

CONFIDENTIAL – DO NOT COPY

New Route Investigation and Process Development in the Synthesis of GSK221149

Thesis submitted to the University of Strathclyde for the
degree of Doctor of Philosophy

Alastair Roberts

April 2015



This thesis is the result of the author's original research. It has been composed by the author and has not been previously submitted for examination which has led to the award of a degree.

The copyright of this thesis belongs to the author under the terms of the United Kingdom Copyright Acts as qualified by University of Strathclyde Regulation 3.50. Due acknowledgement must always be made of the use of any material contained in, or derived from, this thesis.

Signed:

Date:

Acknowledgements

I would firstly like to thank my academic supervisor Professor Jonathan Percy. Your guidance, patience and meticulous attention to detail have taught me much, and I have thoroughly enjoyed our collaboration. You have played a huge part in shaping this thesis and I am truly grateful. Thank you also to Professor Colin Suckling, whose thorough examination and thesis review have been highly valuable.

To my industrial supervisors Andy Mason and Mat Whiting, thank you for all your support over the last 4 years, your commitment to me during my studies has been superb. Your scientific critique has been instrumental in my development and has ensured I've gained the maximum benefit from this programme, you have challenged me and encouraged me to think creatively, and dedicated a great deal of your own time in helping me to prepare this thesis. Thank you.

I would like to thank the GSK221149 project leaders Andy Whitehead, Steve Hermitage and Mat. Thank you for giving me the opportunity to work on a project which has lent itself so well to writing a thesis. Combining the requirements of industrial work and studying for a PhD could have been challenging, yet wasn't because of your willingness to allow me scope to explore my own direction.

Thank you also to all the members of the GSK221149 team past and present, Kate Kinnear, Alan Ironmonger, Sandrine Garcia, Jerome Hayes and Mike Webb to name just a few. Your expertise and knowledge provided the starting point for this work and contributed significantly to the success of the project. Thank you in particular to Mark Mitchell, without your deep expertise in catalysis the route would never have got off the ground.

I would also like to thank Professors Harry Kelly and Billy Kerr for setting up this collaborative PhD programme. After joining GSK as a graduate I never expected to get the opportunity to study for a PhD and you have made that happen. Your commitment to the continued development of chemists and chemistry at GSK is commendable.

To Sophie, we can add this to the long list of experiences we've shared!

Abstract

This thesis describes the development of a novel synthetic route to the Oxytocin antagonist GSK221149 developed by GlaxoSmithKline for the treatment of pre-term labour. The case for investigating new synthetic routes is made and retrosynthetic analysis allows the prioritisation of a route employing an asymmetric reductive amination as the key step.

The investigation and development of the prioritised route is then described. The synthetic methods and processes for the synthesis of an α -keto amide using a modification of an existing literature procedure and the application of Lewis acidic conditions to facilitate the synthesis of a challenging imine is detailed. The novel application of a 1st generation Noyori type ruthenium catalyst to the asymmetric hydrogenation of a sterically encumbered and densely functionalised imine is shown and the newly developed route is scaled up to provide material meeting clinical specification. A detailed comparison of the cost and manufacturability implications *versus* the existing chemistry is then performed.

The final section of the thesis describes the investigations to understand the origin of reactivity in, and scope of, the newly discovered asymmetric hydrogenation reaction. A number of alternate imine substrates are hydrogenated leading to the proposition of a 5-membered ruthenacycle as a key intermediate in the catalytic cycle.

Contents

Acknowledgements	ii
Abstract	iii
Abbreviations	vi
1 Introduction Part 1; Oxytocin and Oxytocin Antagonists	1
1.1 Oxytocin and the Oxytocin Receptor.....	2
1.2 Pre-term Birth and Pre-term Labour	5
1.3 Diketopiperazines	9
1.4 Previous Routes to GSK221149	17
2 Introduction Part 2; New Routes to GSK221149 and Asymmetric Synthesis	23
2.1 Process Chemistry.....	24
2.2 Retrosynthetic Analysis of GSK221149	26
2.3 Asymmetric Synthesis	34
2.4 Transition Metal Catalysed Asymmetric Hydrogenation	40
2.5 Research Objectives.....	58
3 Results and Discussion Part 1; A New Route to GSK221149	61
3.1 Ketoamide Synthesis.....	62
3.2 Imine Formation	71
3.3 Imine Reduction.....	88
3.4 Ester Hydrolysis and Diastereoisomer Separation.....	93
3.5 Synthesis of GSK221149.....	97
3.6 Comparison of GSK221149 Derived from the Two Routes.....	100

3.7	Changing the Ester Protecting Group Strategy	107
3.8	Catalytic Hydrogenation of the Benzyl Ester Protected Imine	116
3.9	Catalytic Asymmetric Hydrogenation of the Imine	120
3.10	Analysis of the Amino Acid	144
3.11	Comparison of the Two Routes to GSK221149	149
3.12	Summary and Conclusions	153
4	Results and Discussion Part 2; Investigation of the Asymmetric Hydrogenation	154
4.1	Introduction	155
4.2	Research Plan	155
4.3	Heterocycle Substitution	157
4.4	Imine <i>N</i> -substituent Investigation	171
4.5	Amide <i>N</i> -Substituent Investigation	177
4.6	Summary and Conclusion	179
5	Conclusion	181
5.1	Summary and Conclusions	182
6	Experimental	187
6.1	General Experimental	188
6.2	Experimental Procedures for Results and Discussion Part 1	191
6.3	Experimental Procedures for Results and Discussion Part 2	254
7	References	292

Abbreviations

a/a	area per unit area	<i>m</i> -CPBA	<i>meta</i> -chloroperoxybenzoic acid
Ac	acetyl		
API	active pharmaceutical ingredient	δ	chemical shift in parts per million downfield from tetramethylsilane
aq	aqueous		
Ar	aryl	d	doublet (spectral)
BARF	[B[3,5-(CF ₃) ₂ C ₆ H ₃] ₄] ⁻	<i>d</i>	density
Bn	benzyl	DCM	dichloromethane
Boc	<i>tert</i> -butoxycarbonyl	DEPT	distortionless enhancement by polarization transfer
bp	boiling point		
br	broad (spectral)	DIBALH	<i>diisobutylaluminium</i> hydride
<i>n</i> -Bu	normal (primary) butyl		
<i>s</i> -Bu	<i>sec</i> -butyl	DIPEA	<i>Diisopropylethylamine</i>
<i>t</i> -Bu	<i>tert</i> -butyl	DMA	<i>N,N</i> -dimethylacetamide
Bz	benzoyl	DME	1,2-dimethoxyethane
°C	degrees Celsius	DMSO	dimethyl sulfoxide
calcd.	calculated	<i>de</i>	diastereomeric excess
CatBH	catecholborane	EDTA	ethylenediaminetetraacetic acid
CBz	benzyloxycarbonyl		
CDI	carbonyl diimidazole	EI	electron impact
cm	centimetre(s)	<i>ee</i>	enantiomeric excess
COSY	correlation spectroscopy	ESI	electrospray ionisation
		Et	ethyl

g	gram(s)	lit.	literature value
GC	gas chromatography	μ	micro
h	hour(s)	m	multiplet (spectral); meter(s)
HMBC	heteronuclear multiple bond correlation	M	molar (moles per liter)
HMQC	heteronuclear multiple quantum correlation	M ⁺	parent molecular ion
		MCR	multicomponent reaction
HPLC	high-performance liquid chromatography	MDAP	mass-directed autopreparative chromatography
HRMS	high-resolution mass spectrometry	Me	methyl
HSQC	heteronuclear single quantum correlation	MHz	megahertz
Hz	hertz	min	minute(s)
ICP-AES	inductively coupled plasma atomic emission spectroscopy	mol	mole(s); molecular (as in mol wt)
		mp	melting point
IR	infrared	Ms	methanesulfonyl (mesyl)
<i>J</i>	coupling constant (in NMR spectroscopy)	MS	mass spectrometry
		MW	molecular weight
<i>k_{1a}</i>	volumetric mass transfer coefficient	<i>m/z</i>	mass-to-charge ratio
		NaHMDS	sodium hexamethyldisilazide
L	litre(s)		
LCMS	liquid chromatography mass spectrometry	nm	nanometre(s)
		NMM	<i>N</i> -methyl morpholine
LDA	lithium diisopropylamide		

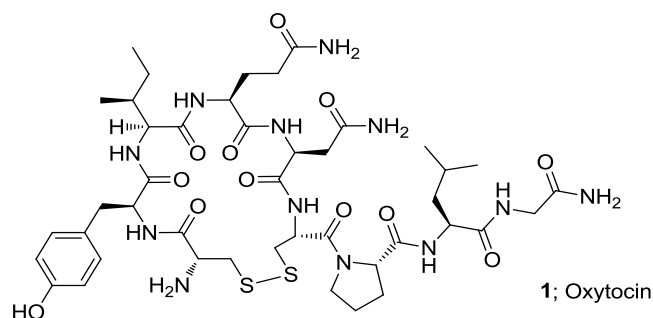
NMR	nuclear magnetic resonance	t	triplet (spectral)
		<i>t</i>	time
NOESY	nuclear Overhauser effect spectroscopy	<i>T</i>	temperature in units of degrees Celsius (°C)
Nu	nucleophile	Tf	trifluoromethanesulfonyl (triflyl)
obsd	observed		
PCA	principal component analysis	TFA	trifluoroacetic acid
		THF	tetrahydrofuran
Ph	phenyl	TLC	thin-layer chromatography
piv	pivaloyl	TMEDA	<i>N,N,N',N'</i> -tetramethyl-1,2-ethylenediamine
ppm	part(s) per million		
PPTS	pyridinium <i>para</i> -toluenesulfonate	TMS	trimethylsilyl; tetramethylsilane
<i>n</i> -Pr	propyl	<i>p</i> -TSA	<i>para</i> -toluenesulfonic acid
<i>i</i> -Pr	<i>isopropyl</i>	<i>T_r</i>	retention time (in chromatography)
q	quartet (spectral)		
ROESY	rotating frame Overhauser effect spectroscopy	Ts	<i>para</i> -toluenesulfonyl (tosyl)
RRT	relative retention time	UV	ultraviolet
RT	room temperature	vol	volume
s	singlet (spectral); second(s)	v/v	volume per unit volume
		wt	weight
T3P [®]	propylphosphonic anhydride	w/w	weight per unit weight
TBME	<i>tert</i> -butyl methyl ether		

1 Introduction Part 1; Oxytocin and Oxytocin Antagonists

1 Introduction Part 1; Oxytocin and Oxytocin Antagonists

1.1 Oxytocin and the Oxytocin Receptor

Oxytocin (**1**) is a cyclic nonapeptide neurohypophysial hormone.¹ It is part of a group of related cyclic nonapeptides which are characterized by a disulfide bridge between cysteine residues 1 and 6. It consists of a cyclic hexapeptide with a C-terminal tripeptide sidechain and has the sequence Cys-Tyr-Ile-Gln-Asn-Cys-Pro-Leu-Gly(NH₂).² This group of neurohypophysial hormones is split into 2 categories based on the polarity of the residue at position 8. The oxytocin family of hormones has a neutral amino acid at this position whereas the vasopressin family typically contains a basic arginine or lysine residue. Hormones of these types are found throughout the animal kingdom, with virtually all vertebrates utilising an oxytocin and a vasopressin derived nonapeptide hormone.



Oxytocin was the first hormone to have its structure elucidated (du Vigneaud *et al.*,³ 1953) and was also the first to be chemically synthesised.⁴ Oxytocin is widely abundant within human tissues⁵ and has many effects on both the central and peripheral nervous systems.⁵

Oxytocin is most commonly known for its effects on the female reproductive system. It has been used for its ability to increase uterine tone since the discovery of the property by Dale⁶ in 1906, and its name is derived from the Greek meaning ‘quick birth’; intravenous oxytocin is commonly used to induce labour. It is also closely involved with lactation in mammals.⁷ However, oxytocin is equally prevalent in both sexes and has

been implicated in various aspects of the male reproductive system including erectile functioning, copulatory activity and ejaculation.⁸

Centrally, oxytocin exerts influence in the regulation of a wide variety of behaviours such as social recognition, parental behaviour and sexual behaviour⁹ leading it to be referred to as the ‘love’ hormone. Oxytocin’s widespread role throughout the cycle of life and reproduction is illustrated by Lee *et al.* (Figure 1).⁹

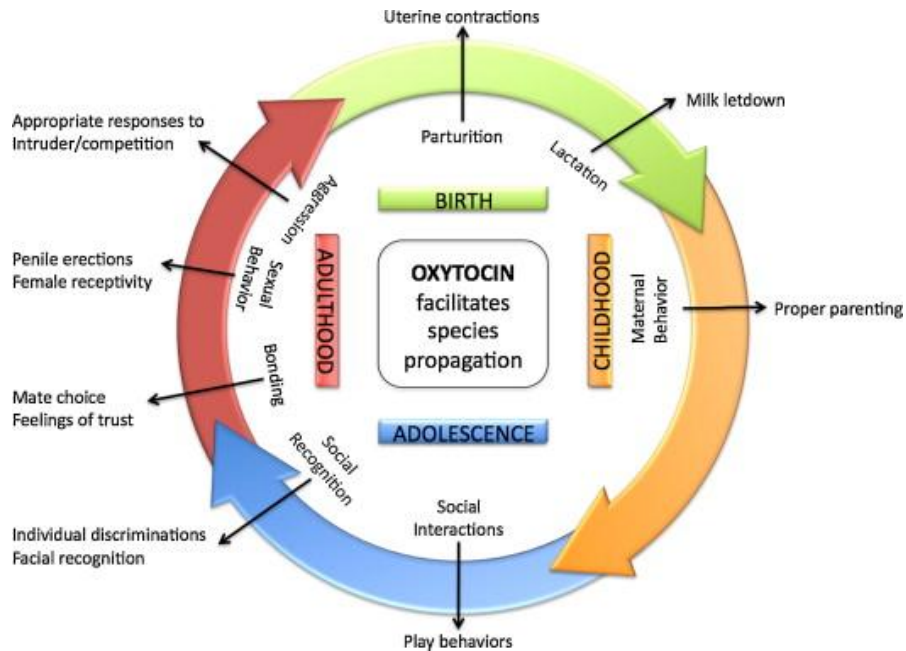


Figure 1 - Role of Oxytocin throughout the cycle of life.⁹

Oxytocin is only known to have one receptor which belongs to a class of G-protein coupled receptors, although the receptor is closely related to the three vasopressin receptors.¹ Like oxytocin itself, the oxytocin receptor is widely distributed throughout the tissues of humans and other vertebrates. It is a seven transmembrane receptor (7TM) characterised by the seven transmembranal helical domains illustrated clearly by Zingg *et al.* (Figure 2).

1. Introduction Part 1; Oxytocin and Oxytocin Antagonists

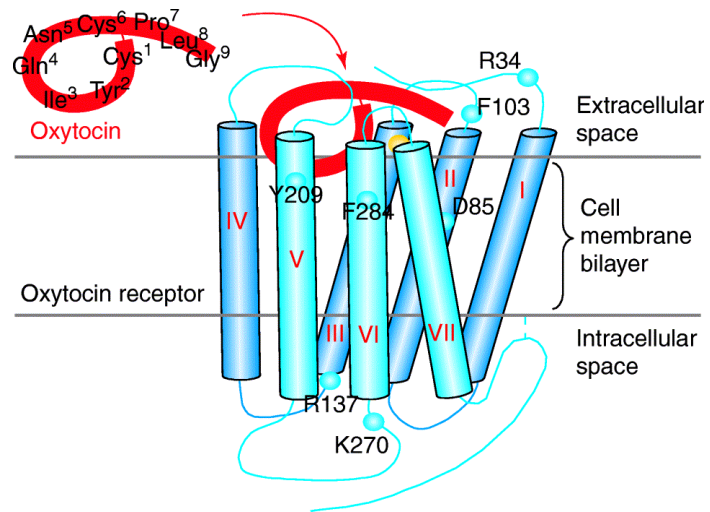


Figure 2 - Structure of the oxytocin receptor.¹⁰

1.2 Pre-term Birth and Pre-term Labour

Pre-term births are defined as births that occur before 259 days (37 completed weeks) of gestational age;¹¹ they are increasingly common in developed countries. A rise from 9.5% in 1981 to 12–13% in 2005 has been observed in the USA¹² and in developed countries, pre-term birth is the leading cause of neonatal mortality (deaths within the first 28 days after birth).¹³ In developing countries, the problem is even more severe. Here, the prevalence of pre-term labour is higher, with estimates placing it at around 25% of all births.¹¹ The World Health Organisation estimates 500,000 deaths per year are caused by prematurity. While pre-term birth and prematurity are two differing concepts they are commonly confused. Pre-term birth relates solely to gestational age at birth, whereas prematurity relates to an infant who has not yet reached the level of maturity required to survive outside the womb. The two concepts, however, are clearly strongly related (Figure 3)¹¹ and increased gestational age reduces the chances of prematurity and associated health problems.

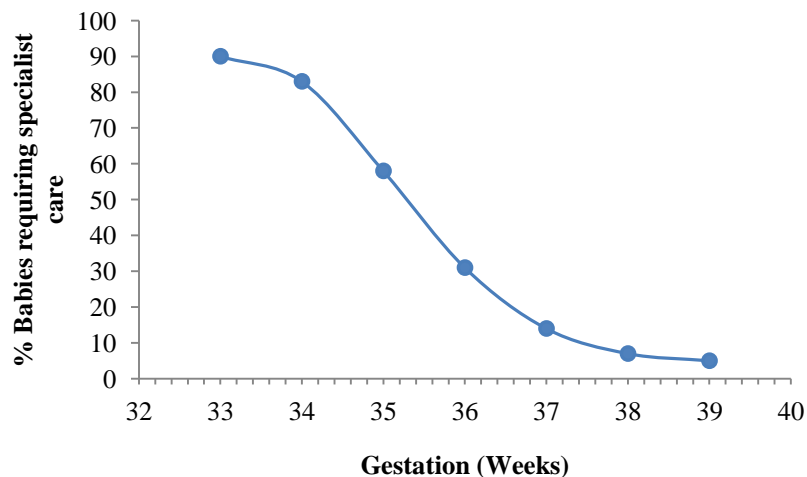


Figure 3 – Babies requiring specialist care based on gestation age

Pre-term infants are at risk of significant medical problems due to the immaturity of their organ systems. Problems typically occur in the respiratory system, as this is one of the last organ systems to develop, and include bronchopulmonary dysplasia (chronic lung disease) and issues with the neurological, cardiovascular and gastrointestinal

systems. Conditions which require long term care, such as cerebral palsy can also be caused by pre-term birth.

Pre-term births can be divided into two main categories; i) delivery for maternal or fetal indications in which labour is induced or the infant is delivered by caesarean section and; ii) spontaneous pre-term labour, although the latter can be classified further depending on whether there is pre-term premature rupture of the membranes (PPROM).¹⁴ Spontaneous pre-term labour accounts for 70% of all pre-term births.

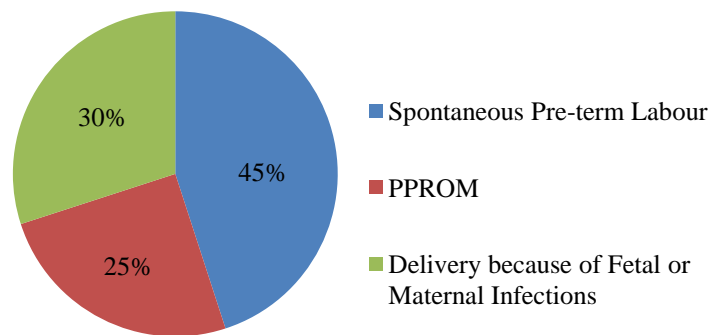


Figure 4 – Obstetric precursors of pre-term birth.¹³

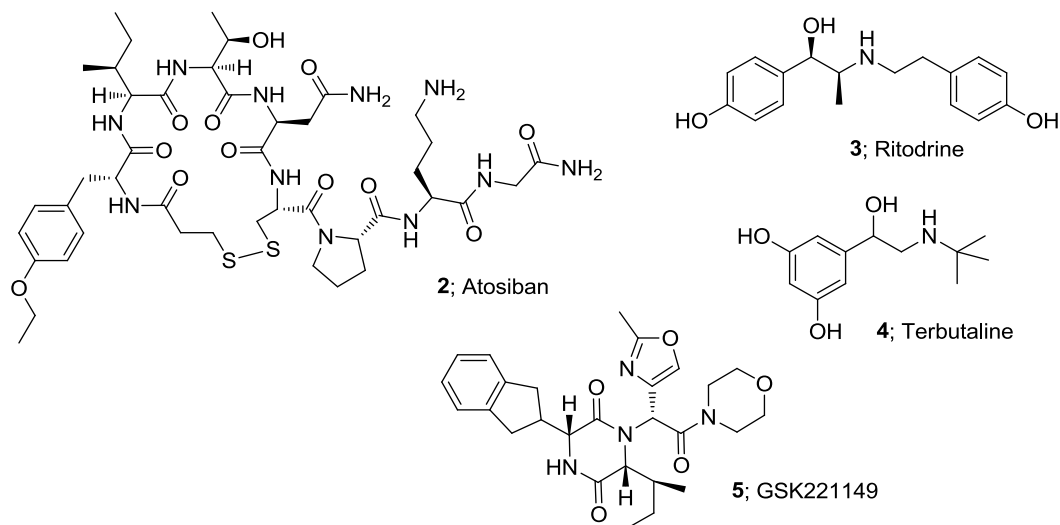
The causes of pre-term labour are complex and not well understood; in most cases a precise mechanism for its cause cannot be established. Generally, pre-term labour is thought to be a syndrome initiated by multiple mechanisms which include infection and inflammation. In the developing world, malarial infection is particularly associated with pre-term labour and neonatal mortality.¹¹

Current treatments to reduce the morbidity and mortality of pre-term labour and associated pre-term births can be classified into primary, secondary and tertiary treatments. Primary treatments are directed at all women before or during pregnancy to prevent and reduce risk of pre-term labour. These may include public educational interventions, nutritional supplements, smoking cessation and pre-natal care. Secondary treatments are aimed at reducing risk in women with known risk factors (e.g. twin pregnancy) and follow similarly to primary treatments. They can also include treatments

such as the prescription of antibiotics to treat infections (such as bacterial vaginosis) which are commonly linked with pre-term labour. Tertiary treatments have the goal of preventing delivery or improving outcomes for pre-term infants.¹⁵ These treatments are given during pregnancy to women with a high risk or history of pre-term labour. Commonly, glucocorticosteroids are given to promote rapid maturation of the foetus prior to birth, which may be combined with tocolytic agents (agents which inhibit uterine contractions and hence delay birth) to prolong gestation.

1.2.1 Tocolytic Agents

A number of tocolytic agents have been shown to be clinically efficacious; importantly, these include the oxytocin antagonist atosiban (**2**) which can delay delivery by 2-7 days and shows fewer maternal side effects than the β_2 -agonists ritodrine (**3**) and terbutaline (**4**).¹⁶ However, the polypeptide atosiban has no oral bioavailability and hence must be delivered intravenously, requiring hospital administration.



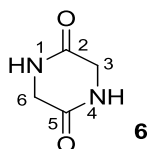
GlaxoSmithKline has developed the orally bioavailable oxytocin antagonist GSK221149 (**5**) for the treatment of pre-term labour; it has recently achieved proof of concept (POC) and is now awaiting phase III clinical trials. Structurally, GSK221149 (**5**) consists of a central 2,5-diketopiperazine core derived from the unnatural amino acids (*R*)-

1. Introduction Part 1; Oxytocin and Oxytocin Antagonists

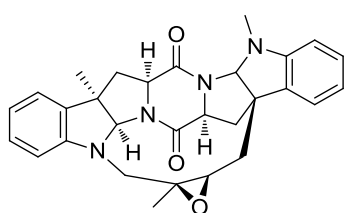
indanylglycine and *D-allo-iso*leucine. It has an important exocyclic stereocentre with a pendant oxazole and morpholinoamide. This thesis is concerned with the development and optimisation of the synthetic route to oxytocin antagonist GSK221149 (**5**).

1.3 Diketopiperazines

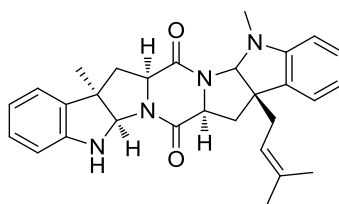
Diketopiperazines (DKP) are 6-membered heterocycles and are the smallest possible cyclic peptides. The simplest example is the anhydride of glycylglycine (2,5-diketopiperazine, **6**); the X-ray structure was first described by Robert Corey in 1938.¹⁷



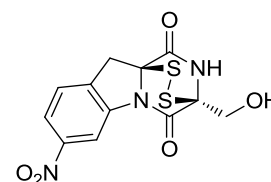
Diketopiperazines are commonly found in nature, being biosynthesized from amino acids by organisms including mammals.¹⁸ They are found in a number of biologically active natural products such as the recently discovered p-glycoprotein inhibiting nocardioazines A and B (**7**, **8**) derived from marine bacteria *Nocardioopsis sp.*,¹⁹ and in glionitrin A (**9**) derived from *Aspergillus fumigates* which shows significant antibiotic activity against a series of microbes including methicillin-resistant *Staphylococcus aureus*.²⁰



7; Nocardioazine A



8; Nocardioazine B



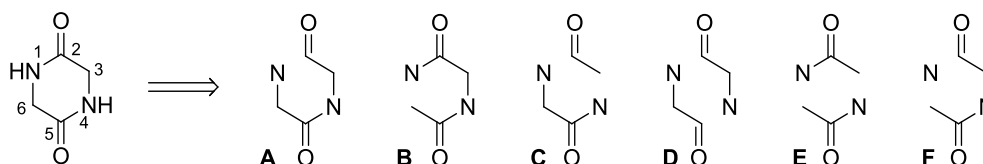
9; Glionitrin A

Many diketopiperazines show plasminogen activator inhibitor (PAI-1) activity which is implicated in a number of conditions including coronary heart disease, thrombosis, atherosclerosis and cancer. In addition, both natural and unnatural 2,5-diketopiperazines have shown activity against targets such as GABAergic, serotonergic 5-HT_{1A} and oxytocin receptors.¹⁸ This biological activity means diketopiperazines have become very interesting targets for medicinal chemistry. In addition, they are resistant to proteolysis²¹ and mimic peptidic pharmacophores, have conformational rigidity and are able to act as donors and acceptors of hydrogen bonds. These properties make them particularly suitable templates for drug molecules. Importantly, they lend themselves well to

combinatorial chemistry, enabling libraries of diketopiperazines to be readily synthesised and tested against disease assays. These factors influenced the early development of GSK's oxytocin antagonist, GSK221149 (**5**).

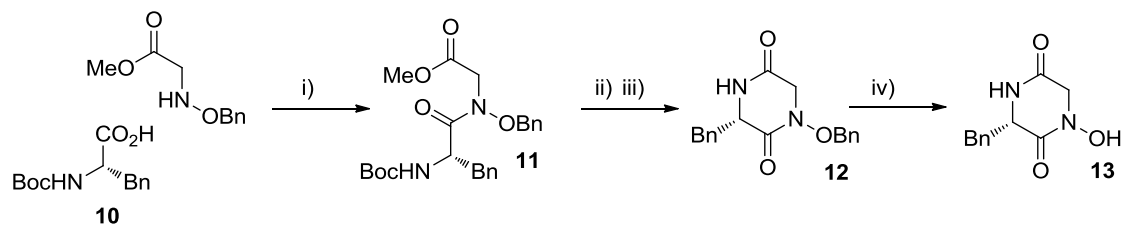
1.3.1 Synthesis of 2,5-Diketopiperazines

The synthesis of 2,5-diketopiperazines (DKPs) is well described in the literature, and summarised excellently by the review of Dinsmore and Beshore²² who discuss the potential approaches according to the retrosynthetic disconnections given below (Scheme 1). Examples of DKP synthesis *via* each of the disconnections are described and discussed.



Scheme 1 – Retrosynthetic analysis of 2,5-diketopiperazines

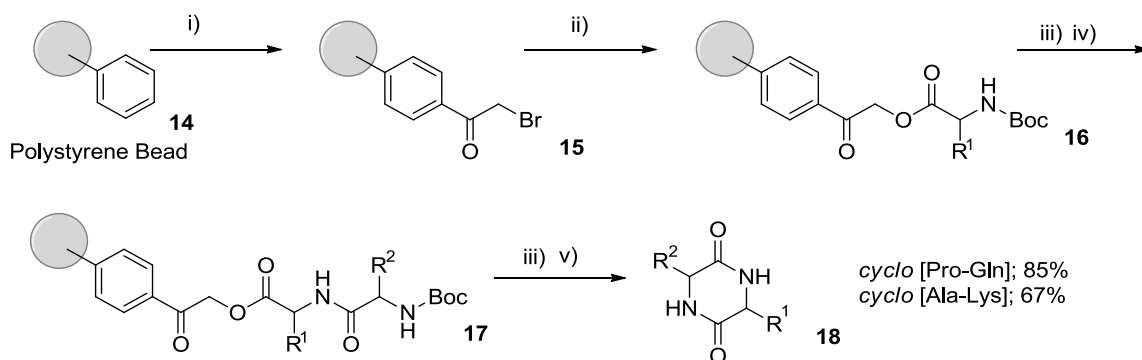
Disconnection **A** provides one of the most common methods of 2,5-diketopiperazine preparation. It involves N_1-C_2 cyclisation and many examples are reported in the literature. A representative example is shown by Akiyama²³ who investigated the synthesis of *N*-hydroxy DKPs (Scheme 2). Condensation of an *N*-protected α -amino acid with an α -amino ester gives an intermediate amide (**11**) which then undergoes acidic Boc cleavage followed by cyclisation, mediated by mild base. Further deprotection gives the desired *N*-hydroxy DKP (**13**).



i) *i*-BuOCOC₂Cl, NEt₃, THF/dichloromethane (69%); ii) TFA, dichloromethane; iii) 5% aq. NaHCO₃ (86%); iv) H₂, Pd/C, EtOH (85%).

Scheme 2 – C₂-N₁ bond formation in the synthesis of DKPs

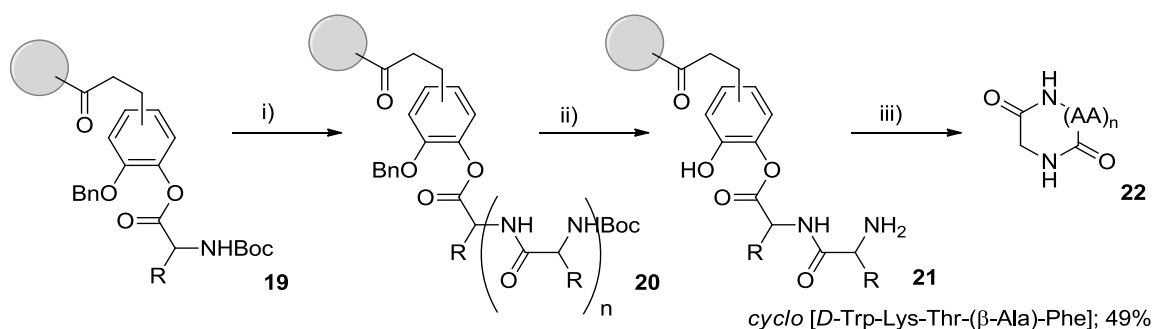
This retrosynthetic strategy has also been commonly implemented using solid phase peptide synthesis methodology, in which the carboxyl terminus remains bound to a polystyrene bead throughout. Wang *et al.*²⁴ exploited the tendency of the phenacyl ester linkage to undergo aminolytic cleavage, which was traditionally seen as problematic for solid phase peptide synthesis. Cyclisation of the resin bound dimer (particularly if the C-terminus residue is the sterically un-hindered proline or glycine) leads to premature cleavage and formation of a 2,5-diketopiperazine. Wang prepared the functionalised bromoacetyl resin (**15**) from polystyrene beads by Friedel-Crafts acylation. The first amino acid residue was attached by α -bromo substitution (**16**). The second residue was added by Boc group cleavage with HCl, followed by exposure to standard DCC/HOBt coupling conditions (**17**). The desired diketopiperazine (**18**) was obtained by a second Boc cleavage and facile intramolecular aminolysis with NEt₃ in THF (Scheme 3).



(i) BrCH₂COBr, AlCl₃, nitrobenzene-dichloromethane; ii) Boc-AA-OH, NEt₃, DMF; (iii) 3.5 M HCl/AcOH; (iv) Boc-AA-OH, HOBt, DCC, NMM, DMF; (v) 5% NEt₃/THF-H₂O.

Scheme 3 – Solid phase synthesis of DKPs

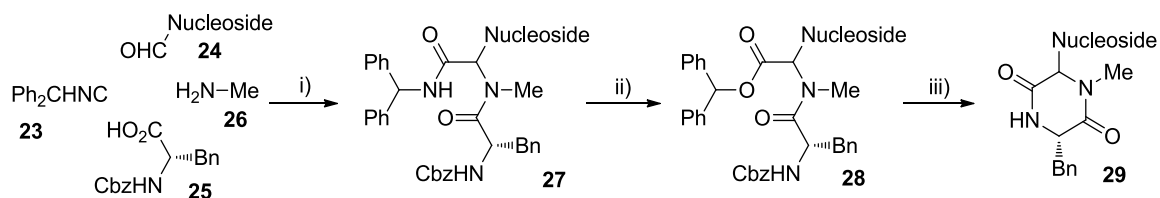
An improvement to this approach was developed by Bourne *et al.*²⁵ who devised the ‘safety catch’ method. Here, the resin linker requires activation before intramolecular aminolysis can take place. This allows the construction of larger cyclic peptides (**22**) and the removal of deprotection by-products prior to cleavage, which greatly simplifies product purification (Scheme 4). The linker is an *O*-alkoxyphenyl ester and the desired peptide is built up while attached to it by standard solid phase techniques. Cleavage of the benzyl group activates the ester and allows cyclisation to generate the desired DKP or cyclic polypeptide (**22**) with concurrent cleavage from the resin. Cleavage has also been shown to occur without racemisation.^{26,27}



i) Solid phase peptide synthesis; ii) HBr/TFA, *p*-cresol, 1 h, RT; iii) DIPEA, DMF, 16 h.

Scheme 4 – ‘Safety catch’ linker technique

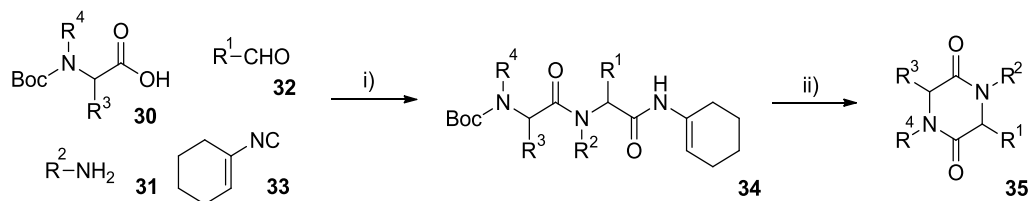
The N₁-C₂ disconnection strategy has also been applied using the 4 component Ugi reaction (section 1.4) to build the cyclisation precursor. Boehm and Kingsbury²⁸ used the multicomponent reaction to give a benzhydryl amide (**27**) which underwent nitrosation and rearrangement to give the cyclisation precursor (**28**). Cbz cleavage initiated cyclisation to give the desired DKP (**29**) (Scheme 5).



i) MeOH H₂O; ii) N₂O₄, NaOAc, dichloromethane; iii) HCO₂H, Pd, MeOH (No yield quoted).

Scheme 5 – Ugi reaction synthesis of 2,5-dikeopiperazines

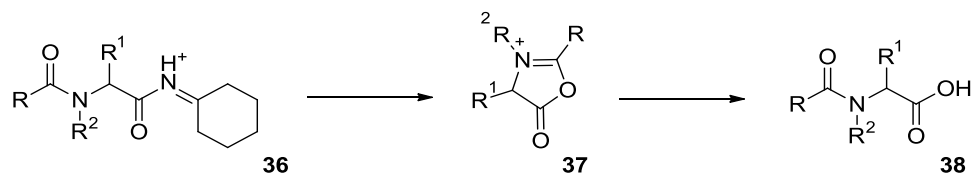
Following this principle, Hulme *et al.*²⁹ elegantly used the Ugi reaction with Armstrong's convertible (cyclohexenyl) isonitrile³⁰ to generate a range of α -acylamino amides. Cyclisation of the deprotected amine affords the desired DKPs (**35**) in 2 steps (Scheme 6).



i) MeOH, RT; ii) H⁺, heat (20 – 95%).

Scheme 6 – Use of Armstrong's convertible isonitrile

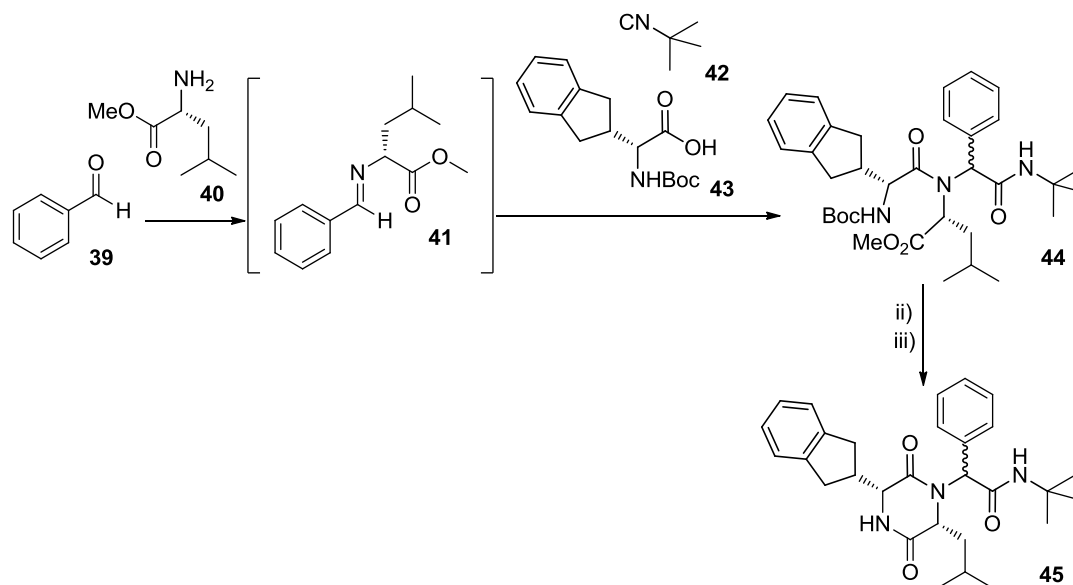
The cyclohexenyl amide is 'convertible' in the sense that protonation provides an *N*-acyliminium species (**36**) which can cyclise and eliminate cyclohexylimine to provide a münchnone (**37**). This species can be hydrolysed to afford an *N*-acyl amino acid (**38**) which can undergo further functionalisation *via* simple amidation (Scheme 7).



Scheme 7 – 'Converting' the cyclohexenyl amide

During the early syntheses of GSK221149 (**5**) and related compounds Sollis used an α -amino ester as the amine component and exploited the Ugi reaction to build an

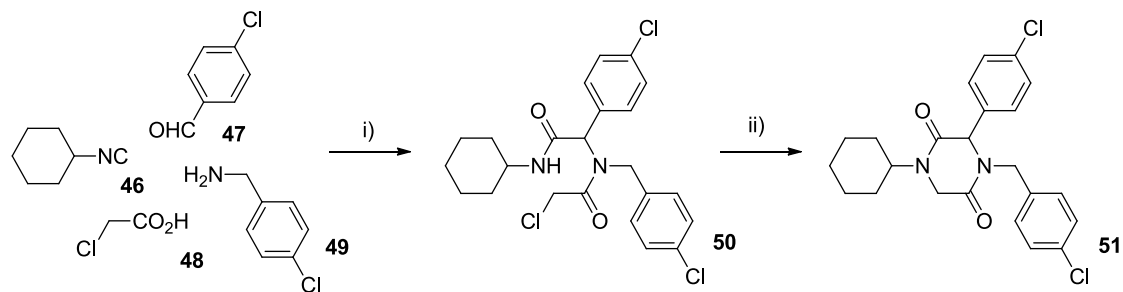
alternative cyclisation precursor (**44**).³¹ Cyclisation give a DKP (**45**) containing an exocyclic stereogenic centre. Partial control of the configuration of the stereocentre was obtained due to attack of the isocyanide on the less hindered face of the imine formed between benzaldehyde (**39**) and *R*-leucine methyl ester (**40**) (Scheme 8). In addition to the above solution phase example, Ugi methodology can be used in combination with solid phase techniques.²¹



i) NEt_3 , MeOH; ii) 4N HCl in dioxane; iii) NEt_3 , dioxane (59%).

Scheme 8 – The use of an α -amino ester in the Ugi reaction to generate cyclisation precursor **44**

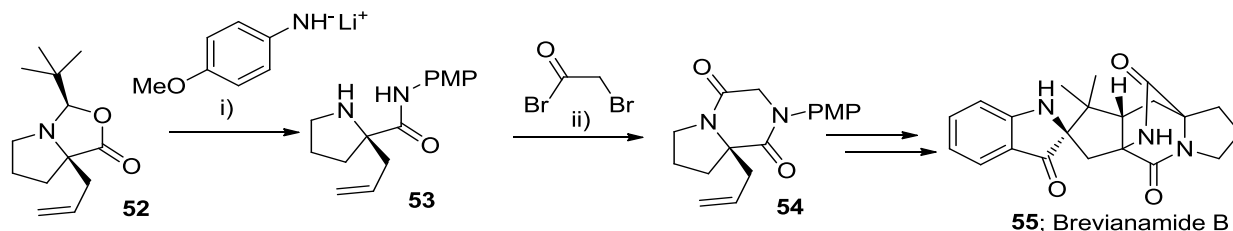
The second approach to 2,5-diketopiperazines (disconnection **B**), involves the formation of the $\text{N}_1\text{-C}_6$ bond. An elegant example of this strategy comes from the group of Marcaccini³² who used the 4 component Ugi reaction using chloroacetic acid (**48**), to generate racemic a chloroacetamide (**50**) which cyclised with sonication to afford the DKP (**51**) in 86% yield (Scheme 9). Marcaccini demonstrated this protocol using a range of aliphatic and aromatic amines and isocyanides, allowing the synthesis of a wide variety of DKPs. However, the reactions were limited to those of aromatic aldehydes.



i) EtOH; ii) KOH, Sonicate (86%).

Scheme 9 – Ugi reaction with chloroacetic acid

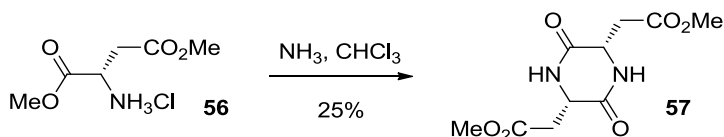
The first of the tandem bond-forming DKP syntheses involves formation of N_1-C_2 and C_3-N_4 bonds (disconnection **C**). This approach typically employs the use of an ambident electrophile. It is exemplified by Williams *et al.*³³ in their synthesis of brevianamide **B** (**55**) in which a proline derivative (**53**) was converted to the desired DKP (**54**) by one-pot *N*-acylation and amide alkylation with bromoacetyl bromide (Scheme 10).



i) *p*-MeO-ArNHLi, THF, (88%); ii) K_2CO_3 /dichloromethane, then NaOH, dichloromethane, (97%).

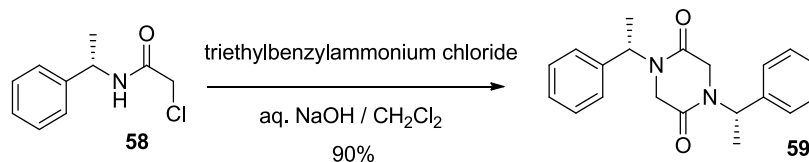
Scheme 10 – Use of bivalent electrophile to form N_1-C_2 and C_3-N_4 bonds

The remaining tandem bond formation strategies, **D** and **E** are usually limited to the formation of symmetrical DKPs and can suffer from low yields due to competing polymerisation pathways. An example is found in the work of Taddei *et al.*³⁴ who investigated dimerisation of aspartic acid methyl ester (**56**) (Scheme 11).



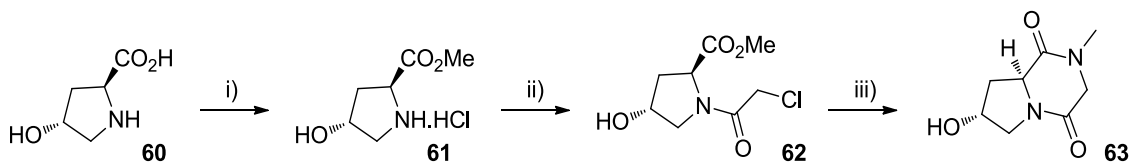
Scheme 11 – Dimerisation of aspartic acid

Paradisi³⁵ employed phase transfer conditions to ensure that cyclisation was favoured over polymerisation, by minimising the concentration of base present in the dimerisation reaction of α -chloro amides (**58**) (Scheme 12).



Scheme 12 – Synthesis of symmetrical 2,5-diketopiperazines

The final tandem bond forming approach, disconnection **F**, allows the introduction of a range of N1 substituents using primary amines. Tronche *et al.*³⁶ used a tandem alkylation-acylation approach in the synthesis of a diazabicyclo[4.3.0]nonane (**63**) derived from *trans*-4-hydroxy-*L*-proline (**60**) (Scheme 13). The approach was shown to be widely applicable to aliphatic and benzyl amines although cyclisation was problematic using aromatic amines owing to their low nucleophilicity.



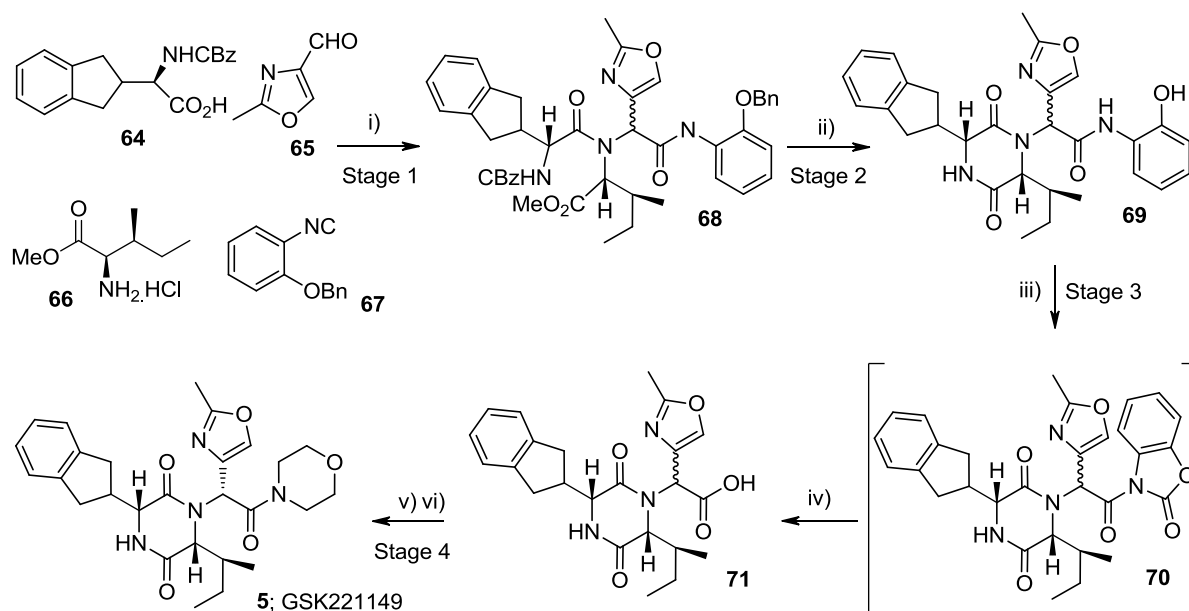
i) SOCl₂, MeOH, (95%); ii) ClCH₂COCl, benzene (87%); iii) MeNH₂, NEt₃, EtOH, (80%).

Scheme 13 – Synthesis of diazabicyclo[4,3,0]nonanes using approach F

1.4 Previous Routes to GSK221149

1.4.1 Route A

The existing route to GSK221149 (**5**) utilising disconnection A above has remained largely unchanged since the compound was discovered. A four component Ugi reaction³⁷ is key to the synthesis; it builds up the required complexity in a single step. The medicinal chemistry lead compound and a number of others like it were discovered from a library of Ugi reaction products. Because of the highly convergent nature of the Ugi reaction, Route A involves a low number of steps considering the complexity of GSK221149. It is for this reason that the route has remained largely unchanged throughout the drug discovery and development process. However, a number of issues mean that while the route appears theoretically sound, it is less practical than desired and significant improvements either to the route or processes are sought.

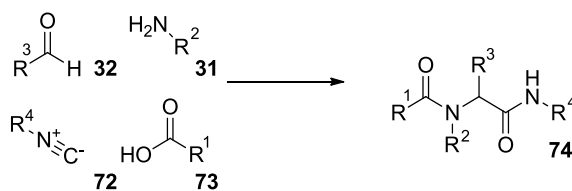


Scheme 14 - Route A to GSK221149

In the route A synthesis of GSK221149, the Ugi reaction, carried out in methanol/trifluoroethanol, combines CBz indanylglycine (**64**), 2-methyloxazole-4-carbaldehyde (**65**), 1-(benzyloxy)-2-isocyanobenzene (**67**) and methyl *D-allo*-isoleucinate (**66**) to afford the desired *bis*-amide (**68**) as shown (Scheme 14). Minimal diastereoselectivity around the newly formed stereocentre bearing the oxazole group is observed (60:40). The almost complete lack of stereocontrol at this point is of little consequence due to epimerisation at a later stage in the synthesis. However, issues with this stage arise from the number of side reactions possible and the resultant loss of yield (up to 50 distinct impurities are observed). The use of expensive trifluoroethanol as solvent is also undesired, but is required to promote efficient reaction as its increased ability to form hydrogen bonds accelerates imine formation.

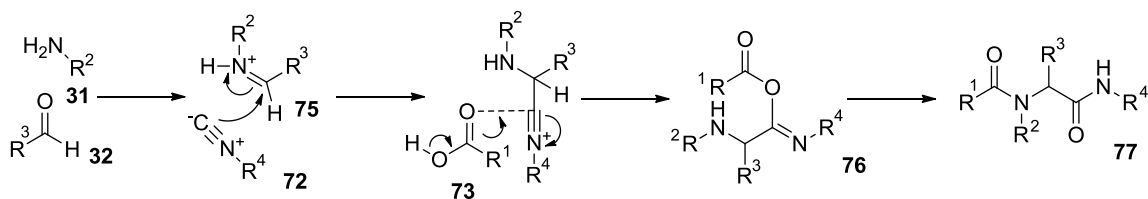
1.4.2 The Ugi Reaction

The Ugi multi component reaction was discovered by Ivar Ugi in the late 1950s.³⁷ It combines a primary amine, an aldehyde or ketone, a carboxylic acid and an isonitrile, and generates α -acylamino amides (**74**) in one step as shown (Scheme 15). The Ugi reaction is often used by combinatorial chemists because significant structural complexity can be built up in a single step; also, being a multicomponent process, it allows a large number of products to be produced from a limited number of monomers.



Scheme 15 - Ugi reaction

The Ugi reaction is thought to take place *via* initial imine formation between the aldehyde (or ketone) and the amine. The imine (**75**) then reacts with the isonitrile and the carboxylic acid to give an intermediate (**76**) which undergoes intermolecular Mumm type rearrangement³⁸ to afford the desired α -acylamino amide (**77**) (Scheme 16).



Scheme 16 – The Ugi reaction mechanism

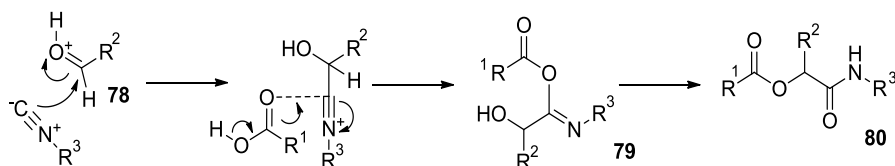
The Ugi reaction has been classified as a ‘green’ reaction³⁹ due to its high atom efficiency, making it a desirable reaction for use on large scale. It has also been shown to operate effectively in aqueous systems, further enhancing its green credentials.⁴⁰ The Ugi reaction’s one-pot, convergent nature can avoid the need for multi-step chemistry; on a small scale, this one-pot nature is desirable. However, on a large scale it can become problematic, when unavoidable delays between material charges may allow undesired reaction pathways to operate. Care must also be taken with the charge order to prevent undesired side reactions (*c.f.* Passerini reaction section 1.4.2.1). Due to these undesired reaction pathways, which may also operate once all materials are charged, the purity of Ugi reaction products is often poor and crystallisation of the product can become a problem particularly as α -acylamino amides are often highly soluble. A wider issue of the Ugi reaction is the low commercial availability of isocyaniles⁴¹ and the fact that only secondary amides can be generated. In efforts to overcome this, convertible isocyaniles are often used; these can be elaborated further to afford more diverse arrays of products. The GSK preparation of GSK221149 using the Ugi reaction is, to the best of our knowledge, the largest scale Ugi reaction performed to date.⁴² This is surprising given the many advantages of the Ugi reaction and its routine use in combinatorial chemistry.

1.4.2.1 Common Impurity Formation Pathways in Ugi Reactions

One of the primary difficulties in performing Ugi reactions on scale is the poor purity profile of the reaction which results in lower yields and causes difficulties in product

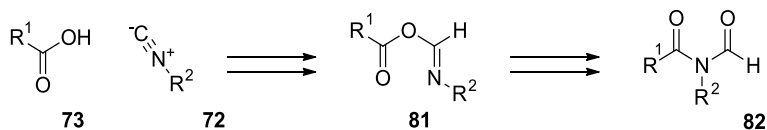
isolation. A number of alternate reaction pathways can occur during Ugi reactions which contribute to their low purity profiles.

The Passerini reaction⁴³ is a related reaction which differs from the Ugi reaction only in the absence of an amine. The Passerini reaction proceeds *via* direct attack of the isonitrile on the aldehyde to afford α -acyloxy amides (**80**), according to Scheme 17. It is a useful reaction in its own right.



Scheme 17 – Passerini reaction mechanism

The three component Ugi reaction is the cause of another commonly observed Ugi impurity. Here, water or solvent intercepts the isonitrile instead of the carboxylic acid to afford α -amino amides. Recently, a two component reaction between isonitriles and carboxylic acids to afford *N*-formylamides (**82**) as shown (Scheme 18), was discovered by the group of Danishefsky.⁴⁴ This reaction can also be expected to occur in Ugi reactions.



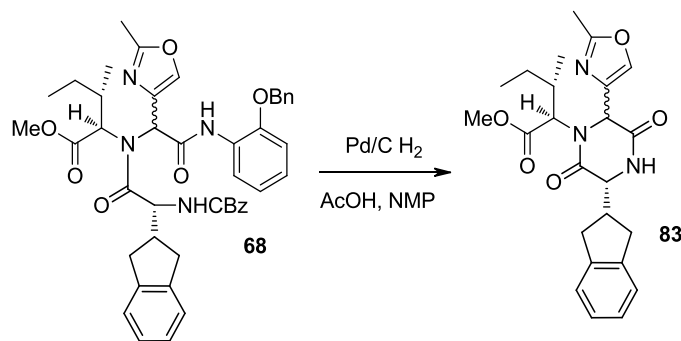
Scheme 18 – Danishefsky two component Ugi reaction

Despite these issues, the Ugi reaction has been successfully used as the key step in the synthesis of GSK221149 on scales of up to 50 kg and this chemistry is discussed further.

1.4.3 Elaboration of the Ugi product to GSK221149

Once the Ugi product (**68**) is formed the hydrogenolysis of the benzylic protecting groups is carried out. As the CBz protecting group is cleaved, cyclisation of the newly revealed primary amine onto the methyl ester proceeds rapidly to afford the

diketopiperazine core. However, the precise reaction pathway is not well understood and a significant impurity is generated by cyclisation of the deprotected indanyl glycine amino-group onto the amide carbonyl, instead of the ester carbonyl (Scheme 19). This impurity (**83**) accounts for 20% of the total product, and results in a significant yield loss.



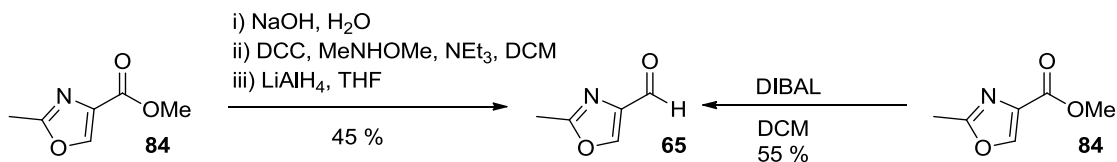
Scheme 19 – Alternative cyclisation pathway

Stage 3 involves the relatively straightforward cleavage of the 2-aminophenylamide *via* activation with CDI and hydrolysis. During this stage, epimerisation of the stereocentre bearing the oxazole group occurs.

At stage 4, a mixed anhydride is formed from the free acid and pivaloyl chloride; reaction with morpholine affords the desired amide (**5**). The reaction is carried out at a low temperature (-78 °C) in order to favour the desired diastereoisomer. An 85:15 ratio of the diastereoisomers is obtained and then improved by crystallisation. However, the scale up of reactions carried out at low temperature is expensive and requires specialised low temperature equipment; it cannot be carried out in general purpose plant which typically does not have the required cooling capacity. The yield of the process is also unsatisfactorily low at 55%.

Route A has a number of more general drawbacks. The synthesis of the oxazole aldehyde (**65**) is difficult resulting in a high cost; there is therefore uncertainty in security of supply. The aldehyde (**65**) is typically made from the corresponding ester *via* either reduction of the Weinreb amide with LiAlH_4 or direct reduction of the ester with

DIBAL. The former suffers from a high number of steps and the latter, whilst more direct, is still low yielding.



Scheme 20 - Synthesis of Oxazole aldehyde 65

Route A also suffers as there are no isolated intermediates throughout. This is an issue firstly, as there are no points of purity control through the synthesis and secondly, as storage of intermediates as solutions is undesirable, especially on large scale since the solutions may have reduced stability and are considerably harder to assay. New synthetic routes to GSK221149 are therefore under investigation in an attempt to circumvent the problems associated with route A as described above.

2 Introduction Part 2; New Routes to GSK221149 and Asymmetric Synthesis

2 Introduction Part 2; New Routes to GSK221149 and Asymmetric Synthesis

2.1 Process Chemistry

There are a number of considerations which must be made when designing chemical processes for the large scale synthesis of pharmaceutical products. Processes should adhere to the general principles of being safe, efficient, economical, environmentally friendly and robust. They must also provide product in high quality.

Firstly, and most importantly, chemical processes must be safe to operate. Whilst the safety of all processes should be thoroughly assessed prior to running on large scale, the following factors require particular consideration. Reactions involving high energy intermediates such as azides should generally be avoided. Care should be taken with reactions which have the potential to evolve significant quantities of gas. Processes which allow a large reactive inventory (reactants in the reaction vessel, yet to react) to accumulate should be avoided. A process whereby a reactive reagent is charged at elevated temperature and immediately consumed is safer than one in which all reagents are charged and the mixture is heated to initiate the reaction. Consideration should be given to the choice of reagents and solvents used in the process; toxic reagents and solvents with low flashpoints should be substituted where possible.

Of equal importance, particularly within the pharmaceutical industry, is that chemical process must be able to provide material in exceptionally high purity. Typically all impurities in API at levels greater than 0.1% need to be fully characterised. Impurities which are genotoxic need to be controlled to very low (parts per million) levels. Therefore processes used to deliver API need robustly and reliably provide material which meets these demanding specifications.

Thirdly, processes and routes need to be economical. This means routes and reagents should be both atom economical and as inexpensive as possible. In addition, consideration should be given to the impact of processing conditions on the overall cost.

2. Introduction Part 2; New Routes to GSK221149 and Asymmetric Synthesis

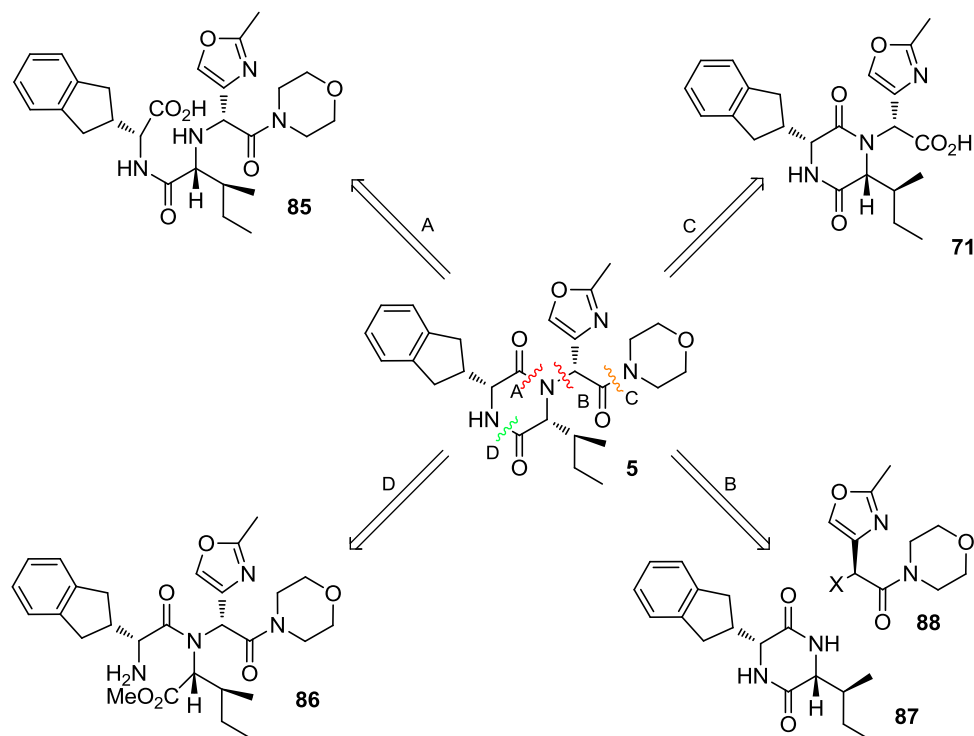
For example, extremes of temperature can be costly both in terms of the energy required for heating or cooling and the equipment needed. As a rule, temperatures between -20 °C and 140 °C are achievable in general purpose plant. Additionally, the cost and availability of the chosen starting materials, reagents, and solvents should be considered. Ideally, all materials should be readily available from multiple suppliers, at low cost.

The environmental impact of the process is of high importance and this is particularly relevant to the waste streams produced by the process. Chlorinated solvents and heavy metals require complex waste treatment procedures and so their use should be avoided, as should reagents which are particularly toxic or harmful to the environment. Extra care should be taken with processes which use or generate harmful gases as accidental release to the environment is often more difficult to prevent.

Lastly, processes and synthetic routes should be designed to be as efficient as possible. This efficiency can relate to the materials used, the time taken and the manpower required. Reagent excesses and solvent volumes should be minimised. Time and material intensive unit operations such as chromatography should be avoided; purifications by crystallisation and aqueous extractions are typically more efficient. Desiccants are also generally best avoided; the use of azeotropic distillation is preferred. A general rule is that processes should be designed to be as simple as possible, utilising minimal equipment, cheap, simple reagents and robust transformations.

2.2 Retrosynthetic Analysis of GSK221149

With these considerations in mind, planning of the synthesis of GSK221149 began. Retrosynthetic analysis was performed and four disconnections for the final bond forming step were envisaged. All four disconnections involve the cleavage of a carbon heteroatom bond and have known associated forward reactions. Each was assessed theoretically and some were investigated practically.



Scheme 21 – Retrosynthetic analysis of GSK221149 (5)

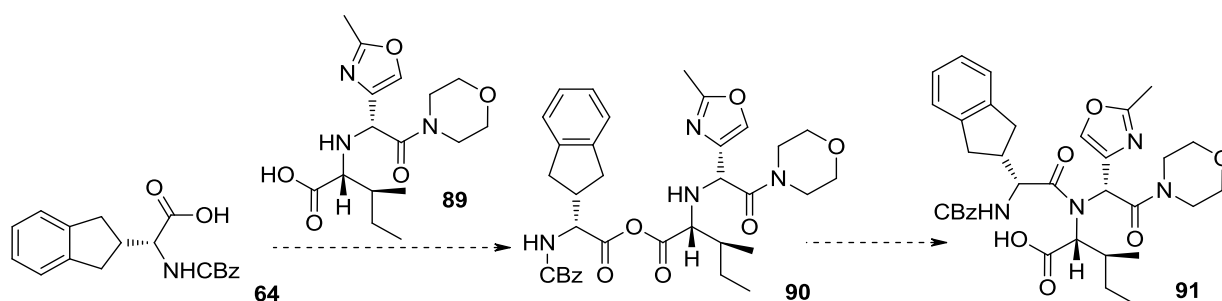
Disconnection A had previously been considered as a potential route and was attractive. Simple amide bond formation is a desirable final synthetic step as amide couplings are generally well understood and there is a broad range of available reagents for performing the transformation.⁴⁵ Amidation reactions typically do not produce unwanted by-products that would need to be controlled to low levels. Unfortunately, this strategy was quickly abandoned due to the difficulties in performing the amidation reaction. Forcing conditions were required to achieve this reaction due to the hindered nature of the amine (85). Under these forcing conditions, epimerisation of the stereocentre bearing the

indanyl glycine moiety was observed. This option was therefore not considered for further investigation.

Disconnection B appeared to be a desirable option due to the convergent nature of a route involving this as a final step. The obvious issue with this strategy was distinguishing between the two diketopiperazine nitrogens in the key alkylation reaction. The transformation was investigated by the project team and quickly discontinued as an option when model chemistry failed to achieve regioselective alkylation at the desired nitrogen.⁴⁶

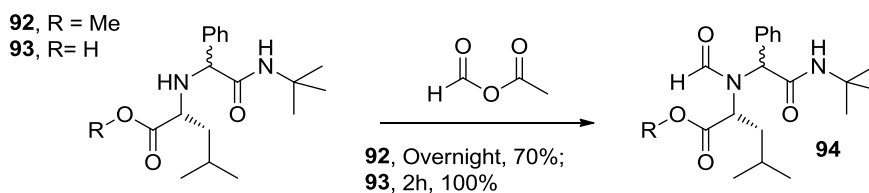
Disconnection C involves amide bond formation at a significantly less hindered centre and is therefore a potentially viable strategy. This strategy, however, makes no disconnection of the diketopiperazine and is the same as that employed in route A, It is known to raise difficulties relating to control of the stereocentre adjacent to the oxazole and, due to the highly convergent nature of the Ugi chemistry, it is difficult to envisage a more expedient synthesis of the precursor (**71**) than that provided by route A.

Disconnection D is therefore the only disconnection to offer a viable new route. Again, it involves a desirable amidation procedure as the final step, but this time it will take place on a relatively unhindered nitrogen, increasing the likelihood of success. This disconnection gives rise to an obvious second disconnection corresponding to the amide bond forming reaction as shown. (Scheme 22)



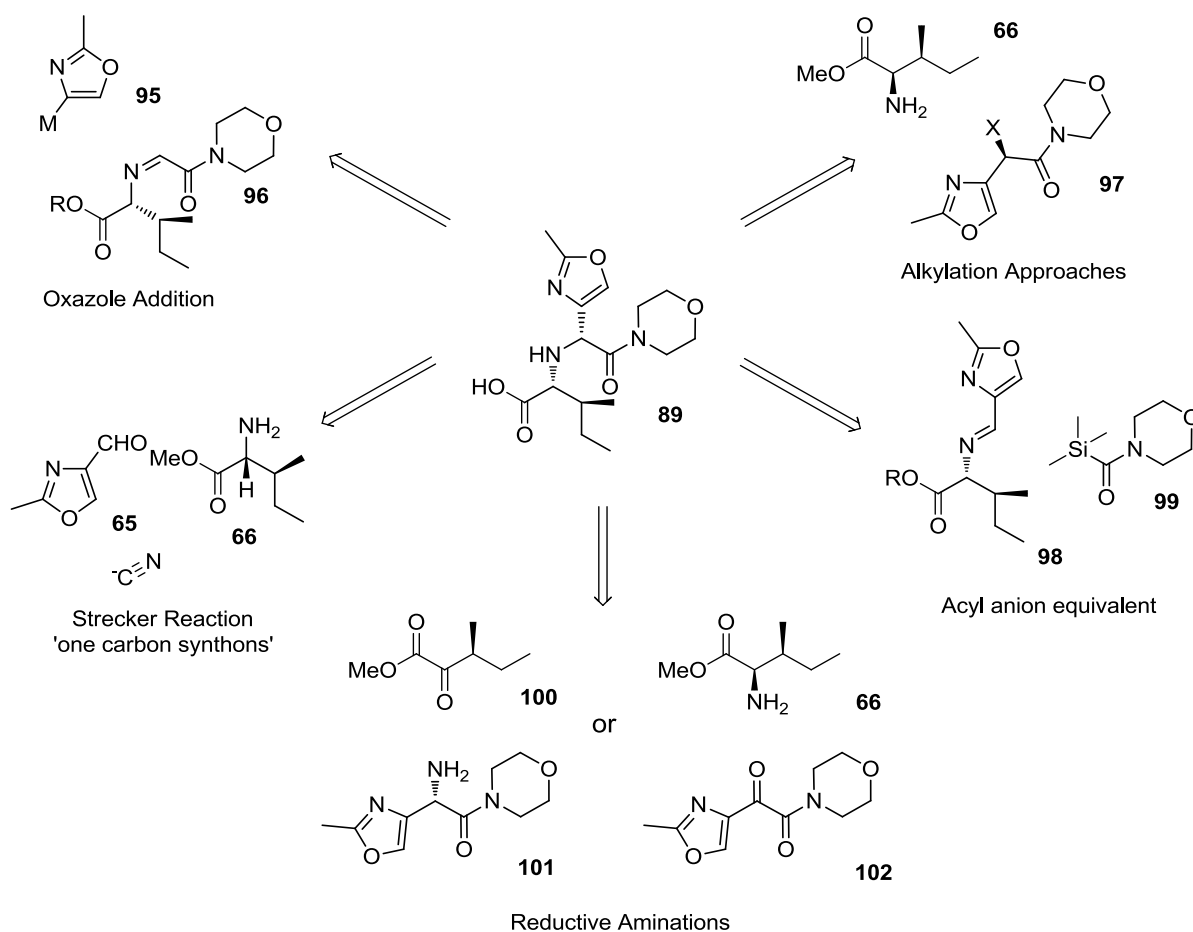
Scheme 22 – Amide bond formation on key amino acid **89**

Precedent for this reaction is found in the work of Sollis,³¹ who investigated this, and similar targets. Acylation of this type of nitrogen centre can be achieved as the reaction proceeds intramolecularly *via* an *O*-acylated intermediate (**90**). Sollis investigated the formylation of similar α -amino acids and amino acid esters and found that the reaction using formyl acetic anhydride was considerably slower with the α -amino acid ester (**92**) than it was with the α -amino acid (**93**) due to the absence of this intramolecular acyl transfer. (Scheme 23)



Scheme 23 – Formylation of α -amino acids and esters³¹

The success of this reaction meant that the route was chosen for further investigation and focus was shifted to the synthesis of the key amino acid precursor (**89**).

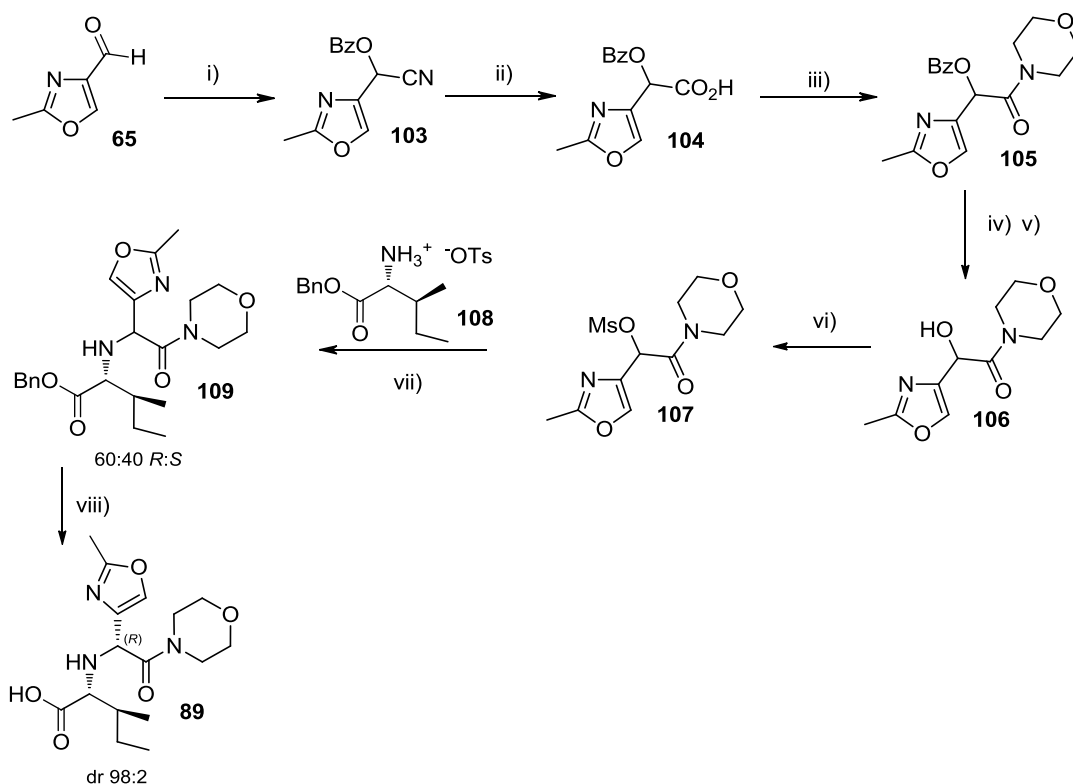
2.2.1 Retrosynthetic Analysis of Amino Acid **89**Scheme 24 – Retrosynthetic analysis of amino acid **89**

Retrosynthetic analysis of the key amino acid fragment (**89**) revealed a number of potential routes (Scheme 24).

2.2.2 Alkylation Approach to Amino Acid **89**

The project team had previously developed a route based on the alkylation disconnection. This route (Scheme 25) proceeded *via* benzoyl cyanohydrin formation from the oxazole aldehyde (**65**) and hydrolysis to the corresponding carboxylic acid (**104**). Amide coupling and deprotection afforded an α -hydroxy amide (**106**) which could be converted to the mesylate (**107**) and then used to alkylate benzyl *D*-*allo*-isoleucinate

(108). Subsequent hydrogenation afforded the amino acid (89). This route, with an overall yield of 18% from the oxazole aldehyde (65), was considered too lengthy to compete with the current Ugi chemistry despite the fact that it consists of effective, robust and reliable chemical steps. Also, due to the stereochemical liability of the mesylate (107) there is no scope for an asymmetric synthesis and so the maximum obtainable yield is severely restricted. An alternative, more expedient synthesis of the amino acid (89) was therefore sought.



i) BzCN, DABCO, dichloromethane, 98%; ii) HCl, dioxane, 79%; iii) T3P[®], NEt₃, morpholine, 98%; iv) LiOH, THF, H₂O; v) Pr₂O 86%; vi) Ms₂O, NEt₃, dichloromethane, 85%; vii) LiBr, NEt₃, MeCN, 60%; viii) H₂, Pd/C, *i*-PrOH, 53%.

Scheme 25 – Alkylation route to amino acid 89

2.2.3 Other Approaches to Amino Acid 89

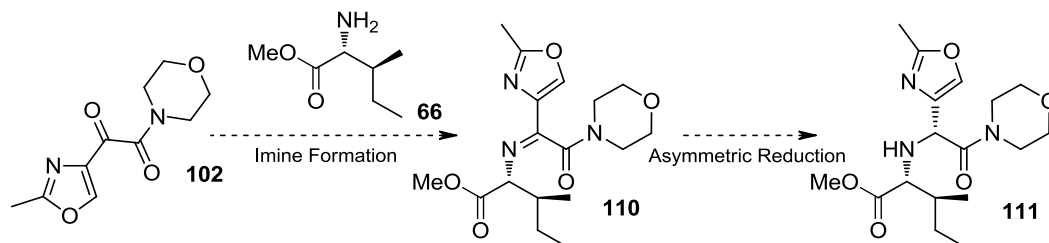
Other approaches suggested by the retrosynthetic analysis include addition of a metallated oxazole species (95) to an imine (96), formed from an α -amido aldehyde and

D-*allo*-isoleucine. This strategy will be investigated, but it is likely to present problems as the regioselective metallation of the oxazole at the 4-position is not trivial.

A number of Strecker-type approaches were also considered; these involve addition of cyanide to an imine formed between the oxazole aldehyde (**65**) and D-*allo*-isoleucine methyl ester (**66**). Some practical work⁴⁶ has been performed to investigate this approach, though without clear success, and this area of research has been suspended pending further results.

An approach worthy of investigation is the addition of acyl anion equivalents such as a carbamoyl silane (**99**) to an imine (**98**). The imine is known to be readily formed in the initial step in the Ugi reaction utilised in route A. Addition of these types of acyl anion equivalents is preceded in the literature^{47,48} and is therefore worthy of practical investigation. Addition to such sterically hindered compounds is less well preceded, so the route may well prove to be challenging.

2.2.4 Reductive Amination Approach to Amino Acid **89**



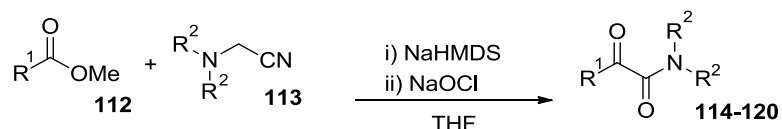
Scheme 26 – Proposed reductive amination strategy

By far the most attractive route to the amino acid is the stereoselective reductive amination strategy shown above. (Scheme 26) Asymmetric reduction of an imine (**110**) could allow the configuration of the centre adjacent to the oxazole to be controlled, removing the requirement for the low temperature chemistry at stage 4 of route A. It could also potentially offer significant savings in the cost of API, as the most expensive starting material, the indanyl glycine fragment (**64**), is introduced at a later stage of the synthesis. Imine formation and asymmetric reduction is a well preceded procedure

and has a good chance of success. However, literature examples are limited to much simpler systems, with no direct precedent for such highly hindered or sterically congested substrates as this. Nonetheless, this strategy appears to be the most attractive of those considered and approaches to the ketoamide (**102**) were therefore sought.

2.2.5 Approaches to Ketoamide 102

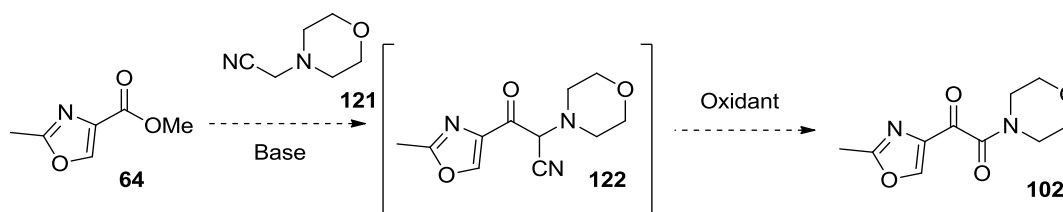
A number of methods for the synthesis of 1,2-diones, and α -ketoamides in particular, are reported in the literature,^{49,50} but the majority of the methods are unsuitable for this system due the preferential functionalisation of the oxazole at the 5-position. Therefore, the method described by Wang and co-workers,⁵¹ in which Claisen condensation between a substituted nitrile (**113**) and an ester (**112**) gives an α -ketonitrile, which can be oxidatively cleaved to afford an α -ketoamide (**114** - **120**) in a facile one-pot procedure, as shown (Table 1), seemed particularly attractive. Wang and co-workers had demonstrated that the chemistry tolerated a number of substituents on both the amine and ester fragments. The reaction of a number of esters with pyridine, *N*-Me-2-pyrrole and 4-*t*-Bu-benzene substituents with aliphatic amino nitriles was described. While the scope of Wang's results is limited, the successful formation of products (**118**, **119**) containing the electron rich heterocycle, *N*-methyl-pyrrole, inspires some confidence that the methodology would be applicable to our system, allowing direct and very concise access to the α -ketoamide (**102**).



Product	R ¹	R ²	% yield
114	2-pyridine	Et	73
115	3-pyridine	<i>n</i> -Pr	57
116	4-pyridine	<i>n</i> -Pr	72
117	4-pyridine	-(CH ₂) ₅ -	92
118	<i>N</i> -Me-2-pyrrole	Et	59
119	<i>N</i> -Me-2-pyrrole	-(CH ₂) ₅ -	40
120	4- <i>t</i> -Bu-benzene	Et	66

Table 1 - Results of Wang⁵¹

This methodology was chosen to be investigated and the proposed scheme is shown. (Scheme 27) It was envisaged that imine formation between the ketoamide (**102**) and *D*-*allo*-isoleucine (**66**) to provide an imine (**110**) would be relatively facile, but that the asymmetric reduction of the imine (**110**) would be challenging. Attention therefore turned to this asymmetric reaction.

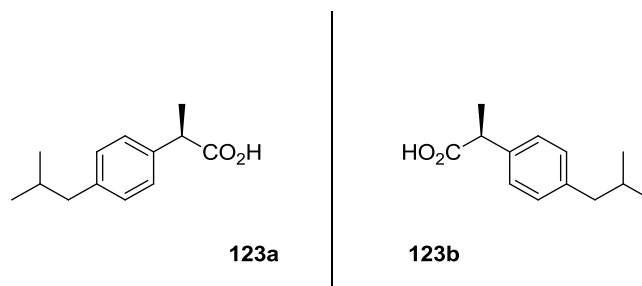


Scheme 27 – Proposed synthesis of ketoamide 3

2.3 Asymmetric Synthesis

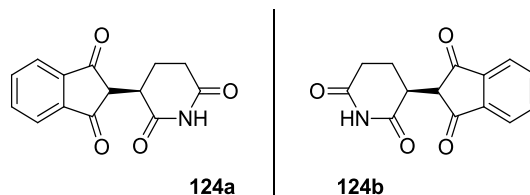
2.3.1 Chirality

The term chiral is derived from the Greek *cheir*, meaning ‘hand’, and is used to describe the non-superimposability of an object on its mirror image. An object that is not superimposable upon its mirror image is said to be *chiral*; if an object is superimposable upon its mirror image it is said to be *achiral*. Everyday objects which display chirality can be readily identified as they have a clear ‘handedness’; examples include gloves and shoes, and the left and right hand spirals of sea shells. Chemical compounds exhibiting chirality have the same atoms bonded by the same sequence of bonds but have different three-dimensional structures. This concept is described as *stereoisomerism*. Pairs of stereoisomers that are mirror images of one another and are non-superimposable are said to be *enantiomers*.⁵² An example of this is the analgesic and anti-inflammatory drug, Ibuprofen (**123**).

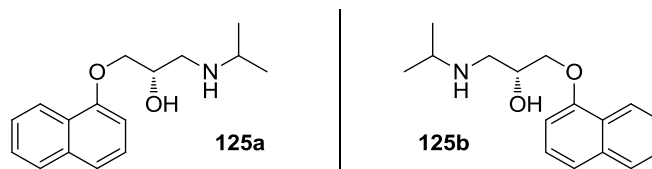


Enantiomers have identical chemical and physical properties within an achiral environment. They have the same melting and boiling points and will have the same chromatographic retention time on an achiral stationary phase. Their properties differ significantly, however, when exposed to a chiral environment. Firstly, they rotate the plane of polarised light in different directions. The isomer which rotates the plane of polarised light to the right is known as the (+)-enantiomer (or the *dextrorotatory* enantiomer) and the isomer which rotates the plane of polarised light to the left is known as the (-)-enantiomer (or the *levorotatory* enantiomer). This property has been used extensively to measure the chiral purity of known samples. Secondly, and importantly,

enantiomers differ in the rate at which they react in, and with, other chiral compounds. This is the reason that many enantiomers can show very different biological activities. Biological systems are, of course, highly chiral environments. Perhaps the most well known example of this is flawed morning sickness treatment thalidomide (**124**). Marketed as a racemic mixture, the (*R*)-enantiomer is a relatively safe and effective antiemetic, yet the (*S*)-enantiomer is teratogenic, and has caused severe birth defects in many thousands of babies.⁵³



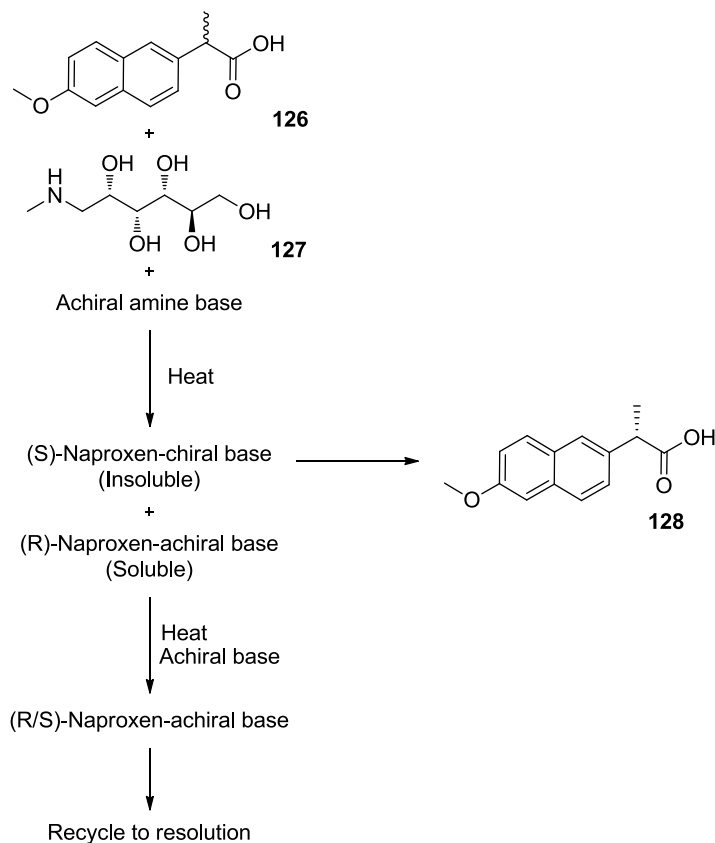
The β -blocker propranolol (**125**) is another compound whose enantiomers exhibit very different biological activities. The (-)-stereoisomer shows the desired β -blocking activity useful in the treatment of heart disease whereas the (+)-isomer acts as a contraceptive.⁵⁴ In this case, the strict control over the enantiomeric purity of the medicine allows its clinical use.⁵⁵ It is therefore clear that the synthesis of enantiomerically pure compounds with high levels of stereochemical control is fundamental to modern synthetic chemistry, and there are a number of methods for the preparation of enantiomerically pure compounds.



2.3.2 Chiral Molecules by Resolution

The preparation of enantiomerically pure compounds can be achieved by a number of methods. The most classical of these methods is preparation of a racemic mixture followed by separation of the enantiomers or *resolution*. The most common method of resolution is by reaction of the racemic mixture with an enantiomerically pure compound to generate a mixture of diastereoisomers. Diastereoisomers, unlike

enantiomers, have different properties in an achiral environment (solubility, crystallinity, chromatographic retention time etc.) and can often be readily separated. An example of this is in the original Syntex synthesis of Naproxen (**128**)⁵⁶ in which a racemic mixture is converted to a pair of diastereomeric salts by reaction with a chiral amine (**127**, *N*-methylglucamine). The desired diastereoisomer is less soluble in the reaction media and crystallises allowing it to be isolated by filtration. The isolated salt can then be broken, yielding both enantiomerically pure Naproxen (**128**) and the chiral amine which can be re-cycled. This is a particularly efficient example of a resolution and builds on the method of Pope and Peachy.⁵⁷ It employs only 0.5 equivalents of the chiral amine; the remaining 0.5 equivalents being a much cheaper achiral material. The (*R*)-Naproxen–achiral base complex is soluble, allowing it to be retained in solution and the pK_a of the base is sufficiently high to promote the racemisation of the unwanted isomer. This allows yields of over 95% of the desired (*S*)-Naproxen to be attained.

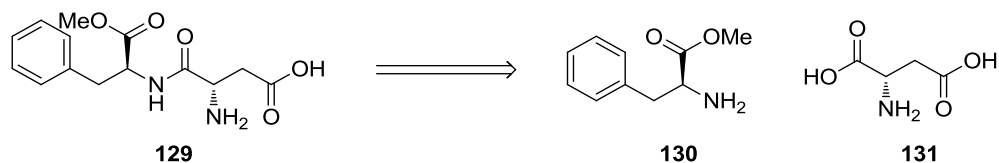


Generally in resolution processes, re-cycling of the unwanted enantiomer is not possible and the yield is limited to a maximum of 50%. This loss of material can sometimes be offset by the simplicity and ease of operability of the process but often the loss is unacceptably high. In this case an asymmetric synthesis of an enantioenriched product is required.

2.3.3 Chiral Molecules from Chiral Starting Materials

Perhaps the most straightforward method of synthesising an enantiomerically pure compound is to begin with a single stereoisomer which contains the required stereogenic centre and modify the structure using a synthesis which does not affect the chiral centre(s). The enantiopure starting material can be prepared by resolution of a racemic mixture (section 2.3.2), a previous asymmetric synthesis, or more commonly, from a natural source. Compounds obtained from nature represent a large resource of enantiopure compounds, particularly sugars, amino acids, terpenes and steroids. These materials are known as *chiral pool* materials and are a collection of cheap, readily available enantiopure products which can be used as starting materials for the synthesis of other chiral products. A drawback of chiral pool materials is that often only a single enantiomer is cheaply available.

A good example of a chiral pool synthesis is provided by the industrial manufacture of the sweetener aspartame (**129**) from (*S*)-phenylalanine methyl ester (**130**) and (*S*)-aspartic acid (**131**).⁵⁸ This synthesis is one of the most simple chiral pool syntheses, with both starting materials containing the required stereochemistry; they are simply combined to provide the product.

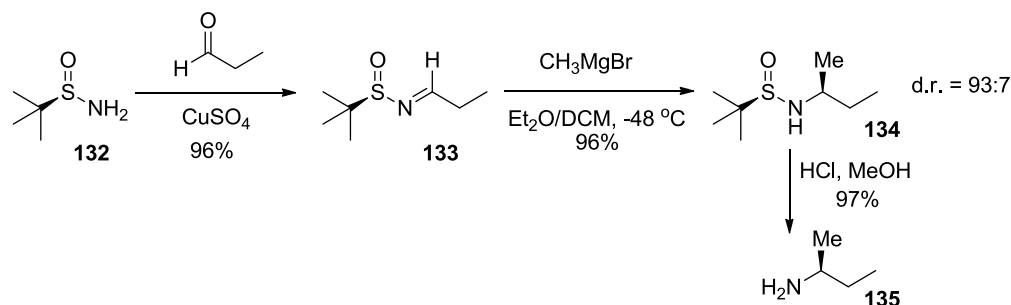


Scheme 29 – Synthesis of Aspartame from chiral pool materials

Chiral pool syntheses of materials that closely resemble the chiral starting materials, as in the case above, are attractive and cost efficient. Chiral pool syntheses become less attractive if the desired product is significantly structurally different from available starting materials or contains stereoisomers not easily available from the chiral pool. In these cases, a long and costly synthesis may be required to provide the desired product. These long syntheses may not compete with a more simple achiral synthesis followed by resolution.

2.3.4 Chiral Molecules using Chiral Auxiliaries

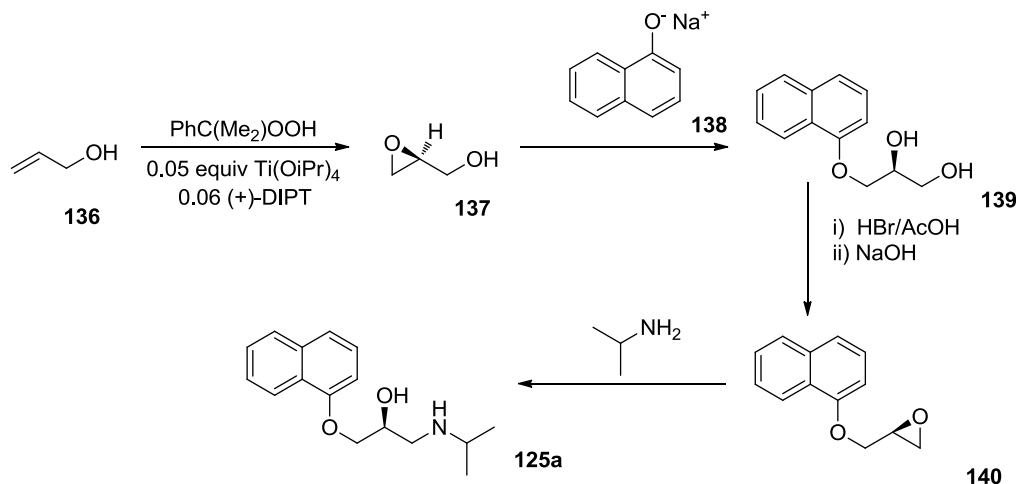
An alternative method for deriving chirality from the chiral pool despite the desired product differing significantly from available materials is to use a chiral pool compound as a *chiral auxiliary*. In this approach a chiral pool material or other cheap chiral material is temporarily incorporated into the synthesis in order to control the stereochemical outcome of a reaction. Once the desired stereocentre has been formed, the chiral auxiliary can be removed and often re-cycled. However, despite the possibility for re-cycling, stoichiometric quantities of the chiral auxiliary are required for each reaction performed and these auxiliaries often contribute significantly to the cost of the synthesis. An example of a chiral auxiliary is Ellman's use of *N-tert*-butanesulfinyl imines for the asymmetric synthesis of amines as shown below. (Scheme 30)⁵⁹ Here, condensation of an enantiomerically pure *t*-butyl sulfonamide (**132**) with an aldehyde gives a chiral intermediate (**133**) which is used to direct the diastereoselective attack of a Grignard reagent. The auxiliary is then cleaved to afford the desired product (**135**).



Scheme 30 – Ellman's *N-tert*-butanesulfinyl chiral auxiliary⁵⁹

2.3.5 Chiral Molecules from Chiral Catalysts

Chiral catalysis is perhaps the most efficient method of asymmetric synthesis; in theory, one molecule of chiral catalyst can transfer its stereochemical information to many thousands of molecules of a prochiral substrate. This eliminates the need for stoichiometric quantities of chiral starting materials or auxiliaries. An example of chiral catalysis can be found in Sharpless' synthesis of the β -blocker propranolol (**125**).⁶⁰



Scheme 31 – Sharpless synthesis of (S)-(-)-Propranolol⁶¹

Sharpless used a catalytic amount of (+)-diisopropyltartrate (DIPT) as the source of chirality in the asymmetric epoxidation of allyl alcohol (**136**). The resultant (S)-glycidol (**137**) is then ring opened *in situ* with sodium naphthoxide (**138**) to generate a diol (**139**) containing the desired chirality. The epoxide (**140**) can then be readily converted to (S)-(-)-propranolol (**125a**) in 98% *ee*.

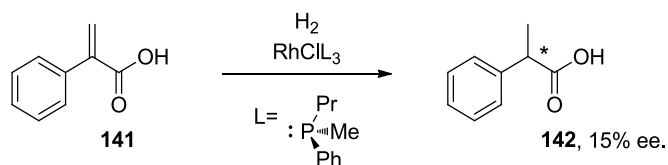
2.4 Transition Metal Catalysed Asymmetric Hydrogenation

2.4.1 A brief history

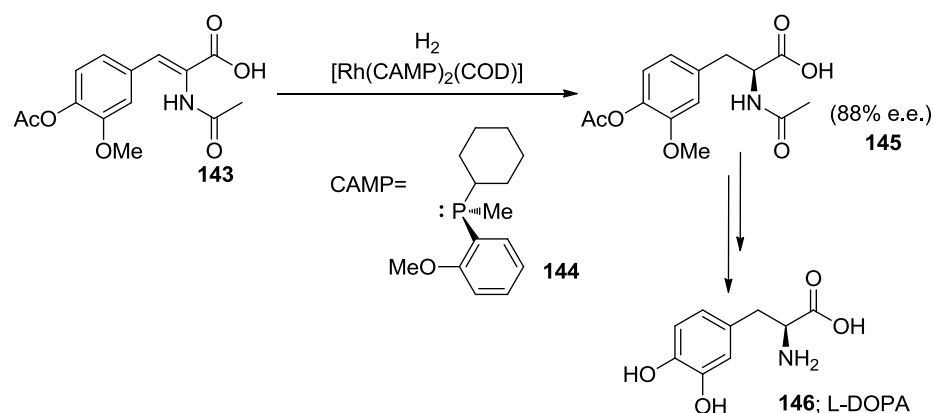
Transition metal-catalysed asymmetric hydrogenation is one of the most widely used and powerful applications of chiral catalysis. The methodology uses clean, inexpensive hydrogen gas and a small amount of chiral catalyst to provide enantioenriched compounds from prochiral substrates, often with high enantioselectivity and with high atom efficiency. Hydrogenation is a scalable process and produces little waste; it can therefore be considered a green process.⁶² Significant advances in recent years have also greatly increased the scope of prochiral substrates that can be efficiently hydrogenated.

Prior to the discovery of chloro*tris*(triphenylphosphino)rhodium [RhCl(PPh)₃] by Wilkinson in 1966,⁶³ catalytic hydrogenation had typically focussed on heterogeneous systems. There are examples of early attempts to employ chiral supports in order to achieve asymmetric induction in heterogeneous catalytic hydrogenations in the literature, but with only a small number of exceptions, enantiomeric excesses were low.⁶⁴

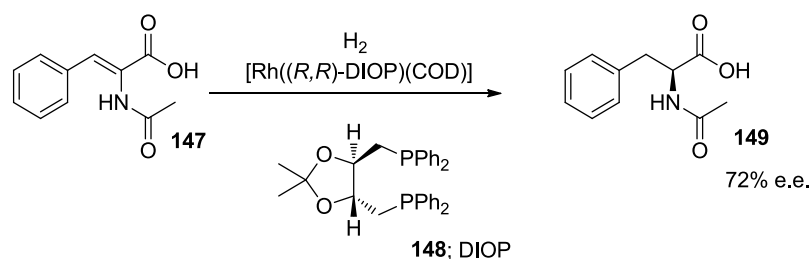
Wilkinson's discovery that [RhCl(PPh)₃], the first soluble transition metal hydrogenation catalyst, showed comparable reaction rates to the well known heterogeneous counterparts of the era, was a landmark event in the field. New opportunities for asymmetric catalysis arose with this discovery. Knowles proposed that replacement of the triphenylphosphine ligand of Wilkinson's catalyst with a chiral counterpart could provide a chiral catalyst which could result in asymmetric induction if used to catalyse the hydrogenation of a pro-chiral olefin.⁶⁵ Knowles initially chose to replace triphenylphosphine with chiral methylpropylphenylphosphine. Hydrogenation of α -phenylacrylic acid (**141**) in the presence of complexes containing this ligand resulted in an enantiomeric excess of 15% (Scheme 32).

Scheme 32 – Knowles' first use of a chiral ligand in the hydrogenation of an olefin⁶⁵

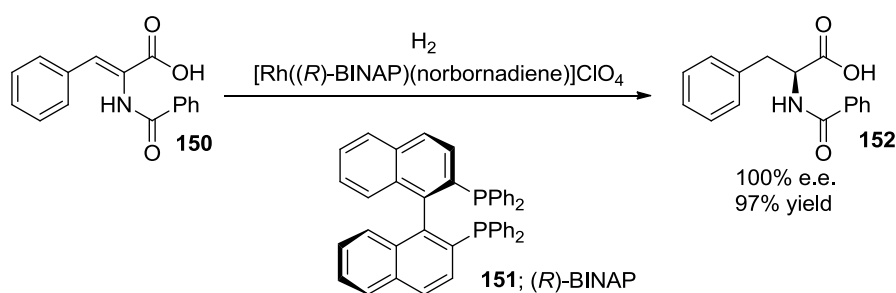
Despite the relatively modest enantioselectivity, this groundbreaking result proved the principle of homogeneous asymmetric catalysis. Knowles went on to optimise the monophosphine ligand series culminating in the use of methylcyclohexyl-*o*-anisylphosphine (CAMP) (**144**) in the commercial synthesis of L-DOPA (**146**), used in the treatment of Parkinson's disease.⁶⁵

Scheme 33 – Monsanto L-DOPA Process⁶⁵

Knowles had proposed that a chiral phosphorus atom was required for efficient asymmetric induction, but this was disproved by Kagan *et al.* in 1971.⁶⁶ Kagan showed that the bisphosphine DIOP (**148**) derived from (+)-ethyl tartrate could be used effectively in the hydrogenation of (*Z*)-*N*-acetylaminoacinnamic acid (**147**) giving an enantiomeric excess of 72% and almost quantitative conversion.

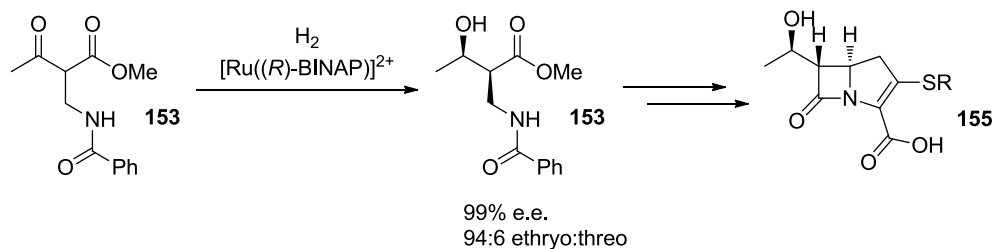
Scheme 34 – Kagan’s use of bidentate DIOP⁶⁶

This discovery paved the way to further research into the use of other bisphosphines as ligands for asymmetric hydrogenation of a variety of substrates. Another landmark discovery came in 1980 when Noyori published work on the asymmetric synthesis of amino acids catalysed by a cationic BINAP-Rh(norbornadiene) complex (Scheme 35).⁶⁷ This catalyst showed unprecedented selectivity which could be attributed to the strong steric influence of the newly discovered ligand.

Scheme 35 – Noyori’s use of BINAP⁶⁸

BINAP (2,2'-bis(diphenylphosphino)-1,1'-binaphthyl) (**151**) is a fully aromatic axially symmetric C_2 -chiral diphosphane that exerts strong steric and electronic influences on transition metal complexes. It is chiral, despite its lack of an sp^3 carbon, due to hindered rotation around the binaphthyl C(1)-C(1') bond. BINAP can accommodate a number of transition metals and it is the highly skewed positions of the two PPh_2 groups which exert the stereochemical influence upon the substrate. BINAP, being a synthetic compound, does not suffer from the common problem with chiral pool materials in that only one isomer is readily available. Both isomers are available *via* resolution of a racemic mixture, meaning one can often ‘dial in’ the required stereochemistry of the product simply by choosing the correct ligand stereoisomer.

After Noyori's initial discovery, he, and others,^{69,70} went on to develop a number of catalytic species based on BINAP. Perhaps the most significant has been its use for the asymmetric hydrogenation of β -ketoesters as a $[\text{RuX}_2(\text{BINAP})]$ complex.⁷¹ This is exemplified in the industrial synthesis of carbapenam antibiotics (**155**) at Takasago International Co. (Scheme 36).⁷²

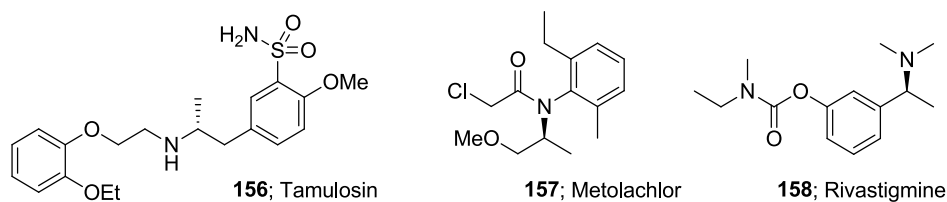


Scheme 36 – Takasago International Co.'s synthesis of carbapenam antibiotics⁷²

Asymmetric hydrogenation has continued to receive much interest in the scientific literature in recent years with development in substrate scope and with ligands and metal centres. The following discussion will focus on the developments in the asymmetric hydrogenation of imines.

2.4.2 Transition Metal Catalysed Asymmetric Hydrogenation of Imines

Chiral amines are an important class of intermediates and products in chemical synthesis. Their use is widespread throughout the pharmaceutical and agrochemical industries⁷³ and they also find synthetic utility as chiral ligands, auxiliaries and catalysts. Examples of important chiral amine containing compounds include tamulosin (**156**), an α_1 antagonist used for the treatment of benign prostatic hyperplasia under the trade name Flomax®,⁷⁴ metolachlor (**157**) a herbicide used for the control of grasses in a variety of crops^{75,76} and rivastigmine (**158**) a parasymphathomimetic agent for the treatment of mild to moderate dementia due to Alzheimer's disease.



A number of methodologies for the synthesis of chiral amines are available, with one of the most attractive being the hydrogenation of prochiral imines. The hydrogenation of imines is often complicated by a number of issues which make high conversions and selectivities more difficult to achieve than with the hydrogenation of either olefins or ketones. Firstly, catalyst poisoning resulting from competitive binding of the product amine to the metal centre is common. Secondly, imines can be sensitive to water, resulting in hydrolysis of the substrates. Thirdly, acyclic imines are often isolated as mixtures of *E/Z*-isomers which may hydrogenate to give mixtures of enantiomers. Despite this, the field of asymmetric imine hydrogenation is broad and many examples of reductions which exhibit high selectivities and conversions can be found. To date, a variety of highly efficient catalyst systems based on iridium, rhodium, titanium, palladium and ruthenium have been reported and the recent literature has been reviewed a number of times.⁷⁷⁻⁸⁰ The following sections will examine each metal in isolation by highlighting a few noteworthy examples.

2.4.2.1 Iridium Based Catalysts

Iridium is by far the most widely described metal for the catalytic asymmetric hydrogenation of imines in the literature.⁸¹ The first example of asymmetric iridium catalysis was described by Osborn *et al.*^{82,83} in 1990; a number of iridium(III)-diphosphine-monohydrido complexes [Ir(L-L)HI₂]₂ were prepared that were effective for the asymmetric reduction of prochiral imines in quantitative conversions and moderate to good enantioselectivities (Figure 5). Osborn's work laid the foundation for further research into iridium catalysis.

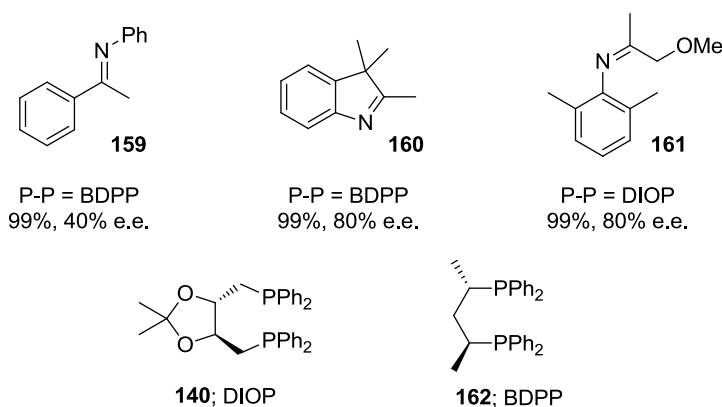
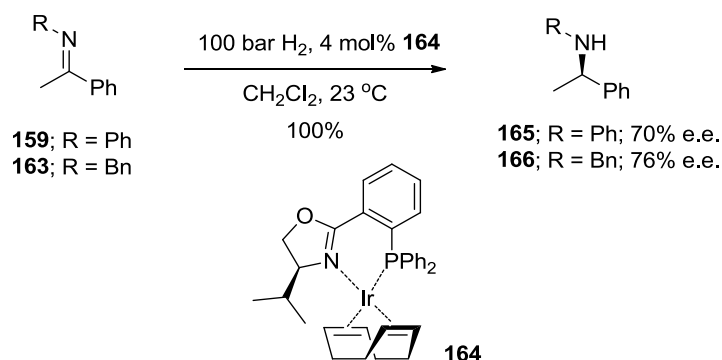


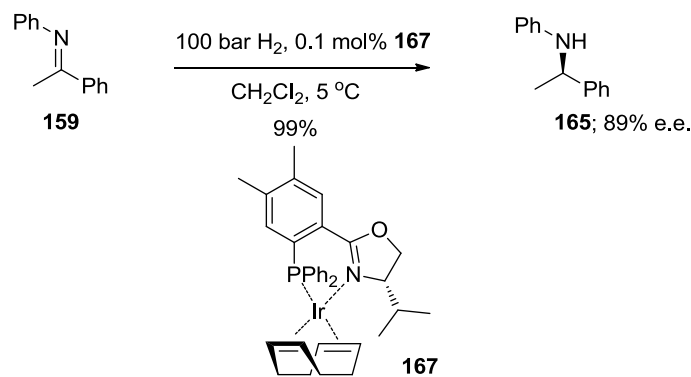
Figure 5 – Iridium(III) catalysed asymmetric hydrogenation of imines.⁸²

The next major milestone in iridium catalysis came in 1997 when Pfaltz,⁸⁴ inspired by Crabtree's work on bidentate phosphorus/nitrogen (PN) ligands,⁸⁵ identified (phosphanodihydrooxazole)-iridium (I) complexes (**164**, **167**) which were effective in the asymmetric hydrogenation of both *N*-alkyl and *N*-aryl imines. Pfaltz's catalysts were air stable crystalline solids that could be readily prepared and were easy to handle. Quantitative conversions, and selectivities of up to 76% *ee* were achieved in the hydrogenation of ketimines (**159**, **163**) (Scheme 37). Despite the hydrogenations typically being performed at 100 bar, Pfaltz observed very similar enantioselectivities and yields when the reactions were run under 1 bar of hydrogen. Interestingly, no correlation was observed between the enantioselectivities in the hydrogenations and the measured *E/Z* ratios of the imines.



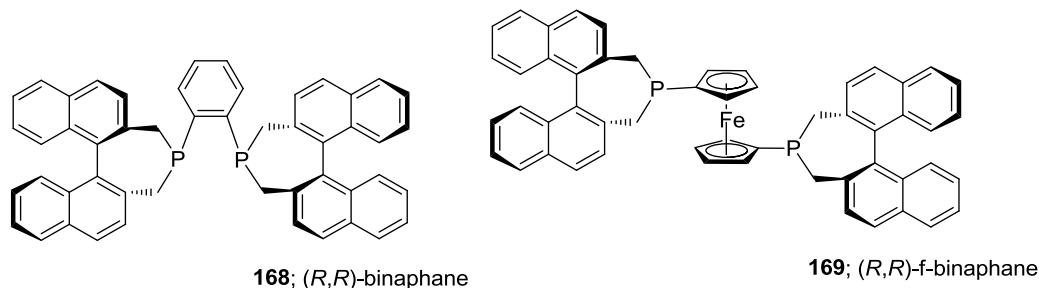
Scheme 37 – Asymmetric hydrogenation of *N*-alkyl and *N*-aryl imines using a (phosphanodihydrooxazole)-iridium(I) complex⁸⁴

Pfaltz also found he could lower the catalyst loading to 0.1 mol% under optimised reaction conditions (increased dilution and a reaction temperature of 5 °C) (Scheme 38) and still achieve excellent conversion and enantioselectivity. This compared favourably to the best results reported up to that time.



Scheme 38 – Pfaltz’s optimised reaction conditions⁸⁴

A noteworthy example of the iridium catalyzed asymmetric hydrogenation of imines is Xiao and Zhang’s use of the chiral ferrocene binaphane ligand f-binaphane (**169**).⁸⁶ Related to binaphane (**168**), f-binaphane contains a highly electron back donating ferrocene backbone, a moiety which has been used extensively in catalyst design for a range of applications.⁸⁷



Zhang and Xiao suggest there are multiple advantages to an f-binaphane containing catalyst system. Ferrocene has a low barrier to rotation which gives flexibility and a larger P-M-P bite angle than binaphane. This can allow large, sterically demanding imines to bind. They also suggest that the highly electron donating nature of the ferrocene enhances Ir-imine complexation by back donation. Zhang and Xiao applied

the catalyst to reduction of a range of *N*-phenyl imines (**159**, **170** - **174**) and observed significantly increased enantioselectivity when $R^2 = 2,6$ -dimethylphenyl compared with $R^2 = \text{Ph}$, which they attribute to the increased steric demand of the substituent. They also observed poor enantioselectivities using imines derived from di-alkyl ketones (Figure 6).

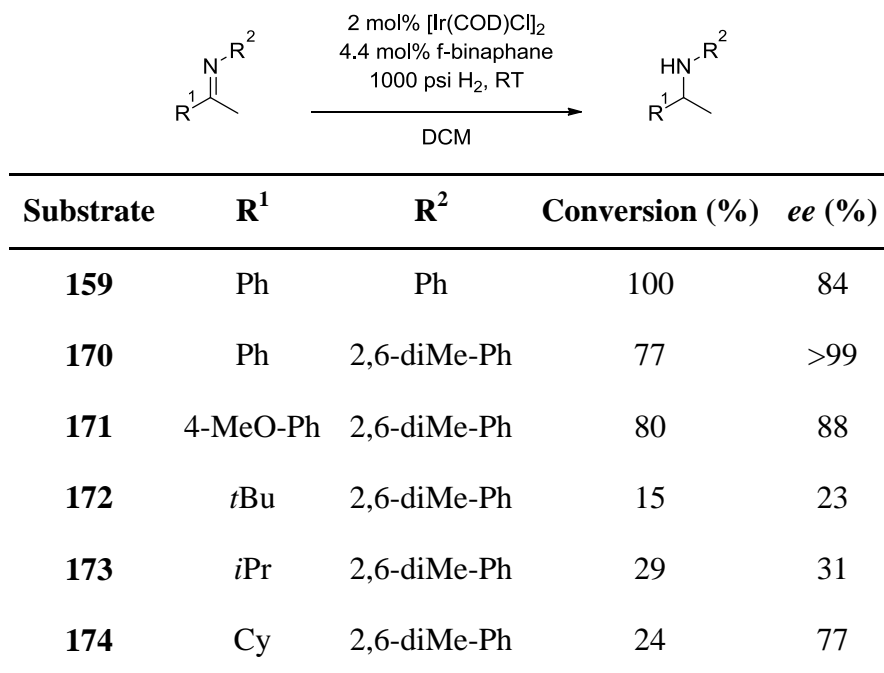
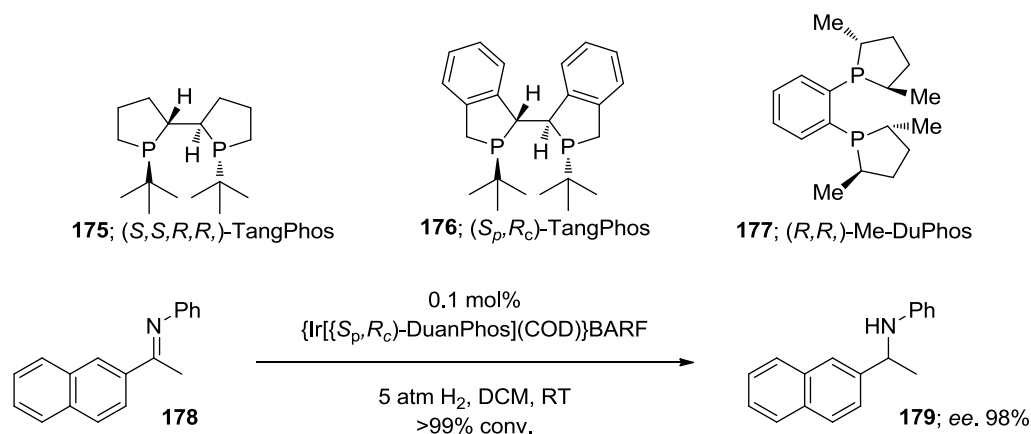


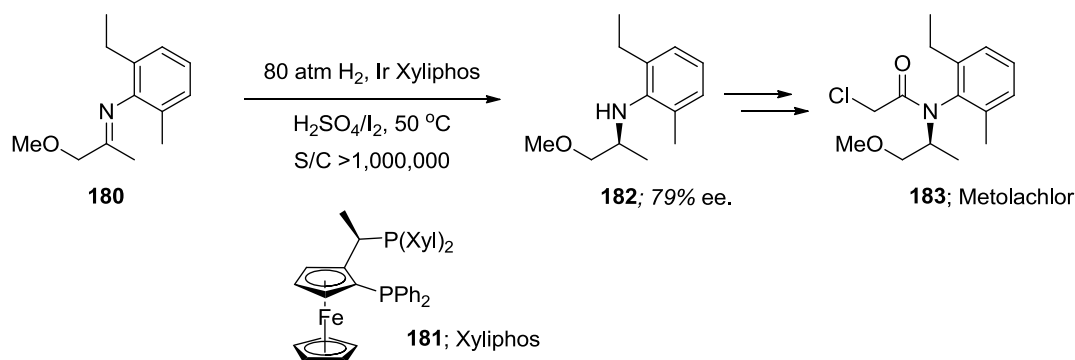
Figure 6 – Use of Ir f-binaphane for the asymmetric hydrogenation of imines⁸⁶

The group of Zhang has continued to be active in the field and has recently developed a series of ligands (TangPhos **175**, DuanPhos **176**, DuPhos **177**); excellent turnover numbers (TONs) were obtained when these ligands were used in the asymmetric hydrogenation of *N*-aryl imines (Scheme 39).⁸⁸ These high TONs allow for very low catalyst loadings, down to 0.01 mol%. It also makes them particularly attractive for industrial applications where the cost of expensive metals and ligands need to be limited.

Scheme 39 – Very high TONs using DuanPhos⁸⁸

The catalytic asymmetric hydrogenation of imines is often plagued by low catalyst TONs which may be attributed binding of the product amine to the metal centre.⁸⁹ Zhang suggests that highly electron-donating and sterically hindered ligands such as these bisphospholanes (**175** - **177**) exert a strong *trans* effect and thus favour release of the amine product from the catalyst.

Probably the most well known example of iridium catalysed hydrogenation, and arguably the most important, is the stereoselective synthesis of the herbicide, metolachlor (**183**). The synthesis uses the electron rich ferrocene containing xylyphos ligand (**181**) which allows for exceptionally high TONs of up to 10⁶. (Scheme 40)⁹⁰

Scheme 40 – Enantioselective synthesis of metolachlor⁹⁰

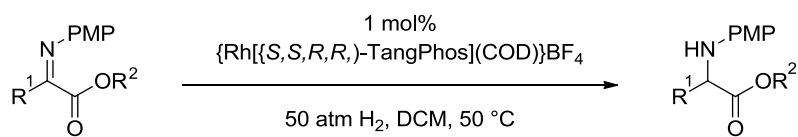
This extremely low catalyst loading is important as the compound is required in quantities of >10,000 tons per year and the cost would quickly become prohibitive if

large quantities were required. In this case, enantioselectivity can be sacrificed for catalyst activity since the (*R*)-enantiomer retains some modest herbicidal activity. The reaction rate is also important for such a high tonnage product as cycle times need to be minimised in order to provide the required volume.

2.4.2.2 Rhodium Based Catalysts

Chiral rhodium catalysts have received less attention than their iridium counterparts over the past two decades, but there are some noteworthy examples to be found in the literature. Particularly using diphosphines and other chiral ligands which have proved successful in iridium catalysis.

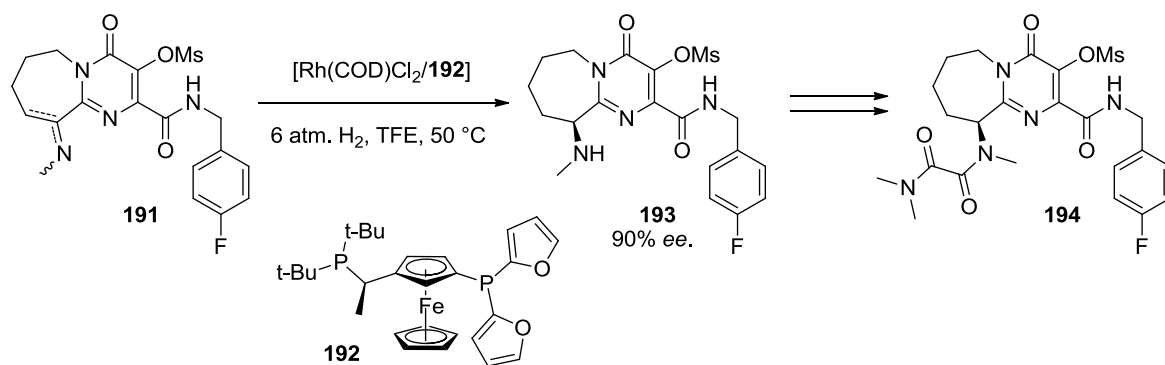
Zhang has shown that a rhodium catalyst based on the TangPhos (**176**) ligand can be used to successfully hydrogenate a series of *N*-aryl α -imino esters (**184** - **189**) with high enantioselectivity (Figure 7).⁹¹ This reaction provides a useful synthetic method for the synthesis of aryl glycine derivatives, since the *para*-methoxyphenyl (PMP) nitrogen substituent can be readily cleaved.



Substrate	R ¹	R ²	Conversion (%)	ee (%)
184	Ph	Me	>99	95
185	3-F-Ph	Me	>95	94
186	3-MeO-Ph	Me	>99	93
187	2-naphthyl	Me	>99	91
188	Ph	Et	>95	84
189	Cyclohexyl	Me	84	94

Figure 7 – Rh TangPhos catalysed asymmetric reduction of α -imino esters⁹¹

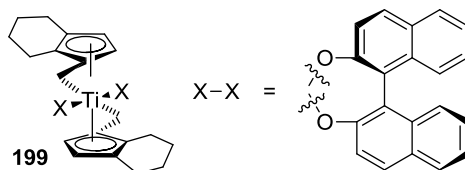
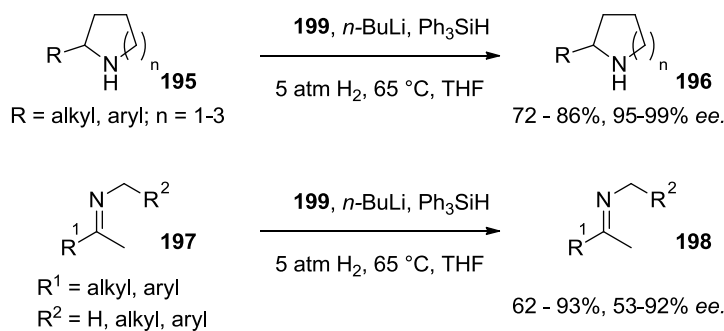
In addition to Zhang's TangPhos ligands, a Rh catalyst based on a Josiphos⁸⁷ type ligand (**192**) has been used to enantioselectively hydrogenate a highly functionalised imine (present as an interconverting mixture of imine and enamine) as part of the synthesis of an HIV integrase inhibitor (**194**) (Scheme 41).⁹² The protocol has been performed on 500 g scale and demonstrates the applicability of such reductions to larger scale synthesis of pharmaceuticals.



Scheme 41 – Enantioselective imine reduction as part of the synthesis of HIV integrase inhibitor **194**.⁹²

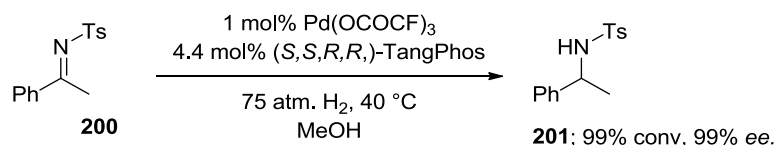
2.4.2.3 Titanium and Palladium Based Catalysts

In 1993 Buchwald discovered a chiral titanocene catalyst^{93,94} derived from Brintzingers's *ansa*-titanocene complex.⁹⁵ The catalyst demonstrated remarkable selectivity in the hydrogenation of *N*-alkyl imines (**195** - **197**) and particularly cyclic imines. Lower selectivity was observed for their acyclic counterparts; this is likely to be due to interconversion between *E* and *Z*-isomers possible with acyclic imines, but not with cyclic imines.⁹⁶



Scheme 42 – Use of Buchwald's titanocene catalyst⁹⁶

Palladium catalysed hydrogenation of imines has been largely restricted to the investigation of activated imines such as the *N*-tosyl derivative (**200**) exemplified below (Scheme 43).⁸⁹ Examples are limited to these substrates as the tosyl group is beneficial in two ways. Firstly, *N*-tosyl imines are relatively stable and can be prepared exclusively as the *E*-isomer.⁹⁷ Secondly, the electron withdrawing nature of the tosyl group reduces the inhibitory effect of the amine product on the catalyst.

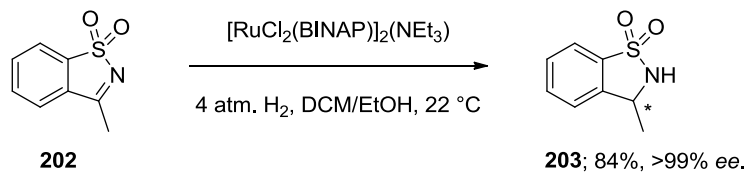


Scheme 43 – Hydrogenation of *N*-tosyl imines catalysed by Palladium⁸⁹

2.4.2.4 Ruthenium Based Catalysts

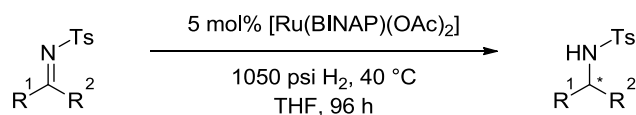
Ruthenium is the second most widely reported metal used in the asymmetric hydrogenation of imines after iridium. Many of the catalysts used are those derived from Noyori's seminal work into the asymmetric hydrogenation of ketones.^{98,99} There are a few examples of the use of Noyori's 1st generation catalysts of the type [RuX₂(BINAP)] in the literature; those which can be found are described below.

In 1990, Oppolzer *et al.*¹⁰⁰ discovered a highly enantioselective reduction of a cyclic *N*-sulfonyl imine (**202**) catalysed by the 1st generation complex [RuCl₂(BINAP)]₂(NEt₃) (Scheme 44). The work was groundbreaking in that catalysts of this type had not been applied to the hydrogenation of imines; either product enantiomer could be readily formed in high *ee* by varying the choice of BINAP antipode.



Scheme 44 – Oppolzer's use of a 1st generation Noyori complex for asymmetric imine reduction¹⁰⁰

Subsequently, Charette⁹⁷ showed that a similar ruthenium-based catalyst could be used to achieve the hydrogenation of acyclic *N*-tosyl imines (**200**, **204** - **209**) in moderate yields and enantioselectivities (Figure 8).

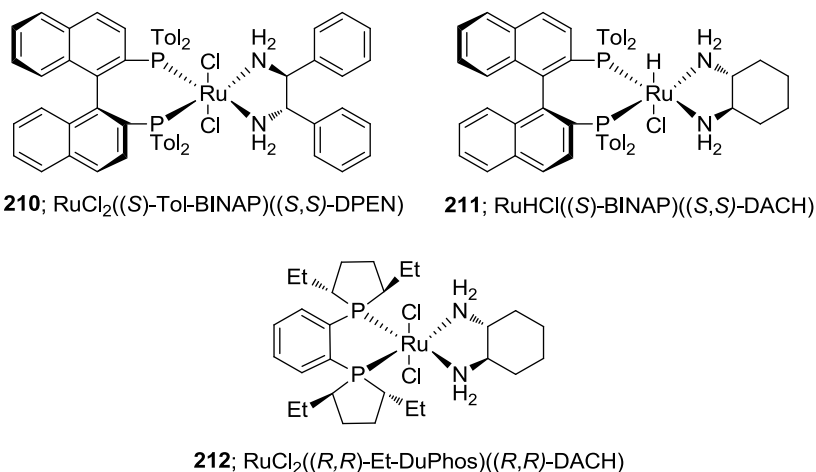


Substrate	R ¹	R ²	Conversion (%)	ee (%)
200	Ph	Me	82	62
204	Ph	Et	80	84
205	Ph	<i>i</i> -propyl	<5	17
206	-naphthyl	Me	80	44
207	-naphthyl	Me	60	18
208	cyclohexyl	Me	52	17
209	<i>i</i> -butyl	Me	48	48

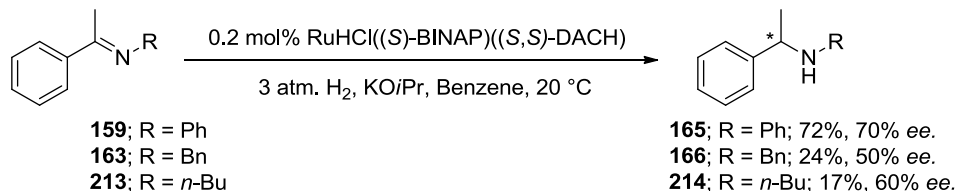
Figure 8 – Charette’s use of [Ru(*R*)-BINAP(OAc)₂] in the hydrogenation of acyclic imines⁹⁷

The majority of ruthenium-catalysed imine hydrogenations found in the literature use Noyori’s 2nd generation catalysts of the type [RuX₂(diphosphine)(diamine)], exemplified by RuCl₂((*S*)-Tol-BINAP)((*S,S*)-DPEN) (**210**).¹⁰¹ These catalysts are highly effective in the hydrogenation of prochiral ketones. The addition of a chiral diamine allowed substrates which lacked a secondary heteroatom capable of anchoring to the Ru metal center to be hydrogenated. This was a limitation of the 1st generation catalysts. The diamine ligand also allowed the selective hydrogenation of carbonyl groups in the presence of olefins.⁹⁹

2. Introduction Part 2; New Routes to GSK221149 and Asymmetric Synthesis

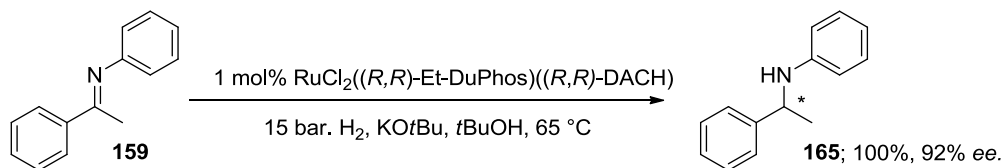


The application of the newly developed catalysts to imine reductions was quickly investigated. In 2001, Morris *et al.*¹⁰² demonstrated the application of the RuHCl((S)-BINAP)((S,S)-DACH) catalyst (**211**) to the reduction of a number of *N*-aryl and *N*-alkyl imines (**159**, **163**, **213**), obtaining the corresponding amines in up to 70% *ee*.



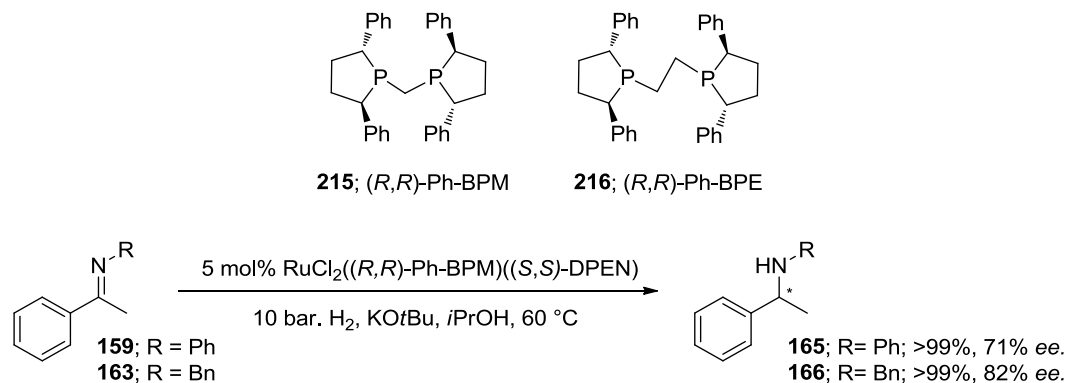
Scheme 45 – Morris' use of RuHCl((S)-BINAP)((S,S)-DACH) (**211**)¹⁰²

Cobley *et al.*¹⁰³ expanded this work by undertaking a thorough investigation into the combination of chiral phosphine, amine and imine substrate, and although they found it difficult to predict the best diphosphine/diamine combination for any particular substrate, they were able to identify conditions which gave complete conversion and 92% *ee* in the hydrogenation of *N*-(1-phenylethylidene)aniline (**159**).



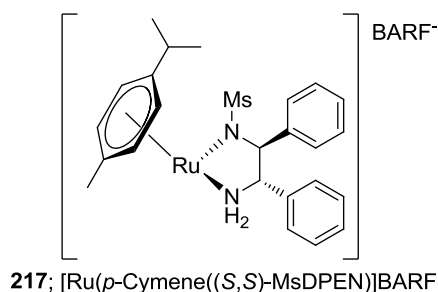
Scheme 46 – Coley's asymmetric hydrogenation of *N*-(1-phenylethylidene)aniline (**159**)¹⁰³

More recent work into these catalytic systems has focussed on the discovery of alternative diphosphine ligands in attempts to increase reactivity and selectivity. Jackson and Lennon¹⁰⁴ described the synthesis of 1,2-bis(2,5-diphenylphospholano) ligands BPE (**216**) and BPM (**215**) and their application to the hydrogenation of a number of model imines (**159**, **163**) with excellent conversion, but moderate enantioselectivity.



Scheme 47 – Asymmetric hydrogenation of imines catalysed by Ru BPM complex

The most recent developments in the field of asymmetric hydrogenation of imines using ruthenium catalysts comes from the group of Fan.⁹⁸ Fan has investigated a number of phosphine free Ru diamine catalysts exemplified by MsDPEN (*N*-(methanesulfonyl)-1,2-diphenylethylenediamine (**217**)).



Fan has used the catalyst to successfully hydrogenate a broad range of often problematic *N*-alkylketimines (**163**, **218** - **225**), achieving selectivities of up to 97% *ee*. (**225**, R = 2-thiophene, Figure 9).

2. Introduction Part 2; New Routes to GSK221149 and Asymmetric Synthesis

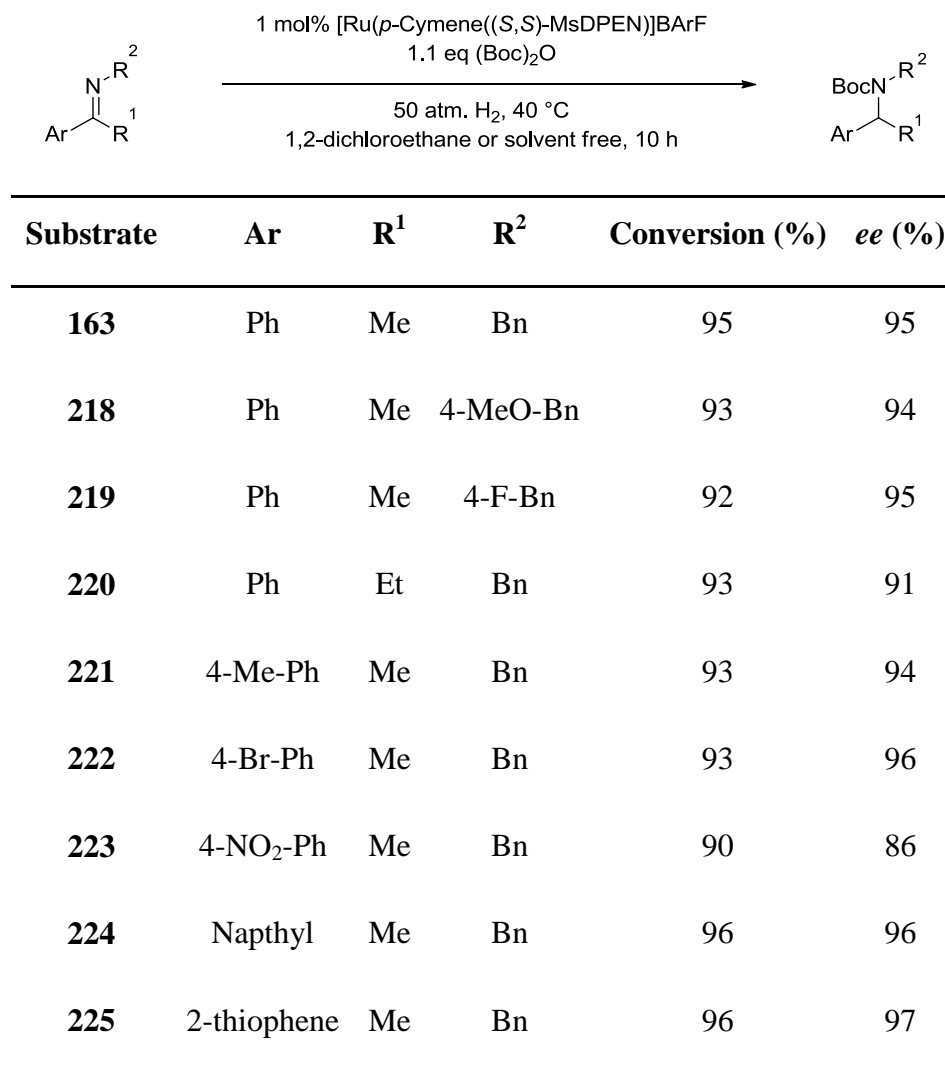
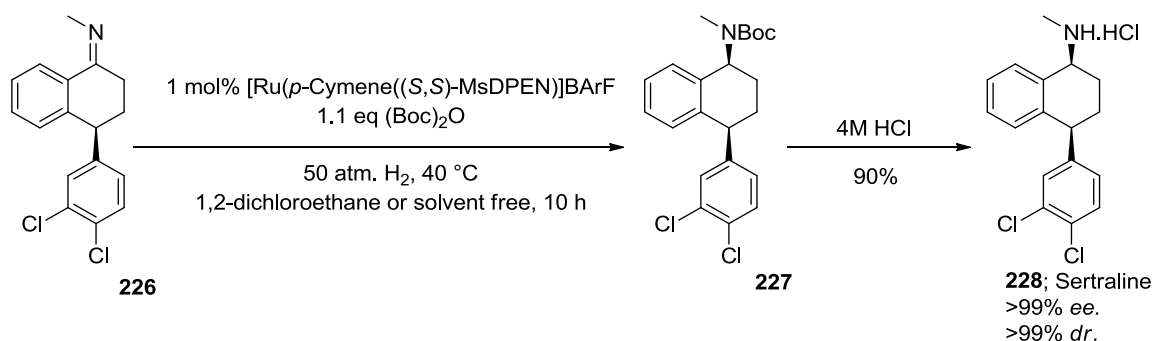


Figure 9 – Fan’s use of phosphine free Ru diamine catalyst⁹⁸

In addition, the effectiveness of the catalyst was demonstrated by lowering the loading to just 0.05 mol% and achieving complete hydrogenation of the *N*-benzylimine of acetophenone (**163**) in 89% *ee*. Fan also demonstrated the synthetic utility of the methodology in the synthesis of the antidepressant sertraline (**228**).

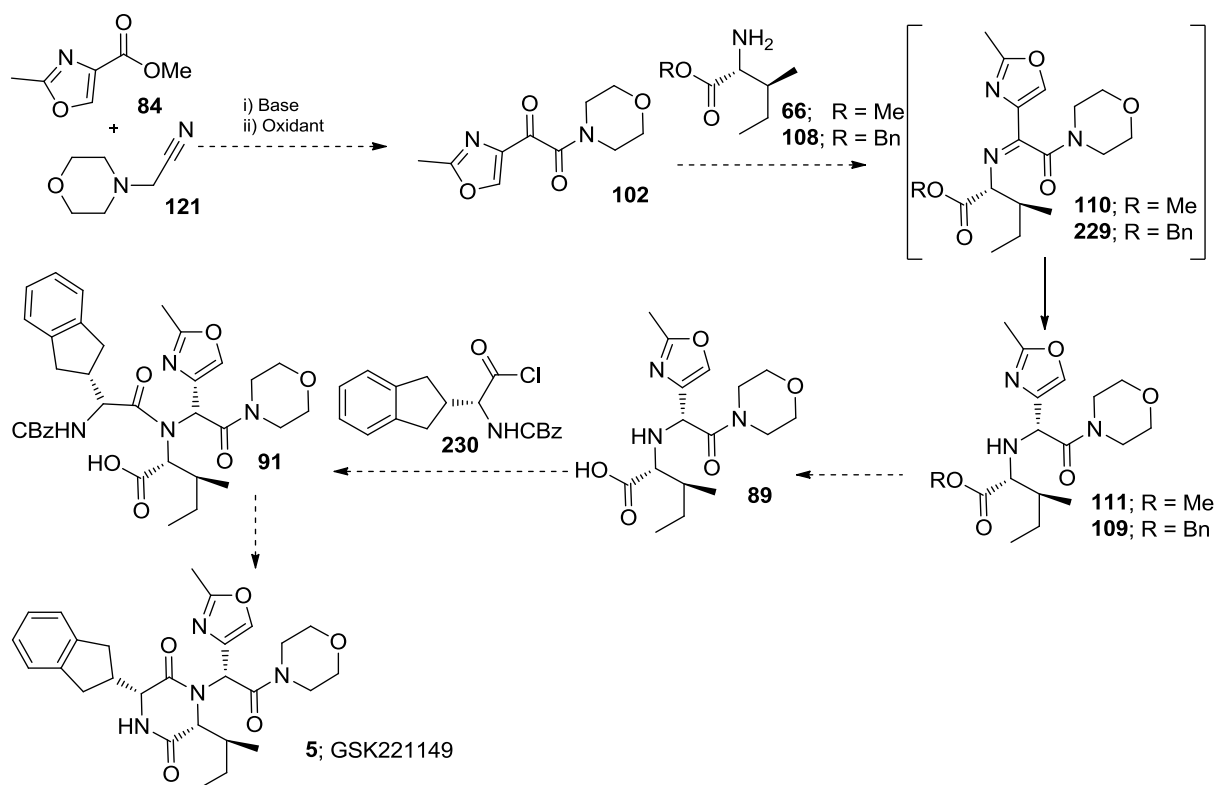


Scheme 48 – Synthesis of sertraline hydrochloride⁹⁸

This review has shown that there are a wide variety of hydrogenation catalysts, based on a number of metals, which can be applied to the asymmetric hydrogenation of imines. However, a number of challenges remain, particularly in the hydrogenation of *N*-alkyl imines and those which can readily interconvert between their *E* and *Z*-isomers. In addition, catalyst systems often suffer from product inhibition due to competitive binding of the product amine. This means that, whilst theoretically possible, development of an asymmetric reductive amination route to GSK221149 could prove challenging.

2.5 Research Objectives

Pre-term labour is the cause of 500,000 infant deaths per year and a lack of effective current treatments means that an efficacious oxytocin antagonist could fill significant unmet medical need. GSK has developed oxytocin agonist GSK221149 (**5**), which is currently awaiting Phase III clinical trials. New synthetic routes to GSK221149 capable of providing material for long term toxicology and ultimately manufacture are required to overcome issues with the current route. Any new route developed will need to provide API within specification and at lower cost than the current Ugi chemistry. The processes developed on a new route should be robust and scalable. Retrosynthetic analysis of GSK221149 was performed, generating a number of potential avenues of research; surveying the literature allowed prioritisation of the strategies. The following synthetic scheme was chosen as the start point for new route investigation. The route provides an opportunity to control absolute configuration *via* asymmetric reduction and will give a number of isolable intermediates which are not accessible *via* the current route.



Scheme 49 - Proposed new route to GSK221149

A number of challenges are envisaged during the forthcoming work. The Claisen condensation and oxidation reaction to generate the ketoamide (**102**) has limited precedent. It is known that the corresponding oxazole aldehyde (**65**) is unstable and such instability may also be evident with the reactive α -amidoketone. Careful considerations of the oxidant and oxidation conditions will also be required to ensure that a sufficiently safe process can be developed to allow use in large scale plant. The most significant challenge is the development of asymmetric imine reduction conditions to provide the desired amino acid (**89**). There is little precedent for this transformation on such highly functionalised and sterically hindered substrates, yet asymmetric reduction will be crucial in generating material in a sufficiently high yield for the route to compete with the existing Ugi chemistry. More generally, API produced *via* any new route developed will have to meet a stringent purity specification. Meeting this specification may be particularly difficult as impurities tend to be specific to individual synthetic routes.

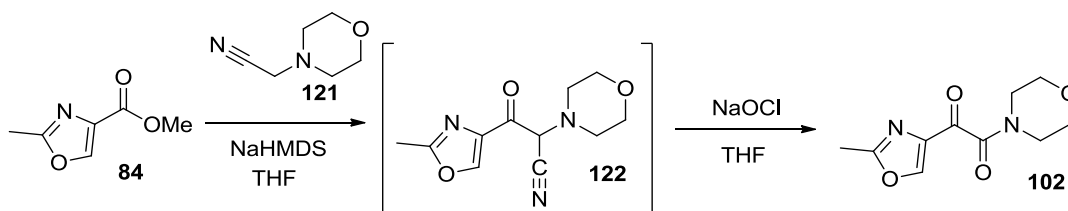
2. Introduction Part 2; New Routes to GSK221149 and Asymmetric Synthesis

Tolerance of impurities commonly observed in API produced by the existing chemistry will be higher since toxicological studies have been performed with this material. Impurities which have not previously been observed will have to be controlled to very low levels due to a lack of toxicological information. Finally, the Ugi chemistry has been well developed over a number of years and, despite the issues associated with this chemistry, it may be difficult for a new route to compete in terms of cost of goods, purity and manufacturability.

3 Results and Discussion Part 1; A New Route to GSK221149

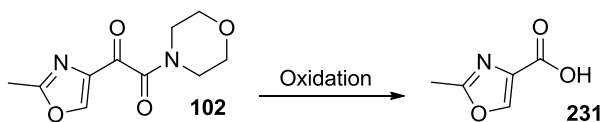
3 Results and Discussion Part 1; A New Route to GSK221149

3.1 Ketoamide Synthesis



Scheme 50 – Synthesis of ketoamide **102**

The first stage in the proposed new route towards GSK221149 is the synthesis of the ketoamide (**102**). Literature precedent in the form of one-pot Claisen condensation and oxidative nitrile cleavage as described by Wang⁵¹ was chosen as the start point for investigations. Wang's conditions were initially applied to the oxazole/morpholine system (Scheme 50); addition of NaHMDS resulted in formation of the intermediate nitrile (**122**) as observed by LCMS. However, on addition of sodium hypochlorite solution, complete conversion to the corresponding carboxylic acid (**231**), rather than the desired ketoamide (**102**) was observed (Scheme 51). The ketoamide (**102**) was only observed transiently by LCMS during the oxidation. It is postulated that further reaction of the ketoamide is the cause of this undesired product, which prompted us to ponder the nature of the mechanism of both the desired oxidation reaction, and that of the over-oxidation pathway.

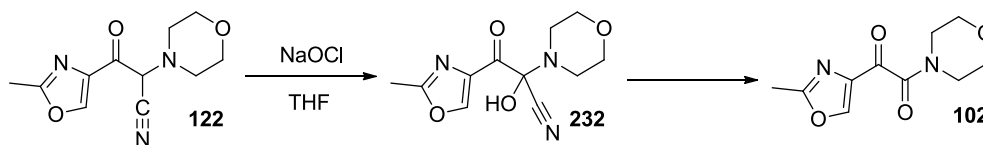


Scheme 51 – Over oxidation of ketoamide **102**

3.1.1 Mechanism of Ketonitrile Oxidation

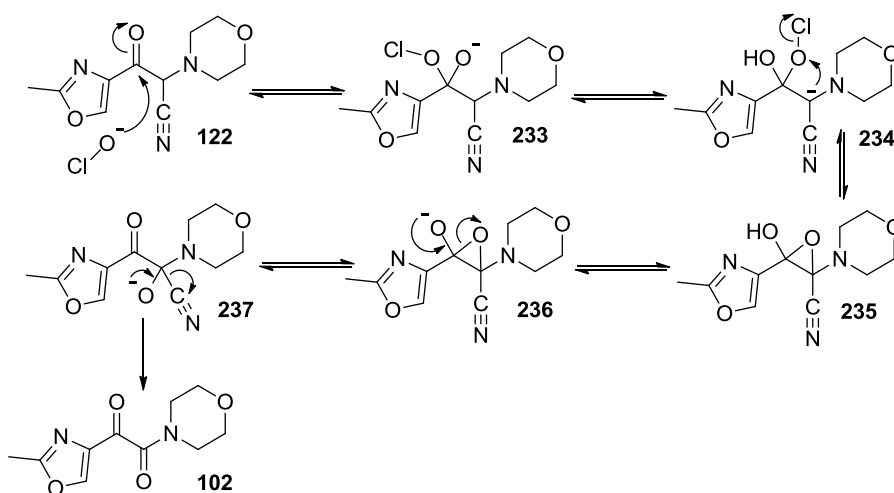
The mechanism of 1,2-dione formation from the ketonitrile intermediate (**122**) is unknown, with Wang suggesting only that the reaction may proceed *via* a cyanohydrin.

Two quite different pathways for the formation of cyanohydrins from the intermediate can be envisaged.



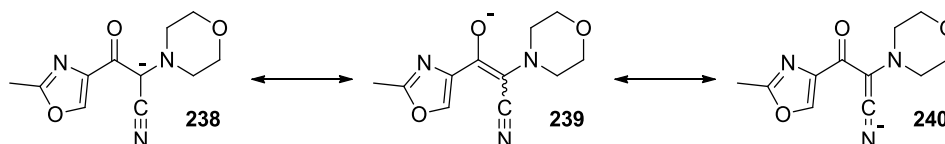
Scheme 52 – Oxidation of ketonitrile 122 via cyanohydrin formation

The first involves nucleophilic attack at the ketone carbonyl by a hypochlorite anion. Proton transfer *via* solvent then enables epoxide formation which can undergo scission resulting in oxygen transfer and cyanohydrin formation. Loss of cyanide generates the ketoamide (**102**) (Scheme 53).



Scheme 53 – Nucleophilic oxidation mechanism

The main issues arising from this mechanism are the ionization state of the ketonitrile (**122**) and the status of the epoxide (**235**). The reaction is carried out under basic conditions, so it may be that the ketonitrile is present as its enolate (**239**) (Scheme 54).



Scheme 54 – Resonance forms of the conjugate base of ketonitrile 122

The pK_a of the ketonitrile (**122**) is unknown, but related related 3-oxo-3-phenylpropanenitrile (**241**) has a measured pK_a of 10.2 in DMSO. The presence of π -donor dialkylamino group may raise the pK_a , but it would appear that the ketonitrile (**122**) would remain quite acidic (Figure 10).¹⁰⁵

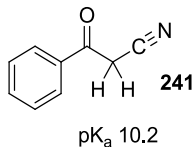
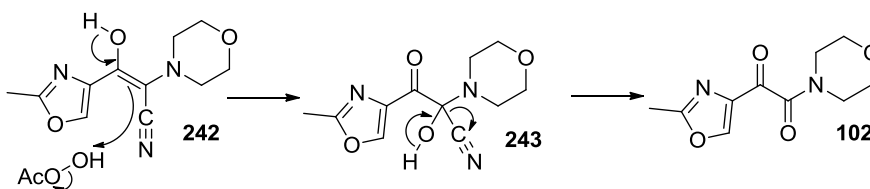


Figure 10 – pK_a of 3-oxo-3-propanenitrile **241**

Aqueous pK_a s are often ~ 3 units lower than those in DMSO (eg. HCN, $(pK_a)_{DMSO} = 12.9$, $(pK_a)_{H_2O} = 9.4$)¹⁰⁶ and so the ketonitrile (**122**) should be significantly ionized under our conditions. The presence of a significant amount of enolate will disfavour the nucleophilic addition of hypochlorite anion. An alternative mechanism which uses the enolate is shown below (Scheme 55). The oxidation of enolates by hypochlorite and related species is a known process. For example, the haloform reaction^{107,108} uses hypochlorite, hypobromite or iodine to oxidize and cleave methyl ketones to carboxylic acids, while the Rubottom reaction^{109,110} oxidises silyl enol ethers to α -hydroxy ketones using *m*-CPBA, and the oxidation of enolates with TMS peroxide is also well established.¹¹¹

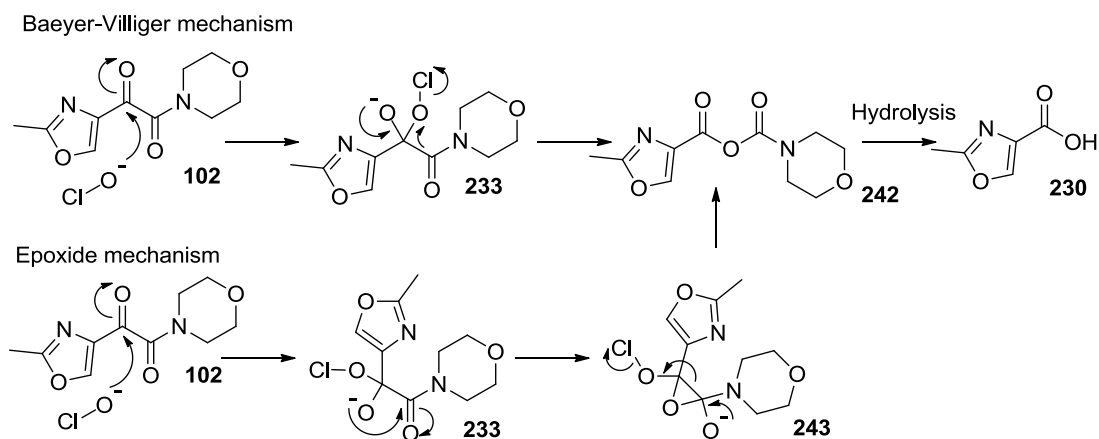


Scheme 55 – Electrophilic oxidation mechanism

3.1.2 Mechanism of Oxidative Cleavage of 1,2-diones

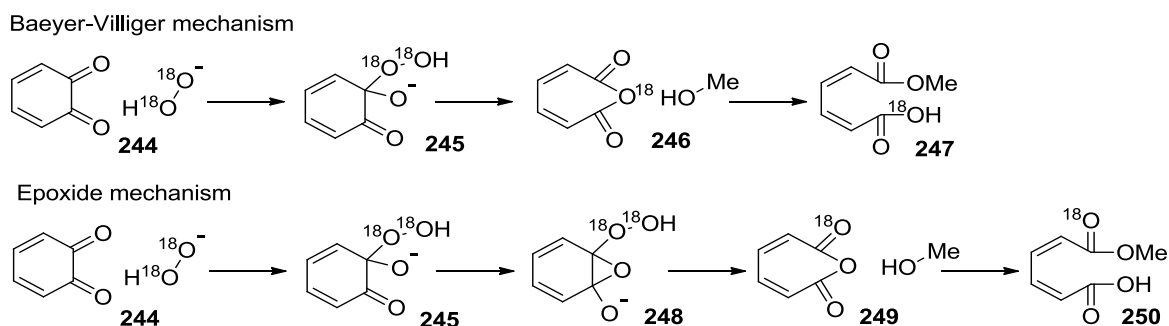
A number of mechanisms have been proposed for the oxidative cleavage of 1,2-diones.¹¹²⁻¹¹⁴ Of these, the two most common are Baeyer-Villiger type reaction involving migration of the amide carbonyl, and epoxide formation and opening. Both these over-

oxidation mechanisms proceed *via* initial attack of a nucleophilic oxidant followed by anhydride formation (Scheme 56).



Scheme 56 – Over-oxidation mechanisms

Though the amide migration looks questionable as the key step in the Baeyer-Villiger type mechanism, Foote *et al.*¹¹⁵ used ¹⁸O labeling techniques to show this was the predominant pathway in the related oxidative cleavage of 1,2-benzoquinone (**244**). The absence of labelled oxygen in any of the methyl ester (**250**) formed on quench proving that the epoxide mechanism was not the predominant pathway.



Scheme 57 – ¹⁸O labeling in the oxidative cleavage of 1,2-benzoquinone

3.1.3 Application of Mechanistic Understanding to the Oxidation

Working on the hypothesis that the desired nitrile cleavage oxidation could occur by either a nucleophilic or electrophilic oxidation mechanism, but that the over-oxidation can only proceed *via* nucleophilic attack, it was proposed that reducing the

3. Results and Discussion Part 1; A New Route to GSK221149

nucleophilicity of the oxidant may reduce the propensity for over-oxidation of the system. In order to test this, a quantity of the intermediate ketonitrile (**122**, p 62) was isolated by column chromatography and was used to screen a range of oxidants. The oxidants chosen were based on a number of the more readily available reagents used by the group of Wang in later papers.^{116,117} Oxidations were performed in THF with or without NaHMDS (to simulate a one-pot reaction) and with sodium hydroxide in water.

Entry	Base	Equivs	Solvent	Oxidant	Equivs	102 (% a/a)
1	NaHMDS	1.2	THF	Bleach (15% wt soln)	2	27
2	NaHMDS	1.2	THF	<i>m</i> -CPBA	2	60
3	NaHMDS	1.2	THF	TMS Peroxide	2	0
4	NaHMDS	1.2	THF	Peracetic Acid (32% w/w in AcOH)	2	65
5	None		THF	Bleach (15% wt soln)	2	68
6	None		THF	<i>m</i> -CPBA	2	6
7	None		THF	TMS Peroxide	2	0
8	None		THF	Peracetic Acid (32% w/w in AcOH)	2	18
9	NaOH(aq)	1.2	Water	Bleach (15% wt soln)	2	67

Table 2 – Effect of varying oxidant and conditions

The results appear to indicate that the reaction is disfavoured by the presence of enolate and electrophilic oxidants, and that nucleophilic attack on the ketone is taking place. The reactions showing significant product formed from NaHMDS-derived enolate are those which have been acidified by peracid oxidants (entries 2 & 4) and the concentration of enolate in these reactions may be assumed to be low. In addition, the electrophilic TMS peroxide generated no product. The differences between entries 6 vs 2 and 8 vs 4 may be explained by the presence of the more nucleophilic carboxylate in entries 2 and 4, further supporting a nucleophilic mechanism. It is possible that bleach is a successful

3. Results and Discussion Part 1; A New Route to GSK221149

oxidant in aqueous NaOH and water, as at those pHs, the concentration of enolate is low, whereas in entry one, where the ketonitrile (**122**) is expected to exist primarily as the enolate, low conversion to the ketoamide (**102**) was observed. This would suggest that the pK_a of the ketonitrile is somewhere between the pK_a of hydroxide and NaHMDS.

Further work on this reaction¹¹⁸ suggests that the peak area of product in the reaction is primarily dependent on the pH of the oxidation reaction, due to differing stabilities of starting material and product. The ketonitrile (**122**) is unstable at $pH < 5$ and ketoamide **3** is unstable at $pH > 9$, therefore a narrow window exists where reaction can take place. The most simple explanation of the above results is that, regardless of mechanism, reactions are successful in the correct pH range. Peracid oxidations may lower the pH of the NaHMDS entries into a range where reaction can take place and sodium hypochlorite is basic enough to raise the pH into a range where reaction can take place. This hypothesis however, cannot explain the success of reaction 9.

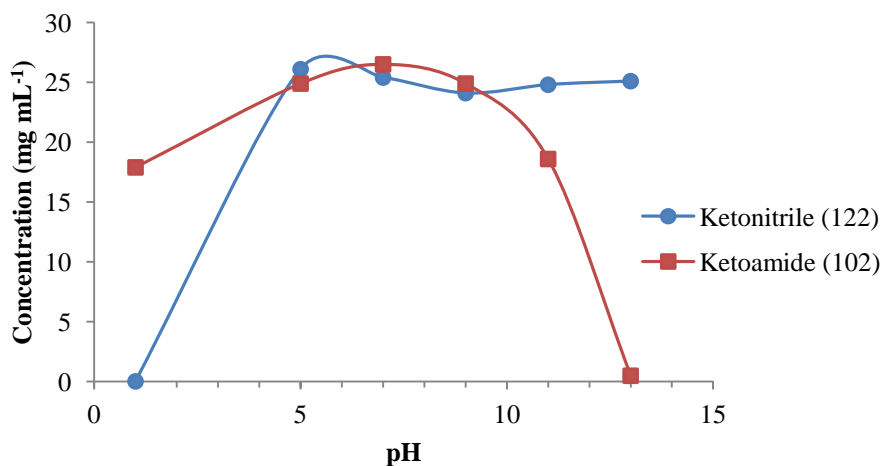


Figure 11 – Stability of ketonitrile **122** and ketoamide **102** vs pH¹¹⁸

Due to the difficulty in isolating the highly water soluble intermediate nitrile, it was decided to further investigate a one-pot procedure using a peracid as oxidant. Peracetic acid was chosen for further investigation as it offered practical advantages over *m*-CPBA; liquids are easier to dispense affording more accurate control of stoichiometry, and acetic acid is much easier to remove than benzoic acid.

3. Results and Discussion Part 1; A New Route to GSK221149

The first attempt at isolation of the ketoamide (**102**) resulted in a yield of 20% after column chromatography. This result was somewhat disappointing given that the major component visible by HPLC was the desired product at over 60% a/a. More thorough reaction investigation using standardised sampling clearly showed loss of product peak area over time. More startlingly, loss of product was observed once the samples had been quenched into dilute sodium sulfite solution, the standard sample preparation prior to HPLC (Figure 12).

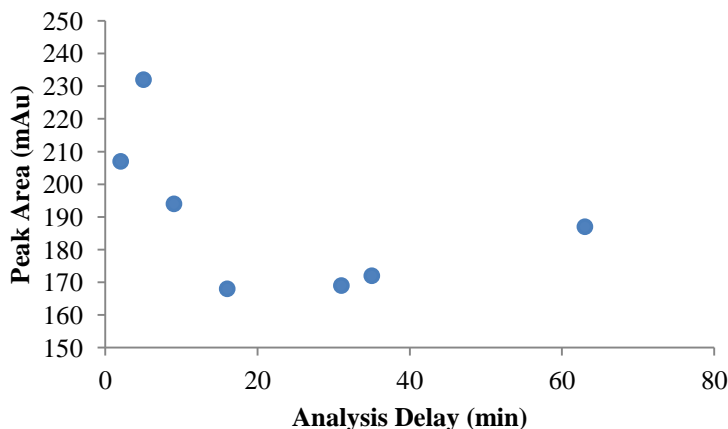


Figure 12 – Peak area vs analysis delay

Sodium thiosulfate solution proved to be a more suitable alternative quench; the product was more stable under these conditions.

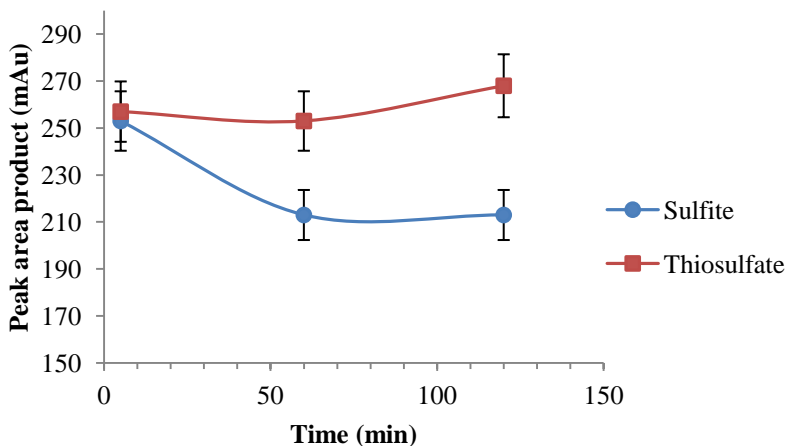
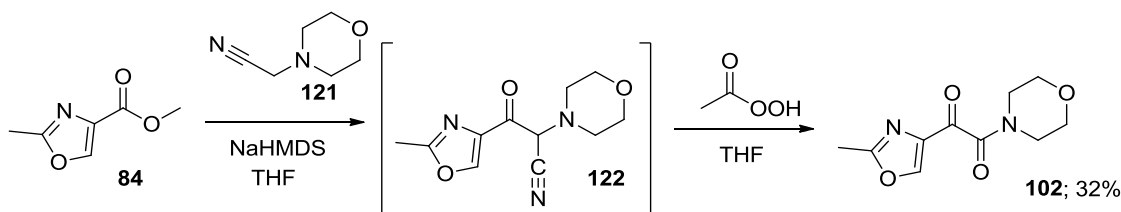


Figure 13 – Sample stability

3. Results and Discussion Part 1; A New Route to GSK221149

Brief optimisation of the reaction conditions, in which the temperature was lowered to 0 °C, and the amount of peracetic acid was raised to 2.15 equiv., gave a reduction in the levels of a number of impurities. The primary impurity was still the oxazole acid (**231**), but this was readily removed by a basic aqueous work-up.

Before scale up, two important safety points were taken into consideration. Firstly, all of the excess oxidant would need to be effectively quenched prior to evaporation. Sodium thiosulfate is a common mild reducing agent and it was anticipated that there would be no issue with destruction of the excess peracetic acid. Indeed, this was quickly proved by testing the quenched reaction mixture with Merckoquant semi-quantitative peroxide test. Secondly, due to the potential for cyanide generation during the oxidative cleavage, the absence of cyanide needed to be confirmed. It is believed that cyanide liberated during the oxidative cleavage reaction is quickly oxidized. This is supported by the requirement of 2 equiv. of peracetic acid to ensure complete reaction. The cyanide oxidation closely mirrors that described by Payne.¹¹⁹ However, application of the Merckoquant semi-quantitative cyanide test yielded a positive result on the quenched reaction mixture. Washing the organic phase with a saturated aqueous sodium bicarbonate solution did not show reduction in the cyanide levels detected which suggested that free cyanide was not present. It is hypothesised that cyanide reacts with the ketoamide (**102**) to form a cyanohydrin which can slowly release cyanide under the test conditions and thereby give a positive result. This is an issue which has not previously been reported, and investigations to understand and overcome it are ongoing.¹¹⁸ Despite this positive cyanide result, it was decided to scale up the reaction, but to include added safety precautions. The reaction was scaled up successfully to provide 7.7 g product (**102**) in 32% from the oxazole ester (**84**). (Scheme 58)



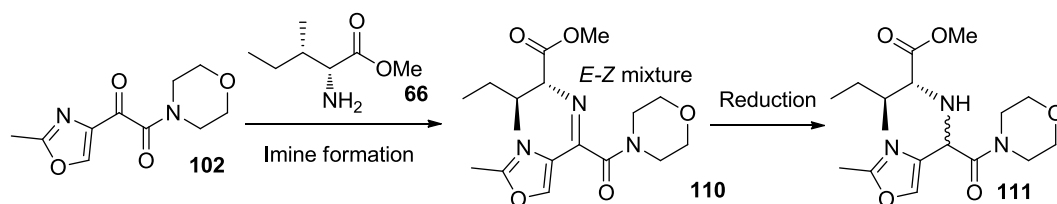
Scheme 58 – Synthesis of ketoamide **102**

3. Results and Discussion Part 1; A New Route to GSK221149

The reaction optimisation described in this section has allowed a process to be developed which is suitable for the preparation of small quantities of material in order to investigate the subsequent transformations of the proposed new route. However, a number of limitations remain which would need to be addressed in order for this chemistry to form part of a long term manufacturing route. Firstly, the use of column chromatography would need to be avoided since this operation is particularly time consuming and inefficient on a large scale. Secondly, the safety of the highly exothermic, cyanide liberating oxidation reaction would need to be studied in detail to ensure it could be performed safely in pilot plant and manufacturing equipment. Thirdly, the yield would need to be improved in order for the process to be economically viable.

3.2 Imine Formation

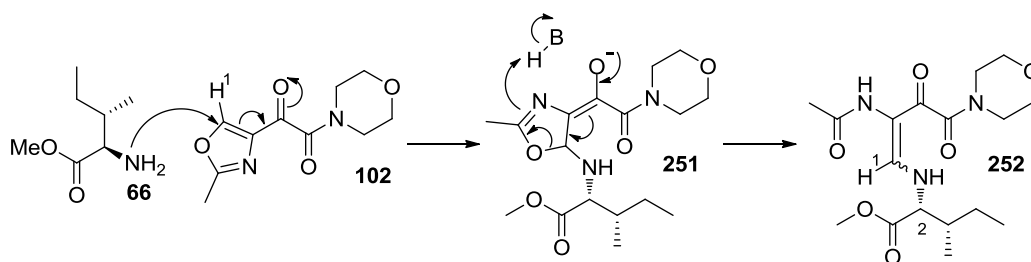
The exploration of the reductive amination as shown (Scheme 59) began with an investigation of the imine-forming step. Due to the instability of imines under aqueous acidic conditions and the consequent difficulty in monitoring reactions by standard TFA modified HPLC methods, it was decided to monitor imine formation by quenching small portions of the reaction mixture into an excess of sodium borohydride in methanol. Based on the assumption that the imine (**110**) would readily reduce under these conditions, its presence could be inferred by observation of the corresponding amine (**111**). The presence of the unreacted ketone (**102**) could be inferred by observation of the corresponding alcohol and it was confirmed that reduction of the ketone occurred readily on the timescale of the reaction, before the work was started.



Scheme 59 – Reductive amination

3.2.1 1,4-Addition to the Oxazole

Initial attempts to form the imine (**110**) were made using molecular sieves to aid dehydration and drive the equilibrium to product. These initial attempts failed, due to the rapid formation of a ring opened species (**252**) (Scheme 60). Confirmation of the product structure was obtained using ^1H and HMBC NMR analysis which showed an upfield shift of proton 1 from 8.37 ppm to 6.97 ppm, indicative of a loss of aromaticity and also showed $^3J_{\text{C-H}}$ connectivity between proton 1 and carbon 2. HRMS provided evidence of molecular formula. A postulated mechanism for the formation of the ring opened acetamide (**252**) via 1,4-addition and ring opening is given. (Scheme 60)



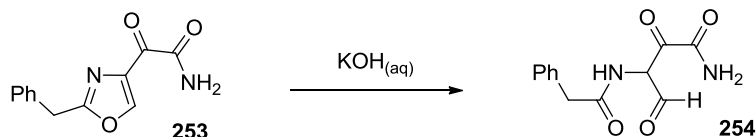
Scheme 60 – Mechanism for the formation of 252

In a mixture of MeOH/THF under basic conditions, the acetamide (**252**) was formed to 75% a/a after 18 hours. However, the reaction was much slower in THF alone. In the absence of added base, the ketoamide (**102**) did not react with methyl D-*allo*-isoleucinate (**66**).

Solvent	Base	% a/a 252 after 18h
MeOH/THF	1.5 equiv NEt ₃	75%
THF	1.5 equiv NEt ₃	10%
MeOH	None	0%
THF	None	0%

Table 3 – Formation of acetamide 252

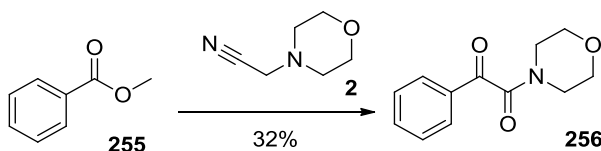
The observation of this unexpected product, particularly given the ease with which it formed, was significant. On further investigation in the literature, the work of Cornforth *et al.*¹²⁰ provides a precedent for the reaction in the hydrolysis of an oxazole (**253**) with aqueous potassium hydroxide (Scheme 61). This, coupled with the empirical data, meant alternative reaction conditions were required for the formation of the imine (**110**).

Scheme 61 – Hydrolysis of oxazole 253¹²⁰

3.2.2 Investigation into Model Systems

It was decided to use a model system in order to investigate imine formation without the complication of 1,4-addition to the oxazole. This would allow an understanding of the factors important in imine formation, and the knowledge gained could then be applied to the real system. It was decided to use a phenyl derivative (**256**) as the model system as methyl benzoate (**255**) was readily available and the phenyl substituent was not expected to undergo 1,4-addition.

The optimised conditions developed for formation of the oxazole derivative (**102**) were used to synthesise the phenyl ketoamide (**256**) (Scheme 62).



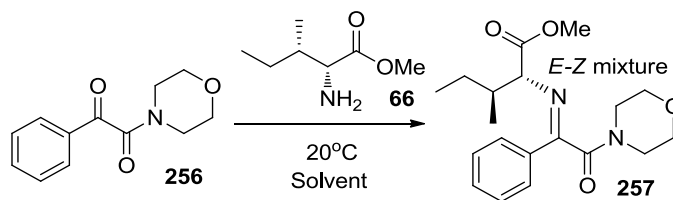
i) NaHMDS, THF; ii) AcOOH, THF, 0 °C.

Scheme 62 – Synthesis of phenyl ketoamide 256

The Claisen condensation reaction proceeded quantitatively without the darkening of the reaction mixture that occurred with the oxazole methyl ester (**84**). Moreover, the reaction profile was cleaner, demonstrating the increased propensity of the oxazole system to undergo side reactions. Oxidative cleavage of the nitrile again proceeded smoothly with the primary impurity being benzoic acid, formed presumably *via* an over-oxidation pathway analogous to the formation of the oxazole acid (**231**) (Scheme 56). The yield of this reaction was not representative of the ease with which the transformation was carried out compared with the oxazole substrate. This was due to the difficulty of separating the benzoic acid by-product from the phenyl ketoamide (**256**) by column chromatography. Presumably, including a simple basic wash would improve the yield significantly, a procedure which could be included in further preparations.

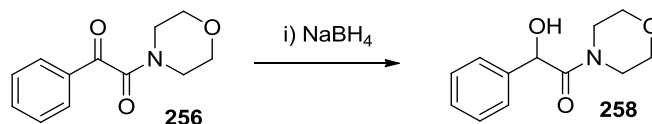
3.2.2.1 Imine Formation with Phenyl Ketoamide 256

Reaction was attempted using the model phenylketoamide (**256**) and methyl *D*-allo-isoleucinate (**66**) as shown (Scheme 63).



Scheme 63 - Imine formation with phenyl ketoamide 256

Imine formation was attempted under a range of conditions (Table 4), but the imine (**257**) could not be detected in any of the reactions. Quenching the reactions with NaBH₄ led to the formation of a hydroxyamide (**258**) in each case.

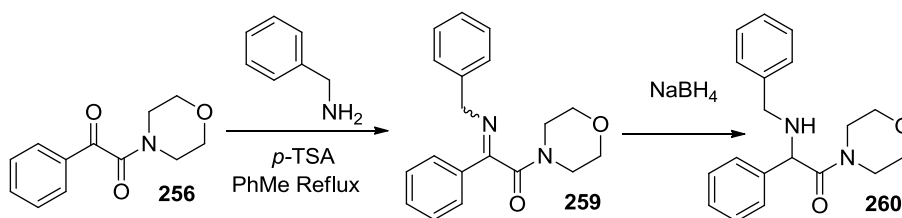


Scheme 64 – Reduction of ketoamide to give hydroxyamide 258

Solvent	Additive	4Å Molecular Sieves	% Conversion to 257
Toluene	10 mol% <i>p</i> -TSA	Yes	0
Toluene	None	Yes	0
Dichloromethane	MgSO ₄	No	0
THF	None	Yes	0

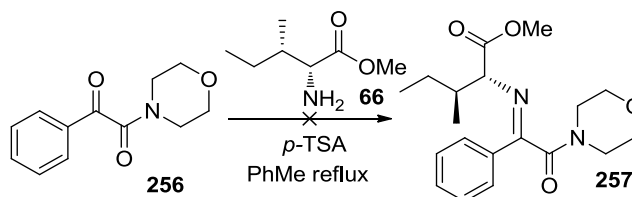
Table 4 – Imine formation with phenyl ketoamide 256

The model was further simplified by using benzylamine instead of the sterically encumbered methyl *isoleucinate* (Scheme 65). The primary goal was to confirm that the reaction monitoring system of quenching into sodium borohydride was valid.

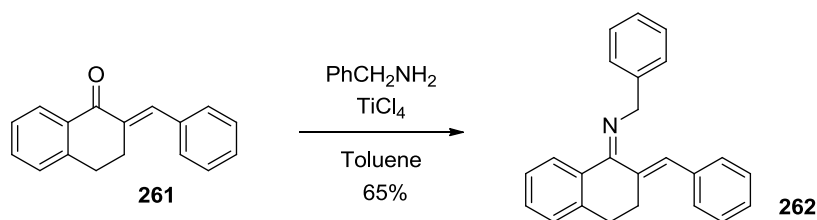
Scheme 65 – Reductive amination with phenyl ketoamide **256** and benzylamine

Mild conditions were explored in the first instance; carrying out the reaction in dichloromethane in the presence of MgSO₄ as both Lewis acid and dehydrating agent failed to deliver the imine (**259**). Under more forcing conditions (refluxing toluene with 10 mol% *p*-TSA) the imine was formed, and reduced successfully to give the amine (**260**) upon quench with sodium borohydride. Brief assessment of the reduction conditions showed that the ketone (**256**) and the benzyl imine (**260**) were reduced rapidly to the corresponding alcohol and amine.

Unfortunately, reaction was not observed when these conditions were applied to the phenylketoamide (**256**) with methyl *D*-*allo*-isoleucinate (**66**), presumably due to the increased steric hindrance of the methyl *D*-*allo*-isoleucinate and lower nucleophilicity because of the electron-withdrawing alkoxy carbonyl group.

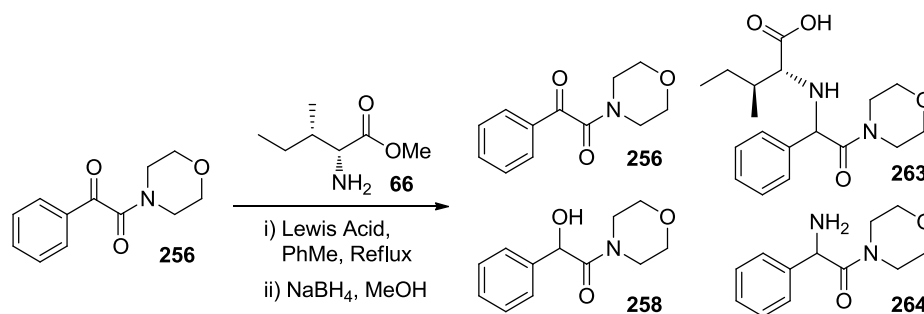
Scheme 66 – Imine formation with phenyl ketoamide **256**

Work by the groups of Barney and Gamble suggested that imines were difficult to form from hindered amines and ketones^{121,122} and that the addition of a strong Lewis acid and dehydrating agent may be essential to achieve the desired transformation.^{123,124} The work of Brunel *et al.*^{125,126} also showed that minimal 1,4-addition was observed when forming imines from α,β -unsaturated ketones such as 1-(furan-2-yl)ethanone and 4-phenylbut-3-en-2-one with Ti(IV) reagents. The work of Henin *et al.*¹²⁷ also showed the absence of conjugate addition when forming imines using α,β -unsaturated ketones (**261**) with TiCl₄ (Scheme 67).



Scheme 67 – Using TiCl₄ to form imines using α,β unsaturated ketones¹²⁷

A screen of readily available Lewis acids of differing strengths was performed in attempt to begin to map the required reactivity. Reaction in refluxing toluene, followed by quenching with NaBH₄ in MeOH, gave multiple products in all reactions, tentatively assigned (from the ion masses) as the structures below (**256**, **258**, **263**, **264**) (Scheme 68).

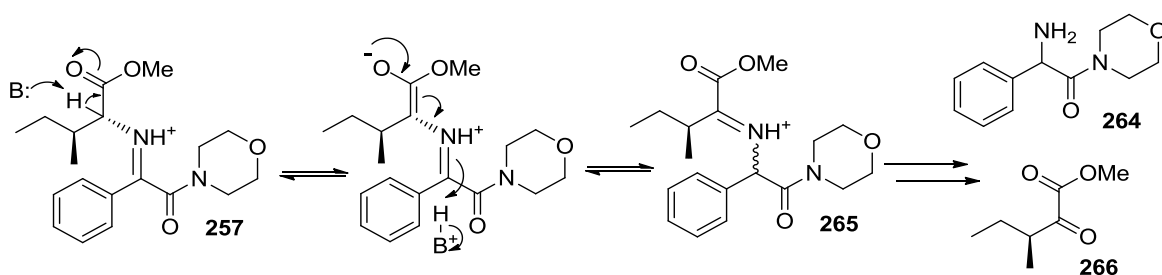


Scheme 68 – Reaction products of reductive amination

Lewis Acid	256 (% a/a)	258 (% a/a)	264 (% a/a)	263 (% a/a)
AlCl ₃	17.3	58.5	8.7	15.9
ZnCl ₂	10.9	82.0	1.8	5.3
TiCl ₄	1.2	0	68.2	30.6
Ti(OEt) ₄	83.8	6.4	1.7	7.9

Table 5 – Effects of varying Lewis acid on reaction products

The observation of small amounts of the amino acid (**263**) was encouraging and implied that the desired imine was being formed and reduced effectively. Ester hydrolysis, presumably facilitated by TiCl₄ and either *via* the acid chloride or by direct attack on the methyl group, suggests that the conditions are too harsh. More worrying was the observation of a species which appeared to be the amino amide (**264**). This species could potentially be formed *via* tautomerism of the imine into conjugation with the ester and hydrolysis (Scheme 69). Formation of this compound alerted us to the possibility of scrambling of the *isoleucine* stereocentres and was something which needed close monitoring. The presence of the hydroxyamide (**258**) was expected, and arised from reduction of the unreacted ketone (**256**). The presence of the ketone itself (**256**) was more surprising because reduction would be expected. Analysis of the reaction mixtures by proton NMR failed to shed any further light.

Scheme 69 – Mechanism for the formation of amino amide **264**

As TiCl₄ was successful in effecting the imine formation, a limited solvent screen was performed with the reactive Lewis acid and only minor differences were observed

3. Results and Discussion Part 1; A New Route to GSK221149

(Table 6). Approximately 1:1 mixtures of the ketone (**256**) and the hydroxyamide (**258**) were seen (on quench with excess NaBH₄) after addition of 0.5 equiv TiCl₄ but this increased to around 3:1 after addition of a further 0.5 equiv. Extending the quench time did not affect the observed mixture.

Solvent	Temperature	256 (% a/a)	258 (% a/a)
Toluene	20 °C	70.7	15.1
Dichloromethane	20 °C	55.0	17.3
THF	20 °C	70.7	16.7
DMF	20 °C	58.5	16.0

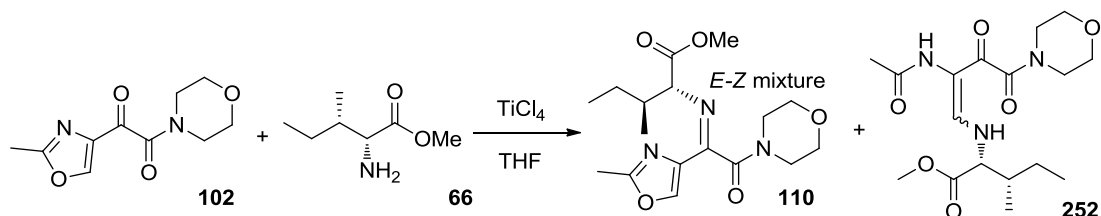
Table 6 – Solvent screen for imine formation with model ketoamide 256

One of the drawbacks associated with the current strategy of reaction investigation is the assumption that imine reduction occurs immediately when a sample is quenched with NaBH₄. Ideally, a method of observing the imine directly would be preferred. Proton NMR was ineffective due to the number of components within the reaction mixture. Application of a high-pH LCMS method using an ammonium bicarbonate buffer at pH 10 enabled us to observe the imine. It showed us that the species observed as the ketoamide (**256**) was in fact the desired imine (**257**). Crucially, this showed that our assumption that the imine would be reduced rapidly was incorrect. Research by Banik and co-workers confirmed that reduction of sterically hindered imines with sodium borohydride was more difficult than anticipated.¹²⁸

The real system could now be re-examined with a significantly improved method of reaction monitoring available, and conditions to give conversion to the desired imine in hand.

3.2.3 Imine Formation with Ketoamide 3

Using this newly discovered analytical method and the strongly Lewis acidic conditions the reaction time course of imine formation with the oxazole derived system was studied (Scheme 70, Figure 14). The desired imine (**110**) was observed as a mixture of *E*- and *Z*-diastereoisomers (**110a,b**) by LCMS (Method C). However, relatively rapid decay of this desired product to the 1,4-addition product (**252**) occurred due to the reversibility of the imine formation (Figure 14).



Scheme 70 – Imine formation of oxazole ketoamide

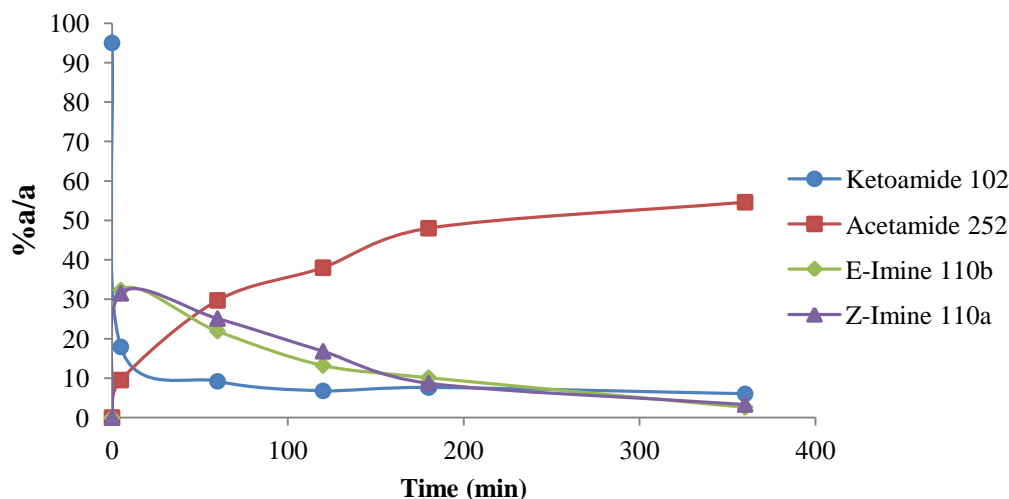


Figure 14 – Reaction profile of imine formation

The desired imine appears to be the kinetic product with the undesired 1,4-addition product acetamide (**252**) the thermodynamic sink. Attempted reduction of this imine with sodium borohydride was unsuccessful and confirmed the difficulties in reducing such hindered systems.

3.2.3.1 Optimisation of the Imine Formation Conditions

The imine (**110**) appeared to be formed rapidly under the Lewis acidic conditions, but turned over to the 1,4-addition product (**252**) more slowly, so the reaction temperature was reduced to prolong its lifespan (Figure 15).

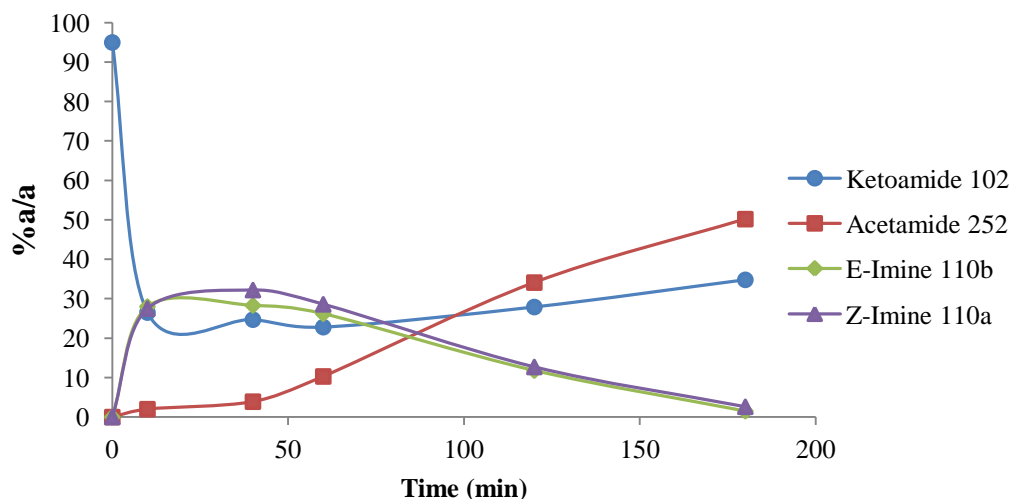


Figure 15 – Reaction profile of imine formation at 0 °C

It was surprising that complete consumption of the ketoamide (**102**) was not observed; only 0.5 equiv of TiCl_4 should be required to facilitate imine formation. In practice however, dispensing this highly water reactive material as a neat liquid provides ample opportunity for the material to hydrolyse, causing the stoichiometry in the reaction mixture to be lower than desired. In addition, metering such small quantities accurately (*ca.* 30 μL) is difficult. Brief assessment of the amount required showed up to 1.5 equiv was required for achieving >95% conversion to the imine (**110**). To help reduce the hydrolysis of TiCl_4 , it was decided to use the material as the commercially available 1 M solution in dichloromethane. Using this form, only 1 equiv. was required for smooth conversion to the imine. Using dichloromethane as the solvent also gave an improved reaction profile over that obtained in THF. However, use of dichloromethane on scale is undesirable due to its environmental impact. A selection of alternative Lewis acids including various trifluoromethanesulfonates were trialled to replace titanium tetrachloride, but none were as effective.

3. Results and Discussion Part 1; A New Route to GSK221149

Clearly, base is required in the reaction to prevent protonation of the amine by HCl released from the TiCl₄. A 2-3 fold excess of the methyl D-*allo*-isoleucinate (**66**) was used initially; however, it was soon shown that 1 equiv was sufficient when combined with 3 equiv. triethylamine as a sacrificial base.

The work-up procedure was then investigated; the key aim of this optimisation was to find conditions for the isolation of the imine, or at least for the preparation of a stable stock solution. With the knowledge that the stability of imines is greater under neutral to basic conditions, and the direct evidence that the imine was stable at pH 10 under the ammonium bicarbonate modified LCMS conditions, aqueous sodium hydroxide washes were tried initially. When the reaction was carried out in both THF and dichloromethane, 5 M NaOH solution could be added to give a biphasic system in which the desired imine was stable and remained in the organic phase. However, on addition of the NaOH solution, precipitation of a fine white solid was observed. The solid, assumed to be titanium dioxide, was difficult to filter and obscured the phase separation. To avoid the precipitation of solids, acid and neutral work-ups were investigated. When the dichloromethane reaction mixture was quenched with water instead of NaOH solution, the solids did not precipitate, and the pH of the aqueous phase was measured at 2. To our surprise, the imine was retained solely in the organic phase and was sufficiently stable under these conditions to allow removal of the titanium dioxide. This unexpected stability can potentially be rationalised, as the water content of the dichloromethane layer is low, limiting the rate at which hydrolysis can take place. Simply concentrating the washed organic phase afforded the desired imine.

3.2.4 Characterisation of Imine 110

The imines could now be characterized thanks to the fortuitous discovery that the by-products could be washed from the reaction mixture with water allowing facile isolation. Throughout the investigation of this reaction, two peaks were observed by high pH LCMS with molecular ions corresponding to the desired imines. It was assumed that these two peaks were the *E*- and *Z*-diastereoisomers, but this assumption needed to be tested. It was also noted that in dichloromethane, one of the peaks appeared to be formed more quickly, but when the reaction was allowed to stand, the mixture equilibrated to an approximately 1:1 mixture of the two peaks. The crude mixture was purified by high pH MDAP which readily separated the two isomers. The earlier running (thermodynamic) product was isolated cleanly, whereas the later running (kinetic) product was isolated cleanly initially, but isomerised to a mixture of the two by the time evaporation of fractions was complete. Spectral analysis was used to show that the two compounds both fitted the structure of the imines. However, there were significant differences in proton chemical shifts between the two isomers, particularly in the methine proton α -to the methyl ester. A significant downfield shift in the kinetic isomer suggested an interaction with an aromatic π -system. In order to gather more information on the structure of the isomers, the through-space correlative technique ROESY was used.¹²⁹ By this time, both samples had begun to isomerise to form mixtures, but with one clean NMR spectrum in hand, correlations could be assigned to the correct isomer.

3. Results and Discussion Part 1; A New Route to GSK221149

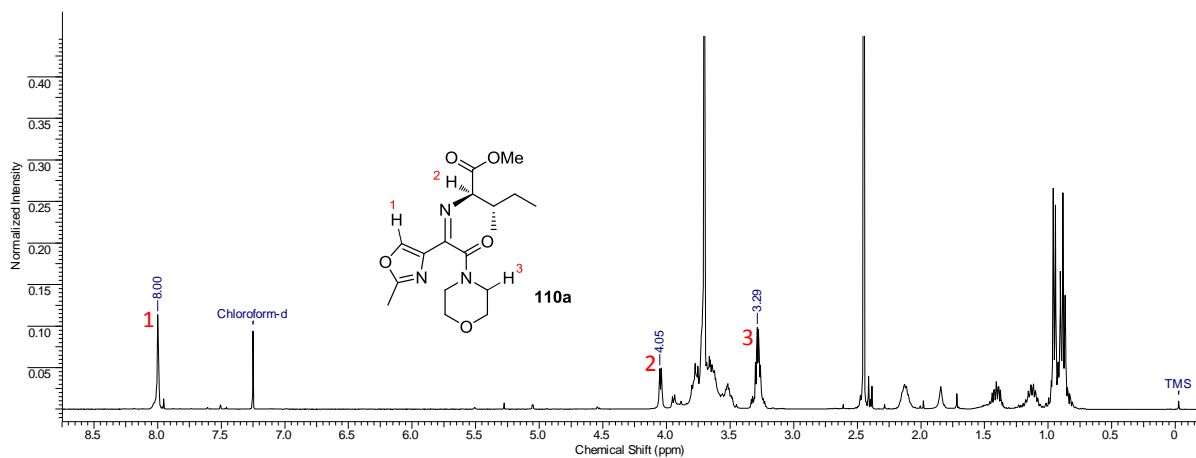


Figure 16 – Thermodynamic (*E*) imine isomer (110a), prior to isomerisation

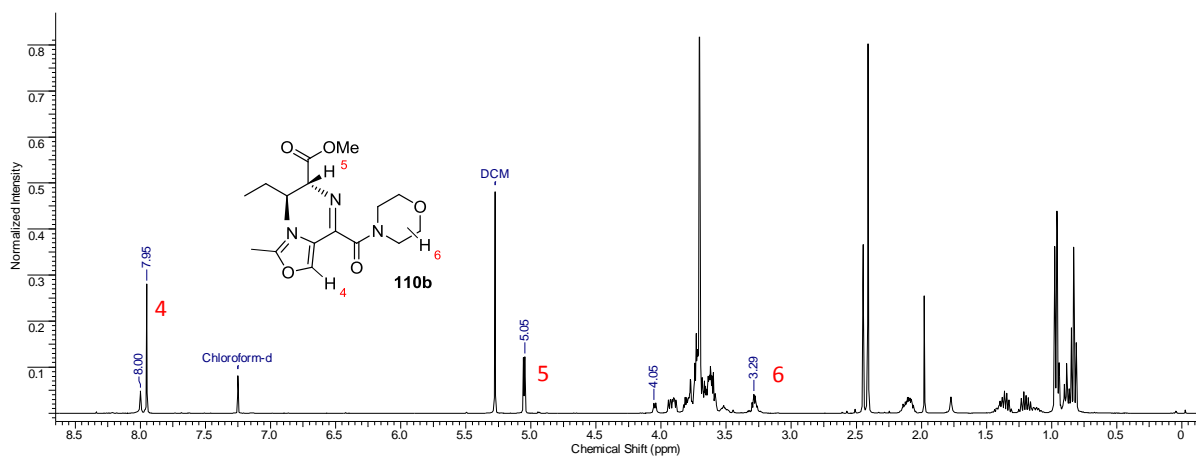


Figure 17 – Mixture enriched in kinetic (*Z*) imine isomer (110b)

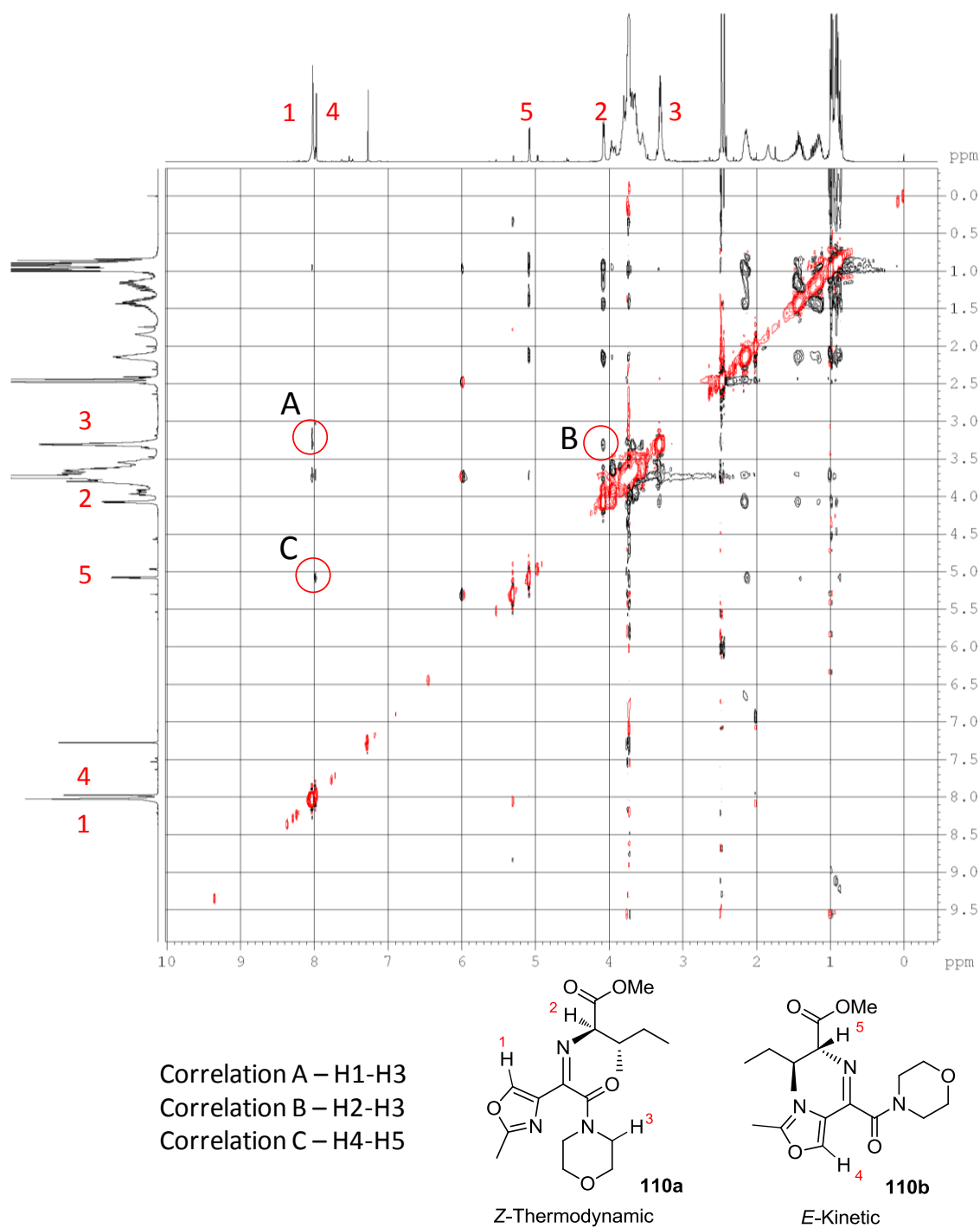


Figure 18 – ROESY plot of a mixture of *E* and *Z* imine isomers (110a & 110b)

Correlation C between protons 4 and 5 (Figure 18) in the kinetic product suggests this isomer is in the *E*-configuration. Correlations A and B between morpholine protons 3

3. Results and Discussion Part 1; A New Route to GSK221149

and both protons 1 and 2 in the thermodynamic product suggests that this is in the *Z*-configuration. It also suggests that the conformation of the *Z*-isomer has changed with a rotation around the central bond, bringing the oxazole and morpholine into close proximity. This would provide a structure in which the two polarized carbonyl and imine bonds are in an unfavourable *syn* relationship, but would allow the bulky *iso*-butyl moiety to be adjacent to only the amide oxygen, which would be sterically favoured. These observations can be rationalised by assuming that the ketoamide (**102**) sits in a conformation in which the two carbonyls are *anti* to each other, a conformation likely to be preferred as the two dipoles are diametrically opposed. Initial attack of the bulky *D-allo-isoleucine* (**66**) would then occur from the direction of the oxazole moiety, being considerably smaller than the morpholine, and initially afford the *E*-imine (**110b**).

Energy minimization calculations using MOE 2009.1001 software applying the MMFF94x forcefield identified a number of low energy conformations for the two isomers. The structures shown (Figure 19 - Figure 21) are consistent with the correlations seen in the ROESY spectra.

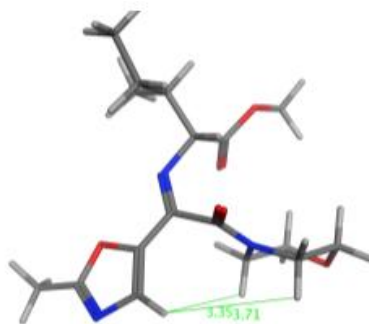
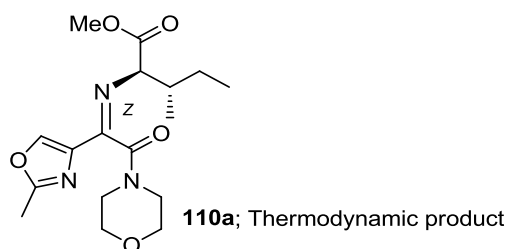


Figure 19 – A low energy conformation showing the origin of correlation A

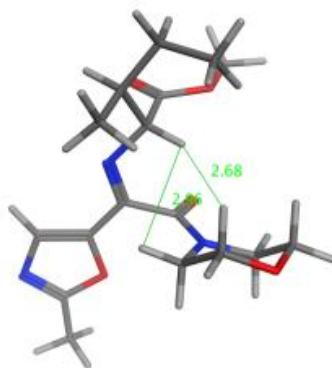


Figure 20 – A low energy conformation showing the origin of correlation B

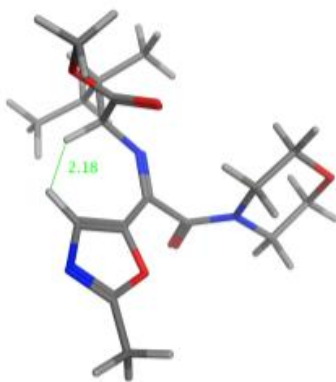
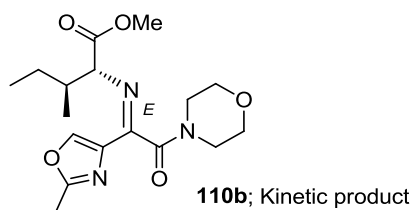


Figure 21 – A low energy conformation showing the origin of correlation C

These structural representations are also supported by analysis of the energies over a number of conformations (Figure 22). A number of low energy conformations exist for the kinetically preferred *E*-isomer (**110b**) in which H4 and H5 are within 3Å, distances which would be expected to give a ROESY correlation, as observed. However, none of the low energy conformations generated for the thermodynamically preferred *Z*-isomer (**110a**) showed an H1-H2 distance of less than 4Å, which is consistent with the absence of an H1–H2 cross peak in the ROESY spectrum.

3. Results and Discussion Part 1; A New Route to GSK221149

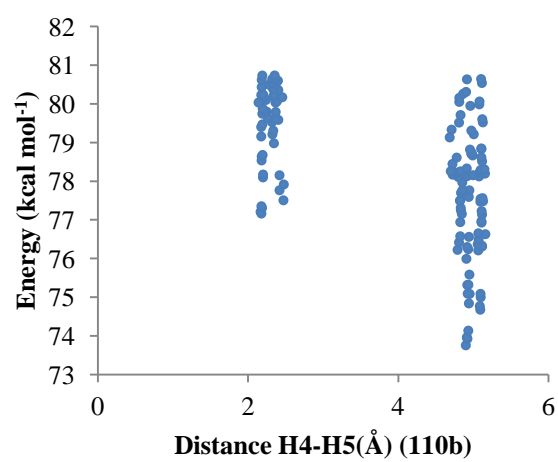
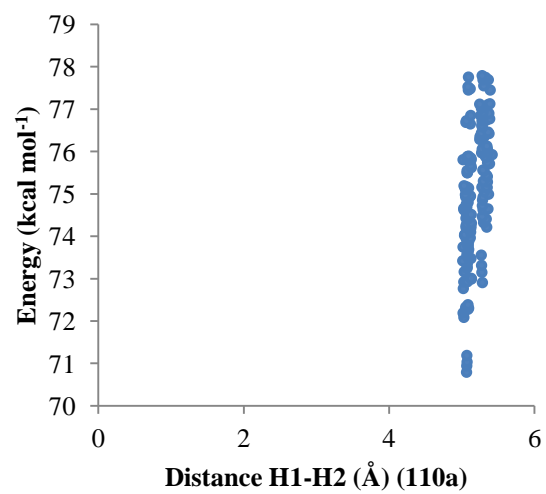
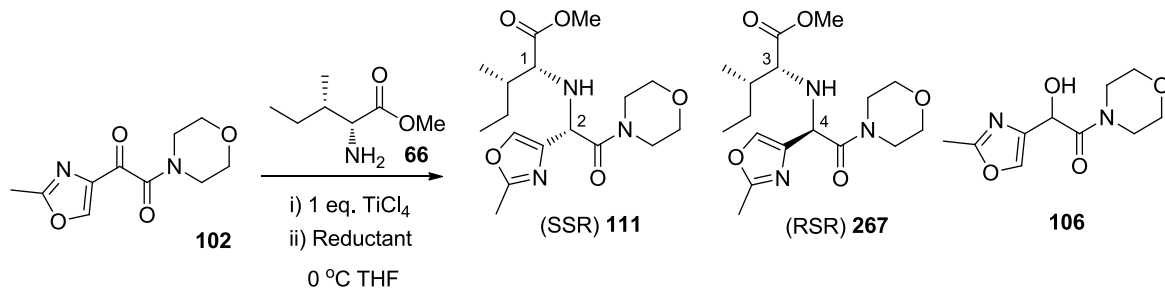


Figure 22 – Conformer energy vs inter atomic distance

3.3 Imine Reduction

With a method in place to prepare the imine, attention turned to its reduction to provide the amine (**111**). A range of commonly used reducing agents was screened and the results are given below.

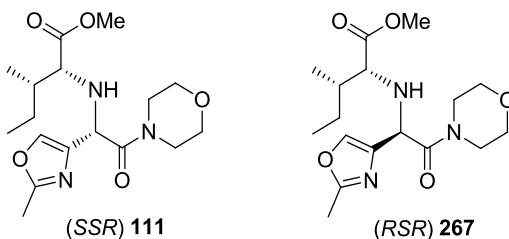


Reductant	Catalyst	111 (% a/a)	267 (% a/a)	106 (% a/a)	102 (% a/a)
$\text{BH}_3 \cdot \text{THF}$	None	5.9	4.2	38.5	24.8
CatBH	None	16.7	8.8	37.5	10.6
DIBALH	None	1.9	0	4.7	7.2
LiAlH_4 (1 eq.)	None	13.5	6.8	23.8	19.9
LiAlH_4 (4 eq.)	None	0	0	12.8	0
$\text{NaBH}_4/\text{ZnCl}_2$	None	26.2	18.9	32.6	5.9
$\text{NaB}(\text{OAc})_3\text{H}$	None	4.0	7.7	21.7	39.2
LiBH_4	None	7.8	8.3	36.4	12.8
LiBEt_3H	None	5.0	3.5	17.4	23.9
Et_3SiH	$\text{RhCl}(\text{PPh}_3)_3$	0	0	0	22.6
Cl_3SiH	$\text{RhCl}(\text{PPh}_3)_3$	1.0	3.4	10.9	9.4
PhSiH_3	$\text{RhCl}(\text{PPh}_3)_3$	0	0	2.3	16.7

Table 7 – Reducing agent screen.

3. Results and Discussion Part 1; A New Route to GSK221149

In a number of reactions, two resolved peaks were observed in the HPLC. Both had ion masses corresponding to the desired amine; they are presumably diastereoisomers arising from the newly created stereocentre. An authentic sample of the desired isomer (**111**), synthesised *via* the existing alkylation route (Scheme 25), was used to confirm its identity.



The NaBH₄/ZnCl₂ and catecholborane systems were effective in reducing the imine; the NaBH₄/ZnCl₂ system was particularly effective because minimal ketone formation occurred. Whilst not the cleanest reaction, it was decided to use this hit to isolate product as attention was still focussed on proving the viability of the route rather than optimising the processes.

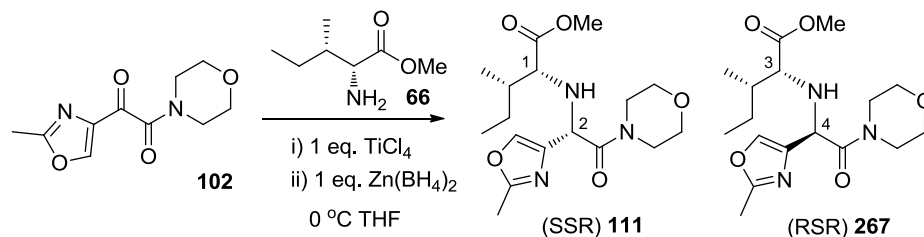
3.3.1 Reduction of Imine 110 using ZnCl₂/NaBH₄

Although the HPLC retention times from the reduced reaction mixtures matched closely with a sample of the authentic amino ester (**111**), isolation and characterisation of the compound produced *via* ZnCl₂/NaBH₄ reduction was required for confirmation of structure.

Rather than preparing the Zn(BH₄)₂ *in situ*, as in the screening experiment, a stock solution was prepared. This would allow less ambiguous assignment of the species present in solution. The stock solution was prepared according to the method of Narasimhan,¹³⁰ by reacting sodium borohydride with zinc chloride in THF. In our case, a standard solution of anhydrous zinc chloride was used instead of freshly fused solid. The sodium chloride precipitate was simply filtered off and the resulting Zn(BH₄)₂ solution was used as required.

3. Results and Discussion Part 1; A New Route to GSK221149

The reductive amination reaction was then scaled up to 500 mg (Scheme 71) with the aim of isolating and characterising both diastereoisomers (**111**, **267**).



Scheme 71 – Reductive amination

Imine formation and reduction were performed successfully, and the diastereoisomers were separated by preparative chromatography in low yield (15%). Analysis by LCMS, ^1H NMR, ^{13}C NMR and HMBC was concordant with the desired products. In particular, HMBC $^3J_{\text{C}2-\text{H}1}$ and $^3J_{\text{C}4-\text{H}3}$ correlations were indicative of the desired connectivity and thereby validated the initial stages of the route.

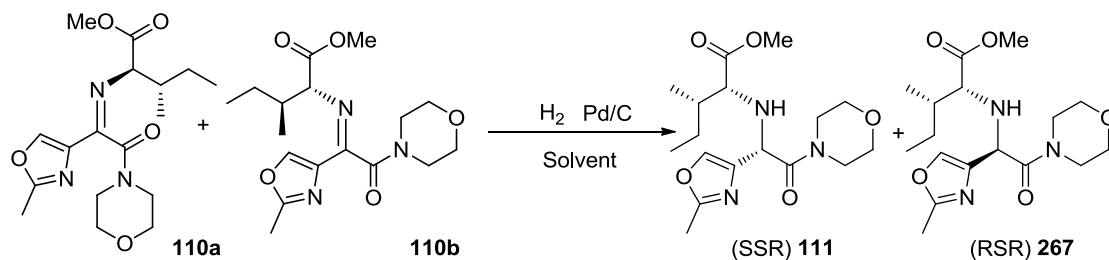
It was observed that the intensities of the product peaks in the HPLC decreased with time during the zinc borohydride reduction, with long reaction times yielding no product. It was postulated that instability of the product to the reaction conditions was the cause of the low yielding reaction. This instability was confirmed by exposing the isolated amine **111** to TiCl_4 and $\text{Zn}(\text{BH}_4)_2$ in THF. The amine was stable to titanium tetrachloride; however on addition of zinc borohydride, the amine decomposed to a number of impurities with low UV response at 220 nm. It is thought that reduction of the oxazole destroys the chromophore and yields products which are non-UV active. This result may also help to explain why incomplete reaction is observed even when a full molar equivalent of zinc borohydride is used (a four-fold excess of hydride assuming all four equivalents can be transferred).

3.3.2 Catalytic Hydrogenation of Imine **110**

As the best metal hydride conditions for the reduction of the imine (**110**) were still not ideal, transition metal catalysed hydrogenation was investigated as an alternative. The optimised imine formation conditions (1 equiv. of methyl D-allo-isoleucinate, 3 equiv. of

3. Results and Discussion Part 1; A New Route to GSK221149

NEt₃, 1 equiv. TiCl₄, dichloromethane, 0 °C) were scaled up to provide 7.26 g of a roughly 1:1 mixture of isomers in 93% yield. A screen of hydrogenation conditions was then performed with the material, using readily available 10% Pd/C as catalyst at 25 °C in different solvents and under different pressures.



Scheme 72 – Hydrogenation of imine 110

Reaction	Solvent	Catalyst	Temperature	Pressure	Product observed?
1	THF	Pd/C - 0.5 wt	25 °C	1 bar	Yes
2	Toluene	Pd/C - 0.5 wt	25 °C	1 bar	Yes
3	EtOH	Pd/C - 0.5 wt	25 °C	1 bar	Yes
4	THF	Pd/C - 0.5 wt	25 °C	3 bar	Yes
5	Toluene	Pd/C - 0.5 wt	25 °C	3 bar	Yes
6	EtOH	Pd/C - 0.5 wt	25 °C	3 bar	Yes

Table 8 – Hydrogenation reaction screening results

The reactions were monitored by high pH LCMS in order to observe the imine directly. Using this system, poor peak shape and overlap of both isomers of the imine with both diastereoisomers of the product amine meant that quantitative analysis was difficult. Product was observed in all reactions and reaction rates could be inferred from the hydrogen uptake curves generated by the hydrogenation instrument. Once it was known that there was minimal hydrolysis of the imine under the reaction conditions (by high pH HPLC, Method C), it should be possible to quantify the reaction progression by quenching into dilute acid and monitoring by generic TFA-modified HPLC (Method A)

for future experiments. Any imine would be observed as ketone, which is readily resolved from the product amines.

It is possible to compare rates of reaction using the hydrogen uptake curves (Figure 23), with the reactions corresponding to those in above (Table 8). As expected, reactions performed at lower pressure (1 bar), are generally slower than the comparable reactions run at higher pressure (3 bar). Hydrogen uptake rates in THF and toluene were comparable, whereas those in ethanol were considerably higher. This was also expected due to the increased solubility of hydrogen in ethanol over THF and toluene. Analysis of reaction 6 by generic TFA-modified HPLC (Method A) showed the reaction to be remarkably clean, with only minimal impurities in addition to the desired product diastereoisomers. The product could be further purified, if required, by a simple acid/base extractive work-up.

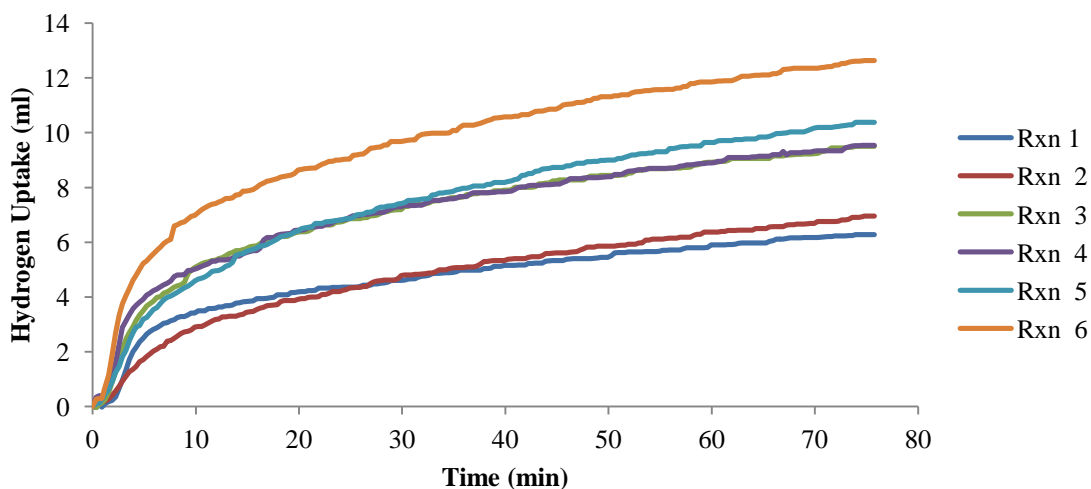
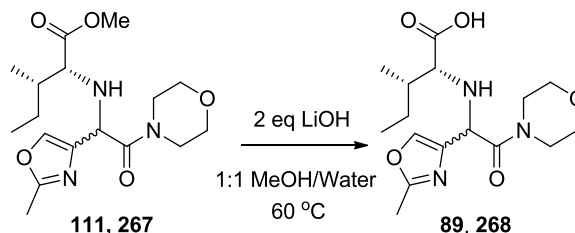


Figure 23 – Hydrogen uptake curves of reactions in Table 8

The hydrogenation at 3 bar in EtOH was immediately scaled up to ~7 g with the ultimate goal of providing API from this material in order to assess the ratio of *D-allo-isoleucine* diastereoisomers. Hydrogenation proceeded smoothly to give the desired amine as a 1:1 mixture of diastereoisomers (**111**, **267**) in 84% yield. NMR analysis suggested the material was of sufficient purity to use crude in the following step (hydrolysis of the ester).

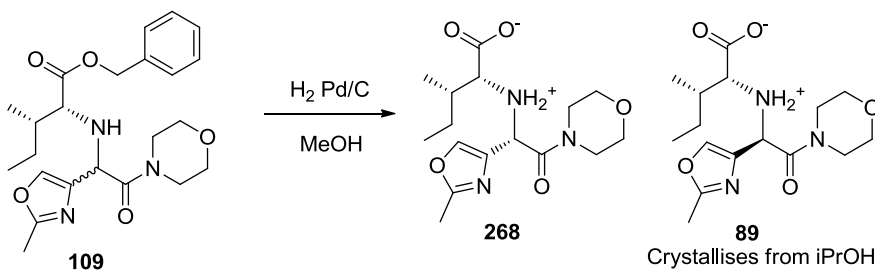
3.4 Ester Hydrolysis and Diastereoisomer Separation

The initial conditions investigated for the hydrolysis of the methyl esters (**111**, **267**) (LiOH, MeOH, Scheme 73) were successful in giving complete conversion to a 1:1 mixture of diastereoisomers of the amino acid (**89**, **268**) with no decrease in purity. Separation of the diastereomeric mixture of amino acids was now the goal.



Scheme 73 – Hydrolysis of amino ester **111**, **267**

Whilst working on the alkylation route (Scheme 25), a previous team member¹³¹ had observed that following hydrogenolysis of the benzyl ester (**109**) under neutral conditions (Scheme 74), the zwitterion form of the desired diastereoisomer (**89**) could be preferentially crystallised from *i*-PrOH.



Scheme 74 – Hydrogenolysis of benzyl amino ester **109**

Adjustment of the pH of the hydrolysis reaction mixture to the *iso*-electric point (pI) and crystallization was explored to allow the isolation of the desired diastereoisomer (**89**).

The pI was measured by titrating 0.1 M HCl_(aq) into a sample of authentic, pure zwitterion (**89**) treated with excess base and produced *via* the alkylation route. The pH curve is shown (Figure 24).

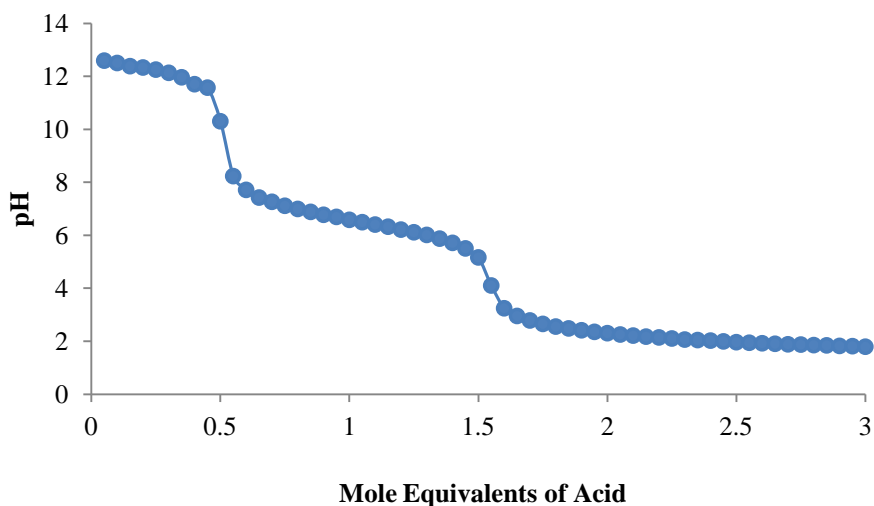


Figure 24 – pH curve of amino acid 89

The addition of the first 0.5 equivalents of acid changes the pH minimally as at this point excess NaOH is being protonated. Once the excess NaOH is fully protonated, the pH drops rapidly to around 8, where protonation of the amine begins to buffer the system. After addition of 1.5 equiv. of acid, the amine is now fully protonated and again the pH drops to the point where the carboxylate begins to be protonated, again buffering the system. After the addition of 2.5 equiv of HCl, another step in the curve should be observed; however, due to the particularly acidic nature of the carboxylic acid, the pH of 0.1 M HCl_(aq) is not sufficiently low to cause a step to be observed.

From the curve, the pK_a of the protonated amine can be measured at 6.6 (the point where 50% of the amine is protonated) and the pK_a of the acid can be measured as 2. From these measurements, the pI can be calculated as 4.3.

These pK_a values are largely typical of amino acids of this type and can be readily rationalized.¹³² The carboxylic acid of an amino acid is significantly more acidic than other carboxylic acids due to the inductive effect of the electronegative cationic nitrogen. This is exemplified by glycine, which has a measured carboxyl pK_a of 2.79.¹³³ The reduction in basicity of the amine over typical nitrogen bases, such as triethylamine, is attributable to the electron withdrawing nature of both the morpholine amide and aromatic oxazole in close proximity.

3. Results and Discussion Part 1; A New Route to GSK221149

These measurements could then be re-applied to the real system, with the aim of careful adjustment of the pH to the isoelectric point followed by removal of water, either by extraction or concentration, and then crystallisation of the desired diastereoisomer from *i*-PrOH. Acetic acid was chosen for acidification as it is sufficiently acidic to protonate the amine, but not the carboxylic acid. This would mean that excess acetic acid could be removed by evaporation. After pH adjustment to pH 4.7, the aqueous solution was freeze dried. Attempted crystallisation from *i*-PrOH unfortunately yielded the undesired isomer (**268**) in 93:7 *dr*. Ion chromatography showed that the sample contained 2.2% w/w lithium, consistent with the presence of the lithium carboxylate (calcd. 2.01% w/w) plus a small amount of lithium acetate. It was already known that the lithium carboxylate of the undesired diastereoisomer (**268**) would readily crystallize from *i*-PrOH. However, it was expected that adjustment of the pH to 4.7 would ensure that only zwitterion was present, thereby preventing crystallisation of the undesired diastereomer. Freeze-drying may perturb the equilibrium between lithium acetate and the lithium carboxylate in the direction of the lithium carboxylate, due to evaporation of acetic acid. The resulting salt then crystallises from *i*-PrOH.

3.4.1 Crystallisation of the Amino Acid (**89**)

It was decided to re-acidify the mother liquors containing the desired diastereoisomer (**89**) with a stronger acid since the crystallisation of the undesired diastereoisomer can potentially be explained by an equilibration with a relatively weak, volatile acid. Aqueous HCl was titrated into the evaporated liquors to adjust the pH to 2.8. Again the aqueous solution was freeze dried and the residue was dissolved in *i*-PrOH. No crystallization was observed despite seeding with authentic material. Another trial was run in which the solution was acidified to pH 1.5 to ensure complete protonation of all species, but again, no crystallisation of the desired isomer was observed from *i*-PrOH. The hypothesis as to why crystallisation could not be established now shifted as pH effects had been ruled out by investigation. It was postulated that the effect of dissolved salts carried through from the hydrolysis were inhibiting crystallisation. In order to

3. Results and Discussion Part 1; A New Route to GSK221149

remove the dissolved lithium acetate from solution, extraction of the amino acid (**111**) into an organic solvent at its isoelectric point was attempted. Unfortunately, extraction failed at all pHs and the compound remained in the aqueous phase. Presumably, the charged molecule, in combination with the polar oxazole and morpholine moieties, do not allow solubility in the organic solvent.

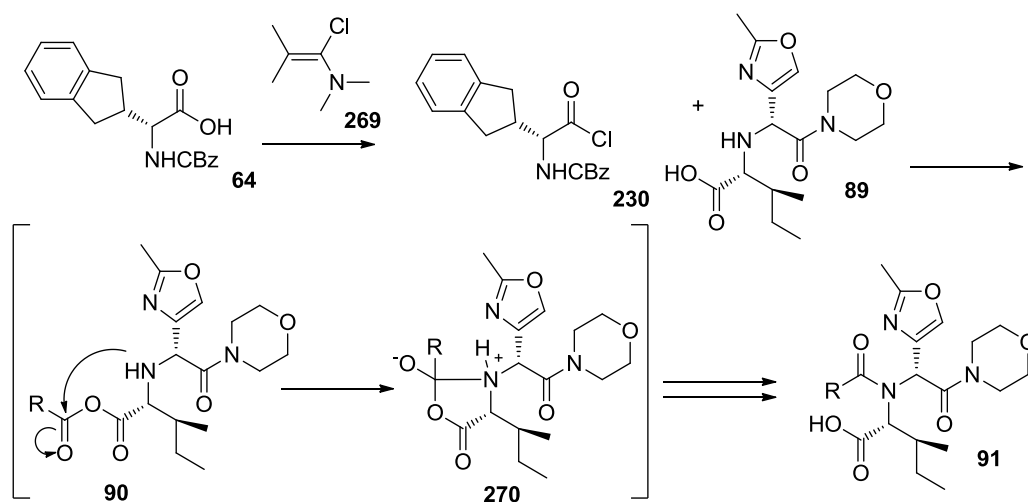
The removal of salts was then attempted by solid phase extraction. This is a powerful technique, but is not a preferred method as it cannot be readily scaled up. An aqueous solution of the desired amino acid (**89**) at pH 4.7 was loaded onto a C₁₈ column, which was eluted with water to remove the polar lithium salts. Once the removal of salts was complete, as observed by a reduction in the UV absorption of the solution (LiOAc absorbs weakly at 220 nm), methanol was used to flush the product and any other adsorbed compounds from the column. This provided a solution of the desired diastereoisomer and related impurities in methanol, with only a minimal amount of water present. The solution could then be concentrated and the residue dissolved in *i*-PrOH. Crystallisation of the desired diastereoisomer initiated, to afford material of high purity. It is assumed that the hypothesis was correct, and that dissolved salts alter the polarity of the *i*-PrOH sufficiently to inhibit the crystallization.

3.5 Synthesis of GSK221149

With pure material in hand, and with spectral data consistent with the material produced *via* the alternative alkylation route, the proof of principle of the reductive amination route was complete. However, data on the enantiomeric purity of the sample was not available as an analytical method had not yet been developed. In order to assess the enantiomeric purity, the material was progressed to API *via* the existing acylation and hydrogenation/cyclisation chemistry. At the API stage there were analytical methods available to distinguish between the diastereoisomers.

3.5.1 Acylation of the Amino Acid (89) with Protected Indanyl Glycine (64)

The acylation of the amino acid (89) had been previously investigated as part of the alkylation route. Optimal conversions were obtained by forming the acyl chloride of the protected indanyl glycine (64) which could then be reacted with the amino acid (89) in the presence of pyridine. The mechanism of acylation is believed to involve initial acylation of the carboxylate to give a mixed anhydride which then undergoes intramolecular acyl transfer (Scheme 75). This is thought to be the case because of the significant steric bulk of the amine which prevents its direct acylation. This type of acyl transfer mechanism was first proposed by Sollis when investigating similar acylation reactions.³¹ Further evidence for this mechanism is that acylation of the corresponding amino ester (111) is unsuccessful.



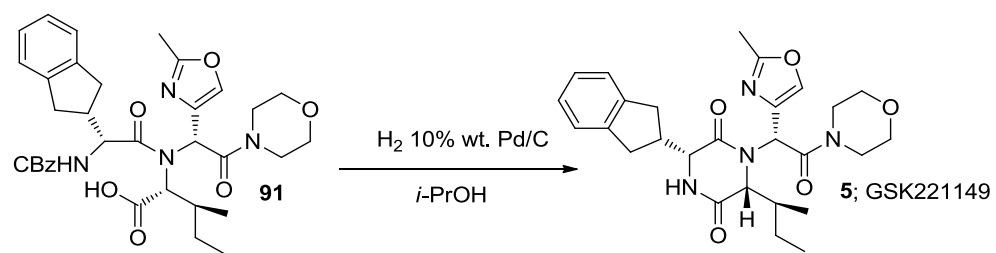
Scheme 75 – Acyl transfer mechanism

Formation of acid chlorides from *N*-protected α -amino acids is an extensively studied field, and racemisation of the α -stereocentre is a well known problem.⁴⁵ In our case, racemisation was not observed; however, acid mediated deprotection of the CBz group was observed.⁴⁶ In order to overcome this problem the mild chlorinating reagent 1-chloro-*N,N*-2-trimethylprop-1-en-1-amine (Ghosez's Reagent, **269**) was used.¹³⁴ This allows the formation of acid chlorides under neutral conditions by a mechanism similar to that of the Vilsmeier reagent. Once the desired amide had been formed, the by-product *iso*-butyramide could be washed out and the product crystallised in 43% yield.

3.5.2 Deprotection and Cyclisation of the GSK221149 Precursor (**91**)

Hydrogenolysis of the amide (**91**) catalysed by palladium-on-carbon facilitated facile CBz cleavage; the resultant amino acid then cyclised spontaneously to afford the API, GSK221149. This was crystallized as an EtOAc solvate and was re-crystallised from *s*-BuOH/heptane to provide the desired polymorphic form.

3. Results and Discussion Part 1; A New Route to GSK221149



Scheme 76 – Synthesis of GSK221149

3.6 Comparison of GSK221149 Derived from the Two Routes

The GSK221149 produced *via* this new chemistry was analysed by ^1H NMR alongside equivalent GSK221149 produced from the existing Ugi route; the spectra are shown (Figure 25). The material is crystallised as an ethyl acetate solvate in both cases and the spectra are concordant. This result confirms that the new reductive amination chemistry is capable of forming the correct product, GSK221149.

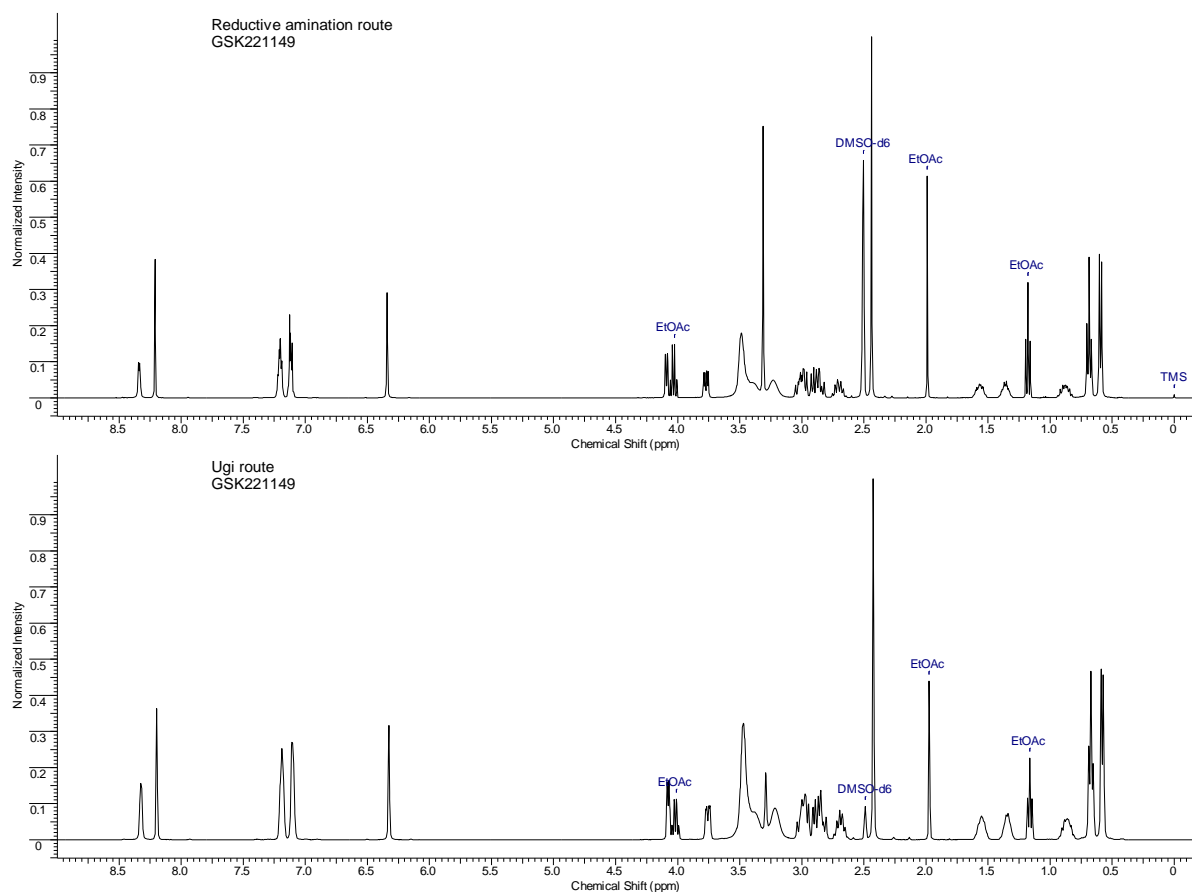


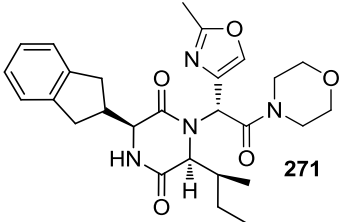
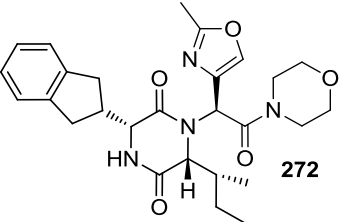
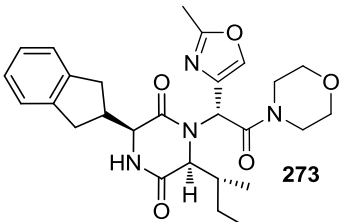
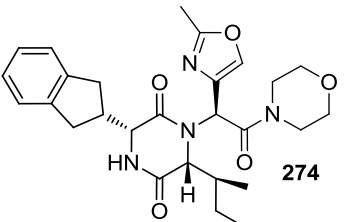
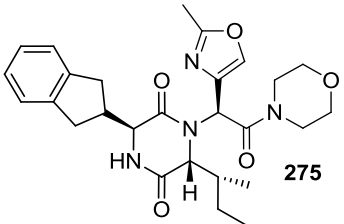
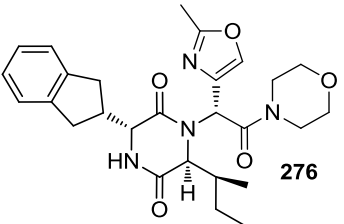
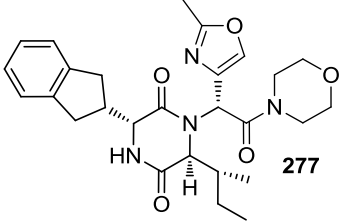
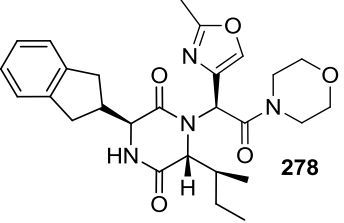
Figure 25 – Comparison of ^1H NMR from GSK221149 produced by different routes.

3.6.1 Analysis of New Route GSK221149

While proof that the new route chemistry is capable of forming the correct product is crucial, the purity of the product, in particular with respect to the contaminant isomer content, is also important. There are 16 stereoisomers of GSK221149 and all have been

3. Results and Discussion Part 1; A New Route to GSK221149

previously synthesised.⁴⁶ They are shown (Table 9) as pairs of enantiomers, and are numbered by elution order for convenience.

No	Enantiomer 1	Enantiomer 2
1	 (S)-Indanyl glycine-L-isoleucine	 (R)-Indanyl glycine-D-isoleucine
2	 (S)-Indanyl glycine-L-allo-isoleucine	 (R)-Indanyl glycine-D-allo-isoleucine
3	 (S)-Indanyl glycine-D-isoleucine	 (R)-Indanyl glycine-L-isoleucine
4	 (R)-Indanyl glycine-L-allo-isoleucine	 (S)-Indanyl glycine-D-allo-isoleucine

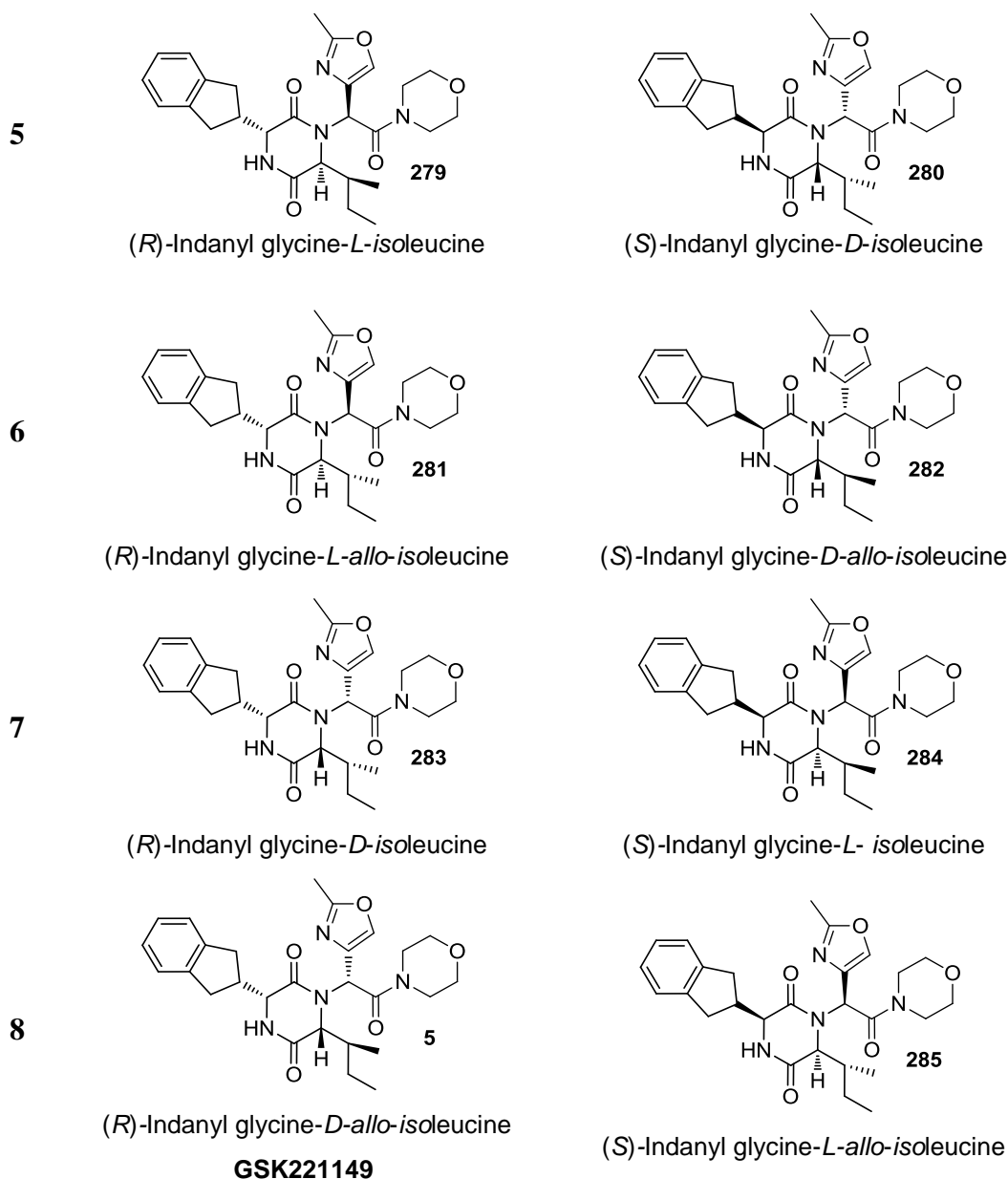


Table 9 – Diastereoisomers of GSK221149

The API release method is an HPLC method which is validated to analyse, and approve for use, APIs destined for use in clinical trials. The method is capable of separating the eight pairs of enantiomers and it was used to analyse the material synthesised *via* this new reductive amination route; the results are shown (Table 10). Diastereoisomers not detected by the analysis are not listed.

Peak Name	RRT	Peak Area (%)
RRT = 0.51	0.51	0.10
Diastereoisomer pair 2 (273 , 274)	0.67	0.07
Diastereoisomer pair 5 (279 , 280)	0.78	0.07
Diastereoisomer pair 6 (281 , 282)	0.88	0.06
Diastereoisomer pair 7 (283 , 284)	0.97	0.19
GSK221149 (5)	1.00	99.05
RRT = 1.15	1.15	0.13
RRT = 1.25	1.29	0.35

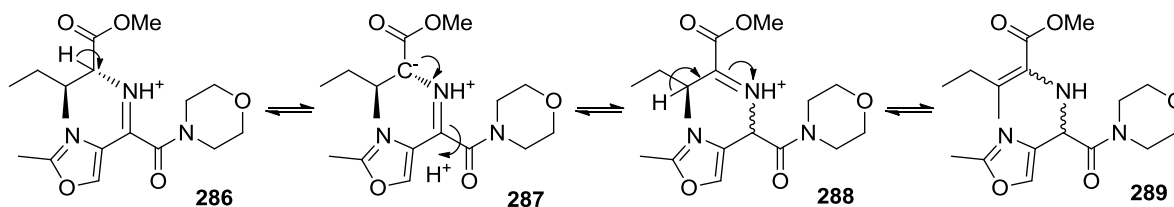
Table 10 – HPLC analysis of GSK221149 made using reductive amination route¹³⁵

Impurities at RRT = 0.51 and 1.15 have not been previously observed in API samples and are therefore new to this route. Impurity with RRT = 1.25 has previously been observed in API produced *via* Route A, and is known to be purged during the final stage re-crystallisation. Several diastereomeric impurities were also observed. The presence of diastereoisomer pair **7** (**283**, **284**) at a level approaching 0.2% a/a is of particular importance as this would currently fail to meet the API specification.

Diastereoisomer pair **7** (**283**, **284**) differs from GSK221149 only by the inversion of the β -isoleucine stereocentre (**283**). It is assumed that it is not the enantiomer (**284**), where all stereocentres apart from that in the β -isoleucine have undergone inversion (which seems unlikely). Inversion of the β -centre may occur during the reductive amination procedure by a mechanism depicted (Scheme 77). Deprotonation of the α -hydrogen to give an imine in conjugation with the ester (**288**), then tautomerisation to the corresponding enamine (**289**), is possible. If this mechanism were in operation, it would be expected to also see significant quantities of diastereoisomer pair **3** (**275**, **276**) due to

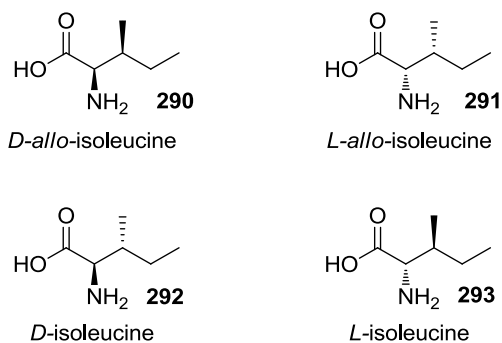
3. Results and Discussion Part 1; A New Route to GSK221149

inversion of only the α -stereocentre, and diastereoisomer pair 4 (**277**, **278**) due to the epimerisation of both. The absence of these impurities casts doubt over whether the tautomerisation mechanism is operative.

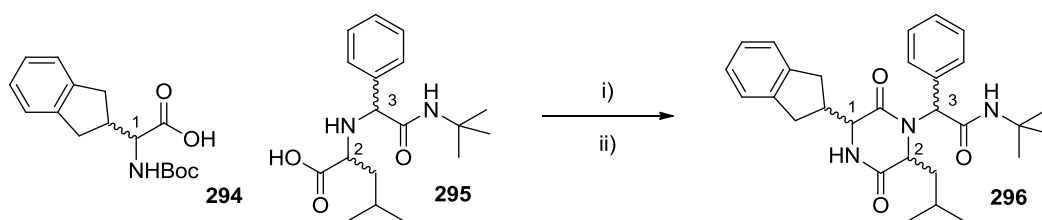


Scheme 77 – Possible mechanism for epimerisation of isoleucine stereocentres

The most likely alternate source of the β -epimer (**283**) is contamination of the *D*-allo-isoleucine (**290**) used in the process with *D*-isoleucine (**292**). However, analysis of this material did not reveal the presence of any of the contaminant isomer.



The β -epimer (**283**) is therefore a process impurity (formed during chemistry). The enamine mechanism described (Scheme 77) is still the most plausible hypothesis. It may be that the conformation of the molecule strongly dictates from which side re-protonation of the imine occurs, meaning little epimerization at the α -centre is observed and little of **276** is formed. Alternatively, it may be that **276/275** is formed, but is removed in one of the crystallisations more effectively and is therefore not detected in the API. Another possibility is that the configuration of the α -centre is inverted during the acyl transfer amidation chemistry which would render the effects of α -epimerization during the imine formation invisible. Whilst investigating a similar acyl transfer reaction, Sollis noted inversion of the leucine α -stereocentre apparently controlled by the phenylglycine stereocentre (Scheme 78, Table 11).³¹



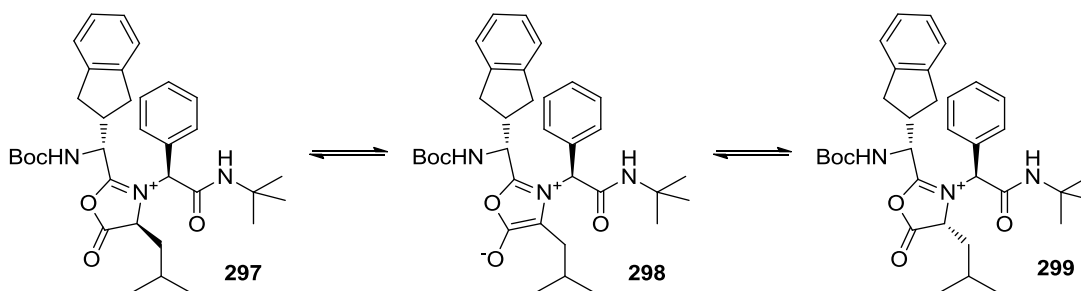
i) *i*-PrOCOCl, *N*-methyl morpholine, THF; ii) HCl, dioxane, 3 h.

Scheme 78 – Acyl transfer reaction investigated by Sollis³¹

Indanyl Glycine Stereochemistry	Amino acid Stereochemistry		Reaction Temperature	Product Stereochemistry		
	1	2		3	1	2
<i>R</i>	<i>R</i>	<i>S</i>	-20 °C to RT	<i>R</i>	<i>S</i>	<i>S</i>
<i>R</i>	<i>R</i>	<i>S</i>	-20 °C to -10 °C	<i>R</i>	<i>R/S</i>	<i>S</i>
<i>S</i>	<i>R</i>	<i>S</i>	-20 °C to RT	<i>S</i>	<i>S</i>	<i>S</i>
<i>R</i>	<i>S</i>	<i>R</i>	-20 °C to RT	<i>R</i>	<i>R</i>	<i>R</i>

Table 11 – Inversion of α -stereocentre³¹

He reasoned this inversion was occurring *via* a Münchnone intermediate (**297**) and, by molecular modelling, showed that intermediate **297** was 40 kJmol⁻¹ more stable than intermediate **299**. He also showed that epimerisation to afford the more stable diastereoisomer could occur readily at room temperature.



Scheme 79 – Inversion of leucine α -stereocentre *via* münchnone intermediate **298**

It is possible that a similar mechanism is active in our case and that epimerization of both α - and β -stereocentres occurs during imine formation, but that the corresponding α -

3. Results and Discussion Part 1; A New Route to GSK221149

epimer is not observed due to inversion during the acyl transfer reaction. In addition to this being an interesting area for investigation in itself, complete inversion could allow readily available *L-iso*leucine to be used to provide GSK221149 instead of the more expensive *D-allo-iso*leucine. Further investigation into this area was not carried out, but could, however, form the basis of future work.

Up to this point the investigations have been concerned primarily with the feasibility of the synthesis of GSK221149 by the proposed reductive amination chemistry. It has now been demonstrated that the route is viable and can produce material very close to the required clinical specification. However, in order to form part of a long term manufacturing route the processes need to be optimised to improve the yields and manufacturability attributes. The following pages document these investigations.

3.7 Changing the Ester Protecting Group Strategy

One significant problem in the ability of the route to provide material on a large scale was the difficult isolation of the amino acid (**89**) after ester hydrolysis. Currently, solid phase extraction using a C₁₈ column was required to separate the polar zwitterion from inorganic salts which inhibit crystallisation. A significant body of work was undertaken attempting to extract the zwitterion (**89**) into organic solvent, without success.¹³⁶ It was postulated that cleavage of an ester under non-hydrolytic conditions could allow direct crystallization of the desired amino acid without the requirement for solid phase extraction.

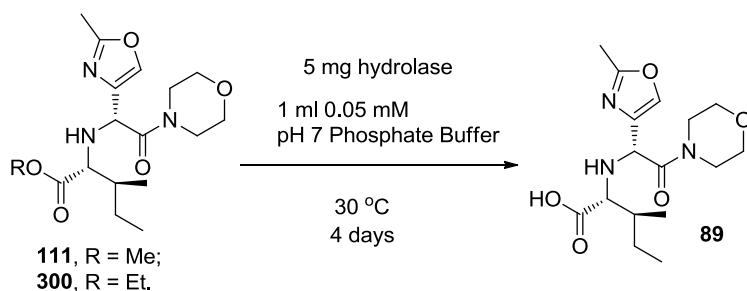
3.7.1 Enzymatic Ester Cleavage

There are a number of methods for alkyl ester cleavage under neutral conditions; for example the use of trimethylsilyl iodide as described by Olah *et al.*¹³⁷ is mild and effective. However, concerns remained that methods such as this use highly reactive reagents and could still suffer from crystallisation inhibition.

A neutral, catalytic method of ester cleavage was therefore sought, and it was postulated that enzymatic ester cleavage methodology could be applicable. Our strategy was to screen a wide range of commercially available hydrolases against both the methyl and ethyl esters in aqueous media in order to give the best chance for ester cleavage to occur. From this initial screen, it was hoped to find a shortlist of enzymes that effectively catalysed the hydrolysis which could then be applied to a second set of reactions. These reactions would investigate the catalytic hydrolysis reaction in water-wet organic solvent which might allow crystallisation of the amino acid without the need for solid phase extraction.

Initially, both the methyl and ethyl ester substrates (**111/267**, **300**) were screened (Scheme 80) due to concern that the methanol released may de-nature the enzymes and inhibit further hydrolysis.

3. Results and Discussion Part 1; A New Route to GSK221149



Scheme 80 – Enzymatic ester cleavage in pH 7 buffer

The results of the initial screen are presented (Table 12) and show the six enzymes from the 46 screened which gave over 1% conversion to the desired amino acid from either the methyl or ethyl ester. Perhaps unsurprisingly, the majority of active enzymes were proteases; because the substrate contains an amino acid and an amide bond, it does bear some resemblance to a peptide. However, amide cleavage was not observed in these reactions. Although the conversion to amino acid was low, it was hypothesised that the activity could be sufficiently different in organic solvents to warrant further investigation. A similar phenomenon had been observed by Karube *et al.*¹³⁸ whilst investigating the enzymatic hydrolysis of polysaccharides.

Type	Strain	Methyl		Ethyl	
		% a/a Desired	% a/a Undesired	% a/a Desired	% a/a Undesired
Lipase	<i>Pseudomonas cepacia</i>	0.49	0.07	1.34	0.26
Alkaline Protease B	N/A	6.17	4.17	8.01	7.84
Protease B	<i>Bacillus subtilis</i>	1.70	0.58	0.87	0.41
Protease C	<i>Bacillus subtilis</i>	7.06	5.69	6.05	7.00
Protease	<i>Bacillus sp.</i>	1.23	1.05	2.28	2.44
Protease B	<i>Bacillus sp.</i>	1.12	0.89	2.03	2.11

Table 12 – Enzymatic ester cleavage in aqueous media

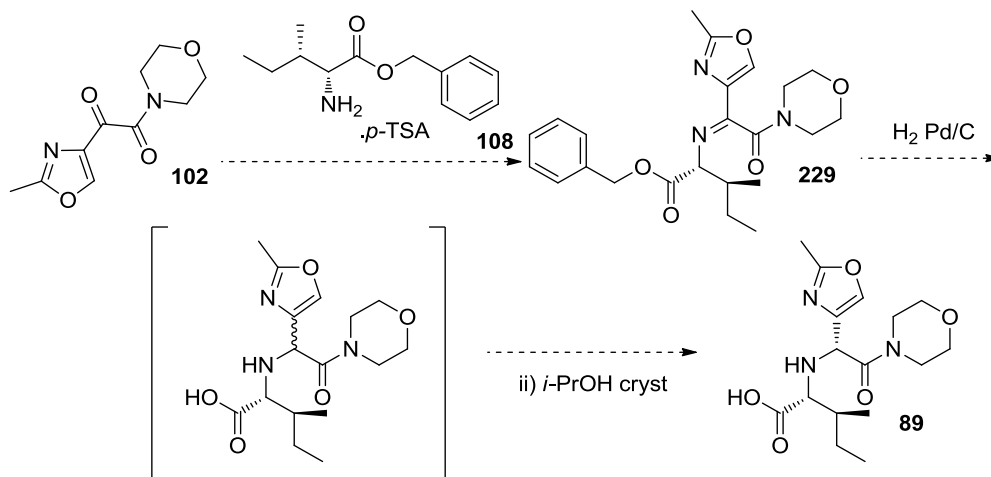
3. Results and Discussion Part 1; A New Route to GSK221149

These six hits were then screened against the methyl ester in a range of water-wet organic solvents. It was decided to use solely the methyl ester in this study as minimal differences were observed between the two substrates when carrying out the hydrolysis in aqueous media. The organic solvents chosen were selected based on their suitability for water removal by azeotropic distillation; it was anticipated that this would be required prior to crystallisation. The solvents chosen were toluene, 2-Me THF, *t*-butyl methyl ether, methyl *i*-butyl ketone, diisopropyl ether and acetonitrile (10% wet) and 36 experiments were run so that each solvent was used in conjunction with each enzyme. Disappointingly, no ester cleavage was observed in any of the reactions. It is possible the enzymes are not stable in the solvents investigated (which would be easy to test with model substrates), but it is more likely that the significantly reduced concentration of water retards the reaction rate. It is also possible that due to the long reaction times the proteases are beginning to self digest; a process which had been previously observed by Mitchell *et al.*¹³⁹ Increased activity may occur using the lipase in a biphasic system as these enzymes typically operate in micelles and at phase boundaries. However, given that the activity in aqueous media was low, and that no increase in activity was observed in organic solvents, it was decided to suspend this avenue of research. It was believed that enzymatic ester cleavage under neutral organic conditions is a viable strategy to allow the isolation of the amino acid (**89**), but that enzyme evolution will be required in order to obtain a sufficiently active strain.^{140,141} Due to the time constraints of this project, no further work was performed at this time.

3.7.2 Catalytic Hydrogenolysis of Benzyl Ester 229

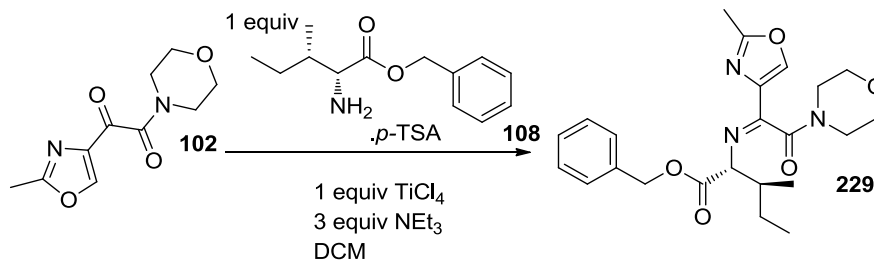
With the failure of neutral enzymatic cleavage of a methyl ester, it was envisaged that hydrogenolysis of a benzyl ester could be a successful alternative. This approach had been previously shown to allow crystallisation of the amino acid directly from *i*-PrOH, when new routes to GSK221149 were investigated by an earlier project team.⁴⁶ It was reasoned that since the corresponding methyl ester (**110**) could be reduced to the amine by catalytic heterogeneous hydrogenation, the imine reduction and benzyl ester cleavage

could be carried out concurrently, and that crystallisation from *i*-PrOH would provide the desired diastereoisomer (**89**) cleanly (Scheme 81). However, the earlier research was performed using the alkylation method of generating the hydrogenolysis precursor amino ester (**109**), and a method did not exist for generating the desired imine (**229**).



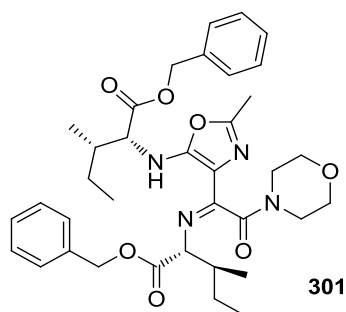
Scheme 81 – Synthesis of amino acid **89** via benzyl ester

3.7.3 Synthesis of Imine **229**

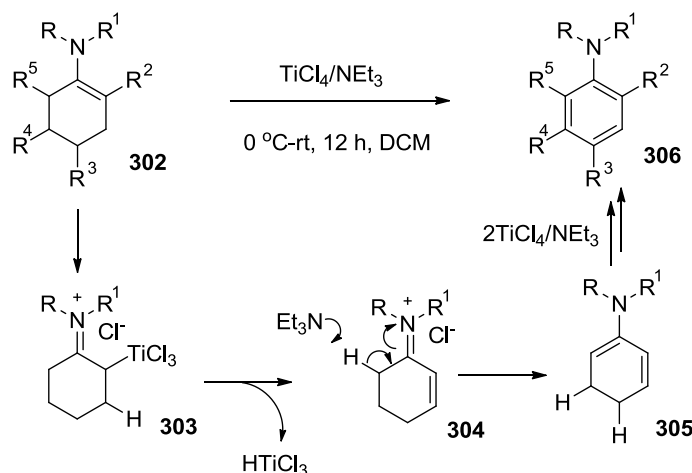


Scheme 82 – Imine formation conditions applied to benzyl ester **229**

Initially, the formation of the benzyl ester protected imine was attempted using the conditions that had provided the methyl congener (Scheme 82). However, the HPLC profile of this reaction showed considerably more impurities than the one with the methyl ester. A significant quantity of impurity with mass MH⁺ = 646 was generated upon reaction quench. Isolation of this impurity by MDAP and analysis by NMR gave a complex spectrum which could not be assigned, but the lack of an oxazole C-H at ~8.4 ppm resonance was noticeable.



The imine above (**301**) is the proposed structure for this impurity; benzyl *D-allo-isoleucinate* has added to the oxazole in a manner similar to that seen in the formation of a previously observed 1,4-addition product (**252**) (Section 3.2.1, page 71). Rather than ring opening to provide an acetamide (**252**), it is proposed that the compound undergoes re-aromatization facilitated by the reduction of TiCl_4 to TiCl_3 in a manner similar to that described by Srinivas and Periasamy (Scheme 83).¹⁴² Further reaction optimization was required in order to prevent the formation of this impurity.

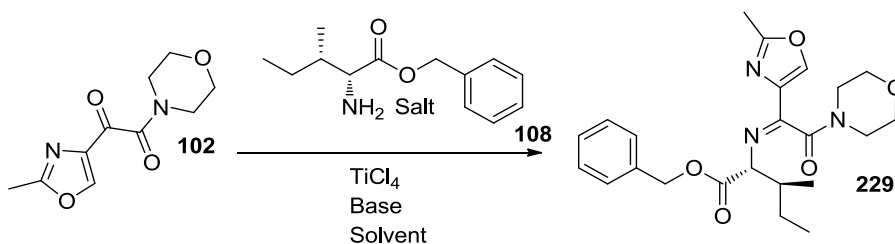


Scheme 83 – Aromatisation of enamines using $\text{TiCl}_4/\text{NEt}_3$ ¹⁴²

Imine formation from the methyl ester was carried out predominantly using the *D-allo-isoleucine* freebase, so this was the first modification to the conditions to be tried with the benzyl ester. Generation of the benzyl *D-allo-isoleucinate* free base was readily achieved by washing a toluene solution with dilute K_2CO_3 and drying by azeotropic distillation, but no improvement in the reaction profile was observed. The use of benzyl *D-allo-isoleucinate* hydrochloride was investigated, but again, no significant

3. Results and Discussion Part 1; A New Route to GSK221149

improvement in the reaction profile was observed. Further investigative work was therefore carried out with the more readily available *p*-TSA salt. Significant improvement was observed when the base was switched from triethylamine to TMEDA, accompanied by longer reaction time. It is thought that coordination of the TMEDA to the highly electron deficient titanium tempers its reactivity and gives milder reaction conditions, and hence a better purity profile. Pleasingly, an improvement in the reaction profile was observed when performing the reaction in toluene rather than dichloromethane. Toluene is preferred over dichloromethane for use at scale, because of easier waste disposal and lower environmental impact. The results described above are summarised below (Table 13).



Scheme 84 - Investigation of benzyl ester imine formation conditions

Solvent	Base	Base Equivs	Amine Version	229 (% a/a)	Rxn time
THF	NEt ₃	3	<i>p</i> -TSA	41.1	5 min
DCM	NEt ₃	4	<i>p</i> -TSA	62.2	5 min
DCM	NEt ₃	3	Freebase	66.2	5 min
DCM	TMEDA	2.5	<i>p</i> -TSA	77.2	2 h
DCM	TMEDA	2.5	HCl	77.4	2 h
Toluene	TMEDA	2.5	HCl	88.7	2 h
Toluene	TMEDA	2.5	<i>p</i> -TSA	87.3	2.5 h
Toluene	TMEDA	2.0	<i>p</i> -TSA	76.0	2.5 h

Table 13 – Investigation of benzyl ester imine formation conditions

3.7.4 Characterisation of the Imine (229)

Once the imine could be formed successfully in acceptable purity, further studies were performed on the material. In particular, we were interested in how the *E/Z*-ratio might affect selectivity or reaction rate during the reduction. It seemed likely that only one of the isomers would be reduced rapidly, making interconversion between isomers crucial for an acceptable reaction rate. In order to assess this turnover rate, the mixture of imines was separated by high pH mass directed preparative HPLC and the eluent solutions were analysed by the equivalent high pH HPLC method at regular intervals.

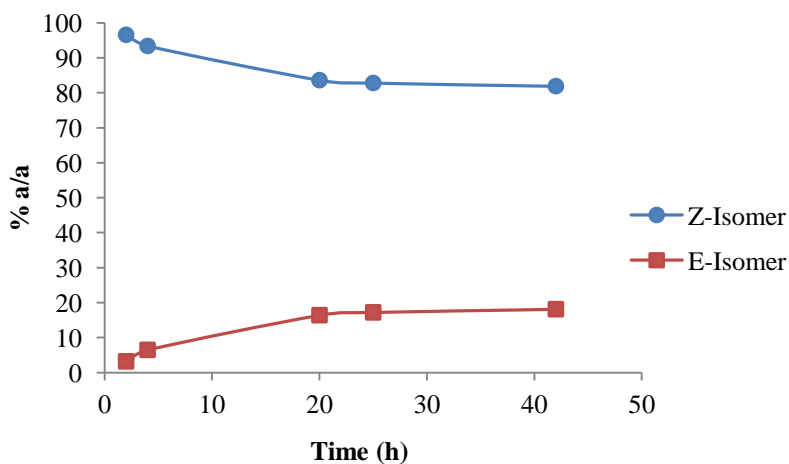


Figure 26 – Equilibration of Isomer 1

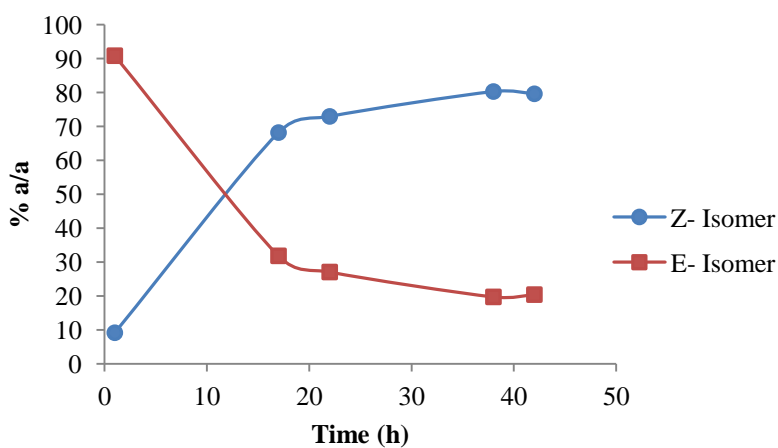


Figure 27 – Equilibration of Isomer 2

3. Results and Discussion Part 1; A New Route to GSK221149

The analysis showed that the equilibrium ratio of approximately 4:1 was reached after 40 hours at ambient temperature in an acetonitrile/ammonium bicarbonate (10 mM aqueous solution) buffer, but this is likely to be dependent on the solvent system. In order to assess the effect which imine isomerisation has on the reduction reaction, the equilibration rate in the reaction medium would need to be assessed.

We were also interested in the geometry of the two isomers and specifically whether differences existed between the methyl and benzyl esters. A sample of partially equilibrated imine was analysed by ROESY and the spectrum is shown (Figure 28). Peak assignments were made based on analysis of ^1H NMR data of the isolated imines.

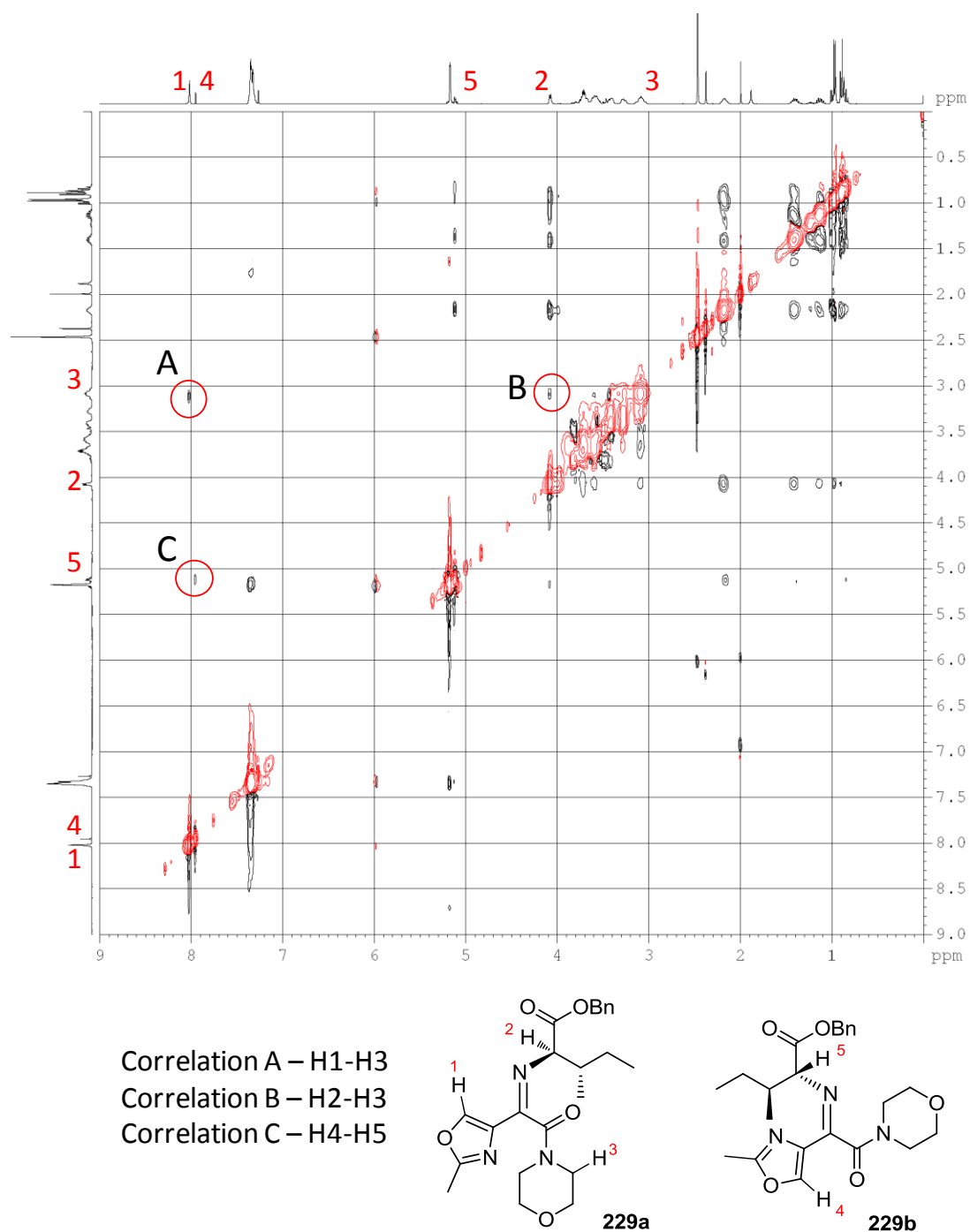
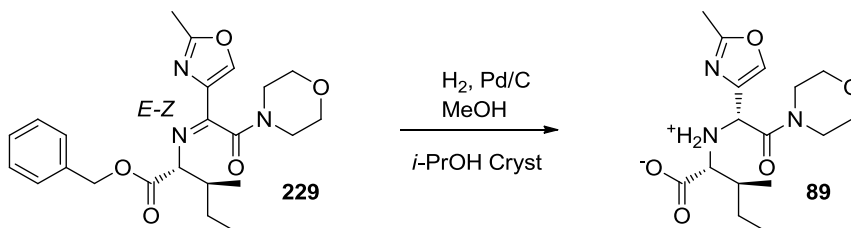


Figure 28 – ROESY spectrum of partially equilibrated imines

Similar correlations can be observed for the benzyl variant as were seen for the methyl ester imine (**110**). It appears that the *E*-imine (**229b**) is formed more rapidly, but the *Z*-imine (**229a**) is more stable, presumably for similar reasons to those discussed in section 3.2.4.

3.8 Catalytic Hydrogenation of the Benzyl Ester Protected Imine

With a way of making the benzyl imine (**229**) in acceptable purity in hand, attention shifted to the reduction by catalytic heterogeneous hydrogenation. Application of the conditions which were used successfully to hydrogenate the methyl ester protected imine (**110**) (3.5 bar H₂, 0.5 wt 10% Pd/C (50% wet), 25 °C, MeOH) were also effective in reducing the imine and cleaving the benzyl ester to generate the zwitterion (**89**) directly.



Scheme 85 – Heterogeneous imine hydrogenation

The desired diastereoisomer could be crystallized from the mixture of diastereoisomers in *i*-PrOH directly from the hydrogenation, with no SPE required. Unfortunately, the imine formation afforded a 5:4 mixture in favour of the undesired diastereoisomer (-10% *de*), which limited the yield of the reaction; only 26% was isolated. It is presumed that the increased steric bulk or electronic properties of the benzyl ester influences the binding mode of the catalyst causing the change in selectivity. A number of reactions were performed to investigate whether the selectivity was affected under other heterogeneous reaction conditions.

Rxn	Solvent	Catalyst	Temp	Pressure	111 (% a/a)	de (%)
1	EtOH	Pd/C – E101	25 °C	3 bar	33	-17.6
2	EtOH	Pd/C – E101	25 °C	1 bar	32	-13.6
3	EtOH	Pd/C – E101	50 °C	1 bar	33	-14.3
4	EtOH	Pd/C – 39	25 °C	3 bar	27	-23.5
5	EtOH	Pt/C – B103032	25 °C	3 bar	1.5	N/A
6	EtOH	Rh/C – 592	25 °C	3 bar	11	-16.3
7	EtOH	Rh-Ru/C - 118072	25 °C	3 bar	2.7	N/A
8	EtOH	Rh/Alumina	25 °C	3 bar	4	N/A
9	EtOH	Pd(OH) ₂	25 °C	3 bar	26	-10.5
10	EtOH	Pd/C - Type 457	25 °C	3 bar	26	-20.5
11	PhMe	Pd/C - E101	25 °C	3 bar	2.6	-17

* A negative value of *de* denotes preference for the undesired diastereoisomer

Table 14 – Investigation of heterogeneous hydrogenation

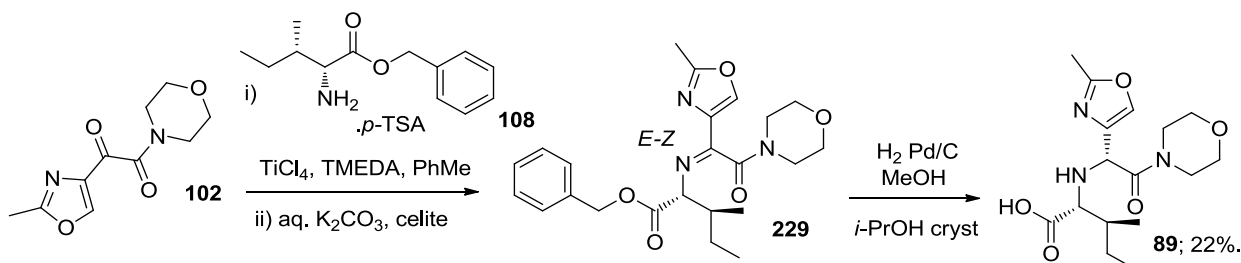
A range of different Pd/C types were screened, with no significant effect on the selectivity of the imine reduction. Neither temperature, pressure nor solvent had significant effects. Alternative metals were largely unsuccessful as catalysts, and although some reduction was observed with Rh/C, no change in selectivity was seen. These results prompted us to abandon heterogeneous hydrogenation and focus in more detail on asymmetric homogeneous catalysis.

3.8.1 Scale Up of Benzyl Ester Protecting Group Route

Prior to starting investigations into asymmetric hydrogenation, it was decided to scale up the chemistry despite having shown that a heterogeneous hydrogenation would be low yielding and therefore ultimately not a viable long term option. Such a scale-up is a useful exercise as, not only does it instil confidence that the route is able to provide

3. Results and Discussion Part 1; A New Route to GSK221149

material in quantity, but that it also allows the material to be progressed to API on a representative scale, allowing important purity data to be generated. A large (50 g) batch of the ketoamide (**102**) was taken through the benzyl route to give the amino acid (**89**) in 22% yield (Scheme 86); the intermediate was elaborated to API *via* the existing acyl transfer chemistry.



Scheme 86 – Scale up of imine formation and reduction with benzyl ester

The scale-up of both imine formation and reduction proceeded as expected; however, the acyl transfer chemistry afforded a low (26%) yield of product. The cause of this is currently being investigated.¹⁴³ Despite this low yield, material of good purity was produced and progressed to API, with the chemistry also performing as expected. The material was analysed using the API release HPLC method¹³⁵ and the results are shown (Table 15).

Peak Name	RRT	Peak Area (%)
RRT = 0.74	0.74	0.07
Diastereoisomer pair 2 (273 , 274)	0.67	<0.05
Diastereoisomer pair 5 (279 , 280)	0.78	ND
Diastereoisomer pair 6 (281 , 282)	0.88	<0.05
Diastereoisomer pair 7 (283 , 284)	0.97	<0.05
GSK221149	1.00	99.9
RRT = 1.22	1.22	0.06

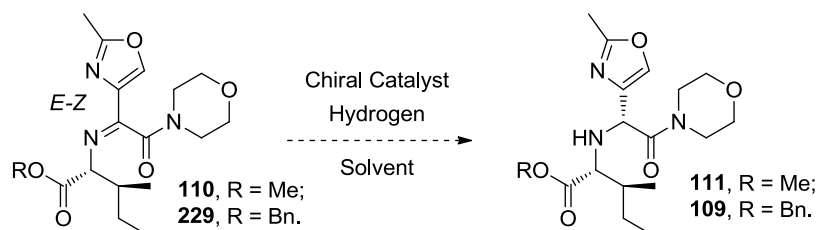
Table 15 – Analysis of GSK221149 derived from the benzyl protected route

3. Results and Discussion Part 1; A New Route to GSK221149

The purity of this material was considerably higher than the API derived from the route from the methyl ester (Table 10) and exceeded the current API specification. With only this single data point available, it is unclear why this material is of higher purity than previous material. In order to make an accurate assessment, more sensitive analytical methods were required to probe the purity of the intermediates, particularly the purity of the amino acid (**89**). Nonetheless, this result represented an important step for the project. It showed that API of sufficiently high purity to exceed specification can be generated from the new route and facilitated the decision to continue work to develop the route. Work now focussed on the development of asymmetric hydrogenation conditions.

3.9 Catalytic Asymmetric Hydrogenation of the Imine

As the selectivity of imine hydrogenations with heterogeneous catalysts had been unaffected by a range of catalyst types and reaction conditions, it was decided to investigate the use of chiral homogenous catalysts to try to improve the selectivity (Scheme 87). Expertise and the facilities for the rapid screening of catalytic reactions exists at a partner GSK site. It was therefore decided that the initial reaction screens and investigations should be performed using that facility.



Scheme 87 – Proposed asymmetric reduction reaction

3.9.1 Initial screens¹⁴⁴

Initially, reaction screens were run using the imine methyl ester substrate (**110**) as the work was carried out prior to the knowledge that this substrate would be difficult to progress. The first reaction screen focused on iridium catalysts. These have been shown to be highly active in reductions of related imines¹⁴⁴ and the study aimed to identify the ligands that were most effective in giving good conversion and high diastereoselectivity. Dichloromethane was chosen as the solvent, to give the best chance for dissolution of a wide range of catalysts, and the reactions were run at high pressure (30 bar) to ensure adequate concentrations of dissolved hydrogen in the reaction mixtures. This type of strategy is commonplace when screening for catalytic reaction conditions. The initial screens sought conditions that would deliver high conversion; potential for scale up was not a primary consideration at this time.

The strategy for screening a large number of categoric factors such as ligands or solvents is to use the mathematical technique known as principal component analysis (PCA) in order to group the items under investigation by properties or combinations of properties.

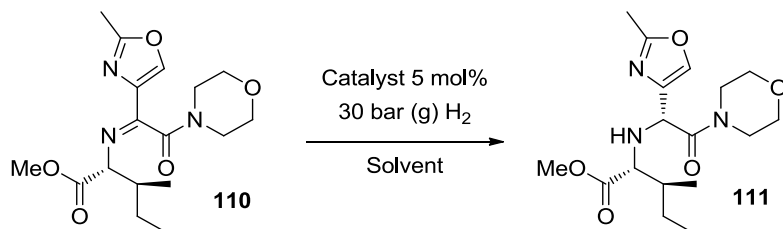
3. Results and Discussion Part 1; A New Route to GSK221149

Principal component analysis is a mathematical technique by which a large number of potentially correlated variables are reduced to a smaller number of uncorrelated variables (principal components) in order to expose the main factors underlying the variability contained within the data set. For example, phosphine ligands can be described in a number of ways according to various calculated and measured properties (including bite angle, dihedral angle, electron density *etc.*). As the high dimensionality of these variables makes visualisation difficult, PCA condenses these variables down to three dimensions which can be plotted and readily visualised. Ligands that are alike can be found grouped in the same area of the 3D plot. By selecting ligands from across the principal component space, diversity in the ligand set can be ensured without the need to screen every ligand available. If ligands from a particular area in the PCA space prove to be effective in the desired transformation, the remainder of the ligands in that particular space can be screened in subsequent experiments in order to find the most effective.

Unfortunately, the first screen yielded no hits; product was not observed in any of the reactions. This meant that the PCA results could not be modelled and the approach was not taken further in this instance. In order to identify successful reaction conditions the scope of the screen was widened to include different metals in combination with a number of solvents at elevated temperature (Table 16). In order to keep the number of experiments to a manageable level, 8 ligands which had been noted to be particularly effective in related transformations were selected. Product was not observed in any of the reactions using rhodium catalysts with these ligands, nor when a number of pre-prepared 2nd generation Noyori-type ruthenium catalysts were employed.^{99,145,146} However 1st generation Noyori-type catalysts,^{72,147} which differ from the 2nd generation variants by the lack of an additional chiral diamine ligand, showed some conversion to product. During the first experiment (*S*)-BINAP was the only ligand of this type to be screened. This gave exclusively the undesired diastereoisomer in low yield when run in dichloromethane. Reaction did not occur in THF and higher conversion, but lower selectivity was observed in toluene. It is not unsurprising that high selectivity is observed in the system which results in low conversion as there may be insufficient energy for the non-preferred reaction to occur. Immediately, the antipodal (*R*)-BINAP

3. Results and Discussion Part 1; A New Route to GSK221149

was screened, and similar conversion and high selectivity for the required stereoisomer was observed.¹⁴⁴ This confirmed the anticipated presence of double stereodifferentiation with the chirality in (*R*)-BINAP being matched with the inherent chirality of the substrate.



Scheme 88 – Initial asymmetric hydrogenation screen conditions¹⁴⁴

Metal	Ligand	Solvent	Temp	Conversion	<i>de</i> (%)
Ir(COD)BARF	48 across PCA	DCM	25 °C	0%	N/A
Ir(COD)BARF	8 ligands	DCM, MeOH, THF, PhMe	50 °C	0%	N/A
Rh(COD) ₂ BF ₄	8 ligands	DCM, MeOH, THF, PhMe	50 °C	0%	N/A
Ru	2 nd gen. Noyori†	DCM, MeOH, THF, PhMe	50 °C	0%	N/A
[Ru (<i>p</i> -cymene)Cl ₂] ₂	1 st gen. Noyori (<i>S</i>)-BINAP	DCM	50 °C	30%	<-99%*
[Ru (<i>p</i> -cymene)Cl ₂] ₂	1 st gen. Noyori (<i>S</i>)-BINAP	THF	50 °C	0%	N/A
[Ru (<i>p</i> -cymene)Cl ₂] ₂	1 st gen. Noyori (<i>S</i>)-BINAP	PhMe	50 °C	76%	-50%
[Ru (<i>p</i> -cymene)Cl ₂] ₂	1 st gen. Noyori (<i>R</i>)-BINAP	PhMe	50 °C	94%	>99%

* -*de* denotes preference for undesired diastereoisomer

† - refers to complete catalyst system

Table 16 – Initial asymmetric hydrogenation screens¹⁴⁴

3. Results and Discussion Part 1; A New Route to GSK221149

From here a much larger range of 39 ligands was screened using 1st generation Noyori conditions in an attempt to explore the ligand scope and find the most active catalyst system. These experiments yielded a set of six ligands which gave over 90% conversion to product all with undetectable levels of the undesired diastereoisomer.

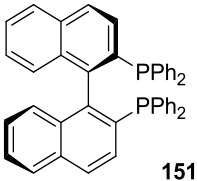
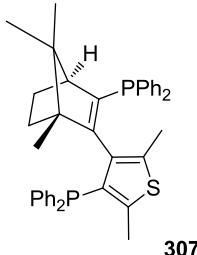
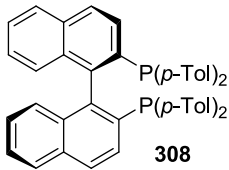
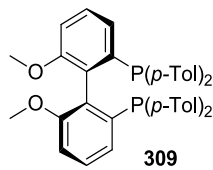
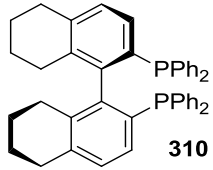
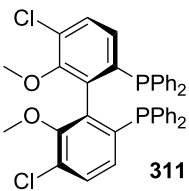
Ligand	Conversion (%)	de (%)	Ligand	Conversion (%)	de (%)
 (R)-BINAP	93.7	>99%	 catASium® T1	92.5	>99%
 (R)-Tol BINAP	95.6	>99%	 (R)-Tol MeO-BIPHEP	92.7	>99%
 (R)-H₈ BINAP	96.9	>99%	 (R)-Cl-OMe-BIPHEP	87.2	>99%

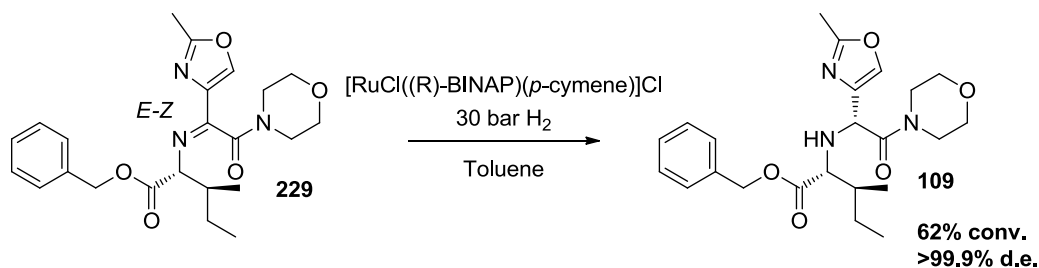
Table 17 – 1st generation Noyori screen¹⁴⁴

These results show that it is likely that a process suitable for large scale use could be developed. However, it became clear that use of the methyl ester was not a viable strategy due to the difficulty in isolating a zwitterion from the aqueous solvent system required for the hydrolysis of a methyl ester. Attention turned to the benzyl ester

3. Results and Discussion Part 1; A New Route to GSK221149

substrate which had already proven useful in non-stereoselective reductions. Application of the successful 1st generation Noyori (*R*)-BINAP conditions to the benzyl ester substrate showed lower conversion, but the same high selectivity. Unlike in the heterogeneous hydrogenation conditions, the benzyl ester was not cleaved using the homogeneous catalysts; a separate benzyl cleavage step would be required to provide the amino acid (**89**).

It is not immediately obvious why the benzyl substrate is so much less reactive than the methyl ester, but there are two hypotheses. Firstly, and most simply, the increased steric bulk of the benzyl group may inhibit coordination to the metal centre. Secondly, η^6 -coordination of the benzyl group to the catalyst could inhibit catalytic activity. This type of coordination to Ru is commonly observed and is exemplified by the commercially available Ru source $[\text{Ru}(\eta^6\text{-}p\text{-cymene})\text{Cl}_2]_2$.



Scheme 89 – Application of (*R*)-BINAP conditions to benzyl ester substrate¹⁴⁴

In an attempt to improve the conversion of the reaction, a factor screen was carried out.¹⁴⁴ This screen investigated the effects of ligand, solvent, reaction concentration, pressure and temperature. Solvents and ligands were investigated using a Latin square design¹⁴⁸ so that each solvent was combined with each ligand in order to identify any unique combinations that performed well. Typically, these type of experimental designs are not used due to the χ^n dependence on the number of individual experiments which must be performed, but they are useful when unique, interactions between categorical factors may exist and give rise to well performing reactions. The ligands selected were previously shown to be effective for the methyl ester substrate, and the solvents were selected to cover a wide range of PCA space (DCM, EtOH, trifluoroethanol, trifluorotoluene, toluene and DME). Statistically, the most significant factor affecting

3. Results and Discussion Part 1; A New Route to GSK221149

the reaction conversion was the solvent, with DME shown to be most effective. The ligand was also influential with Cl-OMe-BIPHEP (**311**) and H₈-BINAP (**310**) effecting the highest conversion. Higher conversion was also observed at 50 °C, but pressure and dilution were not found to be statistically significant over the ranges investigated (15 – 30 bar & 0.12 – 0.23 M). However, significantly lower conversion was observed when the reaction was run at 5 bar. This posed a problem due to the lack of high pressure hydrogenation equipment available on scale within GSK.

Lig/Solv	311	308	309	307	310	151
Toluene	α	β	χ	δ	ε	φ
TFT	β	χ	δ	ε	φ	α
EtOH	χ	δ	ε	φ	α	β
DCM	δ	ε	φ	α	β	χ
DME	ε	φ	α	β	χ	δ
TFE	φ	α	β	χ	δ	ε
	α	β	χ	δ	ε	φ
Temp (°C)	50	25	50	25	50	25
Pressure (bar)	30	30	30	15	15	15
Concentration (M)	0.12	0.12	0.12	0.23	0.23	0.23
Conversion	> 75%	25 - 50%	1 - 25%	0%		

Table 18 – Latin square design ¹⁴⁴

3.9.2 Investigation into Lower Pressures

With the initial screens and some optimisation of the asymmetric reduction performed at our partner site, the investigation of the reaction returned to the Stevenage site. Our main goal was to find conditions which allowed the reaction to be run at pressures lower than 5 bar. The reason for this is primarily the availability of large scale high pressure hydrogenation apparatus is limited. Although hydrogenation plant can be found which operates at extremely high pressures, it is much less readily available than equipment designed to run at more moderate pressures (< 5 bar). The first set of hydrogenation reactions investigated were therefore run at 4 bar.

Solvent	Temp	Ligand	109 @ 4 h (% a/a)	109 @ 28 h (% a/a)	313 @ 4h (% a/a)
Toluene	50	(<i>R</i>)-BINAP	4.2	9.0	9.2
Toluene	80	(<i>R</i>)-BINAP	16.5	23.3	22.6
Toluene	50	(<i>R</i>)-H ₈ BINAP	9.6	11.2	17.8
Toluene	80	(<i>R</i>)-H ₈ BINAP	19.2	20.3	29.4
DME	50	(<i>R</i>)-BINAP	X	X	X
DME	80	(<i>R</i>)-BINAP	26.5	30.8	19.6
DME	50	(<i>R</i>)-H ₈ BINAP	27.8	27.5	11.1
DME	80	(<i>R</i>)-H ₈ BINAP	31.4	32.5	23.4

Table 19 – Hydrogenation investigation at 4 bar

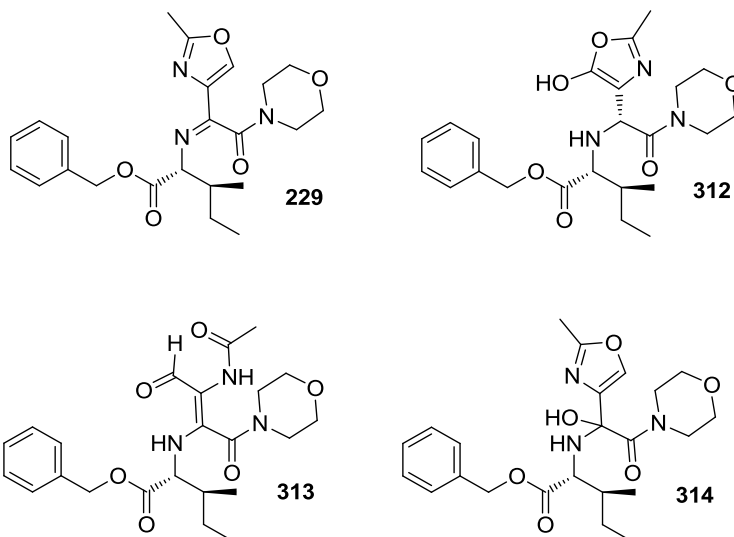
As with previous experiments, the diastereoselectivity was excellent (>99%), and the best results were obtained with (*R*)-H₈ BINAP (**310**) as the ligand and DME as solvent. Some conversion was observed with both (*R*)-BINAP (**151**) and toluene. The increase in temperature above that investigated in the initial screens was significant in giving higher conversion. However, the most striking observation was the generation of high levels of

an impurity which appeared to have a mass of 18 mass units higher than that of the starting imine, by LCMS.

3.9.3 Characterisation of Impurity 313

It was important to isolate and characterise this impurity since it was being formed in such high levels; at this stage of the synthesis impurity formation could jeopardise the entire route. Elucidation of the structure of the impurity may allow control of its formation to be achieved.

Initial LCMS data showed the molecular ion to be 445, 18 mass units higher than the imine (**229**) (mwt = 427); overall addition of water to the molecule would cause this +18 mass increase. Three potential structures (**312** - **314**) were proposed.



It was envisaged that water could be adding to the oxazole (its electrophilic nature when adjacent to a carbonyl has already been shown (section 3.2.1) and then either re-aromatising to afford hydroxyl oxazole (**312**), or ring opening to afford an acetamide (**313**). Alternatively, a simple hemi-aminal (**314**) could be present, but this was deemed unlikely due to the stability of the compound to TFA modified preparative HPLC during initial attempts to isolate it.

3. Results and Discussion Part 1; A New Route to GSK221149

In previous screens,¹⁴⁴ this impurity formed quantitatively in alcoholic solvents, and so methanol was employed to allow access to larger quantities of the impurity. Though the compound could be purified to a single peak by HPLC (Figure 29), a number of components seemed present by NMR (Figure 30) which hampered characterisation.

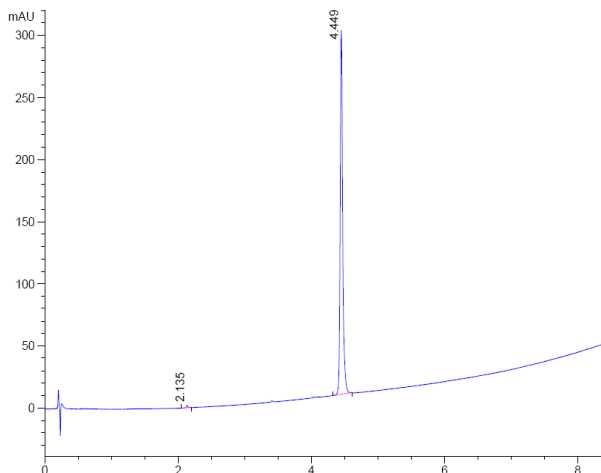


Figure 29 – HPLC of impurity 313

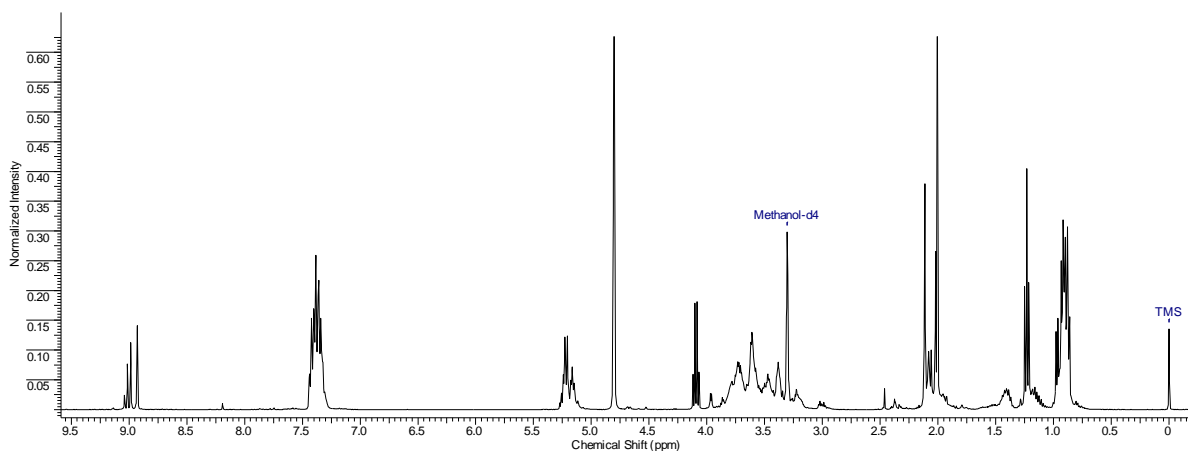


Figure 30 - ¹H NMR of impurity 313

However, the absence of oxazole protons at $\delta = 8\text{--}8.5$ ppm was immediately noticeable, which enabled the hemi-aminal structure (**314**) to be discounted. A chemical shift of 2.0–2.1 ppm rather than 2.4–2.5 ppm is more consistent with the presence of an acetamide than an oxazole methyl group (c.f. compounds **252** and **229**). This prompted an investigation into the possibility of structures similar to **313**, rather than a hydroxy-oxazole (**312**). The HSQC spectrum confirms the absence of oxazolyl protons and shows

3. Results and Discussion Part 1; A New Route to GSK221149

that the protons at $\delta \sim 9$ ppm correlated with carbons with shifts of $\delta \sim 190$ ppm, characteristic of an α,β -unsaturated aldehyde,¹⁴⁹ thus providing further evidence for the ring opened structure such (313).

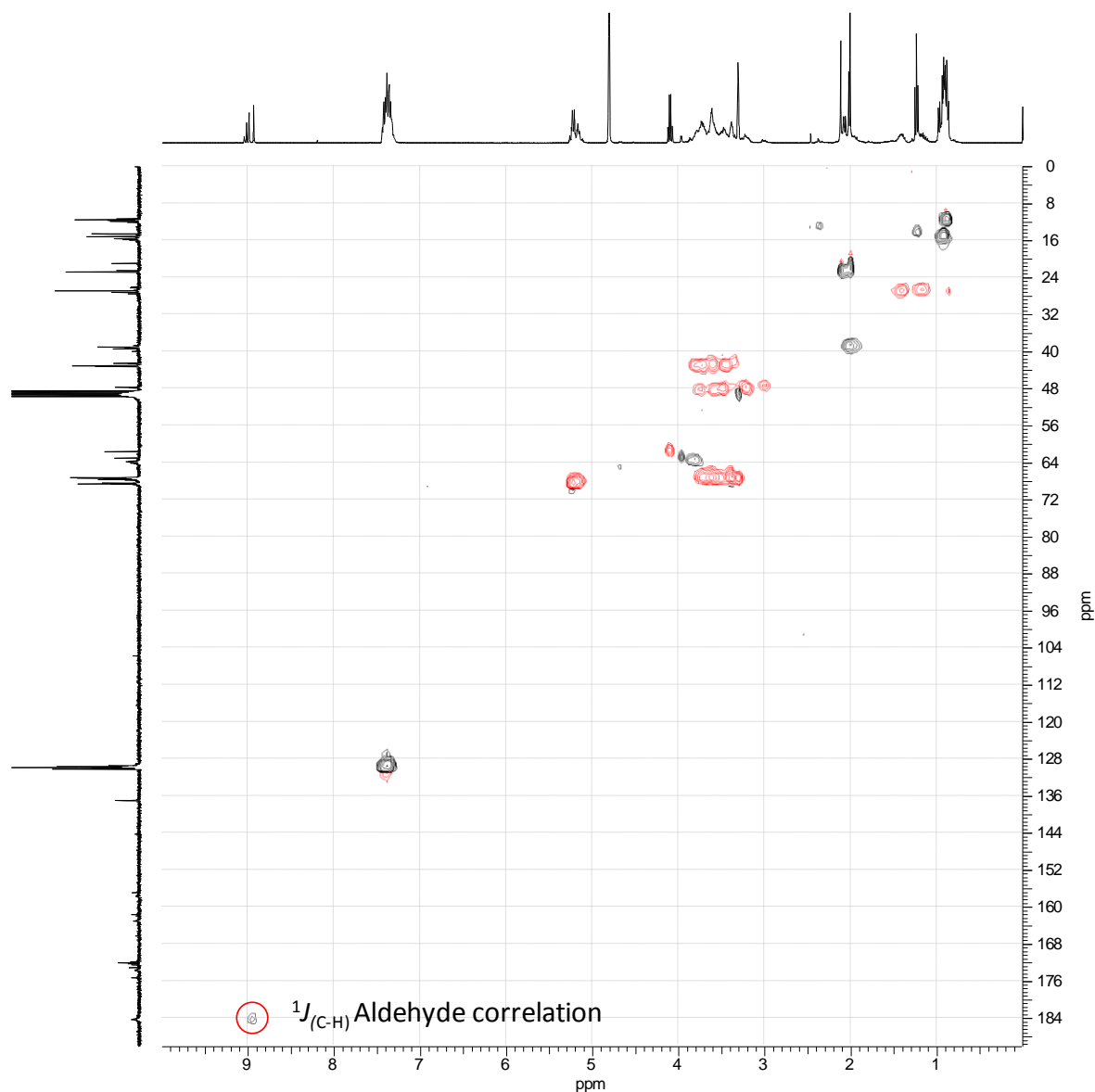
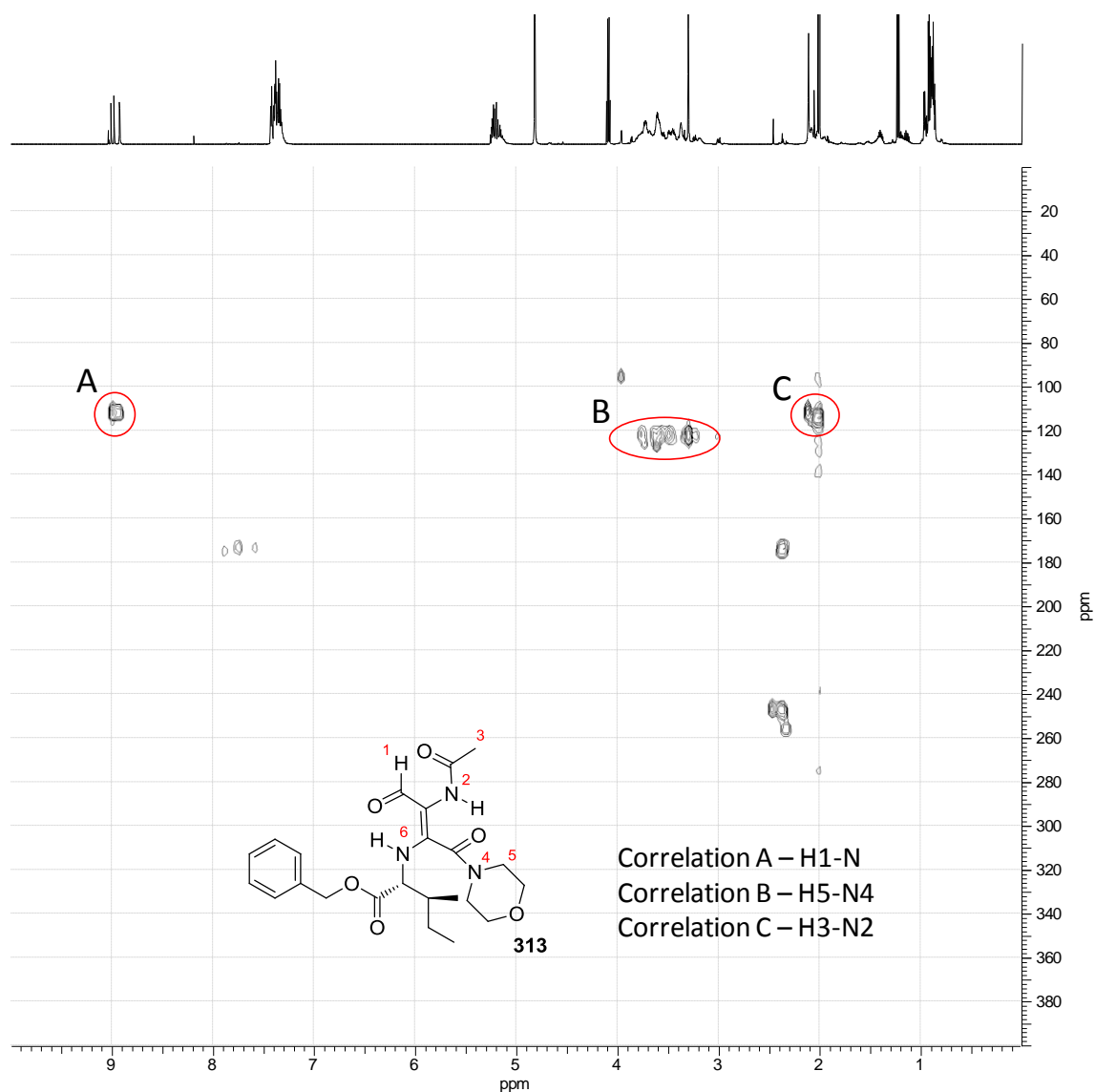


Figure 31 – HSQC of impurity 313

The most compelling evidence for ring opening comes from the $^1\text{H} - ^{15}\text{N}$ HMBC experiments which clearly show the disappearance of the oxazolyl nitrogen at 250 ppm, replaced by a resonance at 114 ppm which is characteristic of an amide. These observations led us to propose the following structure for the impurity (313).

Figure 32 – ^{15}N HMBC of impurity 313

A number of inconsistencies remain unexplained. Firstly, protons 1 and 3 correlate to different nitrogens ($\delta_{\text{N}} = 111$ ppm and 114 ppm). Whilst this is possible, as $^4J_{(\text{N-H})}$ correlations which would allow H1 to correlate to N6 can occur, particularly in ^{15}N HMBC, it seems unlikely that a $^3J_{(\text{N-H})}$ correlation between H1 and N2 would not occur. Secondly, the presence of multiple components by NMR remains unexplained. However, it is possible that two components could arise from *cis* and *trans* double bond isomers, with the presence of either amide rotamers or *isoleucine* diastereoisomers accounting for the other resonances.

3. Results and Discussion Part 1; A New Route to GSK221149

Variable temperature NMR experiments showed coalescence of some resonances to give a slightly simplified spectrum, but no further conclusions could be drawn. Variable temperature ^{15}N HMBC would be required to gain further information.

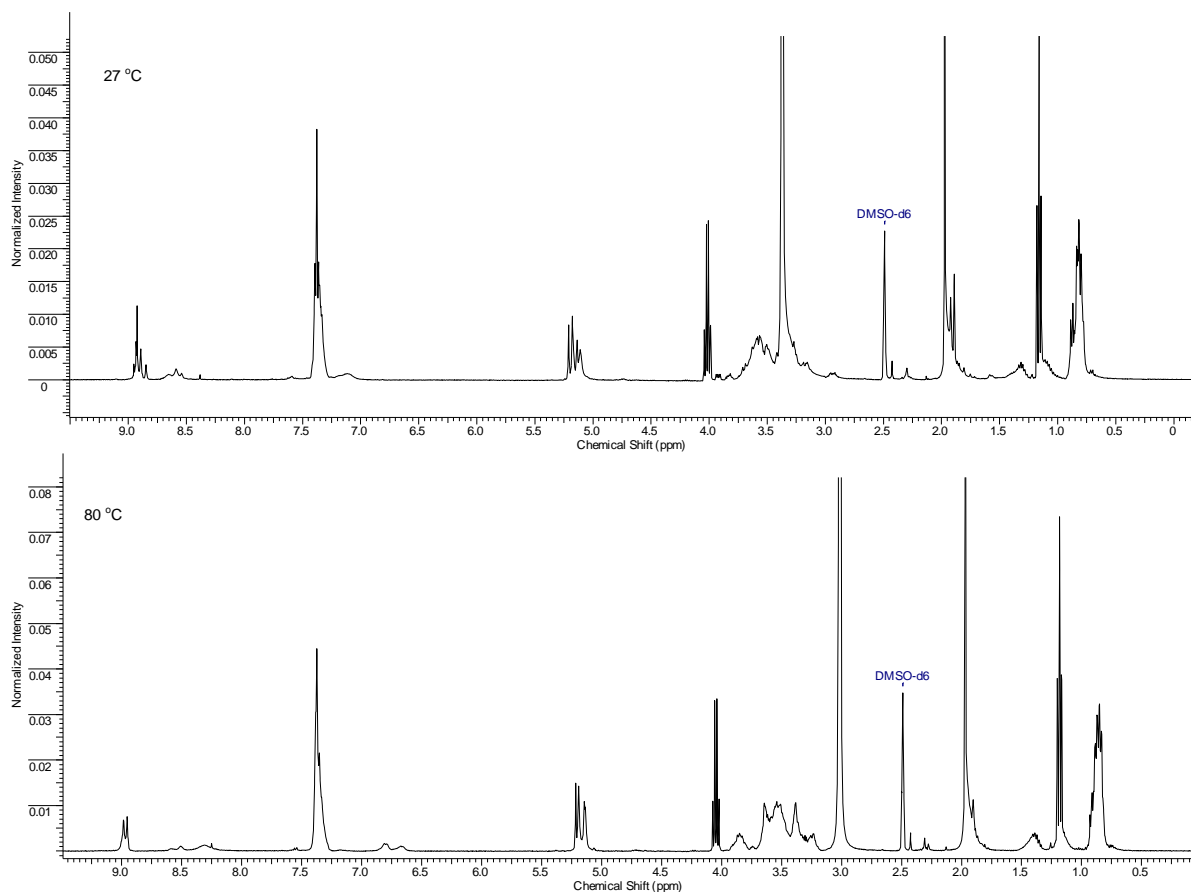


Figure 33 – Variable temperature NMR of impurity 313

Assuming that our tentative structure for the impurity was correct, strict exclusion of water from the reaction mixture should prevent its formation. Spiking water into reactions gave an increase in levels of the impurity, providing further evidence. However, strict exclusion of water from the reactions was difficult to achieve using our available laboratory hydrogenators which use hydrogen generated from the on-line electrolysis of water. This hydrogen is invariably wet, despite attempts to dry it using activated molecular sieves or silica gel dessicants. Small hydrogen lecture bottles were attached to the hydrogenator in order to provide dry hydrogen, but this showed no real effect in lowering the levels of the impurity (**313**) when running optimised reaction

3. Results and Discussion Part 1; A New Route to GSK221149

conditions. As the use of dry hydrogen could not completely eliminate the formation of the impurity (**313**), it was presumed that the source of the adventitious water was the solvent. The DME was analysed by Karl Fischer and found to contain 469 ppm (0.047% w/w) water, which equates to 15 mol% at the current reaction dilution. This appears to fit well with the observed levels of impurity observed in reactions run using dry hydrogen (*Catalyst A; [RuCl((R)-SEGPHOS)(*p*-cymene)]Cl

Table 20).

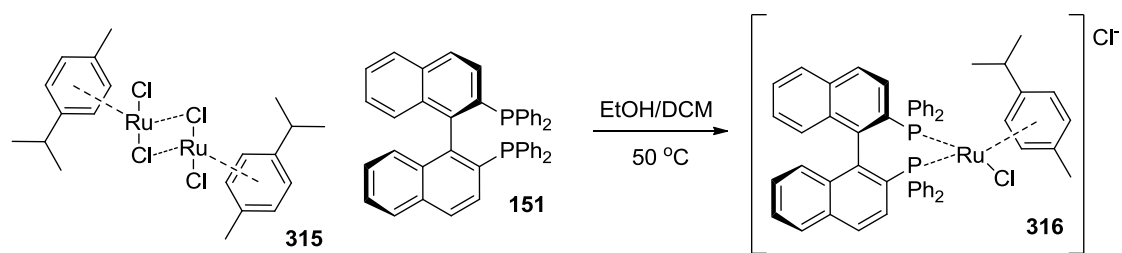
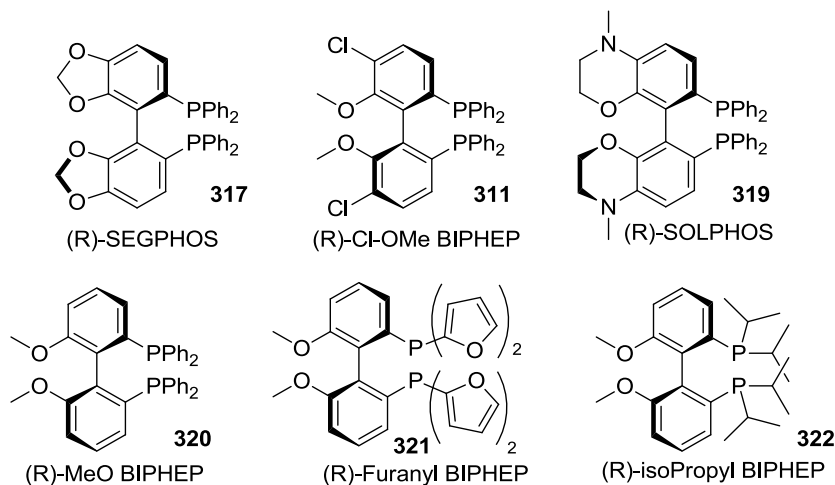
Catalyst*	Solvent	Pressure	Hydrogen	109 (%a/a)	313 (%a/a)
A	DME	4 bar	Generator	38.2	9.4
A	DME	4 bar	Generator 5 equiv water	13.8	32.4
A	DME	4 bar	Bottle (dry)	46.3	10.7

*Catalyst A; [RuCl((R)-SEGPHOS)(*p*-cymene)]Cl

Table 20 – Effect of water on +18 impurity 165

3.9.4 Further Catalyst Screening

The conversion of the imine (**229**) to the amine (**109**) under these revised conditions was still disappointingly low and significant improvements would be required before a cost effective process was available. This is particularly true given the current high (5 mol%) catalyst loading required. Further ligands and pre-catalysts were screened in attempt to increase the catalytic activity, and allow catalyst loading to be reduced. A ligand set (**317-322**) was chosen based primarily on the basis of structural similarity to the hits from the initial screens. As pre-formed catalysts of the 1st generation Noyori type were not readily available, the ligands were purchased and the pre-catalysts made in the laboratory according to a procedure used in the initial screens¹⁴⁴ which was based on literature precedent.¹⁵⁰

Scheme 90 – Preparation of 1st generation Noyori pre-catalysts

(*R*)-SEGPHOS (**317**) was of particular interest due to the commercial availability of both the ligand and pre-formed catalyst on large scale. Two reactions were run using this catalyst; the first used commercially sourced pre-catalyst and the second material made in the laboratory. The latter would serve as a control for the other catalysts, which were all made in the laboratory. The Cl-OMe BIPHEP ligand (**311**) was selected because it was observed to be one of the better ligands in previous screens. We wanted to confirm these results and observe how this ligand behaved at lower (< 5 bar) pressures. SOLPHOS (**319**) was included due to structural similarity with the existing hits and availability. The remaining ligands (**320-327**) would allow us to probe the structure activity relationship around the pendant groups on phosphorus in more detail. A reduction in conversion had been observed as more bulky pendant groups on phosphorus had been used with (*R*)-BINAP based catalysts in the initial 1st generation Noyori screens (with the methyl ester substrate); this is exemplified by the use of (*R*)-Xylyl BINAP (**151**) which gave < 70% conversion compared to (*R*)-BINAP which gave > 90% conversion. We were interested to see if moving to pendant groups with even lower

3. Results and Discussion Part 1; A New Route to GSK221149

steric bulk raised the conversion. This seemed feasible, particularly if the increased bulk of the benzyl substrate was responsible for the poor reactivity compared to the methyl ester. The ligands based on MeO BIPHEP (**320-322**) are commercially available, and (*R*)-Tol-MeO BIPHEP (**309**) had been shown to be effective previously (Table 17). It was therefore decided to use this template to probe the question, the results are shown below (Table 21).

Entry	Ligand	Solvent	Pressure	Temp	109 (%a/a)	229 (%a/a)	313 (%a/a)
1	317^a	DME	4 bar	80°C	36.4	4.7	17.2
2	317^b	DME	4 bar	80°C	16.3	7.5	34.1
3	311	DME	4 bar	80°C	0.7	23	29.1
4	319	DME	4 bar	80°C	5.4	7.4	-
5	320	DME	4 bar	80°C	16.1	12.3	28.9
6	321	DME	4 bar	80°C	43.2	6	9.7
7	322	DME	4 bar	80°C	1.1	36	28.2

* a. Commercial material. b. Made in house

Table 21 – Catalyst screen

Significantly, a large difference in the profile of the reactions in entries 1 and 2 was observed; the difference between them being only that entry 1 was catalysed by commercially acquired SEGPHOS based catalyst whilst entry 2 was catalysed by material prepared in the laboratory. There was no obvious reason as to why this should be the case. Similarly, the catalyst system based on Cl-OMe BIPHEP (**311**) showed poor activity despite high conversions being observed in previous screens. Further investigation into these results are required. The results also show that the furanyl ligand (**321**) gave the highest conversion of the catalyst systems based on MeO BIPHEP (**320-322**), with the phenyl derived ligand (**320**) showing moderate activity and the *iso*-propyl derived ligand (**322**) having poor activity. It is possible that reducing the steric bulk of

the ligand does indeed increase catalytic activity, however, with such a limited data set, no firm conclusions can be drawn. Nonetheless, the furanyl MeO BIPHEP ligand (**321**) and phenyl MeO BIPHEP ligand (**320**) should be investigated in more detail, along with SEGPHOS (**317**).

3.9.5 Catalyst Characterisation

Due to the apparently capricious nature of the SEGPHOS-mediated hydrogenation reaction, it was decided to investigate the structure and purity of the pre-catalyst. It was initially hypothesised that aerial oxidation of the phosphorus ligand in the laboratory-made batch of catalyst was the reason for poor activity, and therefore analysed the material by ^{31}P NMR in an attempt to observe such a species. The analysis of $[\text{RuCl}((R)\text{-BINAP})(p\text{-cymene})]\text{Cl}$ was in agreement with that reported in the literature⁶⁹ and the presence of oxidised species was not identified. $[\text{RuCl}((R)\text{-SEGPHOS})(p\text{-cymene})]\text{Cl}$ was also analysed by ^{31}P NMR and the spectrum is shown (Figure 34).

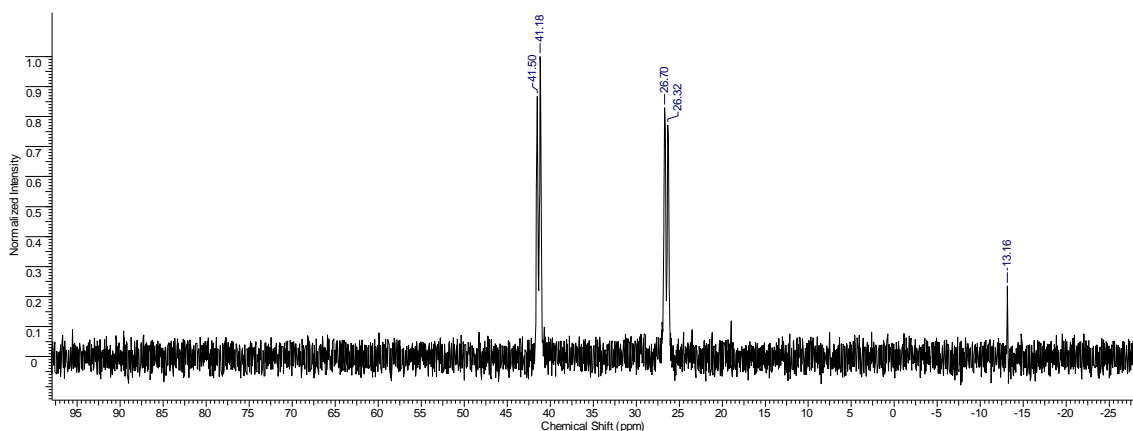


Figure 34 – ^{31}P $\{^1\text{H}\}$ NMR of $[\text{RuCl}((R)\text{-SEGPHOS})(p\text{-cymene})]\text{Cl}$

The presence of the two phosphorus environments at $\delta = 41.3$ and 26.5 ppm indicates that the ligand has bound to the metal centre. The appearance of doublets supports this, as they can only be formed by $^2J_{\text{P-P}}$ coupling through the metal centre. In addition, free ligand gives a single phosphorus signal at $\delta = -13.2$ ppm (a small quantity of unbound ligand can be observed in the above spectrum). There is no evidence for the presence of oxidised ligand, and the spectrum is concordant with that of the commercially made

3. Results and Discussion Part 1; A New Route to GSK221149

catalyst. A second batch of catalyst was synthesised in the laboratory, in air, rather than under the strict anaerobic conditions used for the first batch. This second batch was analysed by ^{31}P NMR and found to be almost identical to the first. When applied to the hydrogenation reaction, its reactivity was comparable to that of the commercial material (Table 22).

Catalyst*	Other	Solvent	Pressure	Temp	109 (%a/a)	229 (%a/a)	313 (%a/a)
A	Ex Aldrich	DME	4 bar	80°C	38.2	22.5	9.4
A	Prepared under air	DME	4 bar	80°C	39.8	26.9	8
A	Prepared anaerobically	DME	4 bar	80°C	22.5	38.3	7.3

*Catalyst A; $[\text{RuCl}((R)\text{-SEGPHOS})(p\text{-cymene})]\text{Cl}$

Table 22 – Effect of catalyst preparation

The reasons for the differences in behaviour between these samples, identical by ^{31}P NMR, remain unclear.

3.9.6 Investigation into the Pre-catalyst Species

Until the reasons behind the capricious nature of the hydrogenation reaction could be resolved, it was decided to investigate pre-cursors to the same active catalyst. Genet *et al.*¹⁵¹ had shown that the pre-catalyst species influenced the kinetic profile of asymmetric β -ketoamide hydrogenation reactions considerably, so similar species using the commercially available SEGPHOS variants were investigated (Table 23).

Catalyst	Solvent	Pressure	Temp	109 (% a/a)	229 (% a/a)	313 (% a/a)
A	DME	4 bar	80°C	38.2	22.5	9.5
B	DME	4 bar	80°C	17.1	19.4	17.7
C	DME	4 bar	80°C	-	75.2	-

*Catalyst **A**; [RuCl((*R*)-SEGPHOS)(*p*-cymene)]Cl, Catalyst **B**; [NH₂Me₂][(RuCl((*R*)-SEGPHOS))₂(μ-Cl)₃], Catalyst **C**; [RuCl(OAc)₂((*R*)-SEGPHOS)]Cl.

Table 23 – Effect of different pre-catalysts

This study clearly showed that η⁶-cymene pre-catalyst gave the highest conversion during the 20h reaction. [RuCl(OAc)₂((*R*)-SEGPHOS)]Cl (**A**) showed no activity whatsoever, possibly because the acetate groups are bound too tightly to dissociate and give the active catalytic species. [NH₂Me₂][(RuCl((*R*)-SEGPHOS))₂(μ-Cl)₃] (**B**) was also shown to be inferior to [RuCl((*R*)-SEGPHOS)(*p*-cymene)]Cl (**C**). Conversion to product was lower and levels of impurities were higher. Therefore, it was decided to focus on the [RuCl((*R*)-SEGPHOS)(*p*-cymene)]Cl pre-catalyst species, but investigate other variables which may be able to increase the conversion.

3.9.7 Return to Increased Pressure

With a number of variables investigated, and in the absence of a clear way of increasing activity further, attention turned back to the reaction pressure in attempt to increase conversion. An hydrogen cylinder was connected to the parallel hydrogenator enabling the pressure to be increased to 8 bar.

Catalyst	Solvent	Pressure	Temp	109 (%a/a)	313 (% a/a)
A	DME	4 bar	80 °C	46.3	10.7
A	DME	6 bar	80 °C	40.0	12.7
A	DME	8 bar	80 °C	51.0	6.0
A	PhMe	8 bar	80 °C	34.5	16.1

*Catalyst A; [RuCl((*R*)-SEGPHOS)(*p*-cymene)]Cl.

Table 24 – Effect of pressure

Raising the pressure does increase the product peak area but there still appear to be some anomalies. However, in toluene, the conversion does not increase with pressure. It was hypothesised that the conditions used above are too forcing since the imine (**229**) is completely consumed, yet only 50% a/a product is present. It is probable that the temperatures required to give activity also give decomposition of the starting material or product, particularly over prolonged reaction times (20 h).

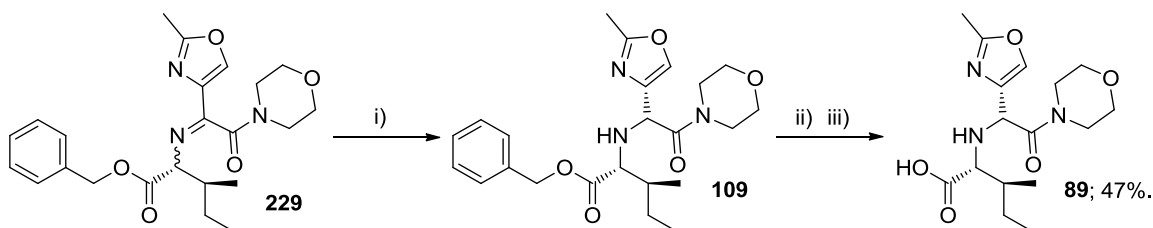
3.9.8 Wider Solvent Screen¹⁴⁴

It is possible that interaction effects between solvent and catalyst could occur in this type of hydrogenation, leading to some unique well performing combinations. In order to investigate this, a wider range of solvents were screened against seven of the best performing ligands.¹⁴⁴ To our surprise, all the reactions performed poorly, even the previously successful (*R*)-SEGPHOS/DME combination. One variable which had changed since the previous screens was the equipment in which the reactions were run. A switch had been made to smaller vials to enable more rapid screening of a large number of reactions and it was postulated that this was the cause of the poorly performing reactions. In smaller vials the gas-liquid mass transfer will necessarily be lower than with larger vials since the surface area to volume ratio is lower and the agitation is also less effective. It was believed that this property, known as k_La (the

volumetric mass transfer coefficient) which correlates with mixing and is characteristic for different vessels at set agitation rates, was the issue. In order to test this, three identical reactions were performed in different sized vials for which the relative $k_L a$ can be estimated. As expected, the vial with the lowest $k_L a$ showed the poorest conversion. In order to understand this dependence further, studies need to be conducted in equipment in which the $k_L a$ has been characterized. A large batch of imine was prepared and dispatched to a partner site which has the facility to perform such experiments.

3.9.9 Scale-out of the Asymmetric Reduction of Imine 229

We wanted to scale our preferred conditions in order to confirm the reaction yielded the correct product and to assess its purity. It was decided to ‘scale out’ rather than scale up the experiment due to the potential dependence on the mass transfer of the reaction system. Five identical reactions were run in parallel hydrogenation equipment, then combined and hydrogenated over Pd/C to cleave the benzyl ester. The crude amino acid (**89**) was crystallised from *i*-PrOH in 47% yield and > 99% a/a by generic HPLC.



i) $[\text{RuCl}((R)\text{-SEGPHOS})(p\text{-cymene})]\text{Cl}$, 8 bar H_2 , DME, 80 °C, 18 h; ii) Pd/C, 1 bar H_2 , MeOH 20 °C, 30 min; iii) *i*-PrOH crystallisation.

Scheme 91 – Scale out of asymmetric reduction

The material was analysed by a more specific HPLC method to determine its isomer content (section 3.10) and by ICP-AES to determine levels of ruthenium. The ruthenium concentration in the product was measured at 1300 ppm (for comparison, the level of metals in API would need to be controlled to < 20 ppm). However, these levels should be achievable with sufficient process development and, for an early attempt, this yield and purity was good enough for progression. The crucial property of this reaction is its

dependence on the $k_{L}a$ described earlier (section 3.9.8). If the reaction cannot be run at $k_{L}a$ values readily achievable in large scale plant, then the whole synthetic route may not be a feasible alternative to the existing Ugi chemistry.

3.9.10 Investigation of the Hydrogenolysis of Imine **229** at a Defined $k_{L}a$

The $k_{L}a$ of a reaction system is characteristic of a particular vessel at a defined vessel fill level and agitation rate. It can be readily calculated for a given system by measuring the rate of hydrogen dissolution in solvent; the larger the gas liquid mass transfer coefficient ($k_{L}a$), the faster the rate of hydrogen uptake. This is practically performed by charging the vessel in question with solvent to the required fill level, pressurising with H₂, commencing agitation and monitoring the decrease in pressure within the system. This procedure has been performed for a number of vessels at our partner site and our hydrogenation was studied using one of these vessels.¹⁵² The reaction was performed on 50 mL scale (3.33 g imine **229**) with an agitation rate of 815 rpm corresponding to a $k_{L}a$ of 0.15, a value which can typically be achieved in large scale hydrogenators. Pleasingly, the reaction appeared to perform similarly to the previous system used to scale out the reaction. Although the impurity (**313**) was present, its levels were not elevated.

The effects of catalyst load and pressure on the reaction were then studied using the same equipment at 50 mL scale. The hydrogen uptake could be readily plotted over the course of the reaction using this same equipment, and the data gathered is shown (Figure 35, Table 25). It was observed that complete conversion to the amino ester (**109**) could be achieved with minimal formation of the impurity (**313**) by increasing the catalyst loading two-fold to 10 mol %. Interestingly, hydrogen pressure appears to have only a minimal influence over the reaction rate when 10 mol % catalyst loadings are used. It was hypothesised that under these conditions the reaction the rate is limited by the gas-liquid mass transfer. However, pressure does appear to influence the rate of reaction when the catalyst loading is returned to 5 mol %. Here it is believed that the reaction rate becomes limited by the kinetics of the catalytic cycle. Under these conditions, increasing

3. Results and Discussion Part 1; A New Route to GSK221149

the reaction pressure increases the equilibrium concentration of hydrogen in solution and therefore increases the reaction rate. It was proposed that the incomplete reaction observed is due to competitive catalyst degradation, and the generation of the impurity (313) by an un-catalysed process. Using higher catalyst loadings allows the reaction to proceed to completion before the concurrent catalyst degradation reactions have consumed the catalyst.

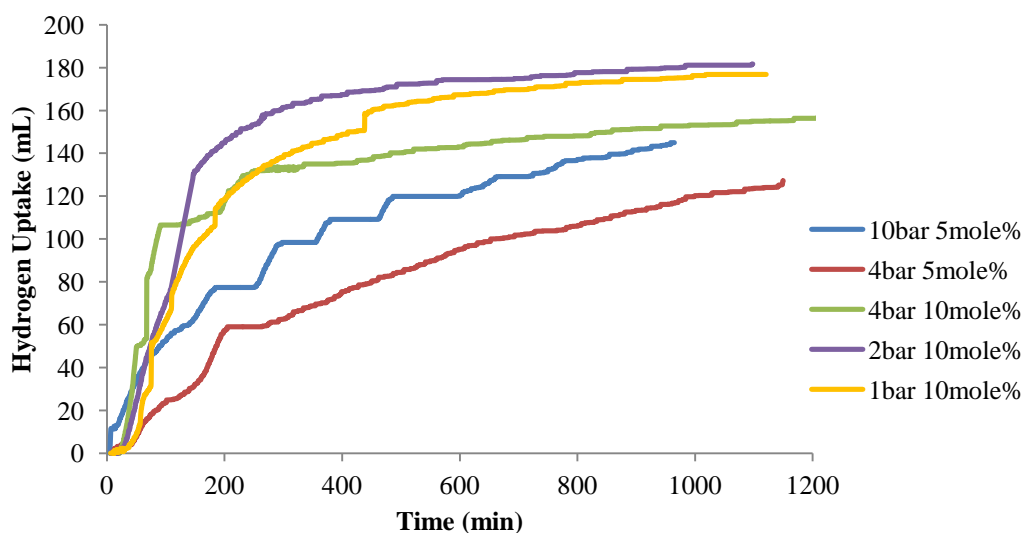


Figure 35 – Hydrogen uptake using varying catalyst loading and pressure¹⁴⁴

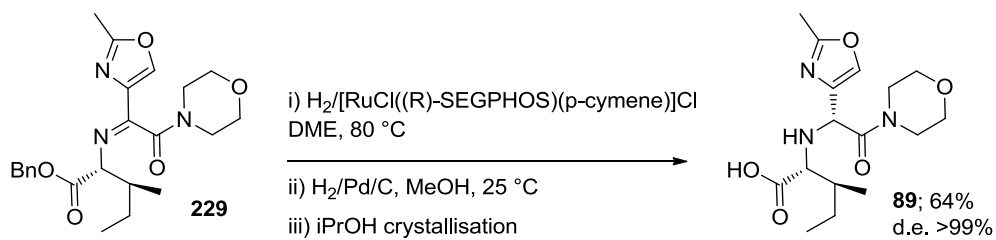
Entry	Conditions	HPLC profile
1	10 bar, 5 mol %	
2	4 bar, 5 mol %	
3	4 bar, 10 mol %	
4	2 bar, 10 mol %	
5	1 bar, 10 mol %	

Table 25 – HPLC profile using varying catalyst loading and pressure¹⁴⁴

The reaction was then scaled up to 39 g (91 mmol), knowing that the reaction could be performed at k_La values typically achievable in larger scale equipment. 10 mol % catalyst at 2 bar H₂ pressure was used and complete reaction in under 4 h was observed, with an isolated yield after de-benylation and crystallisation of 64% (Scheme 92). This pleasing result was indicative of the success of the development work. We now had a process with a viable yield, using a readily achievable temperature and pressure, and a commercially available catalyst (albeit using a loading). Moreover, the application of a 1st generation Noyori catalyst to the reduction of such a densely functionalised *N*-alkyl

3. Results and Discussion Part 1; A New Route to GSK221149

imine in high selectivity represents a significant contribution to the current state of the art. Additionally, this reaction has the potential to be useful in the synthesis of other functionalised aryl glycine derivatives.



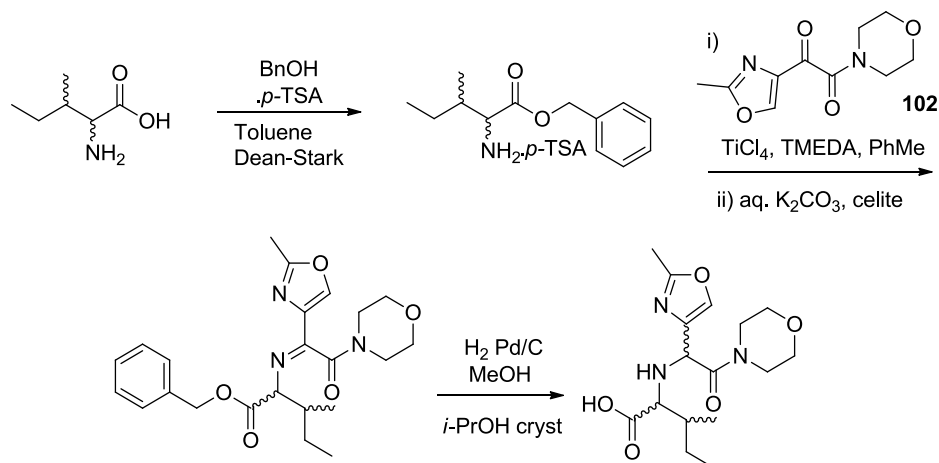
Scheme 92 – Asymmetric hydrogenation to provide amino acid 89

3.10 Analysis of the Amino Acid

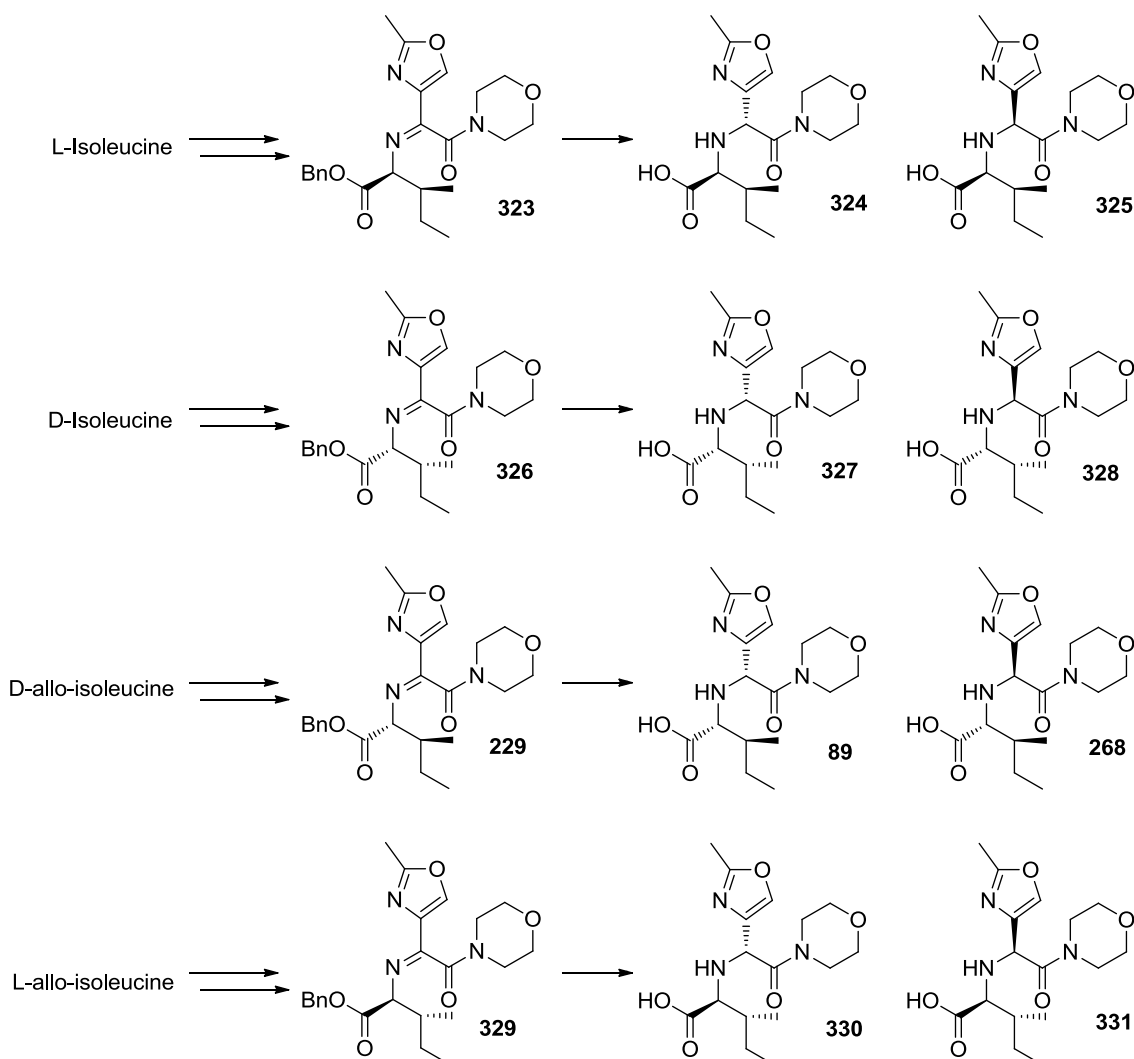
3.10.1 Preparation of Diastereomeric Amino Acids 324-331

In order to fully understand the purity profile of GSK221149 produced *via* a new route, particularly with respect to the isomeric contaminants, it is important to understand the purity profile of the intermediates. This allows understanding of the generation and fate of impurities throughout the route. The purity of the amino acid (**89**) is particularly important as this is the first stage at which solids are isolated after the introduction of the new chiral centre. It is also prior to the acyl transfer chemistry where precedent exists for the epimerisation of stereocentres within the molecule.³¹ The impurities of most interest are the diastereoisomers of the amino acid (**324** - **331**). A number of undesired diastereoisomers have been shown to be present within GSK221149, yet the formation of these impurities is not understood. An analytical method which can distinguish and quantify isomeric impurities in the amino acid would be a valuable tool in understanding the isomeric impurities in GSK221149.

Before an analytical method could be developed, samples of the impurities in question needed to be synthesised. In the case of this amino acid, 8 stereoisomers derived from *D* and *L* isoleucine and *allo*-isoleucine exist. They were synthesised in diastereomeric pairs as shown (Scheme 93, Scheme 94).



Scheme 93 – Synthesis of amino acid diastereoisomers



Scheme 94 – Preparation of *isoleucine* amino acid diastereoisomers

Esterification of the relevant *isoleucine* isomer with benzyl alcohol and *p*-TSA in toluene under Dean-Stark conditions provided the corresponding benzyl ester as its tosic acid salt. This was then taken through the developed imine formation conditions which performed equally well with each of the diastereoisomers. Hydrogenolysis over Pd/C provided diastereomeric pairs of compounds differing by their configuration around the newly created oxazole-bearing stereocentre. The pairs were separated by mass-directed preparative HPLC, but the stereochemical configuration at the oxazole bearing stereocentre was not determined.

The initial esterification reaction performed well with both L- and D- *isoleucine*, but failed with L-*allo-isoleucine* giving a number of unidentified products. It is thought that the scale of the reaction was the cause of this failure. Due to the high price and low quantities in which L-*allo-isoleucine* is available, the esterification reaction was performed only on a small scale (500 mg). The Dean-Stark process was inefficient on this scale and so the reaction time was longer than expected and decomposition of the materials was observed. This, however, did not pose issues in the preparation of suitable analytical markers for the development of an achiral analytical method. Since **89** and **331**, and **268** and **330**, are pairs of enantiomers and the same is true of **324** and **328**, and **325** and **327**, a representative selection of all 4 diastereoisomers can be obtained by simply combining the products produced from L-*isoleucine* and D-*allo-isoleucine* (**89**, **268**, **324** & **325**).

3.10.2 Analysis of the Diastereomeric Purity of Amino Acid **89**

A mixture of the key diastereoisomers (**89**, **268**, **324** & **325**) was prepared and analysed by HPLC (Method A); separation of the desired D-*allo-isoleucine* diastereoisomer from one of the L-*isoleucine* isomers could not be achieved, nor could it be separated using an extended 30 min HPLC method. However, separation was achieved using an alternative stationary phase.¹³⁵ Using the method developed, batches of material produced *via* three different routes was analysed for diastereoisomer content.¹³⁵ The first batch (entry 1) was produced *via* the methyl ester protected D-*allo-isoleucine*, with imine formation in dichloromethane using NEt₃ as base and reduction with H₂, Pd/C. The product was progressed to API to provide material containing a number of isomeric impurities (Table 10). The second batch (entry 2) was produced from the benzyl protected D-*allo-isoleucine* *via* imine formation in PhMe with TMEDA as base, followed by reduction over H₂, Pd/C. The product was progressed to API containing levels of diastereoisomeric impurities which meet specification (Table 15). The third batch (entry 3) was produced as above, but was reduced using the Ru-catalysed asymmetric

3. Results and Discussion Part 1; A New Route to GSK221149

hydrogenation conditions. Data for this batch is given for crude material (entry 3a) and after crystallisation (entry 3b) (Table 26).

Entry	Route	Isoleucine A* (% a/a)	Isoleucine B* (% a/a)	268 (% a/a)
1	Methyl - Crystallised	2.57	1.28	0.76
2	Benzyl (Pd/C) - Crystallised	0.09	0.16	2.51
3a	Benzyl (Asymmetric) - Crude	0.17	0.17	0.34
3b	Benzyl (Asymmetric) - Crystallised	<0.05	<0.05	<0.05

* Exact compound is undetermined **324-328**.

Table 26 – Isomer content of Amino acid batches

Pleasingly, crystallised material produced *via* the preferred asymmetric route showed no reportable diastereoisomer content. Using this more sensitive analytical method, the diastereomeric excess of crude material produced during the hydrogenation was measured to be 99.3%. Also pleasing were the low levels of contaminant isomers derived from L- (or D-) *isoleucine* in material produced by heterogeneous hydrogenation of the imine. The level of isomer **268** was expected; it was consistent with levels previously observed. It originates from imperfect diastereoisomer separation during the crystallisation. Interestingly, significant quantities of contaminant isomers were observed in the methyl ester derived material and this correlated well with the contaminant isomers in drug substance produced from it. It is known that the presence of contaminant isomers in API can arise from processing of the methyl ester and can hypothesise that the strongly basic conditions of the ester hydrolysis cause epimerisation of the α -stereocentre. Epimerisation of the β stereocentre to produce the observed diastereoisomer pair 7 (**283**, **284**) is more difficult to propose a reason for. It could be that differences in the imine formation conditions are responsible. Nonetheless, as it had been shown that the amino acid (**89**) produced *via* Pd/C hydrogenation of the corresponding benzyl protected imine (**229**) could be processed to give API within specification, and as amino acid derived from asymmetric reduction had an even better

3. Results and Discussion Part 1; A New Route to GSK221149

purity profile, we were confident that the new asymmetric hydrogenation conditions would also be able to provide API within specification.

3.11 Comparison of the Two Routes to GSK221149

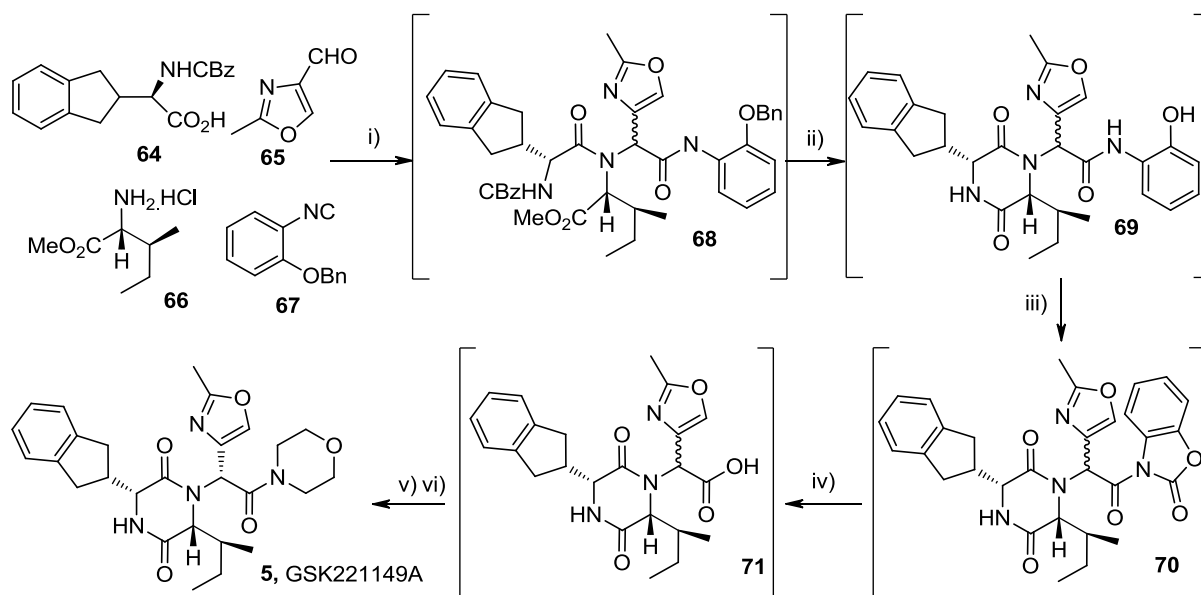
Ongoing development work has been performed on the new route by other members of the team to define processes which can be readily scaled.^{118,143} The key changes which significantly impact the yield of the products or manufacturability of the processes are described below.

The Claisen condensation and oxidation chemistry procedure has been modified to allow extraction of the ketonitrile Claisen condensation product (**122**) into aqueous solution, where the oxidation can be performed using OxoneTM. This greatly improves the manufacturability of the process since oxidations are inherently safer when performed in the absence of large amounts of organic solvents. Crystallisation conditions which allow direct isolation of the ketoamide (**102**) from the reaction mixture have also been developed. This allows the process to be scaled, since chromatography (used previously to isolate the product) is prohibitively expensive to perform on large scale. The robustness of the reaction has also been demonstrated across a range of factors. Despite this development work, the yield of the process (30%) remains low.

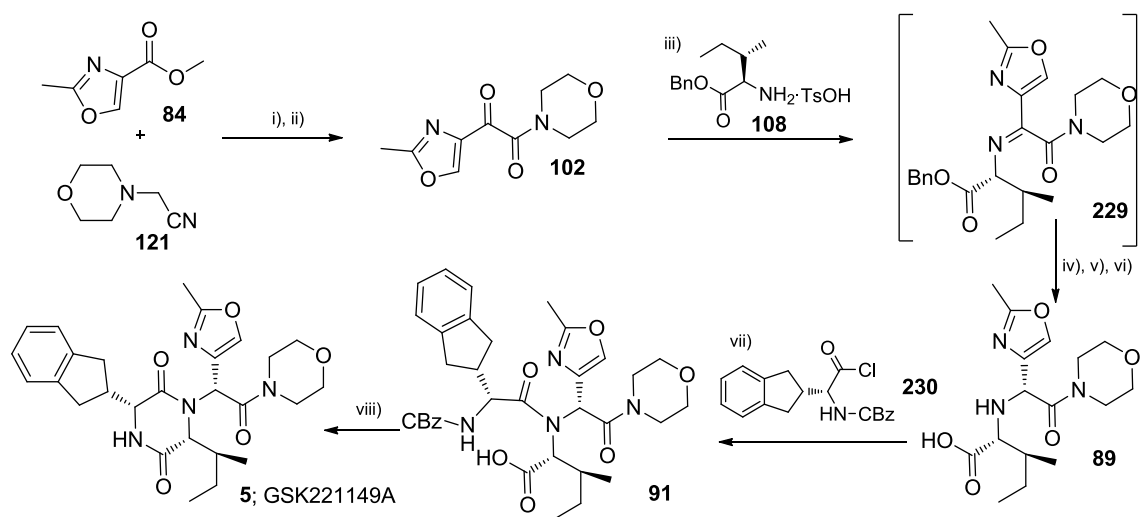
The acyl transfer chemistry has been modified, although a suitable alternative to Ghosez' reagent could not be found. The solvent was changed and the crystallisation improved by addition of an antisolvent and the process now reproducibly yields 75% of the cyclisation precursor (**91**) from the amino acid (**89**). The same antisolvent addition principle was applied to the final hydrogenation and cyclisation chemistry enabling isolation of API meeting specification in 96% yield for the single step.

During the time spent developing the new route chemistry, further developments were made to the existing Ugi route, principally in the development of stage 4, where conditions were defined which allowed the reaction to be run at -20 °C. Project timelines dictated that a decision between the two routes be made in order to prepare for an upcoming manufacturing campaign. The current state of the two routes were compared based on a number of factors (Table 27), with the main focus the cost of API produced *via* each of the two routes.

3. Results and Discussion Part 1; A New Route to GSK221149



Scheme 95 - Route A to GSK221149



Scheme 96 – New route to GSK221149

Property	Ugi Route	Reductive Amination Route
Number of stages	4	5
Yield from 64	27%	72%
Yield from 84	12%	13%
Yield from 66/108	27%	36%
Lowest temperature required	-20 °C	-20 °C
Hydrogenation	Yes (transfer)	x2
Isolated intermediates	None	2
Undesirable solvents	NMP	DME, dichloromethane
Cost of goods (materials)	£6000 kg ⁻¹	£6700 kg ⁻¹
Predicted processing costs	£3500 kg ⁻¹	£4900 kg ⁻¹
Predicted total API cost	£9500 kg ⁻¹	£11600 kg ⁻¹

Table 27 – Comparison of routes to GSK221149

Despite requiring a an extra synthetic step, the reductive amination route compares favourably to the Ugi route (Route A) in terms of yields, particularly based on the indanylglycne fragment (**64**) which is now introduced in the penultimate synthetic step. The yields from the oxazole ester (**84**) are comparable between routes since extra steps are required to reduce to the corresponding aldehyde (**65**) which is required in the Ugi reaction. Both routes require equipment capable of running at a minimum of -20 °C, a temperature which is generally achievable in general purpose plant and therefore causes no issues. Both routes require hydrogenation equipment and both routes use undesirable solvents, although further development work may allow these to be substituted. However, the cost of goods clearly favours the existing Ugi chemistry. Material costs are more than 10% lower than those of the reductive amination route. Processing costs are also predicted to be lower, primarily because of the smaller number of synthetic steps. Despite the increased yields, the reductive amination route is more expensive and this is

3. Results and Discussion Part 1; A New Route to GSK221149

primarily due to the ruthenium hydrogenation catalyst which, at £10000 kg⁻¹ using a 10 mol % loading, contributes to over 30% of the API cost of goods. Clearly, reducing the catalyst loading would enable the route to become competitive with the Ugi chemistry, but approaching a 10-fold reduction in catalyst loading would be required to achieve a real cost advantage.

3.12 Summary and Conclusions

This thesis has described the development of a new synthetic route to Oxytocin receptor antagonist GSK221149 which provides API within clinical specification in 42% overall yield from the ketoamide (**102**) (and 13% from oxazole ester **84**). The route utilises an expedient two step, one-pot process to synthesise an α -ketoamide (**102**) first described by Wang *et al.*⁵¹ The investigation into this reaction raises some interesting questions about the nature of oxidation of ketonitriles and 1,2-diones and it is postulated that a Baeyer Villiger type migration of an amide is taking place. Despite considerable improvements to the process,¹¹⁸ which now provides the ketoamide (**102**) in 30% yield from oxazole aldehyde *via* a method which could be readily scaled, the yield remains low.

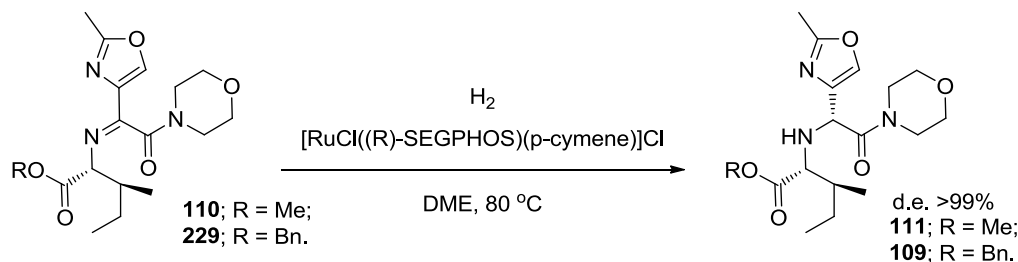
The key reaction in this new route to GSK221149, is the highly selective reduction of a sterically congested imine (**229**) using a first generation Noyori-type ruthenium catalyst. This application is unprecedented, and could find further utility in the synthesis of other *N*-functionalised arylglycine derivatives. The asymmetric reduction allows highly selective introduction of the oxazole-bearing stereocentre, something which the existing Ugi route lacks. However, the success of the reaction is dependent on a high loading (10 mol%) of the relatively expensive [RuCl(*R*)-SEGPHOS](*p*-cymene)]Cl catalyst which contributes significantly to the cost of goods. More generally, the asymmetric reductive amination route allows the late stage introduction of the key indanylglycine subunit (**64**), and provides opportunities to isolate crystalline intermediates, unlike the Ugi chemistry. Despite these advantages, there are still a number of hurdles which would need to be cleared for the asymmetric reductive amination route to be competitive, particularly in terms of cost. This is particularly the case in view of further improvements which have been made to the Ugi chemistry since this work was begun. For these reasons, investigations into the new, asymmetric reductive amination route to GSK221149 have been suspended.

4 Results and Discussion Part 2; Investigation of the Asymmetric Hydrogenation

4 Results and Discussion Part 2; Investigation of the Asymmetric Hydrogenation

4.1 Introduction

The asymmetric hydrogenation of imines remains a challenge despite significant advances being made in the last decade. This is particularly true for the hydrogenation of acyclic *N*-alkyl imines.⁶² More specifically, there are very few reports on the synthesis of chiral aryl glycine derivatives by asymmetric hydrogenation of the corresponding α -imino acid derivatives.¹⁵³ Amongst these there is only a single example of the hydrogenation of an α -imino amide,¹⁵⁴ and to the best of our knowledge no previous successful examples of *N*-alkyl α -imino amide reductions. During the work to develop an alternative route to oxytocin antagonist GSK221149, a highly selective ruthenium catalysed hydrogenation of an *N*-alkyl α -imino amide was discovered (Scheme 97).



Scheme 97 – Asymmetric hydrogenation of an *N*-alkyl α -imino amide in the synthesis of GSK221149

This reaction has the potential to be a useful method for the synthesis of a wide range of functionalised aryl glycine derivatives. Therefore, further mechanistic understanding into the origin of the selectivity and reactivity observed was sought. It was hoped that this mechanistic understanding would then allow the substrate scope to be broadened in order to develop a synthetically useful protocol for the synthesis of functionalised aryl glycine derivatives.

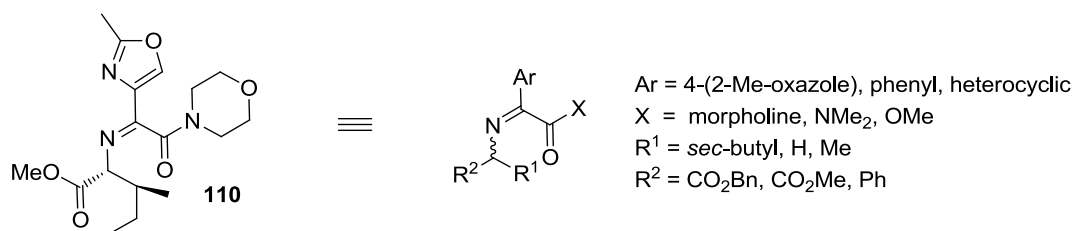
4.2 Research Plan

The initial aim was to explore the reaction scope by preparing a number of structurally related imines and testing them under the optimised asymmetric hydrogenation

4. Results and Discussion Part 2; Investigation of the Asymmetric Hydrogenation

conditions. This would allow the structural features key for the observed reactivity and selectivity to be determined. It was postulated that the highly functionalised nature of the substrate, particularly the density of heteroatoms, could lead to a complex mode of binding to the ruthenium metal centre. It was speculated that the reactivity or selectivity of the system could be significantly impacted by deletion of some key heteroatoms and this may allow hypotheses about the nature of binding to the catalyst to be made.

A number of points of diversity within the molecule were identified (Scheme 98), specifically, the nature of the aromatic substituent, the nature of the amide and the nature of the imine *N*-substituent. The nature of the imine *N*-substituent could be further broken down into the alkyl chain or the ester moiety. Some key changes were then proposed.



Scheme 98 – Points of diversity within the imine substrate

Substitution of the oxazole with other aromatic rings would allow the investigation of the effect of heteroatoms within the ring system and potentially expand the scope to a wider group of synthetically useful substrates. Substitution of the morpholine amide for other amides and esters would allow the structure activity/selectivity relationship to be probed. Substitution of the imine *N*-substituent would again allow us to probe the structure activity/selectivity relationship and may allow a number of other important questions relating to the selectivity of the reaction to be answered. A distinct match/match case between the chirality present in the *D-allo-isoleucine* moiety of the substrate and the (*R*)-enantiomer of the binaphthyl-derived catalyst had been observed, when compared to the opposite (*S*)-enantiomer. We were interested to substitute the *D-allo-isoleucine* with the achiral amino acid glycine to measure the inherent selectivity of the catalyst. Synthesis of substrates derived from amino acids of increasing complexity

4. *Results and Discussion Part 2; Investigation of the Asymmetric Hydrogenation* starting with alanine were then proposed, which would allow investigation of the influence of the bulky *sec*-butyl group upon the diastereoselectivity of the reaction.

Once the key functionality had been determined and some mechanistic insight gained, it was aimed to synthesise a number of further derivatives to demonstrate the scope of the reaction.

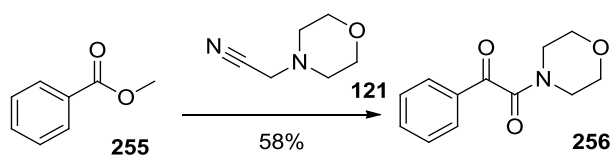
Markers of each of the diastereomeric products would be synthesised in parallel by reduction of the imines using Pd/C. These results could then be used to determine the *de* of the asymmetric reductions by HPLC. It was planned only to investigate the asymmetric hydrogenation under the optimised [RuCl(*R*)-SEGPHOS)(*p*-cymene)]Cl conditions in order to limit the number of variables.

4.3 Heterocycle Substitution

Firstly, the oxazole moiety was replaced with a simple phenyl group whilst retaining all the remaining functionality of the control substrate. This was the first point of investigation primarily because it was felt that the synthesis of aryl glycine derivatives had the greatest synthetic use and applicability in a wider sense. In addition, it was known from previous investigations into model imine formations (c.f. section 3.2) that the synthesis of phenyl imine derivatives was much easier than for their oxazole counterparts. It was hoped that this would allow for rapid generation of results. The strategy was therefore to synthesise a stock of the phenyl ketoamide (**256**) so that a range of phenyl-substituted imines could be prepared and assessed.

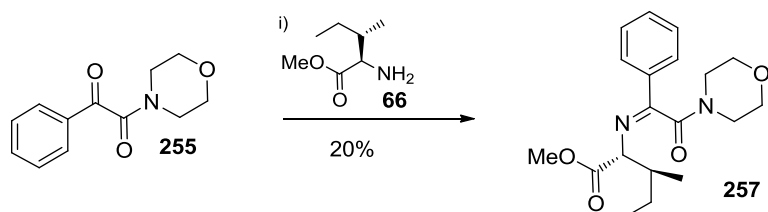
The optimised ketoamide formation conditions were used to provide **256** in moderate yield (Scheme 99) and the corresponding methyl ester protected imine (**257**) was prepared and purified by MDAP to ensure sufficient quality going into the hydrogenation.

4. Results and Discussion Part 2; Investigation of the Asymmetric Hydrogenation



i) NaHMDS, THF; ii) Oxone, Water.

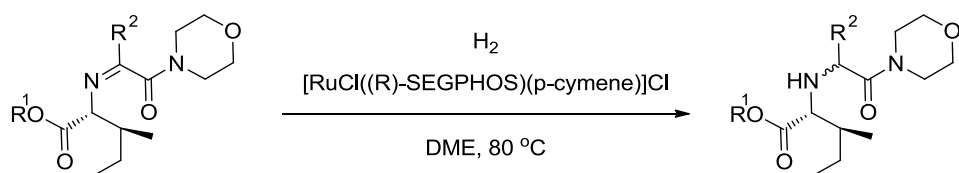
Scheme 99 – Synthesis of phenyl ketoamide 256



i) TiCl₄, TMEDA Toluene.

Scheme 100 – Synthesis of phenyl imine derivative 257

The substrates were subjected to hydrogenation under the optimised [RuCl((*R*)-SEGPHOS)(*p*-cymene)]Cl conditions along with freshly prepared samples of the benzyl and methyl ester protected oxazole imines (**110**, **229**) as positive controls. The results are shown (Table 28).



Imine	R ²	R ¹	Conversion	de (%)
110		Me	98%	>99%
229		Bn	64%	>99%
257		Me	0%	N/A

Table 28 – Asymmetric Hydrogenation

4. Results and Discussion Part 2; Investigation of the Asymmetric Hydrogenation

Somewhat unexpectedly, a complete lack of reactivity was observed for the phenyl substituted derivatives. Conversion to the desired amine was not observed despite the stability of the imines to the reaction conditions. The expected conversions for the control reactions demonstrated there was no issue with either the equipment or the catalyst.

It is possible that a secondary binding mode between the substrate and the catalyst metal centre was taking place. Binding of secondary functionality was observed by Noyori during his investigations into the asymmetric hydrogenation of β -ketoesters and is well documented.^{72,99,147} In these examples, the β -ester functionality co-ordinates to the metal centre giving a 6-membered chelate which facilitates both the reactivity and the selectivity of the reduction. Figure 36 shows the binding mode (**332**), and how it allows the (*R*)-BINAP ligand to exert its stereochemical influence during the transition state.

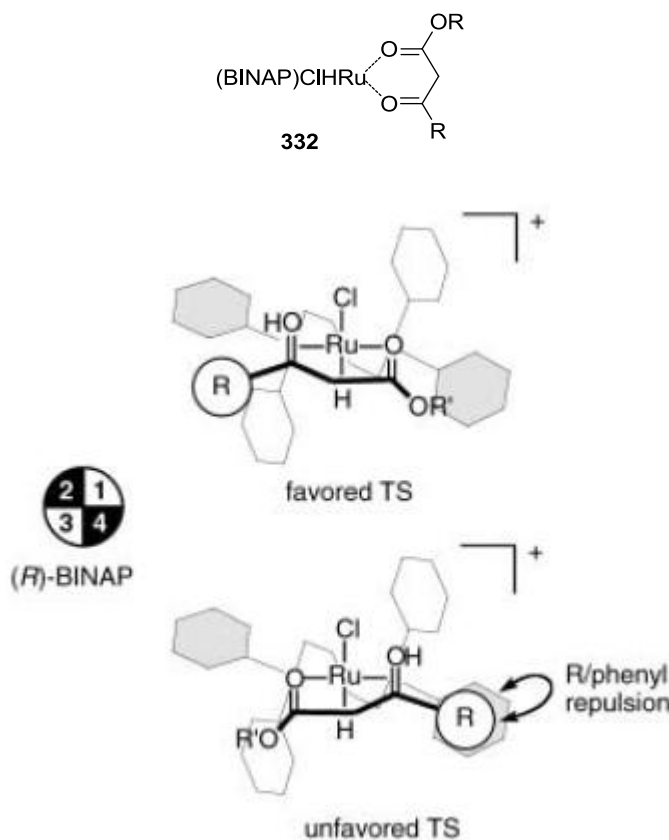


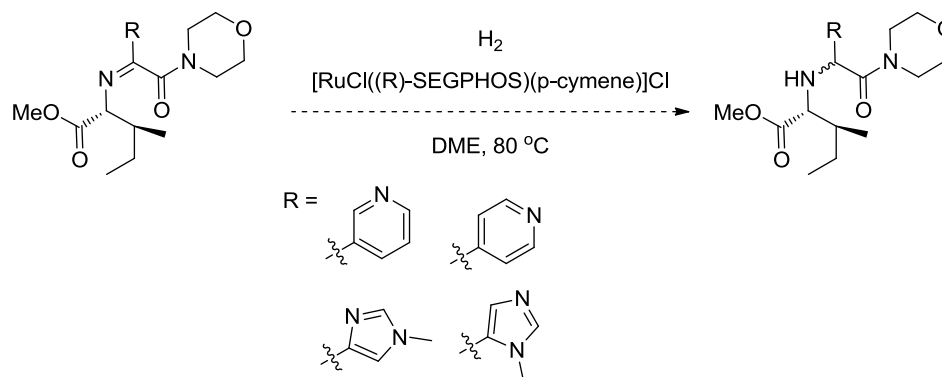
Figure 36 – Stereochemical influence of (*R*)-BINAP.⁷²

4. Results and Discussion Part 2; Investigation of the Asymmetric Hydrogenation

With this in mind, it was proposed that secondary binding of one of the heteroatoms present in our oxazole was taking place, which enabled the observed reactivity, and set out to investigate this with the synthesis and testing of alternative heterocyclic substrates

4.3.1.1 Alternative heterocyclic substrates

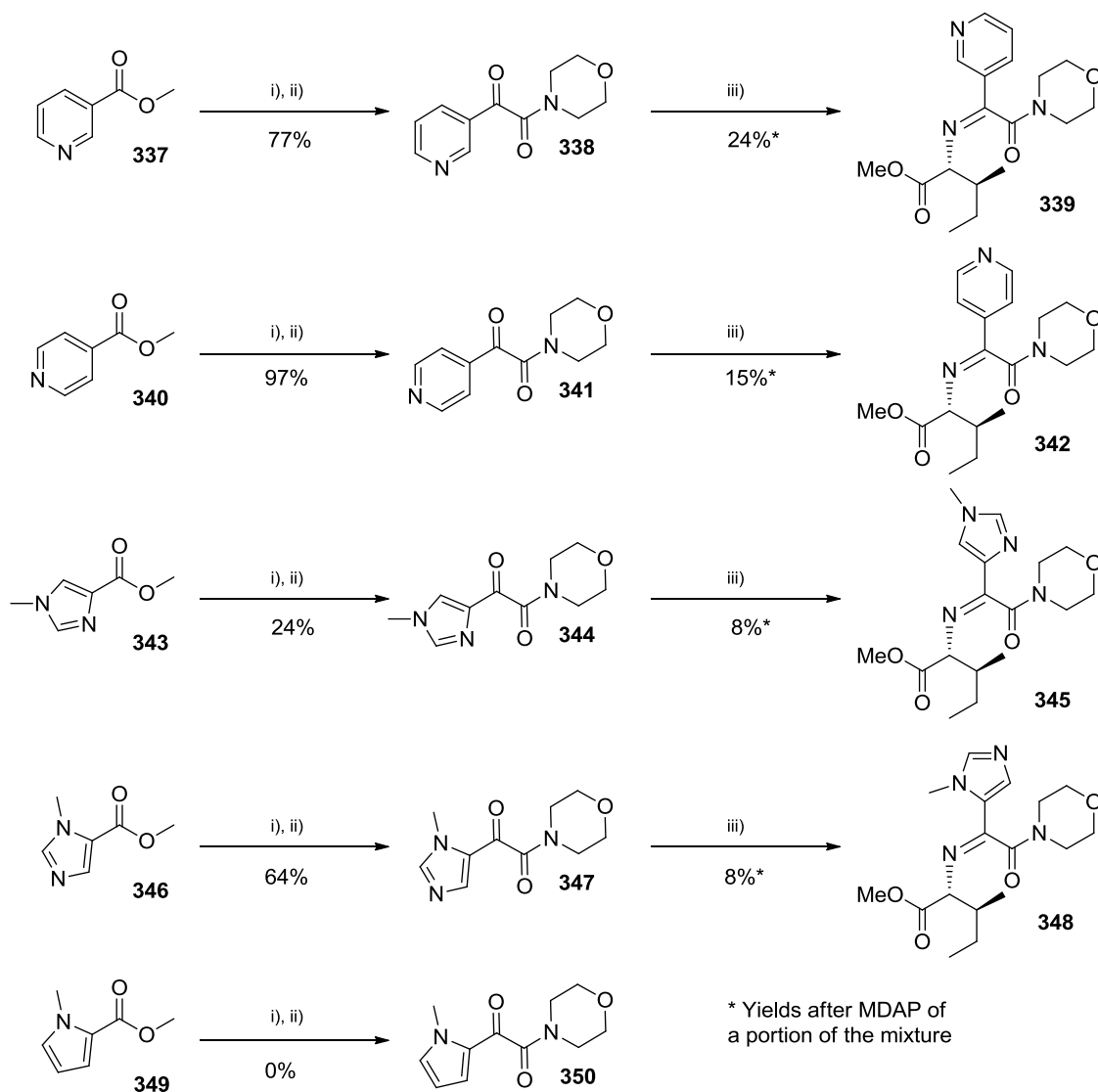
The investigation of the binding phenomenon was performed empirically, since evidence of binding could not be observed spectroscopically; equimolar mixtures of substrate and catalyst were prepared but showed no measurable change in chemical shift compared to the isolated components. Therefore, the syntheses of a number of imines with nitrogen containing heterocycles were proposed to try to re-instate catalytic activity and gain further understanding into the binding of the oxazole. Substrates containing the commonly available heterocycles pyridine, imidazole and pyrrole were initially selected.



Scheme 101 – Proposed reaction of substrates containing commonly available heterocycles

The compounds were synthesised using the Claisen condensation/oxidative nitrile cleavage and TiCl_4 mediated imine formation chemistries optimised for the oxazole containing species (Scheme 102). The methyl esters were chosen in preference to the benzyl esters due to the previously demonstrated ability of the methyl esters to undergo reduction more readily. Here, there was no requirement for isolation of the corresponding amino acids which had previously proven to be troublesome from the methyl esters (c.f. section 3.4). In addition, the proposed strategy of providing markers

4. Results and Discussion Part 2; Investigation of the Asymmetric Hydrogenation of each of the enantiomers by Pd/C reduction of the imines would fail due to concurrent de-benzylation under the Pd/C hydrogenation conditions.



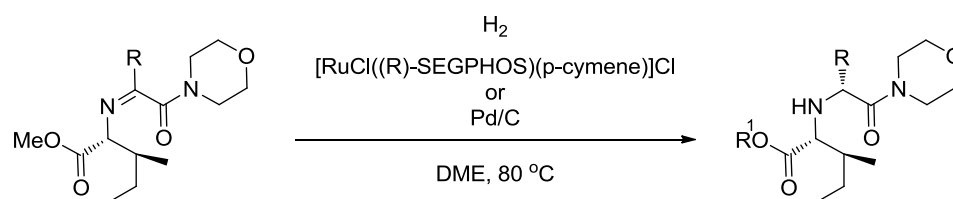
Scheme 102 – Synthesis of imines containing commonly available heterocycles

Synthesis of the heterocycle-containing ketoamides (**338**, **341**, **344**, **347**) proceeded smoothly, in generally higher yields than those obtained for the corresponding oxazole containing species. This is likely to be reflective of the reduced propensity for these heterocycles to undergo 1,4-addition compared to the oxazole (c.f. section 3.2.1).

4. Results and Discussion Part 2; Investigation of the Asymmetric Hydrogenation

Conversion to the pyrrole containing ketoamide (**350**) could not be achieved due to the insolubility of the intermediate ketonitrile in the aqueous media required for the oxidation reaction. The imine syntheses also proceeded as expected and the low yields can be attributed to the fact that only portions of the crude products were taken on and purified by preparative HPLC due to column loading limitations.

The imines (**339**, **342**, **345** & **348**) were subjected to the optimised asymmetric hydrogenation conditions, again using the oxazole imine (**110**) as a positive control. In addition, each of the substrates was reduced using Pd/C to provide a mixture of diastereoisomers which were separated and characterised to allow measurement of the *de* and conversion of the asymmetric reactions by HPLC.

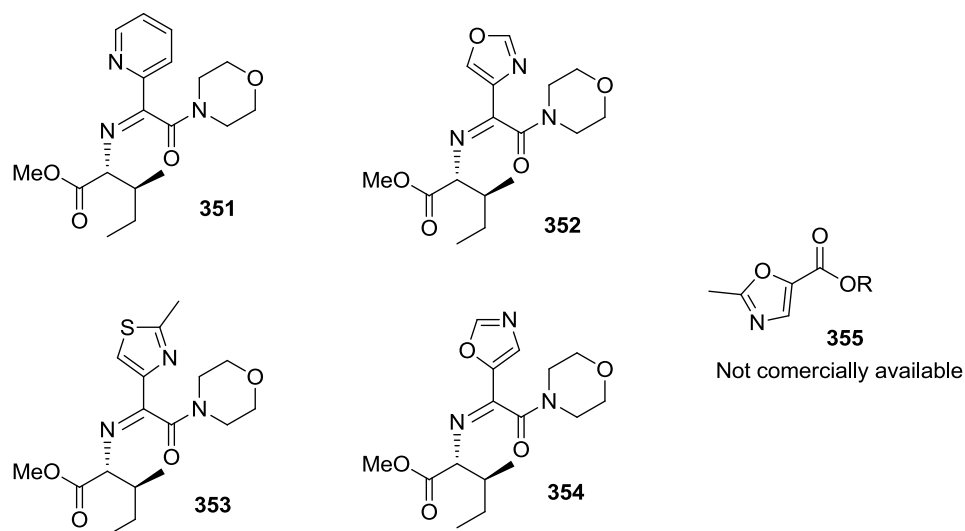


Imine	R	Cat = Ru		Cat = Pd	
		Conversion	<i>de</i> (%)	Conversion	<i>de</i> (%)
110		98%	>99%	84%	0%
339		0%	N/A	37%	0%
342		0%	N/A	>95%	0%
345		33%	N/A	47%	0%
348		0%	N/A	13%	0%

Table 29 - Asymmetric hydrogenation of imines containing pyridine and imidazole

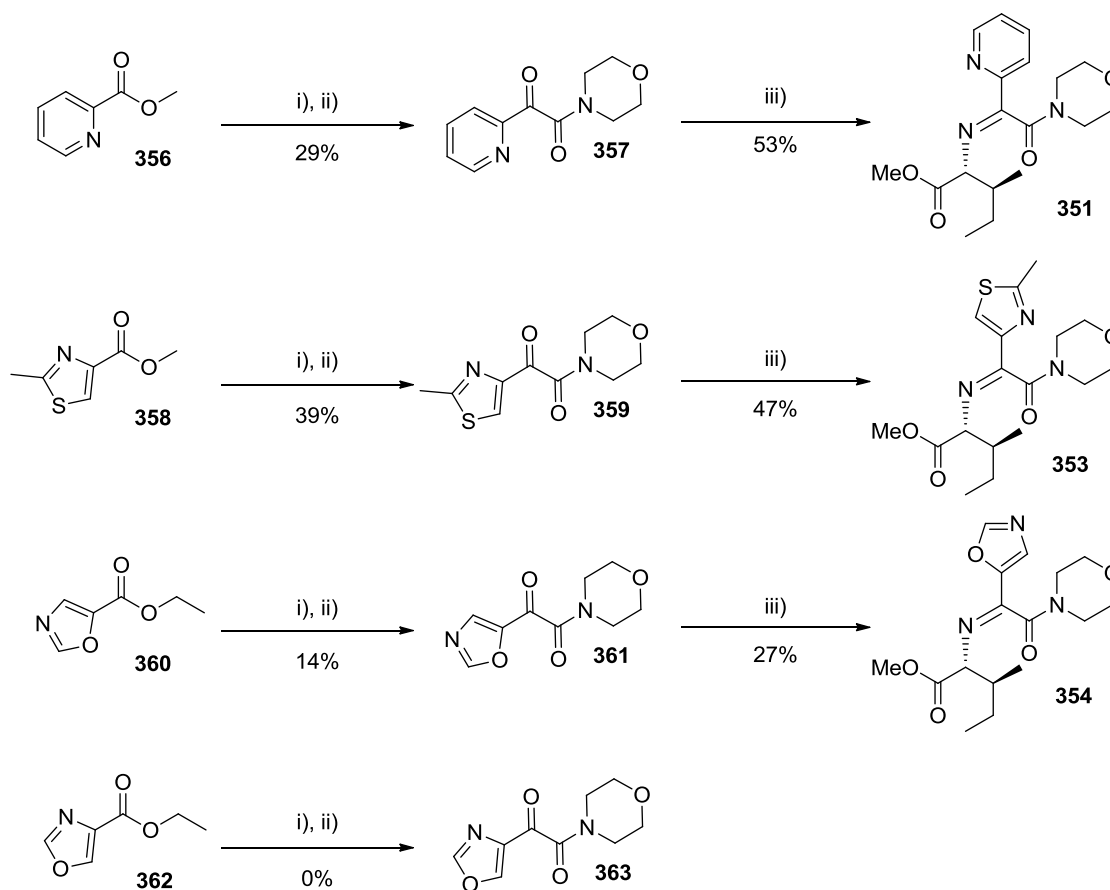
4. Results and Discussion Part 2; Investigation of the Asymmetric Hydrogenation

Interestingly only one of the substrates, the imidazole (**345**), showed conversion to the corresponding amine under the asymmetric hydrogenation conditions, though all were effectively reduced using Pd/C. The structural attribute which both the 4-(2-Me)-oxazole containing substrate (**110**) and the 4-(*N*-Me)imidazole containing substrate (**335**) share, but which differs from the remainder of the substrates, is the presence of an available nitrogen atom within the heterocycle, α to the imine. It was therefore proposed that binding of this nitrogen atom to the ruthenium centre was critical for the observed reactivity and selectivity. We sought to investigate this further with the synthesis and testing of a second round of structurally related heterocycles. The imines shown (**351-354**) were chosen for the next set of syntheses.



The pyridine containing imine (**351**) was chosen as it contains the α -aza substituent in addition to the 6-membered ring and would allow for a direct comparison with the previous two pyridines. The 5-oxazole compound (**354**) was selected as the most direct test of whether the α -nitrogen is indeed crucial for activity. It would also allow the binding affinity of oxygen to be tested. Neither the methyl or ethyl ester of the related 2-methyl oxazole (**355**) were commercially available, and so it was decided to synthesise the des-methyl 4-oxazole derivative (**352**) in order to provide a link between the oxazole (**354**) and the control compound (**110**). The thiazole (**353**) would allow us to investigate the effect of substitution of oxygen with sulphur. As previously, the optimised Claisen

4. Results and Discussion Part 2; Investigation of the Asymmetric Hydrogenation condensation/oxidative nitrile cleavage and TiCl_4 mediated imine formation chemistries as shown were used to prepare the imines (Scheme 103).

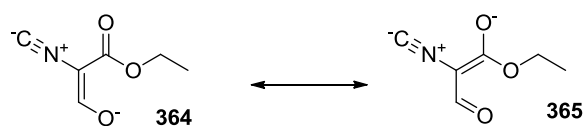


i) Morpholinoacetonitrile, NaHMDS, THF; ii) aq Oxone ; iii) TiCl_4 , TMEDA Toluene.

Scheme 103 – Second round of imine syntheses

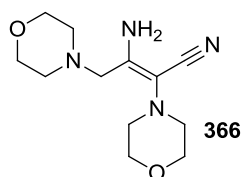
The imines (**351**, **353-354**) were successfully prepared; however, problems were encountered with the synthesis of the 4-oxazole derivative (**363**). This is presumably due to the acidic nature of the proton in the oxazole 2 position. Deprotonation of these oxazole species has been previously reported in the literature.¹⁵⁵ The presence of the pendant ester is likely to make the compound more acidic. It is proposed that deprotonation at C2 and ring opening affords an isonitrile (**364**) which is in equilibrium with its tautomer (**365**). These species are likely to be considerably less electrophilic than the ring closed species (**362**) and therefore formation retards the desired reaction.

4. Results and Discussion Part 2; Investigation of the Asymmetric Hydrogenation



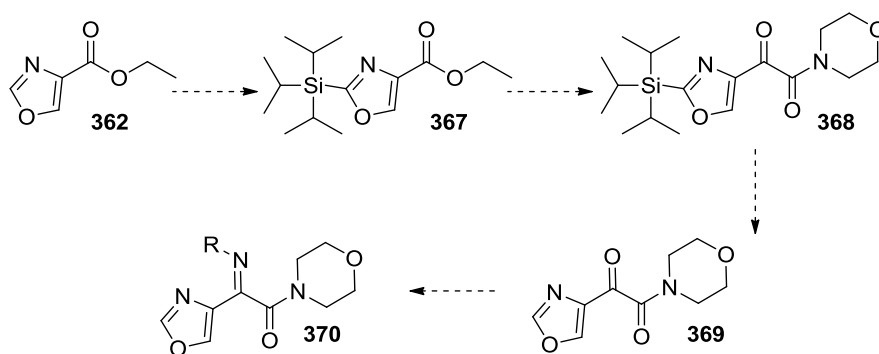
Scheme 104 – Resonance contributors of ring opened oxazole

Support for this hypothesis is provided in the observation of the self condensation product of the morpholinoacetone nitrile (**366**) in the reaction mixture. This presumably occurs in the manner described by Thorpe *et al.*¹⁵⁶ and is consistent with the absence of another electrophile in the reaction mixture.



4.3.1.2 Modified route to 5-oxazole 352

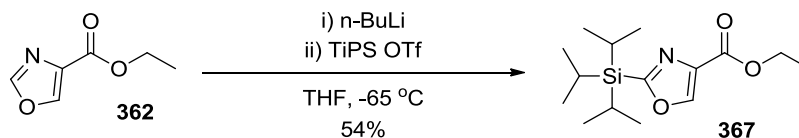
In order to circumvent this deprotonation issue, a method for the C2 protection of the oxazole was found in the work of Miller *et al.*¹⁵⁷ who developed a protocol for the selective C2 silylation of substituted oxazoles. We envisaged that we could protect at C2, perform the Claisen condensation and oxidation to generate the protected ketoamide (**368**) which could be readily deprotected and undergo imine formation to give the desired species (**370**).



Scheme 105 – Proposed route to 5-oxazole imine 370

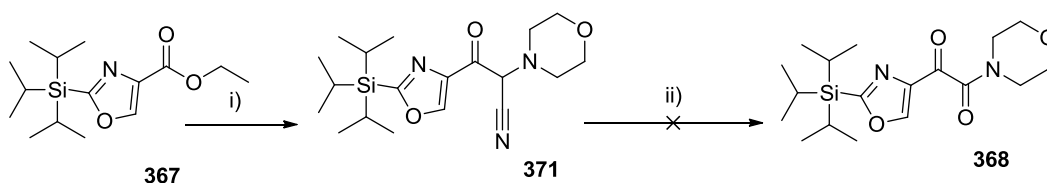
4. Results and Discussion Part 2; Investigation of the Asymmetric Hydrogenation

Using Miller's procedure the silylated oxazole (**367**) was prepared in moderate yield after modification of the reaction conditions to run at lower temperature.



Scheme 106 – Selective C2 oxazole silylation

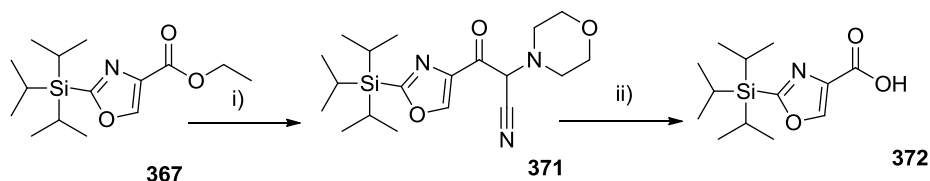
The silylated oxazole (**367**) was then subjected to the Claisen condensation and oxidation conditions. Whilst it successfully underwent Claisen condensation to provide the corresponding ketonitrile (**371**), the oxidation was unsuccessful owing to the poor solubility of the highly lipophilic TIPS protected oxazole in the aqueous reaction media.



i) Morpholinoacetonitrile, NaHMDS, THF; ii) aq Oxone.

Scheme 107 – Formation of silylated ketoamide 368

It had been shown that oxidation to the desired ketoamide using peracetic acid in THF was successful during the initial assessment of the oxidation conditions (section 3.1) and so these conditions were applied to the silylated ketonitrile (**371**). However, under these conditions rapid conversion to the corresponding silylated oxazole acid (**372**) was observed, with no evidence of the desired ketoamide (**368**) (Scheme 108).

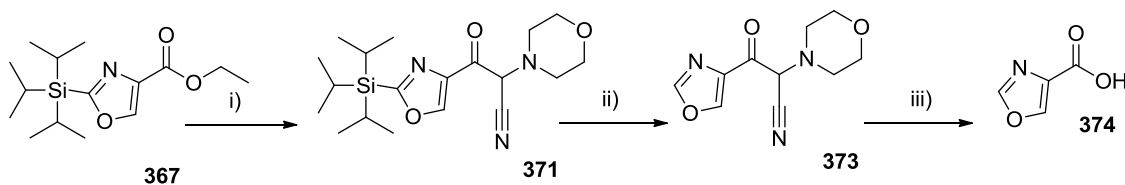


i) Morpholinoacetonitrile, NaHMDS, THF; ii) AcOOH, THF.

Scheme 108 – Oxidation of silylated ketonitrile 371 using peracetic acid

4. Results and Discussion Part 2; Investigation of the Asymmetric Hydrogenation

The synthetic strategy was therefore changed in case the presence of the TIPS group was adversely affecting the oxidation reaction. The TIPS group was removed after formation of the ketonitrile (**371**) and oxidative nitrile cleavage was attempted on the deprotected oxazole (**373**). Despite clean deprotection with TBAF, the oxidation yielded only the undesired oxazole acid (**374**).



i) Morpholinoacetonitrile, NaHMDS, THF; ii) TBAF; iii) AcOOH, THF.

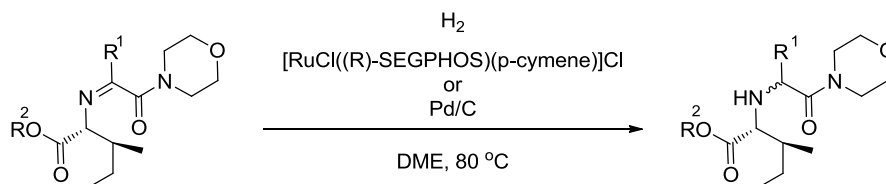
Scheme 109 – Silyl deprotection of ketonitrile 371

Due to the repeated failures in preparing the des-methyl derivative (**369**) the synthesis was abandoned.

4.3.2 Hydrogenation of second round of imines

The successfully prepared imines (**351**, **354** & **354**) were subjected to the optimised asymmetric reduction conditions (Scheme 103) and also to the non-selective Pd/C conditions to provide markers of each of the diastereoisomers. The results are combined with those reported in Table 29 and are shown (Table 30).

4. Results and Discussion Part 2; Investigation of the Asymmetric Hydrogenation

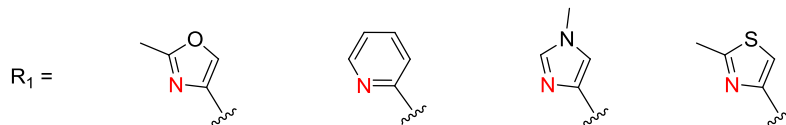


Imine	R ¹	R ²	Cat = Ru		Cat = Pd	
			Conversion (%)	de (%)	Conversion (%)	de (%)
110		Me	98%	>99%	84%	~0%
229		Bn	64%	>99%	100%	-10%
257		Me	0%	N/A	N/A	N/A
351		Me	32%	87%	100%	-10%
339		Me	0%	N/A	37%	~0%
342		Me	0%	N/A	>95%	~0%
345		Me	33%	N/A	47%	~0%
348		Me	0%	N/A	13%	~0%
353		Me	98%	93%	90%	3%
354		Me	1%	N/A	N/A	N/A

Table 30 – Collated asymmetric hydrogenation results

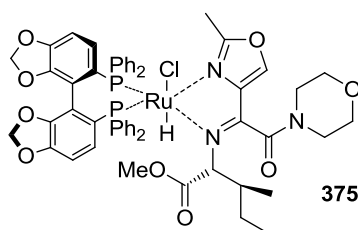
4. Results and Discussion Part 2; Investigation of the Asymmetric Hydrogenation

The successful reduction of the 2-pyridyl (**351**) and 4-(2-Me)-thiazolyl (**353**) imines, and the failure of the 5-oxazolyl imine (**354**) supports the hypothesis that a nitrogen atom within a heterocycle α to the imine is required for the substrate to be reduced effectively by the system.



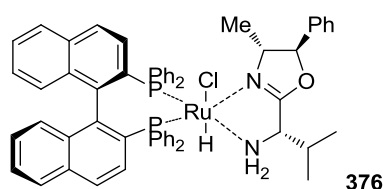
Scheme 110 – Heterocyclic substrates which are effectively reduced

It is therefore proposed that a secondary binding interaction through this α -nitrogen atom is essential for the operation of this catalytic system. The proposed mode is shown below (**373**). The 5-membered ruthenacycle seems plausible based on its size, despite not matching the 6-membered structure proposed by Noyori, as it is believed that the sp² nitrogen lone pairs can adopt the correct orientation to facilitate formation of this type of metalocycle. Moreover, a 6-membered ruthenacycle with the heteroatom contained within the ring would be unlikely to adopt the correct geometry for bidentate binding.



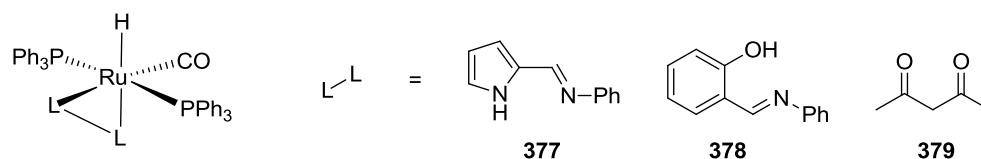
Precedent for these types of 5-membered ruthenacycles can be found within the literature. The most closely related structure is a ruthenium complex (**376**) containing a bidentate aminooxazoline ligand described by Abdur-Rachid and Lough.¹⁵⁸ This complex was shown to be an effective catalyst for the catalytic hydrogenation of acetophenone and was prepared by treating RuHCl(*R*-BINAP)(PPh₃) with a slight excess of the aminooxazoline ligand in THF. The complex was then crystallised from hexanes and characterised by x-ray crystallography.

4. Results and Discussion Part 2; Investigation of the Asymmetric Hydrogenation



The complex shows significant similarity to the proposed binding mode shown above (**375**). Both have the central ruthenium atom in an octahedral co-ordination environment with BINAP or a BINAP-derived axially chiral biphosphine ligand, and both have bidentate co-ordination of two nitrogen atoms to give a 5 membered ruthenacycle. The key difference between the above complex (**376**) and the proposed binding mode is the hybridization state of the coordinating nitrogen atoms. In the case of our proposed mode (**375**), both nitrogens are sp^2 hybridized, whilst Abdur-Rachid and Lough's complex (**376**) is formed by coordination from the sp^2 hybridised oxazoline nitrogen and by the sp^3 hybridized amino nitrogen.

Coordination to ruthenium by two sp^2 hybridised nitrogens creating a 5-membered ruthenacycle is also known, and is exemplified by complex **377** described by Takata and Nakanishi.¹⁵⁹ However, in this example, the ancillary ligands are not as similar to our system as in the example (**376**) above. In addition to the pyrrole derived complex (**377**), Takata and Nakanishi prepared further compounds (**378**, **379**) which demonstrate that the ruthenium metal centre can tolerate coordination of other heteroatoms and larger ring sizes.



Considering both the precedent and the empirical data, it seems reasonable that a binding mode similar to the one proposed above (**375**) is in operation. This model could be used to predict the future applicability of this type of catalytic system to the asymmetric hydrogenation of heterocyclic glycine derivatives and, whilst the requirement for an α -aza substituent does limit the scope of the reaction, it may still find wider synthetic use.

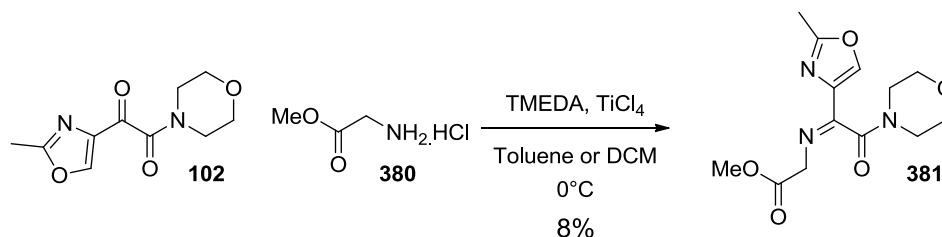
4.4 Imine N-substituent Investigation

With the knowledge of the structural features of the heterocycle required for successful reaction now available, attention turned to investigations of the amino acid fragment.

During the new route development, very high selectivities were observed for the the model system when *D-allo-isoleucine* was coupled with diphosphines of (*R*)-configuration. This is in contrast to diphosphines of (*S*)-configuration, which gave a much lower selectivity (section 3.9). It is possible that a significant match/mismatch case was in operation for the model system. It was therefore necessary to determine the inherent selectivity of the catalyst by investigation of an achiral imine. Doing this would ensure that no chiral induction from the substrate itself was responsible for the reaction outcome. The synthesis and investigation of glycine derivative (**381**) was therefore undertaken.

4.4.1 Synthesis of the glycine derived imine **381**

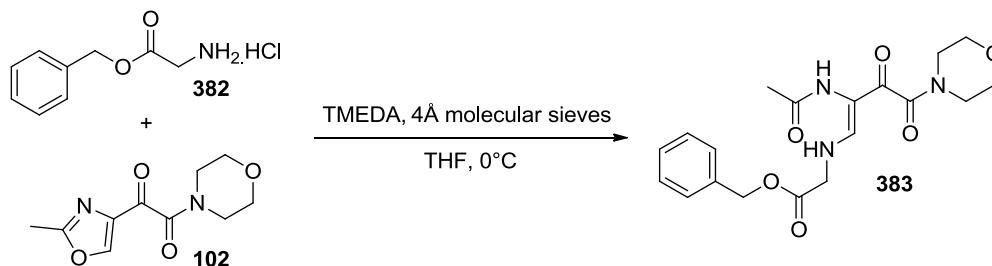
The original 4-(2-Me)-oxazole ketoamide (**102**) was chosen to partner glycine despite our knowledge of its propensity to react with nucleophiles in a 1,4-manner (Section 3.2.1) since supplies of material were plentiful. The optimised, strongly Lewis acidic imine formation conditions were applied according to Scheme 111. However, despite a number of attempts, only very low yields (8%) of the desired imine were obtained. The poor solubility of glycine in both toluene and dichloromethane and the propensity of the methyl ester to undergo hydrolysis on both work-up and purification hampered the reactions. This hydrolysis is presumably due to the much lower steric hindrance caused by the proton compared to the bulky *sec*-butyl group in the *D-allo-isoleucine* equivalent.



Scheme 111 – First attempt at the synthesis of glycine derived imine **381**

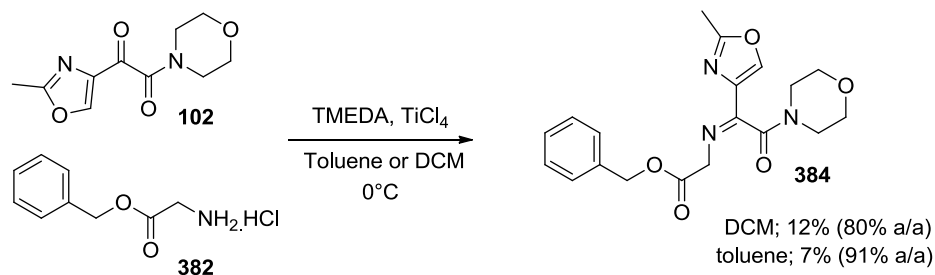
4. Results and Discussion Part 2; Investigation of the Asymmetric Hydrogenation

It is likely that the steric bulk of the amine influences the rate of the 1,4-addition to the oxazole. With this less sterically encumbered substrate, formation under milder, non Lewis acidic conditions was attempted. Unfortunately, rapid 1,4-addition was also observed with this substrate.



Scheme 112 – 1,4-addition of glycine benzyl ester to ketoamide **102**

In a final attempt to synthesise a glycine derived imine glycine benzyl ester (**382**) was used in combination with the Lewis acidic conditions in the hope that the increased lipophilicity would increase the solubility in the reaction solvent, and that the increased steric bulk of the ester would reduce the rate of hydrolysis. This increased the yield marginally, but we were unable to prepare sufficient imine in the required purity to test the hydrogenation.



Scheme 113 – Synthesis of benzyl ester protected glycine imine **384**

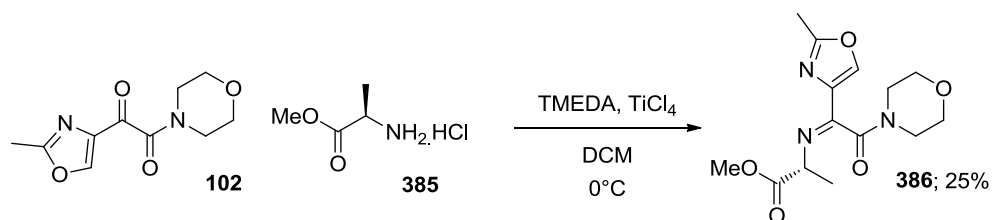
4.4.2 Synthesis of D-alanine derived imine **386**

Due to the failure of the synthesis of the glycine derived imine the synthesis of the next most simple amino acid, alanine, was investigated. This would allow the effect of the steric bulk of the *sec*-butyl group on the selectivity of the reaction to be assessed. D-alanine was chosen so that the stereochemical arrangement of the α -centre matched that

4. Results and Discussion Part 2; Investigation of the Asymmetric Hydrogenation

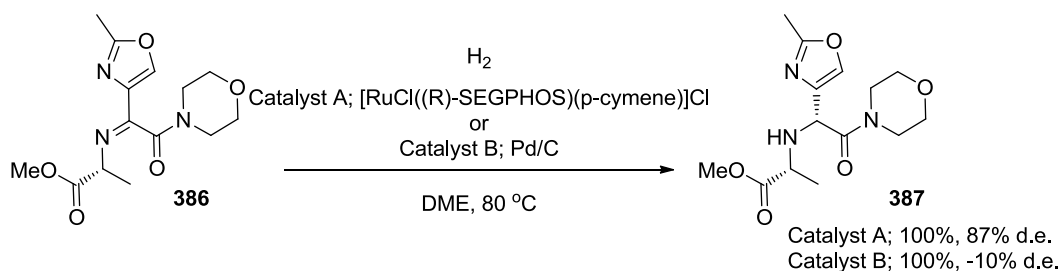
of our control *D-allo-isoleucine* derived substrate. Owing to the chirality of *D-alanine*, the reduction would generate a mixture of diastereoisomers and the diastereomeric excess could be determined by HPLC without the need for development of a suitable chiral method.

The synthesis of the alanine-derived imine (**386**) was achieved more readily than that of the glycine derived imine (**381**) according to the optimised conditions. Despite a moderate yield, the product was prepared in excellent purity after mass-directed preparative HPLC. (Scheme 114)



Scheme 114 – Synthesis of *D-alanine* derived imine **386**

The imine (**386**) was subjected to the hydrogenation conditions with both the ruthenium and Pd/C catalysts; it underwent reduction effectively with the ruthenium SEGPHOS catalyst. The diastereomeric excess of the reaction was reduced from the near perfect selectivity observed with *D-allo-isoleucine* to 87% *de*. This supported the hypothesis that the chirality and steric bulk present within the substrate plays an important role in defining the selectivity of the hydrogenation.

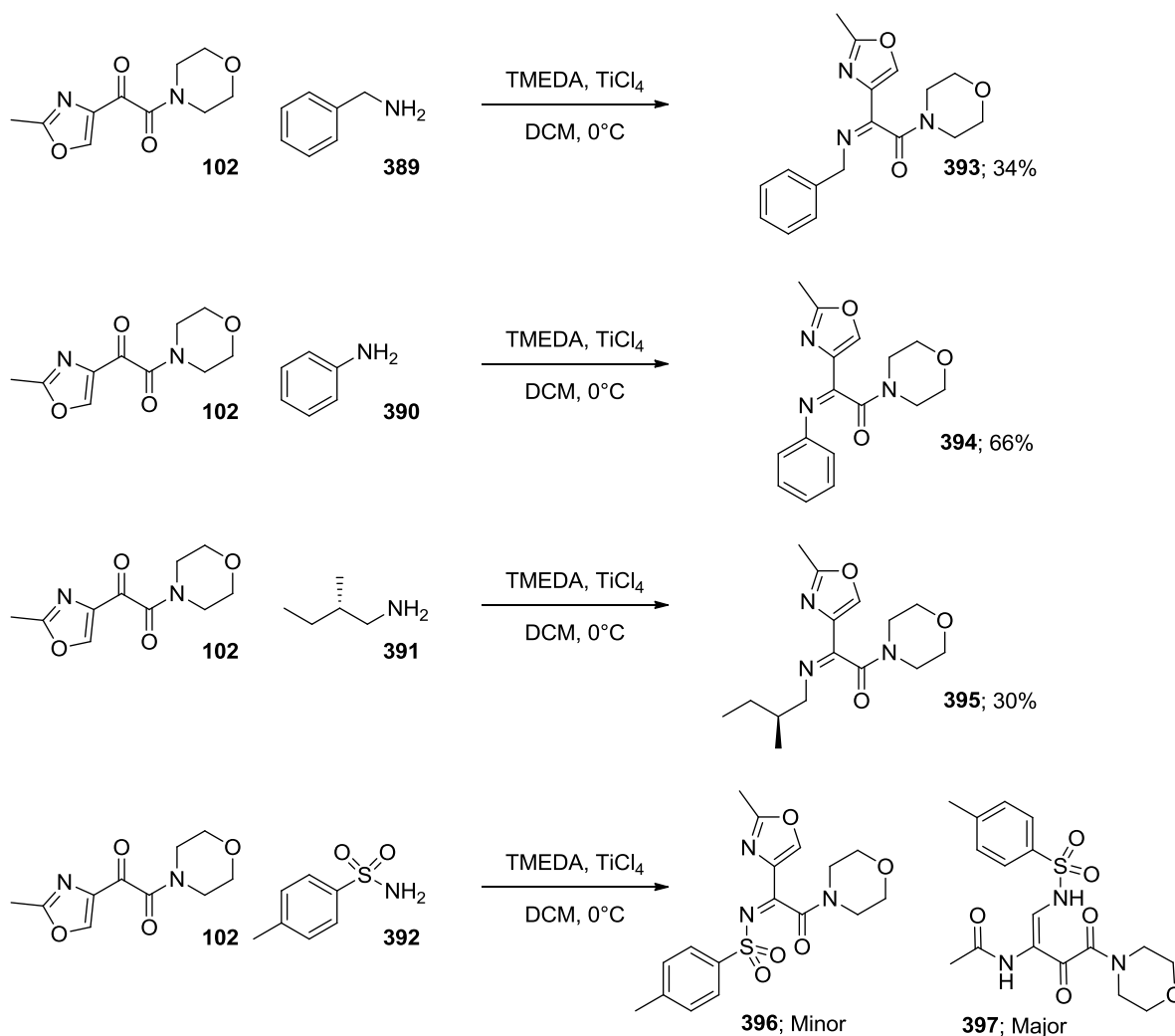


Scheme 115 – Asymmetric hydrogenation of *D-alanine* derived imine

4.4.3 Other amines

The next natural progression in investigating the reaction was to prepare imines derived from simple amines instead of amino acid derivatives. The following compounds (**393-396**) were proposed and synthesised. The imine derived from benzylamine (**393**) would allow the success of the reaction on other alkyl substituents to be assessed. It is also an attractive functionality as a method for the installation of chiral primary amines due to the ease with which it can be de-benzylated. The imine derived from aniline (**394**) was included to assess the applicability of the hydrogenation conditions to simple *N*-aryl imines. These reactions are widely reported in the literature using other catalytic systems, but more rarely using the 1st generation Noyori type catalysts (section 2.4.2). We were interested to see whether these substrates were equally well reduced with this catalytic system. The imine derived from (*S*)-2-Me-butylamine (**395**) would allow the effect of the ester functionality in the control substrate to be directly assessed. It would also demonstrate the applicability of the catalytic system to the typically hard-to-hydrogenate *N*-alkyl imines. Finally, the *N*-tosyl imine (**396**) was chosen for its ability to act as an ammonia equivalent for the synthesis of chiral primary amines.

4. Results and Discussion Part 2; Investigation of the Asymmetric Hydrogenation



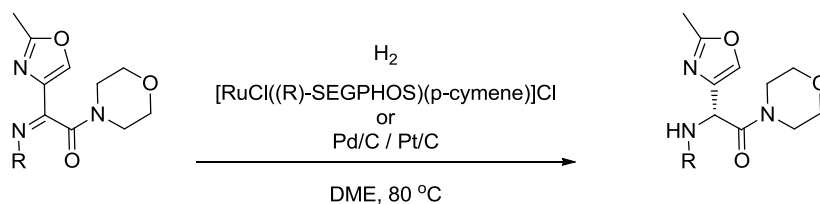
Scheme 116- Synthesis of non-amino acid derived imines

Three of the imines (**393-395**) were synthesised in acceptable yield and high purity after preparative HPLC. The reaction with *N*-tosylamine failed, due to competitive 1,4-addition despite the use of the strongly Lewis acidic conditions.

The imines were subjected to hydrogenation under both the asymmetric hydrogenation and Pd/C conditions (Table 31). The ruthenium-catalysed hydrogenation conditions do not typically catalyse the de-benzylation of amines, unlike Pd/C which rapidly promote de-benzylation. Therefore, reduction using Pt/C was carried out to prevent the debenzylation reaction and prepare analytical markers of the *N*-benzyl amine products

4. Results and Discussion Part 2; Investigation of the Asymmetric Hydrogenation

(**393a**). With the phenyl and benzyl imines (**393**, **394**), chiral HPLC was used to separate the enantiomeric products and measure the *ee*.



Entry	R	Cat = Ru		Cat = Pd/C	
		Conversion	<i>de/ee</i>	Conversion	<i>de/ee</i>
394		100%	98.4%	100%	-1%
393		0%	N/A	100%*	-†
395		84%	28%	92	11%

*Reduction performed with Pt/C. †Enantiomeric excess not determined.

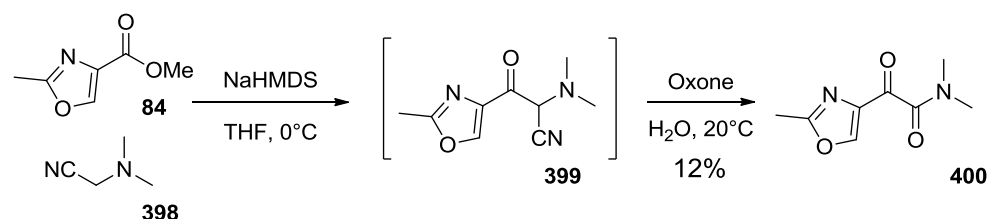
Table 31 - Asymmetric hydrogenation of non-amino acid derived imines

Asymmetric reduction of the *N*-phenyl imine (**394**) occurred readily and with excellent selectivity. Although, asymmetric hydrogenation of *N*-phenyl imines with high selectivity is known using iridium based catalysts,⁸⁰ this result compares favourably to the current state of the art, due to the use of less expensive ruthenium as the metal centre. Further exploration of the reduction of *N*-phenyl imines using this catalyst system could form an interesting area for further work. This high selectivity could be attributed to the significant amount of steric influence of the phenyl moiety as it has fewer degrees of freedom than the *sp*³ *N*-substituents. Reduction of the *N*-benzyl imine was unsuccessful, largely due to competing hydrolysis of the imine. Interestingly, whilst a reasonable conversion is observed with the *N*-(*S*)-(2-methyl)butyl imine, there is a significant reduction in the selectivity of the reaction with this substrate. There are a number of possible reasons as to why this is the case. Firstly, there may be a third

4. Results and Discussion Part 2; Investigation of the Asymmetric Hydrogenation interaction between the substrate and the metal centre involving co-ordination of the ester, which promotes a specific conformation and helps induce the selectivity. Secondly, this substrate is missing an α -stereocentre which may confer a significant degree of selectivity. In the absence of a glycine derived imine (**381**), this phenomenon could be probed by the synthesis of other non-coordinating α -chiral substrates. Thirdly, the effect could be due to the steric bulk of the *N*-substituent. It is likely that the deletion of the α -ester decreases the steric demand of the substrate and allows for other modes of binding to metal centre binding which may ultimately furnish the opposite diastereoisomer.

4.5 Amide *N*-Substituent Investigation

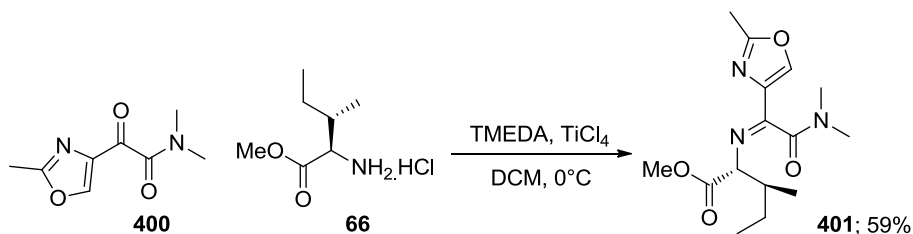
The final point of diversity to be investigated was the morpholinoamide functionality. The synthesis of the *N,N*-dimethyl amide (**41**) was initially proposed in order to explore the effect of steric bulk and the role of the morpholine oxygen atom. As previously, the optimised Claisen condensation/oxidation conditions were used to prepare the ketoamide (**400**) as shown (Scheme 117). The reaction was low yielding due to formation of large quantities of an over-oxidation product, but when performed on large scale it provided sufficient material for onward synthesis.



Scheme 117 – Preparation of *N,N*-dimethyl ketoamide **400**

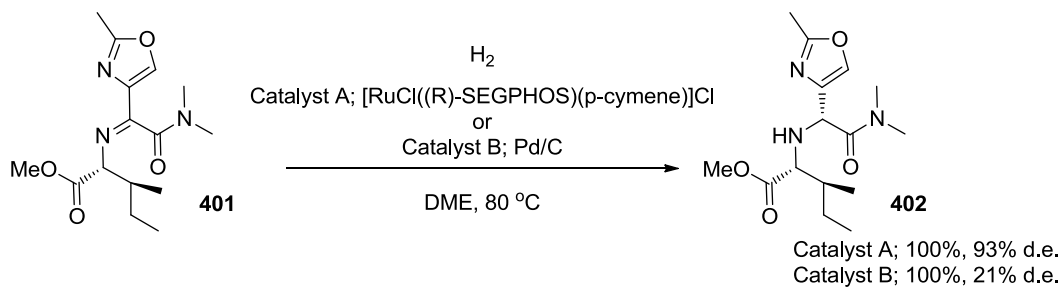
The synthesis of the imine derived from the ketoamide (**400**) and *D*-*allo*-isoleucine (**66**) was performed (Scheme 118), and the product (**401**) was obtained in good yield.

4. Results and Discussion Part 2; Investigation of the Asymmetric Hydrogenation



Scheme 118 – Synthesis of imine 401

The imine (**401**) was subjected to the asymmetric hydrogenation conditions and found to undergo complete reduction with good selectivity.



Scheme 119 – Asymmetric hydrogenation of *N,N*-dimethyl amide imine 401

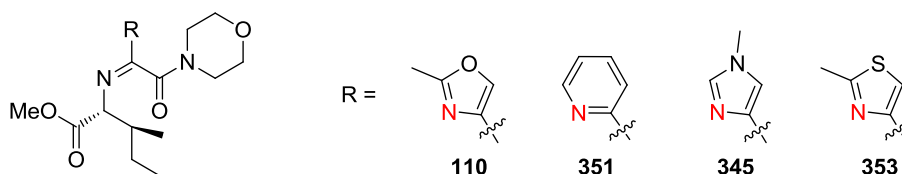
There is some reduction in selectivity over the corresponding morpholine derived imine (**401**) (93% vs >99%) which suggests there is some steric or electronic influence of the morpholine group on the reduction. However, this portion of the molecule does not appear to be crucial for activity and a number of alternative substrates could be synthesised and tested in order to explore this further.

4.6 Summary and Conclusion

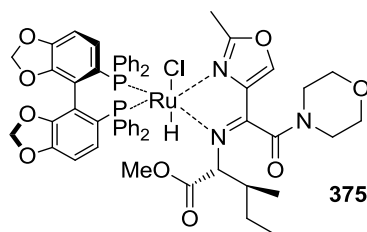
During work to develop an alternative synthesis of the oxytocin antagonist GSK221149 a previously unprecedented application of a 1st generation Noyori ruthenium catalyst to the asymmetric hydrogenation of a sterically congested and densely functionalised imine was discovered. This reaction was particularly noteworthy due to the high selectivity obtained and the structural complexity of the imine. Previous examples of asymmetric imine hydrogenation in the literature are limited to much more simple examples.

The origins of the reactivity and scope of the reaction was explored by synthesising a number of modified imine substrates and subjecting them to the optimised asymmetric hydrogenation conditions.

It was found that only substrates containing nitrogen atoms α -to the imine were reduced effectively (Scheme 120) which led to the proposal of a catalyst-substrate binding mode (**375**) as being key for reactivity and selectivity. This binding mode is complementary to the secondary binding mode of β -ketoesters to ruthenium metal centres described by Noyori⁹⁹ and has structural features in common with the complexes described by Abdur-Rachid and Lough (**376**)¹⁵⁸ and Takata and Nakanishi (**377**).¹⁵⁹



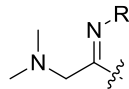
Scheme 120 – Heterocyclic substrates which are effectively reduced



Future work into the investigation of these reductions could look to further simplify the system. It would be particularly interesting to abandon heterocycles as a whole and

4. Results and Discussion Part 2; Investigation of the Asymmetric Hydrogenation

investigate α -amino imines based on the structure below (**403**). This could allow a much broader reaction scope.



403

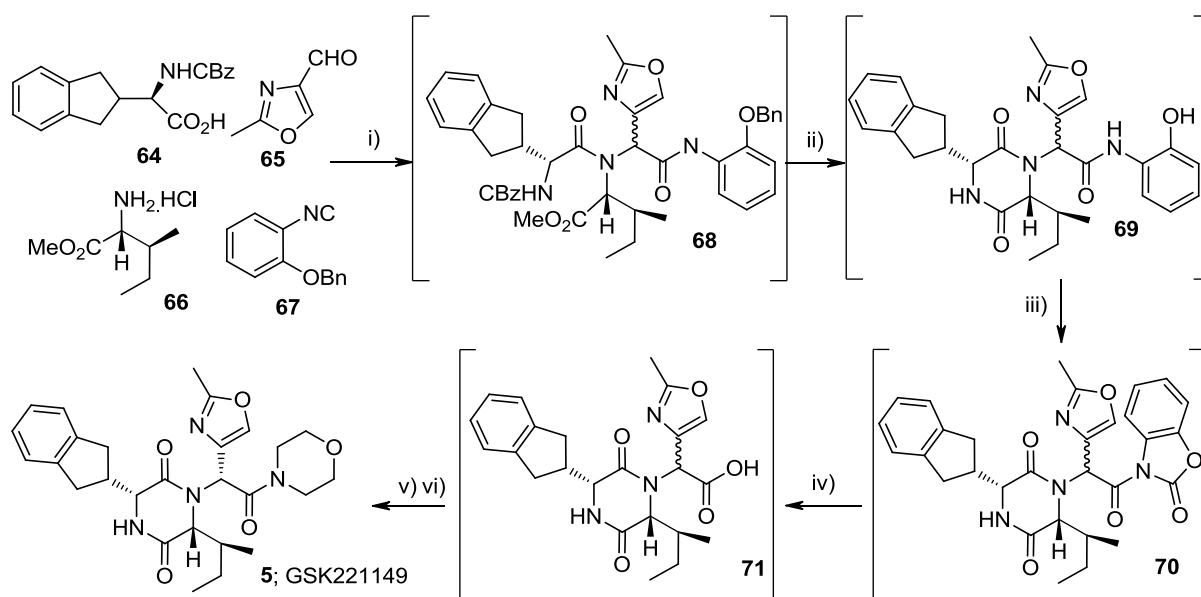
In addition to the requirement for α -aza substituents, the structure activity relationship around the imine *N*-substituent was investigated. Whilst the *N*-glycine derivative could not be satisfactorily synthesised, the *N*-D-alanine analogue showed that the steric bulk of the imine *N*-substituent had an effect on the selectivity of the reaction (87% *de*). Similarly, deletion of the D-*allo*-isoleucine ester group (*N*-(*S*)-(2-methyl)butyl (**395**)) caused a large reduction in selectivity (28% *de*) which may also be attributed to a decrease in steric bulk. Pleasingly, the *N*-phenyl substituent (**394**) showed excellent selectivity (98.4% *ee*). Further work in this area could focus on the use of readily deprotected *N*-phenyl substituents, which would allow access to chiral primary amines.

More generally, this work raises a number of interesting questions about the general experimental strategy employed, and the synthetic usefulness of the methodology. Firstly, throughout these further investigations, it became clear that the poor stability of the imines can become a significant challenge. The oxazolyl imines in particular can undergo not only hydrolysis to the corresponding ketones under acidic conditions, but also 1,4-addition and ring opening under basic conditions. If the methodology is to find true synthetic use, an *in situ* imine formation method would be required. Secondly, the relevance of investigating the scope of a reaction which has been highly optimised for a particular substrate is to be questioned. It appears likely that in optimising the reaction conditions for the original substrate, they have been de-optimised for the subsequent substrates in question. If time and materials allowed, it would be interesting to screen a more generalised set of conditions against a number of these substrates.

5 Conclusion

5.1 Summary and Conclusions

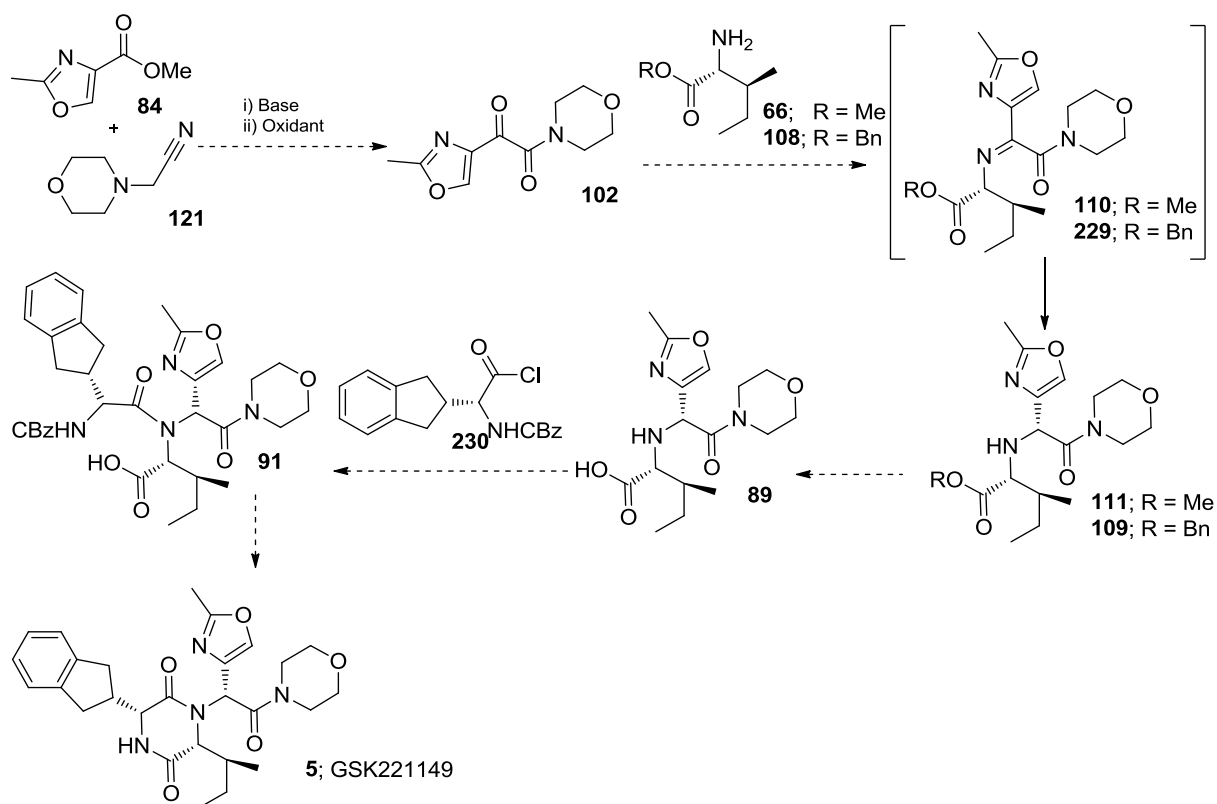
GSK221149 is an oxytocin antagonist indicated for the treatment of pre-term labour, a condition which causes up to 500,000 infant deaths per year and has limited effective treatment options. GSK221149 could fill significant unmet medical need in the treatment of pre-term labour and is currently awaiting phase III clinical trials. The existing synthetic route to GSK221149 (**5**) takes advantage of the multicomponent Ugi reaction to build up the skeleton in a single step. However, whilst the route seems attractive on paper, a number of factors such as the lack of isolated intermediates and the early introduction of the expensive indanyl glycine sub-unit make it less than practical for use on large scale in long term manufacturing. A new route was required to provide material for long term toxicology, phase III clinical trials and ultimately, commercial manufacture.



i) NEt_3 , $\text{MeOH}/\text{CF}_3\text{CH}_2\text{OH}$ 67%; ii) Pd/C , NMP , aq NH_4HCO_2 , 73%; iii) CDI , EtOAc ; iv) H_2O , EtOAc , 90%; v) Me_3CCOCl , *N*-methylmorpholine; vi) Morpholine, EtOAc -20°C , 62%.

Scheme 121 - Route A to GSK221149

Retrosynthetic analysis of the molecule gave a number of potential strategies which were prioritised and an alternative route was proposed. The route utilises an asymmetric reductive amination as the key bond forming step to install the exocyclic oxazole bearing stereocentre selectively.

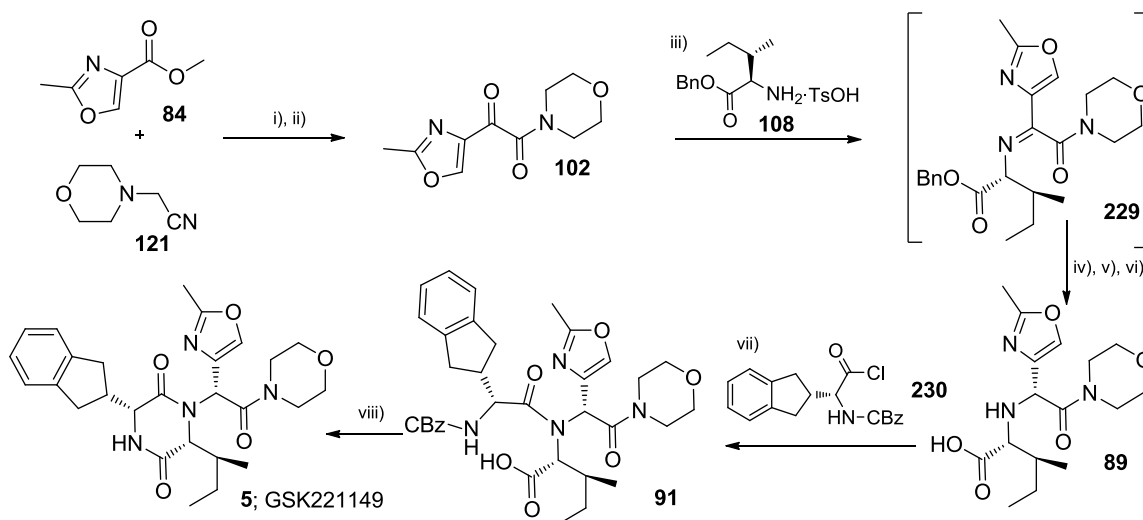


Scheme 122 - Proposed new route to GSK221149

The development work was commenced by investigating the Claisen condensation between the ester (**84**) and the nitrile (**121**) followed by oxidative nitrile cleavage to afford the ketoamide (**102**). Experimentation showed that the nature of the oxidant was important for a high yielding reaction and a process was developed which allowed the scalable formation of product in 32% yield. Attempts to form the imine (**110**) were hampered by the propensity of the oxazole moiety to undergo 1,4-addition and subsequent ring opening. This reaction pathway was disfavoured by the use of strongly dehydrating lewis acidic conditions which allowed the formation of the imine as an interconverting mixture of *E/Z*-isomers. The reduction of the imine (**110**) was achieved by catalytic hydrogenation in the presence of Pd/C which provided a diastereomeric mixture of amino esters. Whilst ester hydrolysis was facile, isolation of the desired diastereomeric product proved challenging which ultimately led to the selection of benzyl as the desired ester. Despite this, we were able to progress material through to GSK221149 where care was taken to demonstrate the purity of the product. The purity

of APIs is of paramount importance and it was demonstrated that material from the new route was very close to the clinical specification.

With the route proven, attention was shifted to the development of scalable, higher yielding chemistry and an asymmetric reduction of the imine. A broad range of catalysts based on a number of metal centres were screened under varying conditions resulting in the identification of 1st generation Noyori type ruthenium catalysts as effective in facilitating the reduction with exceptional diastereoselectivity (>99%). The reaction conditions were optimised in order to use the benzyl ester protected imine (**229**) which allowed for a more facile isolation of the amino acid. The catalyst loading was increased to avoid impurity formation and the reaction was scaled to 39 g in order to demonstrate the reaction and provide material for more detailed API analysis. Here, particular care was taken to demonstrate the diastereomeric purity of the API, which was shown to exceed clinical specification. The final route of synthesis is shown (Scheme 123).



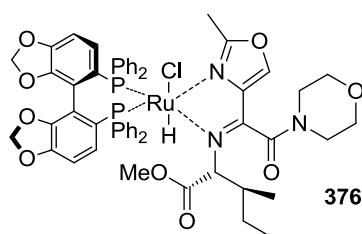
i) NaHMDS, THF; ii) aq Oxone, 30%; iii) TiCl_4 , TMEDA Toluene, 91%; iv) H_2 , $[\text{RuCl}((R)\text{-SEGPHOS})(p\text{-cymene})]\text{Cl}$ (**169a**); v) H_2 , Pd/C; vi) *i*-PrOH cryst, 64%; vii) EtOAc/dichloromethane, 75%; viii) H_2 , Pd/C, 96%.

Scheme 123 – New route to GSK221149

A detailed comparison of the new route versus the existing chemistry was then performed which showed a marginally higher cost of goods (£11,600 kg^{-1} vs £9,500 kg^{-1}) for the newly developed route, primarily due to developments which had

been made to the existing chemistry whilst new route investigations were in progress. This led the new route work being suspended. However, it would make an excellent start point for the development of a future 2nd generation route to the compound if required.

After suspension of the new route work, attention shifted to the investigation of the novel application of Noyori's 1st generation catalyst to the imine hydrogenation. We aimed to understand and expand the scope of the reaction which had the potential to be a useful method for the synthesis of a range of aryl glycine derivatives. The effect of substituting the heterocycle portion of the molecule was shown to severely impact the reactivity of the catalyst system. Only heterocycles containing an available α -nitrogen were shown to undergo hydrogenation. It was proposed that the substrates were involved in secondary binding to the metal centre through this α -aza substituent and this was the mechanism by which hydrogenation took place.



Finally, the effect of substitution of the imine *N*-substituent was investigated. It was observed that, whilst the highest selectivities were observed for an *N*-phenyl substituent (>98% *ee*), stereoselection could be achieved with alkyl substituents ((*S*)-2-Me-butyl (**395**); 28% *de*) and modification of the amino acid fragment showed only a small drop off in selectivity (D-alanine (**386**); 87% *de*). Modification of the morpholine moiety also only showed a small drop-off in selectivity (*N*-Me₂ (**401**); 93% *ee*.)

These results show that whilst the methodology is not broadly applicable as a method for the synthesis of aryl glycine derivatives as hoped, the reaction can be applied to a well defined sub-set of α -nitrogen containing heterocycles and suggests an interesting nitrogen equivalent of Noyori's proposed binding mechanism for β -ketoesters to a ruthenium metal centre.

The chemistry compares favourably to the current state of the art for the asymmetric reduction of *N*-phenyl imines where the use of ruthenium could offer significant cost advantages of commonly used iridium catalysts. Investigation into this area would be an interesting avenue for further research, but will not be undertaken at this time.

6 Experimental

6 Experimental

6.1 General Experimental

All solvents and reagents were standard laboratory grade and purchased from Sigma Aldrich unless otherwise stated, and were used without further purification.

All experiments were carried out under an atmosphere of nitrogen gas unless otherwise stated.

NMR data were obtained on a Bruker DPX400 or Bruker AV400 spectrometer operating at 400 MHz for ^1H spectra, 100 MHz for ^{13}C spectra and 162 MHz for ^{31}P spectra. Chemical shifts in ^1H and ^{13}C spectra are reported on the δ scale relative to tetramethylsilane (TMS). ^{13}C spectra were proton decoupled. All NMR data were obtained at 26 °C unless otherwise stated.

pH was measured using a Jenway Enterprise 350 pH meter calibrated to pH 4.0 and 9.22.

HPLC data were obtained on a number of different methods as detailed below.

6.1.1 HPLC Method A

Instrument	Agilent 1100 series HPLC			
Column	Phenomenex Luna C18(2), 50 x 2.0 mm, 3 μm			
Mobile phase	A	Water + 0.05% v/v trifluoroacetic acid		
	B	Acetonitrile + 0.05% v/v trifluoroacetic acid		
Flow Rate	1 mL/min.			
Gradient Profile	Time (min)	0	8	8.01
	% A	100	5	100
	% B	0	95	0

Column Temp	40 °C
UV Detection	220 nm
Injection volume	1 µL

6.1.2 HPLC Method B

Instrument	Agilent 1100 series HPLC			
Column	Agilent Zorbax SB-C18			
Mobile phase	A	Water + 0.05% v/v trifluoroacetic acid		
	B	Acetonitrile + 0.05% v/v trifluoroacetic acid		
Flow Rate	1.5 mL/min.			
Gradient Profile	Time (min)	0	2.5	3
	% A	100	5	5
	% B	0	95	95
Column Temp	60 °C			
UV Detection	220 nm			
Injection volume	1 µL			

6.1.3 HPLC Method C

Instrument	Agilent 1100 series HPLC	
Column	Gemini NX, 50 x 3 mm, 3 µm	
Mobile phase	A	ammonium bicarbonate (10 mM aqueous solution)

	B	Acetonitrile		
Flow Rate	1.5 mL/min.			
Gradient Profile	Time (min)	0	4	5
	% A	100	5	5
	% B	0	95	95
Column Temp	30 °C			
UV Detection	220 nm			
Injection volume	1 µL			

LCMS data were obtained using one of the above HPLC methods coupled to a Waters ZQ mass spectrometer, running in positive electrospray ionisation mode with a quadrupole detector.

High resolution mass spectrometry data were obtained using the HPLC (Method A) coupled to a Thermo-Finnigan Orbitrap Fourier-transform mass spectrometer running in positive electrospray ionisation mode.

Infra red (IR) spectra were obtained on a Perkin Elmer Spectrum One instrument with diamond attenuated total reflection accessory. Only data for main functional groups and strong peaks are reported.

Screening hydrogenations were carried out in glass tubes in a multi-well steel autoclave with overhead stirring or in multiwell hastelloy autoclave with magnetic stirring, using hydrogen from a hydrogen generator unless stated. Larger scale hydrogenations were carried out in a glass miniclave vessel with a turbine mechanical stirrer, and hydrogen from a hydrogen generator.

Chromatography was carried out using a Biotage SP4 instrument, with pre-packed silica columns; details of solvent system, column size, silica type, flow rate and column loading are provided for individual examples.

6.2 Experimental Procedures for Results and Discussion Part 1

6.2.1 Experimental Procedures for Section 3.1

6.2.1.1 General Procedure 1: Synthesis of Ketoamide 102

Base (A) was added dropwise to a solution of 4-morpholinoacetonitrile (**121**) (B) and methyl 2-methyl-1,3-oxazole-4-carboxylate (**84**) (C) in solvent (D) at temperature (E). The resultant reaction mixture was stirred at temperature (F) for period of time (G) then analysed by HPLC (H). Oxidant (I) was added dropwise to the above solution and the mixture was stirred at temperature (J) for period of time (K) and analysed by HPLC (L).

6.2.1.2 Work-up Procedure 1

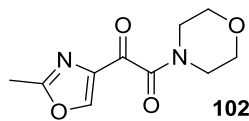
The reaction mixture was quenched (M) and the resultant biphasic mixture was stirred for 5 min. The phases were separated and the organic phase was dried (MgSO_4) and concentrated under reduced pressure to afford the crude product as a brown oil. Purification by flash chromatography (EtOAc) afforded the desired product as a yellow oil which solidified on standing (N).

6.2.1.3 General Procedure 2: Oxidant Screen

Base (O) and oxidant (P) were charged to a solution of the 3-(2-methyl-1,3-oxazol-4-yl)-2-(4-morpholinyl)-3-oxopropanenitrile (**102**) (50 mg, 0.21 mmol) in solvent (Q) (3 mL) and the resultant reaction mixture was stirred at 20 °C for 45 min. An aliquot (20 μL) was removed and quenched into sodium sulphite (1 mL of a 3% w/w aqueous solution) then analysed by HPLC (R).

A series of seven experiments were carried out in this way with variation in all experimental parameters (A) – (R). Only selected experiments are presented more fully.

6.2.1.4 Experimental for the Preparation of 1-(2-Methyl-1,3-oxazol-4-yl)-2-(4-morpholinyl)-2-oxoethanone (**102**)



The experiments documented in section 3.1 were carried out using general procedure 1; details for each entry are provided below. When product was isolated, work-up procedure 1 was followed. Differences in processing are recorded for each entry where applicable. For isolated products, full characterisation was carried out for a single batch; the remainder were analysed by HPLC and ^1H NMR. ^1H NMR spectroscopic data matched that given below with the exception of signals arising from residual solvents and minor impurities.

Experiment 1. A: Sodium bis(trimethylsilyl)amide (19.1 mL of a 1 M solution in THF, 19.1 mmol); B: 0.94 g, 7.4 mmol; C: 1 g, 7.1 mmol; D: THF (10 mL); E: $<30\text{ }^\circ\text{C}$; F: ambient; G: 10 min; H: HPLC showed complete conversion to the ketonitrile (**102**); I: Sodium hypochlorite (10.6 mL of a 10% w/w aqueous solution, 14.2 mmol); J: ambient; K: 5 min; L: Ratio ketoamide (**102**): ketonitrile (**122**): oxazole acid (**231**) = 13.1 : 51.7 : 35.2. Stirring was continued for a further 15 min and the mixture was re-analysed by HPLC. The relative area of the ketoamide (**102**) was reduced; ratio calculations were not completed. Stirring was continued for a further 18 h and the mixture was re-analysed by HPLC. The relative area of the ketoamide (**102**) was reduced; ratio calculations were not completed. A further portion of sodium hypochlorite (10.55 mL of a 10% w/w aqueous solution, 14.17 mmol) was added and the mixture was stirred for 15 min then sampled for HPLC. Ratio ketoamide (**102**): ketonitrile (**122**): oxazole acid (**231**) = 0.8 : 2.2 : 97.0.

Experiment 2. A: Sodium hydride (0.71 g of a 60% dispersion in oil, 19.1 mmol, suspended in 1 mL THF); B: 0.94 g, 7.4 mmol; C: 1.0 g, 7.1 mmol; D: THF (10 mL); E: $<25\text{ }^\circ\text{C}$; F: ambient; G: 15 min; H: an aliquot (20 μL) was quenched into water then diluted with methanol. The ketonitrile (**122**) was not observed. LCMS analysis showed hydrolysis to the acid (**231**). The reaction was re-sampled, quenching into methanol, and

LCMS analysis showed only the oxazole ester (**84**). Stirring was continued overnight and the reaction was re-analysed by HPLC. The ketonitrile (**122**) was not observed. An aliquot (20 μ L) of the reaction mixture was quenched into D₂O (0.75 mL) and analysed by ¹H NMR. Deuteration of morpholinoacetonitrile (**121**) could not be observed due to overlap of the required resonance with THF.

Experiment 3. A: Sodium bis(trimethylsilyl)amide (19.1 mL of a 1 M solution in THF, 19.1 mmol); B: 0.94 g, 7.4 mmol; C: 1 g, 7.1 mmol; D: THF (10 mL); E: <30 °C; F: ambient; G: 10 min; H: HPLC showed complete conversion to the ketonitrile (**122**); I: peracetic acid (2.94 mL of a 32% w/w solution in AcOH, 14.2 mmol); J: ambient; K: 5 min; L: HPLC showed complete conversion to the ketoamide (**102**); M: sodium sulfite (10 mL of a 10% w/w aqueous solution). The separated organic phase was washed with sodium bicarbonate (15 mL of a satd. aqueous solution). HPLC showed there was no change in the composition of the organic phase, but there was some product in the aqueous phase. The aqueous phase was back extracted with iPrOAc (20 mL) and the combined organic phases were washed with water (10 mL). HPLC showed product remained in the aqueous phase; N: 292 mg, 18%, 95% a/a by HPLC. The Biotage column was washed with MeOH and the washings were analysed by TLC (EtOAc); no product was observed. 2D TLC analysis (EtOAc) with 1h between runs showed the compound was stable to silica.

Experiment 4. A: Sodium bis(trimethylsilyl)amide (9.6 mL of a 1 M solution in THF, 9.6 mmol); B: 469 mg, 3.7 mmol; C: 500 mg, 3.5 mmol; D: THF (5 mL); E: <7 °C; F: 0-5 °C; G: 5 min; H: HPLC showed complete conversion to the ketonitrile (**122**); I: peracetic acid (1.47 mL of a 32% w/w solution in AcOH, 7.1 mmol); J: 0-5 °C; K: 2.5 h; L: HPLC showed 3.5% a/a ketonitrile (**122**) remained; M: sodium thiosulfate (5 mL of a 20% w/w aqueous solution); N: 215 mg, 27%.

Experiment 5. A: Sodium bis(trimethylsilyl)amide (9.6 mL of a 1 M solution in THF, 9.6 mmol); B: 469 mg, 3.7 mmol; C: 500 mg, 3.5 mmol; D: THF (5 mL); E: <7 °C; F: 0-5 °C; G: 5 min; H: HPLC showed complete conversion to the ketonitrile (**122**); I: peracetic acid (1.47 mL of a 32% w/w solution in AcOH, 7.1 mmol) added over 30 min

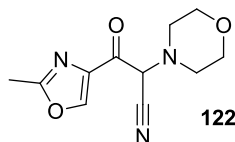
using a syringe pump. Samples were taken for HPLC during addition; J: 0-5 °C; K: 60 min; L: HPLC showed the ketonitrile (**122**) remained. A further portion of peracetic acid (0.074 mL of a 32% w/w solution in AcOH, 0.36 mmol) was charged and HPLC showed the ketonitrile (**122**) remained. A further portion of peracetic acid (37 µL of a 32% w/w solution in AcOH, 0.18 mmol) was charged and HPLC showed the reaction was complete; M: sodium thiosulfate (5 mL of a 20% w/w aqueous solution); N: 276 mg, 35%.

Experiment 6. A: Sodium bis(trimethylsilyl)amide (287 mL of a 1 M solution in THF, 287 mmol); B: 14.1 g, 112 mmol; C: 15 g, 106 mmol; D: THF (150 mL); E: <5 °C; F: 0-5 °C; G: 10 min; H: HPLC showed complete conversion to the ketonitrile (**122**); I: peracetic acid (47.4 mL of a 32% w/w solution in AcOH, 229 mmol); J: 0-5 °C; K: 1h; L: HPLC showed the reaction was complete, 75% a/a ketoamide **3**; M: sodium thiosulfate (150 mL of a 20% w/w aqueous solution); N: 7.68 g, 32%.

Experiment 7. A: Sodium bis(trimethylsilyl)amide (287 mL of a 1 M solution in THF, 287 mmol); B: 14.1 g, 112 mmol; C: 15 g, 106 mmol; D: THF (150 mL); E: <5 °C; F: 0-5 °C; G: 10 min; H: HPLC showed complete conversion to the ketonitrile (**122**); I: peracetic acid (47.4 mL of a 32% w/w solution in AcOH, 229 mmol); J: 0-5 °C; K: 1h; L: HPLC showed the reaction was complete; M: sodium thiosulfate (150 mL of a 20% w/w aqueous solution); N: 7.68 g, 32%.

Data for 1-(2-Methyl-1,3-oxazol-4-yl)-2-(4-morpholinyl)-2-oxoethanone (**102**); ¹H NMR (400 MHz, CDCl₃) δ ppm 2.54 (s, 3H), 3.51 - 3.60 (m, 2H), 3.69 - 3.80 (m, 6H), 8.37 (s, 1H); ¹³C NMR (100 MHz, CDCl₃) δ ppm 13.8 (CH₃), 42.2 (CH₂), 46.3 (CH₂), 66.6 (CH₂), 66.8 (CH₂), 137.9 (CH), 146.7 (C), 163.0 (C), 163.7 (C), 182.5 (C); ν_{max} (neat, cm⁻¹) 2873, 1684, 1626, 1597, 1450, 1248, 1103, 1001; HPLC (Method B) T_R = 1.39 min 95.0% a/a; MS m/z (ESI⁺) 225 ([M+H]⁺); HRMS (ESI⁺) m/z calcd. for C₁₀H₁₃N₂O₄ [M+H]⁺ 225.0870, found 225.0867. Mp 80 – 82 °C (decomp).

6.2.1.5 Experimental Procedures for the Preparation of 3-(2-Methyl-1,3-oxazol-4-yl)-2-(4-morpholinyl)-3-oxopropanenitrile (**122**)



Sodium *bis*(trimethylsilyl)amide (17.7 mL of a 1 M solution in THF, 17.7 mmol) was added to a solution of 2-morpholinoacetonitrile (**121**) (0.94 g, 7.4 mmol) and methyl 2-methyl-1,3-oxazole-4-carboxylate (**84**) (1.0 g, 7.1 mmol) in THF (10 mL); the resulting exotherm was moderated to <30 °C by controlling the addition rate. The reaction mixture was stirred at 20 °C for 5 min and complete consumption of starting material was confirmed by HPLC. The reaction mixture was quenched by the addition of ammonium chloride (5 mL of a 20% w/w solution), diluted with water (30 mL) and washed with EtOAc (2 x 30 mL). The aqueous phase was concentrated to dryness under reduced pressure and the resulting solids were taken up in MeOH (20 mL) and filtered. The solution was again concentrated and the residue purified by flash chromatography (2-10% MeOH in dichloromethane) to afford the desired product as a yellow solid. (850 mg, 51%); ¹H NMR (400 MHz, CDCl₃) δ ppm 2.51 (s, 3H), 2.64 – 2.81 (m, 4H), 3.62 - 3.90 (m, 4H), 8.08 (s, 1H) *CH* not observed; HRMS (ESI⁺) *m/z* calcd. for C₁₁H₁₄N₃O₃ [M+H]⁺ 236.1030, found 236.1022.

6.2.1.6 Experimental Procedures for Table 2

Oxidant screening experiments were carried out according to general procedure 2. HPLC % peak areas for the ketoamide (**102**) are given for each entry.

Entry 1. O: Sodium *bis*(trimethylsilyl)amide (256 μL of a 1 M solution in THF, 0.26 mmol); P: sodium hypochlorite (218 μL of a 10% w/w aqueous solution, 0.43 mmol); Q: THF; R: 27% a/a.

Entry 2. O: Sodium *bis*(trimethylsilyl)amide (256 μL of a 1 M solution in THF, 0.26 mmol); P: *m*-CPBA (105 mg of 70% w/w solid, 0.43 mmol); Q: THF; R: 60% a/a.

Entry 3. O: Sodium *bis*(trimethylsilyl)amide (256 μ L of a 1 M solution in THF, 0.26 mmol); P: *bis*(trimethylsilyl)peroxide (76 mg, 0.43 mmol); Q: THF; R: 0% a/a.

Entry 4. O: Sodium *bis*(trimethylsilyl)amide (256 μ L of a 1 M solution in THF, 0.26 mmol); P: peracetic acid (101 μ L of a 32% w/w solution in AcOH, 0.43 mmol); Q: THF; R: 65% a/a.

Entry 5. O: N/A; P: sodium hypochlorite (218 μ L of a 10% w/w aqueous solution, 0.43 mmol); Q: THF; R: 68% a/a.

Entry 6. O: N/A; P: *m*-CPBA (105 mg of 70% w/w solid, 0.43 mmol); Q: THF; R: 6% a/a.

Entry 7. O: N/A; P: *bis*(trimethylsilyl)peroxide (76 mg, 0.43 mmol); Q: THF; R: 0% a/a

Entry 8. O: N/A; P: peracetic acid (101 μ L of a 32% w/w solution in AcOH, 0.43 mmol); Q: THF; R: 18% a/a.

Entry 9. O: NaOH (128 μ L of a 2 M aqueous solution, 0.26 mmol); P: sodium hypochlorite (218 μ L of a 10% w/w aqueous solution, 0.43 mmol); Q: THF; R: 67% a/a.

6.2.1.7 Experimental Procedures for Figure 12

The reaction was carried out using general procedure 1; details are provided below. Aliquots (20 μ L) of the reaction mixture were removed and quenched into sodium sulfite (0.98 mL of a 3% w/w aqueous solution) and analysed by HPLC (Method B). Product peak areas are recorded.

A: Sodium *bis*(trimethylsilyl)amide (9.6 mL of a 1 M solution in THF, 9.6 mmol); B: 469 mg, 3.7 mmol; C: 500 mg, 3.5 mmol; D: THF (5 mL); E: <7 $^{\circ}$ C; F: 0-5 $^{\circ}$ C; G: 5 min; H: HPLC showed complete conversion to the ketonitrile (**122**); I: peracetic acid (1.47 mL of a 32% w/w solution in AcOH, 7.1 mmol); J: 0-5 $^{\circ}$ C.

Sample time (min)	Analysis Delay (min)	Peak area 102 (mAu)
5	5	232
15	2	207
30	31	169
90	35	172
180	16	168
210	9	194

Table 32 – Data for Figure 12

6.2.1.8 Experimental Procedures for Figure 13

The reaction was carried out using general procedure 1; details for each entry are provided below. Aliquots (20 μ L) of the reaction mixture were removed and quenched into either sodium sulfite (0.98 mL of a 3% w/w aqueous solution) or sodium thiosulfate (0.98 mL of a 3% w/w aqueous solution) and analysed by HPLC (Method B). Product peak areas are recorded. The analytical solutions were left to stand at ambient temperature and then re-analysed.

A: Sodium *bis*(trimethylsilyl)amide (9.6 mL of a 1 M solution in THF, 9.6 mmol); B: 469 mg, 3.7 mmol; C: 500 mg, 3.5 mmol; D: THF (5 mL); E: <7 °C; F: 0-5 °C; G: 5 min; H: HPLC showed complete conversion to the ketonitrile (**122**); I: peracetic acid (1.47 mL of a 32% w/w solution in AcOH, 7.1 mmol); J: 0-5 °C.

Time (min)	Peak area 102	Peak area 102
	in sodium sulfite (mAu)	in sodium thiosulfate (mAu)
0	253	257
60	253	253
120	213	268

Table 33 – Tabulated data for Figure 13

6.2.2 Experimental Procedures for Section 3.2

6.2.2.1 General Procedure 3: Formation of Acetamide 252

4 Å Molecular sieves (50 mg, pre-activated) and base (A) were added to a solution of 1-(2-methyl-1,3-oxazol-4-yl)-2-(4-morpholinyl)-2-oxoethanone (**102**) (50 mg, 0.22 mmol) and methyl *D-allo-isoleucinate* (**66**) (40 mg, 0.22 mmol) solvent (B) (2 mL). The resultant reaction mixture was stirred at 20 °C for 18 h and analysed by HPLC (C)

6.2.2.2 Experimental Procedures for Table 3

Experiments for Table 3 were carried out according to general procedure 3; HPLC peak areas for the acetamide (**252**) are given for each entry

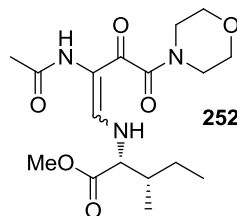
Entry 1. A: Triethylamine (22.6 mg, 0.233 mmol); B: 1:1 v/v MeOH/THF; C: 75%.

Entry 2. A: Triethylamine (22.6 mg, 0.233 mmol); B: THF; C: 10%.

Entry 3. A: None; B: MeOH; C: 0%.

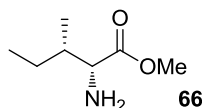
Entry 4. A: None; B: THF; C: 0%.

6.2.2.3 Preparation of Methyl-*N*-[2-(acetylamino)-4-(4-morpholinyl)-3,4-dioxo-1-buten-1-yl]-*D*-*allo*-isoleucinate (**252**)



4 Å Molecular sieves (50 mg, pre-activated) and triethylamine (22.6 mg, 0.223 mmol) were added to a solution of 1-(2-methyl-1,3-oxazol-4-yl)-2-(4-morpholinyl)-2-oxoethanone (**102**) (50 mg, 0.22 mmol) and methyl *D*-*allo*-isoleucinate (**66**) (40.5 mg, 0.22 mmol) in 1:1 THF/MeOH (2 mL). The resultant reaction mixture was stirred at 20 °C for 18 h, then decanted and concentrated to dryness under reduced pressure. The residue was purified by MDAP (MeCN/Water & formic acid) to afford the desired product as a yellow oil. (41 mg, 50%); ¹H NMR (400 MHz, CDCl₃) δ ppm 0.93 (d, *J* = 8.1 Hz, 3H) 0.95 (t, *J* = 7.3 Hz, 3H), 1.24 - 1.35 (m, 1H), 1.38 - 1.49 (m, 1H), 1.97 - 2.06 (m, 1H), 2.19 (s, 3H), 3.37 - 3.44 (m, 2H), 3.62 - 3.70 (m, 4H), 3.70 - 3.75 (m, 2H), 3.78 (s, 3H), 3.93 (dd, *J* = 8.8, 4.4 Hz, 1H), 6.97 (d, *J* = 12.7 Hz, 1H), 7.76 (s, 1H), 8.25 (dd, *J* = 12.7, 8.8 Hz, 1H); ¹³C NMR (100 MHz, CDCl₃) δ ppm 11.5 (CH₃), 14.3 (CH₃), 23.7 (CH₃), 26.0 (CH₂), 38.4 (CH), 41.9 (CH₂), 46.7 (CH₂), 52.6 (CH₃), 65.8 (CH), 66.6 (CH₂), 66.9, (CH₂), 110.4 (C), 146.1 (CH), 165.7 (C), 169.4 (C), 171.3 (C), 182.5 (C); -HPLC (Method B) *T_R* = 1.69 min 100% a/a; MS *m/z* (ESI⁺) 370 ([M+H]⁺); HRMS (ESI⁺) *m/z* calcd. for C₁₇H₂₈N₃O₆ [M+H]⁺ 370.1973, found 370.1972.

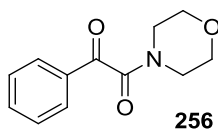
6.2.2.4 Preparation of Methyl *D*-*allo*-isoleucinate (**66**)



Toluene (200 mL) was charged to a solution of methyl *D*-*allo*-isoleucinate hydrochloride (20 g, 110 mmol) in water (100 mL). A solution of potassium carbonate (22.8 g, 165 mmol) in water (100 mL) was added and the resultant biphasic mixture was stirred

vigorously for 5 min. The phases were allowed to separate and the organic phase was washed with water (2 x 100 mL) and concentrated under reduced pressure to afford methyl *D-allo-isoleucinate* (**66**) as a clear liquid with spectral data consistent with the literature.¹⁶⁰ (10.9 g, 75 mmol, 68%). ¹H NMR (400 MHz, CDCl₃) δ ppm 0.84 (d, *J* = 7.1 Hz, 3H), 0.94 (t, *J* = 7.5 Hz, 3H), 1.21 – 1.32 (m, 1H), 1.36 (br. s, 2H), 1.42 – 1.50 (m, 1H), 1.77 - 1.87 (m, 1H), 3.47 (d, *J* = 4.2 Hz, 1H), 3.72 (s, 3H).

6.2.2.5 Preparation of 2-(4-Morpholinyl)-2-oxo-1-phenylethanone (**256**)



NaHMDS (39.7 mL of a 1 M solution in THF, 39.7 mmol) was added to a solution of 2-morpholinoacetonitrile (**121**) (1.95 g, 15.4 mmol) and methyl benzoate (**255**) (1.85 mL, 14.7 mmol) in THF (20 mL) at 0-5 °C under nitrogen. After stirring for 5 min, the reaction was shown to be complete by HPLC. A solution of peracetic acid (6.2 mL of a 32% w/w solution in AcOH, 32 mmol) in THF (20 mL) was then added dropwise keeping the temperature below 10 °C, and the solution was allowed to warm to ambient temperature once the addition was complete. Aqueous sodium thiosulfate pentahydrate (20 mL of a 20% w/w solution) was charged and the resultant biphasic mixture was stirred for 5 min and separated. The organic phase was then dried (MgSO₄) and concentrated to dryness under reduced pressure to afford an orange oil, which was purified by Biotage chromatography (EtOAc) to afford the desired product (**256**) as an orange solid with spectral data consistent with the literature¹⁶¹ (1.05 g, 32%); ¹H NMR (400 MHz, CDCl₃) δ ppm 3.35-3.45 (m, 2H), 3.60-3.70 (m, 2H), 3.70-3.90 (m, 4H), 7.53 (dd, *J* = 7.3, 7.2 Hz, 2H), 7.67 (t, *J* = 7.2 Hz, 1H), 7.97 (d, *J* = 7.3 Hz, 2H); ¹³C NMR (100 MHz, CDCl₃) δ ppm 41.6 (CH₂), 46.3 (CH₂), 66.67 (CH₂), 66.74 (CH₂), 129.1 (2 x CH), 129.7 (2 x CH), 133.1 (C) 135.0 (CH), 165.5 (C), 191.2 (C); HPLC (Method B) *T_R* = 1.77 min 99.3% a/a; MS *m/z* (ESI⁺) 220 ([M+H]⁺); HRMS (ESI⁺) *m/z* calcd. for C₁₂H₁₄NO₃ [M+H]⁺ 220.0968, found 220.0963.

6.2.2.6 General Procedure 4: Formation of Imines

2-(4-Morpholinyl)-2-oxo-1-phenylethanone (**256**) (A) and amine (B) were dissolved in solvent (C) (1mL) and additive (D) was charged. The resultant reaction mixture was stirred at temperature (E) for time (F) then an aliquot (100 μ L) was quenched into a solution of sodium borohydride (6.9 mg, 0.182 mmol) in MeOH (1 mL) and stirred for 30 s. The solution was quenched with HCl (1 mL of a 2 M aqueous solution) and analysed by HPLC (Method B) (G). The reaction was stirred for time (H) and sampled, quenched and analysed by HPLC as above (I). The reaction mixture was filtered, concentrated under an N₂ stream, dissolved in CDCl₃ (1 mL) and analysed by ¹H NMR (J).

6.2.2.7 Experimental Procedures for Table 4

Experiments for Table 4 were carried out according to general procedure 4. HPLC peak areas for amine **6** are given.

Entry 1. A: 20 mg, 0.091 mmol; B: methyl D-*allo*-isoleucinate (**66**) (13.3 mg, 0.091 mmol); C: toluene; D: *p*-toluenesulfonic acid (1.7 mg, 9.1 μ mol), 4 Å molecular sieves (20 mg); E: 20 °C; F: 30 min; G: 0% a/a; H: 18 h; I: 0% a/a; J: ¹H NMR showed no evidence of conversion to the amine (**257a**).

Entry 2. A: 20 mg, 0.091 mmol; B: methyl D-*allo*-isoleucinate (**66**) (13.3 mg, 0.091 mmol); C: toluene; D: 4 Å molecular sieves (20 mg); E: 20 °C; F: 30 min; G: 0% a/a; H: 18 h; I: 0% a/a; J: ¹H NMR showed no evidence of conversion to the amine (**257a**).

Entry 3. A: 20 mg, 0.091 mmol; B: methyl D-*allo*-isoleucinate (**66**) (13.3 mg, 0.091 mmol); C: dichloromethane; D: magnesium sulfate (20 mg); E: 20 °C; F: 30 min; G: 0% a/a; H: 18 h; I: 0% a/a; J: ¹H NMR showed no evidence of conversion the amine (**257a**).

Entry 4. A: 20 mg, 0.091 mmol; B: methyl D-*allo*-isoleucinate (**66**) (13.3 mg, 0.091 mmol); C: THF; D: 4 Å molecular sieves (20 mg); E: 20 °C; F: 30 min; G: 0% a/a; H: 18 h; I: 0% a/a; J: ¹H NMR showed no evidence of conversion the amine (**257a**).

6.2.2.8 Further Experimental Procedures for Section 3.2.2

Further experiments documented in section 3.2.2 were carried out using general procedure 4; details for each entry are provided below. Differences in processing are recorded for each entry where applicable.

Experiment 1. A: 58 mg, 0.265 mmol; B: benzylamine (29 μ L, 0.27 mmol); C: dichloromethane; D: magnesium sulphate (20 mg), 4 Å molecular sieves (20 mg); E: 20 °C; F: 30 min; G: 0% a/a; H: 18 h; I: 0% a/a; J: No evidence of conversion to the imine (**260**).

Experiment 2. A: 58 mg, 0.265 mmol; B: benzylamine (29 μ L, 0.27 mmol); C: dichloromethane; D: *p*-toluenesulfonic acid (5.0 mg, 0.03 mmol), 4 Å molecular sieves (20 mg); E: reflux; F: 72 h, evaporation of the reaction solvent occurred during the reflux period. The residue was re-dissolved in toluene (1 mL) prior to sampling; G: 26% a/a amine (**260**), 13% a/a ketoamide (**256**), 19.5% a/a alcohol (**258**); H: N/A; I: N/A; J: NMR showed the composition of the mixture had changed.

Experiment 3. A: 58 mg, 0.265 mmol; B: benzylamine (29 μ L, 0.27 mmol); C: dichloromethane; D: *p*-toluenesulfonic acid (5.0 mg, 0.03 mmol), 4 Å molecular sieves (20 mg); E: reflux; F: 18 h; G: 20% a/a amine (**260**), 14% a/a ketoamide (**256**), 40% alcohol (**258**); H: N/A; I: N/A; J: N/A.

Experiment 4. A: 58 mg, 0.265 mmol; B: methyl *D*-*allo*-isoleucinate (38 mg, 0.27 mmol); C: dichloromethane; D: *p*-toluenesulfonic acid (5.0 mg, 0.03 mmol), 4 Å molecular sieves (20 mg); E: reflux; F: 18 h; G: 0% a/a amine (**260**), 100% alcohol (**258**); H: N/A; I: N/A; J: N/A.

6.2.2.9 Assessment of Borohydride Reduction

A reaction mixture was prepared according to experiment 4 and aliquots (100 μ L) were taken and quenched into sodium borohydride (6.9 mg, 0.182 mmol) in MeOH (1 mL) and stirred for time (K). These solutions were quenched with HCl (1 mL of a 2 M aqueous solution) and analysed by HPLC (Method B) (L).

Experiment 1. K: 1 min; L: 26% a/a amine (**260**), 13% a/a ketoamide (**256**), 19.5% a/a alcohol (**258**).

Experiment 2. K: 5 min; L: 26% a/a amine (**260**), 13% a/a ketoamide (**256**), 19.5% a/a alcohol (**258**).

Experiment 3. K: 15 min; L: 26% a/a amine (**260**), 13% a/a ketoamide (**256**), 19.5% a/a alcohol (**258**).

6.2.2.10 Experimental Procedures for Table 5

Further experiments documented in Table 5 were carried out using general procedure 4. Differences in processing are recorded for each entry where applicable.

Entry 1. A: 125 mg, 0.57 mmol; B: methyl D-*allo*-isoleucinate (**66**) (166 mg, 1.14 mmol); C: toluene (2 mL); D: aluminium chloride (76 mg, 0.57 mmol), 4 Å molecular sieves (50 mg); E: reflux; F: 2 h; G: 20% a/a ketoamide (**256**), 20% a/a alcohol (**258**); H: 18 h; I: 17.3% a/a ketoamide (**256**), 58.5% a/a alcohol (**258**), 8.7% a/a amine (**264**), 15.9% a/a amino acid (**263**); J: N/A.

Entry 2. A: 125 mg, 0.57 mmol; B: methyl D-*allo*-isoleucinate (166 mg, 1.14 mmol); C: toluene (2 mL); D: zinc chloride (78 mg, 0.57 mmol), 4 Å molecular sieves (50 mg); E: reflux; F: 2 h; G: 77% a/a ketoamide (**256**), 23% a/a alcohol (**258**); H: 18 h; I: 10.9% a/a ketoamide (**256**), 82.0% a/a alcohol (**258**), 1.8% a/a amine (**264**), 5.3% a/a amino acid (**263**); J: N/A.

Entry 3. A: 125 mg, 0.57 mmol; B: methyl D-*allo*-isoleucinate (166 mg, 1.14 mmol); C: toluene (2 mL); D: titanium tetrachloride (63 µL, 0.57 mmol), 4 Å molecular sieves (50 mg); E: reflux; F: 2 h; G: 12% a/a amine (**264**), 88% a/a amino acid **143**; H: 18 h; I: 1.2% a/a ketoamide (**256**), 0% a/a alcohol (**258**), 68.2% a/a amine (**264**), 30.6% a/a amino acid (**263**); J: N/A.

Entry 4. A: 125 mg, 0.57 mmol; B: methyl D-*allo*-isoleucinate (166 mg, 1.14 mmol); C: toluene (2 mL); D: titanium ethoxide (120 µL, 0.57 mmol), 4 Å molecular sieves (50 mg); E: reflux; F: 2 h; G: 38% a/a ketoamide (**256**), 62% a/a alcohol (**258**); H: 18 h; I:

83.8% a/a ketoamide (**256**), 6.4% a/a alcohol (**258**), 1.7% a/a amine (**264**), 7.9% a/a amino acid (**263**); J: N/A.

6.2.2.11 General Procedure 5: Imine Formation using Titanium Tetrachloride

2-(4-Morpholinyl)-2-oxo-1-phenylethanone (**256**) (125 mg, 0.57 mmol) and methyl D-*allo*-isoleucinate (**66**) (248 mg, 1.71 mmol) were taken up in solvent (A) (2 mL) and titanium tetrachloride (31 μ L, 0.29 mmol) was charged. The resultant reaction mixtures were stirred at 20 °C for 30 min then an aliquot (100 μ L) was quenched into a solution of sodium borohydride (10.8 mg, 0.285 mmol) in MeOH (1 mL) and stirred for approximately 30 s. These solutions were quenched with HCl (1 mL of a 2 M aqueous solution) and analysed by HPLC (Method B) (B). The reactions were stirred for a further 4 h and sampled, quenched and analysed by HPLC as above (C). A further portion of titanium tetrachloride (31 μ L, 0.29 mmol) was charged and the reaction mixtures were sampled, quenched and analysed by HPLC as above (D). An aliquot (50 μ L) was also dissolved in ammonium bicarbonate (1 mL of a 10 mM aqueous solution) and analysed by HPLC (Method C) (E).

6.2.2.12 Experimental Procedures for Table 6

The experiments documented in Table 6 were carried out using general procedure 5. Differences in processing are recorded for each entry where applicable.

Entry 1. A: toluene; B: HPLC showed approximately 1:1 ketoamide (**256**): alcohol (**258**); C: HPLC showed no change from previous sample; D: 70.7% a/a ketoamide (**256**), 15.1% a/a alcohol (**258**); E: 70.7% a/a imine (**257**), 15.1% a/a ketoamide (**256**).

Entry 2. A: toluene; B: HPLC showed approximately 1:1 ketoamide (**256**): alcohol (**258**); C: HPLC showed no change from previous sample; D: 55.0% a/a ketoamide (**256**), 17.3% a/a alcohol (**258**); E: 55.0% a/a imine (**257**), 17.3% a/a ketoamide (**256**).

Entry 3. A: toluene; B: HPLC showed approximately 1:1 ketoamide (**256**): alcohol (**258**); C: HPLC showed no change from previous sample; D: 70.7% a/a ketoamide (**256**), 16.7% a/a alcohol (**258**); E: 70.7% a/a imine (**257**), 16.7% a/a ketoamide (**256**).

Entry 4. A: toluene; B: HPLC showed approximately 1:1 ketoamide (**256**): alcohol (**258**); C: HPLC showed no change from previous sample; D: 58.5% a/a ketoamide (**256**), 16.0% a/a alcohol (**258**); E: 58.5% a/a imine (**257**), 16.0% a/a ketoamide (**256**).

6.2.2.13 General Procedure 7: Imine Formation Reaction Profiling

Lewis acid (A) and base (B) were added to a solution of 1-(2-methyl-1,3-oxazol-4-yl)-2-(4-morpholinyl)-2-oxoethanone (**102**) (C) and methyl *D-allo-isoleucinate* (**66**) (D) in solvent (E) at temperature (F) and stirring was continued for time (G). Conversion to the imine (**110**) was monitored by quenching an aliquot (20 μ L) into ammonium bicarbonate (10 mM aqueous solution) and analysing by LCMS (Method C) (H).

6.2.2.14 Experimental Procedures for Figure 14

The experiment documented in Figure 14 was carried out according to general procedure 7. HPLC % peak areas for each time point are given below.

A: Titanium tetrachloride (123 μ L, 1.12 mmol); B: none; C: 250 mg, 1.12 mmol; D: 324 mg, 2.23 mmol; E: THF (2.5 mL); F: 20 $^{\circ}$ C; G & H: See Table 34.

Time (min)	102 (% a/a)	252 (% a/a)	110a (% a/a)	110b (% a/a)
0	95	0	0	0
5	17.9	9.5	32.3	31.5
60	9.2	29.7	21.9	25.1
120	6.8	38	13.2	16.8
180	7.6	48	10.1	8.7
360	6	54.6	2.6	3.3

Table 34 – Data corresponding to Figure 14

6.2.2.15 Experimental Procedures for Figure 15

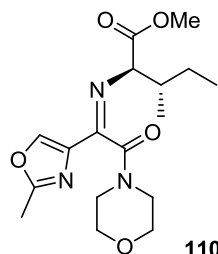
The experiment documented in Figure 15 was carried out according to general procedure 7. HPLC % peak areas for each time point are given below.

A: Titanium tetrachloride (25 μ L, 0.22 mmol); B: none; C: 50 mg, 0.22 mmol; D: 65 mg, 0.45 mmol; E: THF (1 mL); F: 0 $^{\circ}$ C; G & H: See Table 35.

Time (min)	102 (% a/a)	252 (% a/a)	110a (% a/a)	110b (% a/a)
0	95	0	0	0
10	26.5	2	28	27.5
40	24.7	3.9	28.3	32.2
60	22.8	10.3	26.2	28.6
120	27.9	34.1	11.8	12.7
180	34.8	50.2	1.5	2.6

Table 35 – Data corresponding to Figure 15

6.2.2.16 Experimental Procedures for the Preparation of (2*R*,3*S*)-Methyl-3-methyl-2-((1-(2-methyloxazol-4-yl)-2-morpholino-2-oxoethylidene)amino)pentanoate (110)



Mixture of *E* and *Z*-isomers

The experiments documented in section 3.2.3.1 were carried out using general procedure 7; details for each entry are provided below. Differences in processing are recorded for each entry where applicable.

Experiment 1. A: Titanium tetraethoxide (120 μ L, 0.57 mmol); B: none; C: 125 mg, 0.57 mmol; D: 166 mg, 1.14 mmol; E: toluene (2 mL); F: 100 $^{\circ}$ C; G: 4 h 30; H: HPLC showed 3% a/a of the desired imine (**110**) in addition to significant levels of corresponding carboxylic acid and ethyl ester.

Experiment 2. A: Zinc chloride (890 μ L of a 0.5 M solution in THF, 0.45 mmol); B: none; C: 100 mg, 0.45 mmol; D: 130 mg, 0.89 mmol; E: THF (1 mL); F: 20 $^{\circ}$ C; G: 2 h; H: the imine (**110**) was not observed, but some conversion to the acetamide (**252**) was observed.

Experiment 3. A: Trimethylsilyl trifluoromethanesulfonate (81 μ L, 0.45 mmol); B: none; C: 100 mg, 0.45 mmol; D: 130 mg, 0.89 mmol; E: THF (1 mL); F: 20 $^{\circ}$ C; G: 10 min; H: the imine (**110**) was not observed, but some conversion to the acetamide (**252**) was observed.

Experiment 4. A: Bismuth trifluoromethanesulfonate (146 mg, 0.22 mmol); B: none; C: 50 mg, 0.22 mmol; D: 32 mg, 0.22 mmol; E: THF (1 mL); F: 20 $^{\circ}$ C; G: 1 h; H: the imine (**110**) was not observed, some conversion to the acetamide (**252**) was observed.

Experiment 5. A: Hafnium trifluoromethanesulfonate (173 mg, 0.22 mmol); B: none; C: 50 mg, 0.22 mmol; D: 32 mg, 0.22 mmol; E: THF (1 mL); F: 20 $^{\circ}$ C; G: 1 h; H: the imine (**110**) was not observed, but some conversion to the acetamide (**252**) was observed.

Experiment 6. A: Indium trifluoromethanesulfonate (125 mg, 0.22 mmol); B: none; C: 50 mg, 0.22 mmol; D: 32 mg, 0.22 mmol; E: THF (1 mL); F: 20 $^{\circ}$ C; G: 1 h; H: the imine (**110**) was not observed, but some conversion the acetamide (**252**) was observed.

Experiment 7. A: Scandium trifluoromethanesulfonate (110 mg, 0.22 mmol); B: none; C: 50 mg, 0.22 mmol; D: 32 mg, 0.22 mmol; E: THF (1 mL); F: 20 $^{\circ}$ C; G: 1 h; H: the imine (**110**) was not observed, but some conversion to the acetamide (**252**) was observed.

Experiment 8. A: Ytterbium trifluoromethanesulfonate (138 mg, 0.22 mmol); B: none; C: 50 mg, 0.22 mmol; D: 32 mg, 0.22 mmol; E: THF (1 mL); F: 20 $^{\circ}$ C; G: 1 h; H: the

imine (**110**) was not observed, but some conversion to the acetamide (**252**) was observed.

Experiment 9. A: none; B: Potassium carbonate (31 mg, 0.22 mmol); C: 50 mg, 0.22 mmol; D: 32 mg, 0.22 mmol; E: MeOH (1 mL); F: 50 °C; G: 20 min; H: 84% a/a acetamide (**252**). Conditions adapted from those described by Hughes *et al.*¹⁶²

Experiment 10. A: Titanium tetrachloride (13 µL, 11 mmol); B: triethylamine (93 µL, 0.67 mmol); C: 50 mg, 0.22 mmol; D: 32 mg, 0.22 mmol; E: THF (1 mL); F: 0 °C; G: 5 min; H: 55% a/a desired imine (**110**).

Experiment 11. A: Titanium tetrachloride (25 µL, 22 mmol); B: triethylamine (93 µL, 0.67 mmol); C: 50 mg, 0.22 mmol; D: 32 mg, 0.22 mmol; E: THF (1 mL); F: 0 °C; G: 5 min; H: 67% a/a desired imine (**110**).

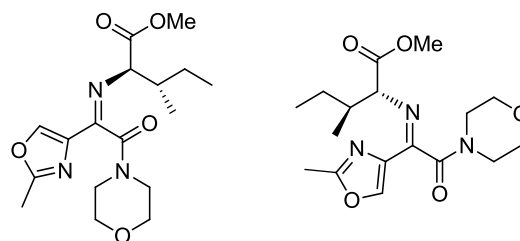
Experiment 12. A: Titanium tetrachloride (196 µL, 1.78 mmol); B: triethylamine (746 µL, 5.35 mmol); C: 400 mg, 1.78 mmol; D: 285 mg, 1.96 mmol; E: THF (8 mL); F: 0 °C; G: 5 min; H: 69% a/a desired imine (**110**), 16% a/a ketoamide remained. Further titanium tetrachloride (98 µL, 0.89 mmol) was charged and the reaction mixture was stirred for 20 min and analysed by LCMS (Method C), <5% a/a ketoamide (**102**) remained. The reaction mixture was treated with NaOH (2.85 mL of a 5 M aqueous solution) which caused solids to precipitate (presumed to be TiO₂) and were difficult to remove by filtration.

Experiment 13. A: Titanium tetrachloride (0.89 mL of a 1 M solution in dichloromethane, 0.89 mmol); B: triethylamine (373 µL, 2.68 mmol); C: 200 mg, 0.89 mmol; D: 130 mg, 0.89 mmol; E: dichloromethane (2 mL); F: 0 °C; G: 5 min; H: 6.6% a/a ketoamide (**102**) remained. Water (4 mL) was charged and the resultant biphasic mixture was stirred vigorously for 2 min and the layers were separated. The precipitation of solids was not observed. The pH of the aqueous phase was measured to be 2 and HPLC showed the absence of product in this phase. The organic phase was held overnight and then analysed by HPLC and found to contain 7.3% a/a ketoamide (**102**).

Experiment 14. A: Titanium tetrachloride (0.89 mL of a 1 M solution in dichloromethane, 0.89 mmol); B: triethylamine (373 μ L, 2.68 mmol); C: 200 mg, 0.89 mmol; D: 130 mg, 0.89 mmol; E: dichloromethane (2 mL); F: 0 $^{\circ}$ C; G: 5 min; H: 4.9% a/a ketoamide (**102**) remained. Water (4 mL) was charged and the resultant biphasic mixture was stirred vigorously for 2 min and the layers were separated. The organic phase was dried (MgSO_4) and concentrated to dryness under reduced pressure to afford (2*R*,3*S*)-methyl-3-methyl-2-((1-(2-methyloxazol-4-yl)-2-morpholino-2-oxoethylidene)amino)pentanoate as a red/brown oil. (250 mg, 80 %)

Experiment 15. A: Titanium tetrachloride (22 mL of a 1 M solution in dichloromethane, 22 mmol); B: triethylamine (9.3 mL, 67 mmol); C: 5 g, 22 mmol; D: 4.05 g, 22 mmol; E: dichloromethane (50 mL); F: 0 $^{\circ}$ C; G: 5 min; H: 5.2% a/a ketoamide (**102**) remained. Water (70 mL) was charged and the resultant biphasic mixture was stirred vigorously for 2 min and the layers were separated. The organic phase was dried (MgSO_4) and concentrated to dryness under reduced pressure to afford (2*R*,3*S*)-methyl 3-methyl-2-((1-(2-methyloxazol-4-yl)-2-morpholino-2-oxoethylidene)amino)pentanoate as a red/brown oil. (7.26 g, 93 %)

6.2.2.17 Characterisation of *E*- and *Z*-isomers of (2*R*,3*S*)-Methyl-3-methyl-2-((1-(2-methyloxazol-4-yl)-2-morpholino-2-oxoethylidene)amino)pentanoate (**110a** & **110b**)



110a; *Z*-Thermodynamic

110b; *E*-Kinetic

The crude (2*R*,3*S*)-methyl 3-methyl-2-((1-(2-methyloxazol-4-yl)-2-morpholino-2-oxoethylidene)amino)pentanoate (**110**) was prepared according to general procedure 7, experiment 15. Approx 200 mg of this isomeric mixture was separated by MDAP (MeCN/10 mM ammonium bicarbonate). The resulting fractions were concentrated,

extracted with dichloromethane (2 x 20 mL) and the extracts were concentrated to dryness under reduced pressure to afford the isomerically pure imines, which isomerised slowly on standing at room temperature.

Z-isomer (**110a**); ^1H NMR (400 MHz, CDCl_3) δ ppm 0.91 (t, $J = 7.6$ Hz, 3H), 0.98 (d, $J = 6.9$ Hz, 3H), 1.11 - 1.21 (m, 1H), 1.38 - 1.52 (m, 1H), 2.11 - 2.19 (m, 1H), 2.47 (s, 3H), 3.25 - 3.36 (m, 2H), 3.52 - 3.85 (m, 9H), 4.08 (d, $J = 5.6$ Hz, 1H), 8.02 (s, 1H); HPLC (Method C) $T_R = 2.21$ min, 86% a/a; MS m/z (ESI $^+$) 352 ([M+H] $^+$).

E-isomer (**110b**); ^1H NMR (400 MHz, CDCl_3) δ ppm 0.86 (t, $J = 7.3$ Hz, 3H), 0.99 (d, $J = 6.8$ Hz, 3H), 1.18 - 1.28 (m, 1H), 1.34 - 1.47 (m, 1H), 2.07 - 2.19 (m, 1H), 2.44 (s, 3H), 3.26 - 3.36 (m, 2H), 3.57 - 3.97 (m, 9H), 5.07 (d, $J = 3.7$ Hz, 1H), 7.98 (s, 1H); HPLC (Method C) $T_R = 2.38$ min, 59% a/a; MS m/z (ESI $^+$) 352 ([M+H] $^+$).

6.2.3 Experimental Procedures for Section 3.3

6.2.3.1 General procedure 6: Reducing Agent Screen

Titanium tetrachloride (590 μL , 5.35 mmol) was added to a solution of 1-(2-methyl-1,3-oxazol-4-yl)-2-(4-morpholinyl)-2-oxoethanone (**102**) (1.20 g, 5.35 mmol) and methyl D-*allo*-isoleucinate (**66**) (1.55 g, 10.7 mmol) in THF (24 mL) at 0 °C and stirring was continued at 0 °C for 5 min. Conversion to the imine (**110**) was monitored by quenching an aliquot (20 μL) into ammonium bicarbonate (10 mM aqueous solution) solution and analysing by LCMS (Method C). The solution was divided into 12 aliquots and each was charged directly to solutions of the reducing agents (A) in THF (2 mL). After stirring at 20 °C for 1 hour the reactions were sampled, quenched into HCl (1 mL of a 1 M aqueous solution) and analysed by HPLC (Method B) and LCMS (B).

6.2.3.2 Experimental Procedures for Table 7

The experiments documented in Table 7 were carried out using general procedure 6. Differences in processing are recorded for each entry where applicable.

Entry 1. A: Borane (444 μL of a 1 M solution in THF, 0.44 mmol); B: 5.9% a/a amine (**111**), 4.2% a/a amine (**267**), 38.5% a/a alcohol (**106**), 24.8% a/a ketoamide (**102**).

Entry 2. A: Catecholborane (96 μL , 0.89 mmol); B: 16.7% a/a amine (**111**), 8.8% a/a amine (**267**), 37.5% a/a alcohol (**106**), 10.6% a/a ketoamide (**102**).

Entry 3. A: Diisobutylaluminium hydride (894 μL of a 1 M solution in THF, 0.89 mmol); B: 1.9% a/a amine (**111**), 0% a/a amine (**267**), 4.7% a/a alcohol (**106**), 7.2% a/a ketoamide (**102**).

Entry 4. A: Lithium aluminium hydride (444 μL of a 1 M solution in THF, 0.44 mmol); B: 13.5% a/a amine (**111**), 6.8% a/a amine (**267**), 23.8% a/a alcohol (**106**), 19.9% a/a ketoamide (**102**).

Entry 5. A: Lithium aluminium hydride (1.79 mL of a 1 M solution in THF, 1.79 mmol); B: 0% a/a amine (**111**), 0% a/a amine (**267**), 12.8% a/a alcohol (**106**), 0% a/a ketoamide (**102**).

Entry 6. A: Sodium borohydride (16.8 mg, 0.44 mmol) and zinc chloride (60.5 mg, 0.44 mmol); B: 26.2% a/a amine (**111**), 18.9% a/a amine (**267**), 32.6% a/a alcohol (**106**), 5.9% a/a ketoamide (**102**).

Entry 7. A: Sodium triacetoxyborohydride (189 mg of 0.89 mmol); B: 4.0% a/a amine (**111**), 7.7% a/a amine (**267**), 21.7% a/a alcohol (**106**), 39.2% a/a ketoamide (**102**).

Entry 8. A: Lithium borohydride (9.7 mg, 0.44 mmol); B: 7.8% a/a amine (**111**), 8.3% a/a amine (**267**), 36.4% a/a alcohol (**106**), 12.8% a/a ketoamide (**102**).

Entry 9. A: Lithium triethylborohydride (894 μ L of a 1 M solution in THF, 0.89 mmol); B: 5.0% a/a amine (**111**), 3.5% a/a amine (**267**), 17.4% a/a alcohol (**106**), 23.9% a/a ketoamide (**102**).

Entry 10. A: Triethylsilane (71 μ L, 0.44 mmol) and *tris*(triphenylphosphine)rhodium chloride (39.6 mg, 0.043 mmol); B: 0% a/a amine (**111**), 0% a/a amine (**267**), 0% a/a alcohol (**106**), 22.6% a/a ketoamide (**102**).

Entry 11. A: Trichlorosilane (45 μ L, 0.44 mmol) and *tris*(triphenylphosphine)rhodium chloride (39.6 mg, 0.043 mmol); B: 1.0% a/a amine (**111**), 3.4% a/a amine (**267**), 10.9% a/a alcohol (**106**), 9.4% a/a ketoamide (**102**).

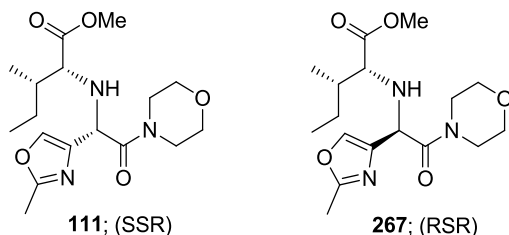
Entry 12. A: Phenylsilane (55 μ L, 0.44 mmol) and *tris*(triphenylphosphine)rhodium chloride (39.6 mg, 0.043 mmol); B: 0% a/a amine (**111**), 0% a/a amine (**267**), 2.3% a/a alcohol (**106**), 16.7% a/a ketoamide (**102**).

6.2.3.3 Preparation of Zinc Borohydride

Zinc chloride (50 mL of a 0.5 M solution in THF, 25 mmol) was added to sodium borohydride (1.9 g, 50 mmol) under nitrogen. The resultant suspension was stirred at 20 °C for 18 h during which time the suspension thickened. The solids were removed by

filtration to afford a (presumed) 0.5 M solution of zinc borohydride which was held under nitrogen and used as required.

6.2.3.4 Preparation of Methyl-*N*-[1-(2-methyl-1,3-oxazol-4-yl)-2-(4-morpholinyl)-2-oxoethyl]-*D*-*allo*-isoleucinate (**111** & **267**)

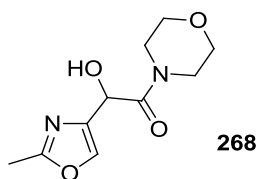


Titanium tetrachloride (0.25 mL, 2.23 mmol) was added to a solution of methyl *D*-*allo*-isoleucinate (**66**) (971 mg, 6.69 mmol) and 1-(2-methyl-1,3-oxazol-4-yl)-2-(4-morpholinyl)-2-oxoethanone (**102**) (500 mg, 2.23 mmol) in THF (10 mL) at 0 °C and the reaction mixture was stirred for 5 min. Zinc borohydride (4.46 mL of a 0.5 M solution in THF, 2.23 mmol) was added at 0 °C and stirred for 30 min. The mixture was quenched by addition of HCl (6 mL of a 2 M aq. solution), neutralised with satd. aq. sodium bicarbonate solution, filtered and extracted with EtOAc (10 mL). The organic phase was dried (MgSO₄) and concentrated to dryness under reduced pressure to afford a mixture of diastereoisomers (**111** & **267**) as a yellow oil, which was separated by MDAP (MeCN/Water & TFA) and concentrated to dryness under reduced pressure to afford clear oils.

Diastereoisomer 1 (**111**) (38 mg, 5%); ¹H NMR (400 MHz, CDCl₃) δ ppm 0.89 (t, *J* = 7.3 Hz, 3H), 0.93 (d, *J* = 6.8 Hz, 3H), 1.10 - 1.27 (m, 1H), 1.37 - 1.51 (m, 1H), 1.71 - 1.83 (m, 1H), 2.41 (s, 3H), 3.24 (d, *J* = 5.6 Hz, 1H), 3.49 - 3.71 (m, 11H), 4.61 (s, 1H), 7.50 (s, 1H), *NH* not observed; ¹³C NMR (100 MHz, CDCl₃) δ ppm 11.7 (CH₃), 13.9 (CH₃), 14.9 (CH₃), 26.2 (CH₂), 38.0 (CH), 42.7 (CH₂), 46.0 (CH₂), 51.6 (CH₃), 55.1 (CH), 63.5 (CH), 66.5 (CH₂), 66.7 (CH₂), 135.8 (CH), 138.8 (C), 161.5 (C), 169.5 (C), 174.9 (C); HPLC (Method B) *T_R* = 1.69 min, 99.3% a/a; MS *m/z* (ESI⁺) 354 ([M+H]⁺); HRMS (ESI⁺) *m/z* calcd. for C₁₇H₂₈N₃O₅ [M+H]⁺ 354.2024, found 354.2025.

Diastereoisomer 2 (**267**) (77 mg, 10%); ^1H NMR (400 MHz, CDCl_3) δ ppm 0.85 (t, $J = 7.3$ Hz, 3H), 0.90 (d, $J = 6.8$ Hz, 3H), 1.15 - 1.31 (m, 1H), 1.35 - 1.49 (m, 1H), 1.72 - 1.84 (m, 1H), 2.41 (s, 3 H), 3.20 (d, $J = 5.6$ Hz, 1H), 3.52 - 3.76 (m, 11H), 4.58 (s, 1H), 7.53 (s, 1H), *NH* not observed; ^{13}C NMR (100 MHz, CDCl_3) δ ppm 9.8 (CH_3), 12.1 (CH_3), 13.0 (CH_3), 24.4 (CH_2), 36.2 (CH), 40.9 (CH_2), 44.3 (CH_2), 47.8 (CH_3), 53.0 (CH), 61.2 (CH), 64.7 (CH_2), 64.9 (CH_2), 134.5 (CH), 137.7 (C), 159.6 (C), 167.6 (C), 173.2 (C); HPLC (Method B) $T_R = 1.75$ min, 96.6% a/a; MS m/z (ESI^+) 354 ($[\text{M}+\text{H}]^+$); HRMS (ESI^+) m/z calcd. for $\text{C}_{17}\text{H}_{28}\text{N}_3\text{O}_5$ $[\text{M}+\text{H}]^+$ 354.2024, found 354.2025.

6.2.3.5 Reduction of Ketoamide 102



1-(2-Methyloxazol-4-yl)-2-morpholinoethane-1,2-dione (**102**) (500 mg, 2.23 mmol) and sodium borohydride (84 mg, 2.23 mmol) were charged to a round bottomed flask, THF (5 mL) was added and the resultant reaction mixture was stirred at ambient temperature for 50 min. An aliquot of the reaction mixture (20 μL) was quenched into HCl (1 mL of a 2 M aqueous solution) and analysed by LCMS (Method B) which showed conversion to the alcohol (**268**). HPLC (Method B) $T_R = 1.27$ min, 75.0% a/a; MS m/z (ESI^+) 227 ($[\text{M}+\text{H}]^+$).

6.2.3.6 Stability of Amine 111 to Reduction Conditions

(2*R*,3*S*)-Methyl-3-methyl-2-((1-(2-methyloxazol-4-yl)-2-morpholino-2-oxoethyl)amino) pentanoate (**111**) (30 mg, 0.085 mmol) was taken up in THF (0.6 mL) and analysed by HPLC (Method B) which showed a single peak ($T_R = 1.70$ min, 97.4% a/a). Titanium tetrachloride (9.4 μL , 0.085 mmol) was charged; the solution turned a dark brown colour and was stirred at ambient temperature for 5 min and analysed by HPLC (Method B) which showed a single peak ($T_R = 1.70$ min, 95.5% a/a). Zinc borohydride (170 μL of a

0.5 M solution in THF, 0.085 mmol) was added and the mixture was stirred for 5 min at ambient temperature and analysed by HPLC (Method B) which showed the absence of a peak at $T_R = 1.70$ min and a number of low intensity peaks.

6.2.3.7 General Procedure 8: Heterogeneous Catalytic Hydrogenation

(2*R*,3*S*)-Methyl-3-methyl-2-((1-(2-methyloxazol-4-yl)-2-morpholino-2-oxoethylidene)amino)pentanoate (**110**) (A) was taken up in solvent (B) and charged to a hydrogenation vessel containing catalyst (C). The resultant reaction mixtures were hydrogenated at pressure (D) and temperature (E) for time (F) and analysed by HPLC. The hydrogen uptake curves were measured and plotted and the total hydrogen uptake after 75 min was recorded (G).

6.2.3.8 Experimental Procedures for Table 8 and Figure 23.

The experiments documented in Table 8, Figure 23 and experiment 1 were carried out using general procedure 8; details for each entry are provided below. Differences in processing are recorded for each entry where applicable.

Entry 1. A: 200 mg, 0.57 mmol); B: THF (3 mL); C: 10% wt Pd/C (100 mg); D: 1 bar; E: 25 °C; F: 75 min; G: 6.3 mL

Entry 2. A: 200 mg, 0.57 mmol); B: toluene (3 mL); C: 10% wt Pd/C (100 mg); D: 1 bar; E: 25 °C; F: 75 min; G: 7.0 mL

Entry 3. A: 200 mg, 0.57 mmol); B: EtOH (3 mL); C: 10% wt Pd/C (100 mg); D: 1 bar; E: 25 °C; F: 75 min; G: 9.5 mL

Entry 5. A: 200 mg, 0.57 mmol); B: THF (3 mL); C: 10% wt Pd/C (100 mg); D: 3 bar; E: 25 °C; F: 75 min; G: 9.6 mL

Entry 6. A: 200 mg, 0.57 mmol); B: toluene (3 mL); C: 10% wt Pd/C (100 mg); D: 3 bar; E: 25 °C; F: 75 min; G: 10.4 mL

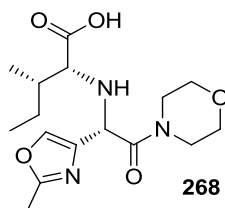
Entry 7. A: 200 mg, 0.57 mmol); B: EtOH (3 mL); C: 10% wt Pd/C (100 mg); D: 3 bar; E: 25 °C; F: 75 min; G: 12.6 mL. The catalyst was removed from the reaction mixture

by filtration and the filtrate was concentrated under reduced pressure to afford a yellow/brown oil. The oil was dissolved in dichloromethane (5 mL) and extracted into HCl (5mL of a 2 M aqueous solution). The aqueous phase was adjusted to pH 11 by the addition of K₂CO₃ (approx 1 g) and extracted with dichloromethane (5 mL). The organic phase was dried (MgSO₄) and concentrated to dryness under reduced pressure to afford (2*R*,3*S*)-methyl 3-methyl-2-((1-(2-methyloxazol-4-yl)-2-morpholino-2-oxoethyl)amino)pentanoate (**111/267**) as a clear, orange oil (74 mg, 37 %).

Experiment 1. A: 5.05 g, 14.4 mmol; B: EtOH (76 mL); C: 10% wt Pd/C (2.5 g); D: 3 bar; E: 25 °C; F: 120 min; G: 12.6 mL. The catalyst was removed from the reaction mixture by filtration through Celite[®] and washed through with EtOH (30 mL) and the filtrate was concentrated under reduced pressure to afford (2*R*,3*S*)-methyl 3-methyl-2-((1-(2-methyloxazol-4-yl)-2-morpholino-2-oxoethyl)amino)pentanoate (**111/267**) as an orange gum which was used without further purification. (4.26 g, 84 %).

6.2.4 Experimental Procedures for Section 3.4

6.2.4.1 Preparation of (2*R*,3*S*)-3-Methyl-2-(((*S*)-1-(2-methyloxazol-4-yl)-2-morpholino-2-oxoethyl)amino)pentanoic acid (**268**)



(2*R*,3*S*)-Methyl-3-methyl-2-((1-(2-methyloxazol-4-yl)-2-morpholino-2-oxoethyl)amino)pentanoate (**111/267**) (4.47 g, 12.7 mmol) was dissolved in MeOH (45 mL) and a solution of lithium hydroxide (0.61 g, 25.3 mmol) in water (45 mL) was added. The reaction mixture was heated to 60 °C and stirred for 3.5 h, until HPLC (Method A) showed absence of ester. The reaction mixture was concentrated to approximately 50 mL under reduced pressure and cooled to 20 °C. A solution of acetic acid (1.81 mL, 31.6 mmol) in water (30 mL) was titrated into the stirring mixture in 0.2 mL portions until the pH reached 4.69. The aqueous solution was then freeze dried, and the resulting solid was triturated with *i*-PrOH (20 mL). The solids were collected by filtration, washed with *i*-PrOH (10 mL) and dried under reduced pressure to afford the undesired diastereoisomer (**268**) as a white solid (947 mg, 22%); ¹H NMR (400 MHz, MeOD) δ ppm 0.83 (t, *J* = 7.5 Hz, 3H), 0.90 (d, *J* = 6.8 Hz, 3H), 1.16 - 1.28 (m, 1H), 1.40 - 1.53 (m, 1H), 1.68 - 1.80 (m, 1H), 2.39 (s, 3H), 2.92 (d, *J* = 4.6 Hz, 1H), 3.41 - 3.52 (m, 1H), 3.53 - 3.70 (m, 7H), 4.75 (s, 1H), 7.72 (s, 1H), COOH and NH not observed; ¹³C NMR (100 MHz, MeOD) δ ppm 12.4 (CH₃), 13.6 (CH₃), 15.6 (CH₃), 27.8 (CH₂), 39.5 (CH), 44.0 (CH₂), 47.4 (CH₂), 55.8 (CH), 66.3 (CH), 67.7 (CH₂), 138.6 (CH), 139.7 (C), 163.7 (C), 171.6 (C), 181.5 (C); HPLC (Method A) *T_R* = 2.30 min, 91.5% a/a. MS *m/z* (ESI⁺) 340 ([M+H]⁺); HRMS (ESI⁺) *m/z* calcd. for C₁₆H₂₆N₃O₅ [M+H]⁺ 340.1867, found 340.1875.

6.2.4.2 pH Titration of Amino Acid **89**

(2*R*,3*S*)-3-Methyl-2-(((*R*)-1-(2-methyloxazol-4-yl)-2-morpholino-2-oxoethyl) amino) pentanoic acid (**89**) (170 mg, 0.5 mmol) was dissolved in water (5 mL) and NaOH (0.38 mL of a 2 M aqueous solution, 0.75 mmol) was added. HCl (3 mL of a 0.1 M aqueous solution) was titrated into the solution, recording the pH after the addition of each 0.2 mL portion.

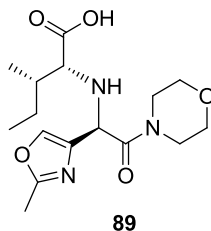
Acid added (equiv)	pH		
0.05	12.6	1.6	3.25
0.1	12.51	1.65	2.96
0.15	12.39	1.7	2.79
0.2	12.34	1.75	2.66
0.25	12.26	1.8	2.56
0.3	12.14	1.85	2.49
0.35	11.97	1.9	2.42
0.4	11.71	1.95	2.36
0.45	11.58	2	2.31
0.5	10.31	2.05	2.26
0.55	8.24	2.1	2.22
0.6	7.72	2.15	2.18
0.65	7.43	2.2	2.15
0.7	7.27	2.25	2.11
0.75	7.12	2.3	2.07
0.8	7	2.35	2.05
0.85	6.89	2.4	2.03
0.9	6.78	2.45	2
0.95	6.7	2.5	1.97
1	6.59	2.55	1.95
1.05	6.5	2.6	1.93
1.1	6.41	2.65	1.91
1.15	6.33	2.7	1.89
1.2	6.22	2.75	1.88
1.25	6.12	2.8	1.86
1.3	6.02	2.85	1.85
1.35	5.88	2.9	1.83
1.4	5.72	2.95	1.82
1.45	5.51	3	1.8
1.5	5.17		
1.55	4.11		

Table 36 - pH curve determination

6.2.4.3 Acidification of Amino Acid **89** with HCl

The mother liquors from the preparation of (2*R*,3*S*)-3-methyl-2-(((*S*)-1-(2-methyloxazol-4-yl)-2-morpholino-2-oxoethyl)amino)pentanoic acid (**268**) (section 6.2.4.1) were concentrated to dryness under reduced pressure to afford an orange residue. A portion of this residue (410 mg) was dissolved in water (5 mL) and HCl (1.43 mL of a 2 M aqueous solution) was added (the pH of the solution was measured to be 1.2). The solution was then concentrated to dryness by freeze drying and the residue was dissolved in *i*-PrOH (2 mL). The solution was seeded with authentic (2*R*,3*S*)-3-methyl-2-(((*R*)-1-(2-methyloxazol-4-yl)-2-morpholino-2-oxoethyl)amino)pentanoic acid (**89**) and stirred at ambient temperature for 16 h. Crystallisation was not observed.

6.2.4.4 Preparation of (2*R*,3*S*)-3-Methyl-2-(((*R*)-1-(2-methyloxazol-4-yl)-2-morpholino-2-oxoethyl)amino)pentanoic acid (**89**)



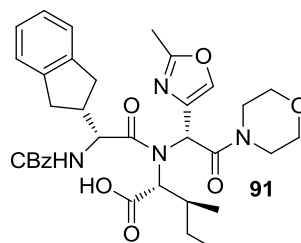
The mother liquors from the preparation of (2*R*,3*S*)-3-methyl-2-(((*S*)-1-(2-methyloxazol-4-yl)-2-morpholino-2-oxoethyl)amino)pentanoic acid (**268**) (section 6.2.4.1) were concentrated to dryness under reduced pressure to afford an orange residue which was dissolved in water (25 mL) and loaded onto a 120 g Phenomenex C₁₈ column. The column was eluted with water (approximately 250 mL) until no further UV active components were removed. The column was then eluted with MeOH (approximately 200 mL) and the solution concentrated to dryness under reduced pressure to afford the crude product free from inorganic contaminants. The residue was dissolved in *i*-PrOH (8 mL) and seeded to initiate crystallisation. The resultant slurry was stirred at 20 °C for 16 hr and the solids were collected by filtration. The solids were washed with *i*-PrOH (2 x 2 mL) and dried at 40 °C under reduced pressure to afford the desired diastereoisomer (**89**)

6. Experimental

as a white solid (854 mg, 20%); ^1H NMR (400 MHz, MeOD) δ ppm 0.96 (t, $J = 7.3$ Hz, 3H), 1.01 (d, $J = 6.8$ Hz, 3H), 1.23 - 1.37 (m, 1H), 1.49 - 1.68 (m, 1H), 1.92 - 2.11 (m, 1H), 2.44 (s, 3H), 3.28 - 3.44 (m, 3H), 3.49 - 3.70 (m, 6H), 5.20 (s, 1H), 7.94 (s, 1H), COOH and NH not observed; ^{13}C NMR (100 MHz, MeOD) δ ppm 12.2 (CH₃), 13.5 (CH₃), 15.3 (CH₃), 26.7 (CH₂), 38.4 (CH), 44.2 (CH₂), 47.1 (CH₂), 55.9 (CH), 66.9 (CH), 67.3 (CH₂), 67.5 (CH₂), 135.0 (CH), 140.1 (C), 164.4 (C), 167.8 (C), 174.1 (C); HPLC (Method A) $T_R = 2.15$ min, 93.6% a/a; MS m/z (ESI⁺) 340 ([M+H]⁺); HRMS (ESI⁺) m/z calcd. for C₁₆H₂₆N₃O₅ [M+H]⁺ 340.1867, found 340.1879.

6.2.5 Experimental Procedures for Section 3.5

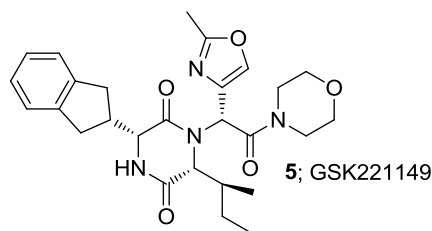
6.2.5.1 Preparation of (2*R*,3*S*)-2-(((*R*)-2-(((Benzyloxy)carbonyl)amino)-2-(2,3-dihydro-1*H*-inden-2-yl)-*N*-((*R*)-1-(2-methyloxazol-4-yl)-2-morpholino-2-oxoethyl)acetamido)-3-methylpentanoic acid (**91**)



1-Chloro-*N,N*,2-trimethylprop-1-en-1-amine (**269**) (350 μ L, 2.7 mmol) was added to a solution of (*R*)-2-(((benzyloxy)carbonyl)amino)-2-(2,3-dihydro-1*H*-inden-2-yl)acetic acid (**64**) (621 mg, 1.91 mmol) in THF (9.1 mL) at 0-2 $^{\circ}$ C and the reaction mixture was stirred for 1 h until the reaction was confirmed complete by HPLC. The reaction was monitored by quenching a portion (50 μ L) into MeCN containing Et₂NH (1 mL of a 5% v/v solution). (2*R*,3*S*)-3-Methyl-2-(((*R*)-1-(2-methyloxazol-4-yl)-2-morpholino-2-oxoethyl)amino)pentanoic acid (**89**) (648 mg, 1.91 mmol) and pyridine (170 μ L, 2.10 mmol) were then added and the mixture was stirred for 30 min at 2 $^{\circ}$ C until the reaction was confirmed complete by HPLC. The mixture was concentrated to dryness under reduced pressure and the residue was taken up in EtOAc (19.5 mL) and washed with HCl (19.5 mL of a 1 M aqueous solution) then water (20 mL). The organic phase was dried (MgSO₄) and concentrated to dryness under reduced pressure to afford the crude product as a clear glass which was triturated with EtOAc (3 mL). The slurry was stirred for 18 h at 20 $^{\circ}$ C and the solids were collected by filtration, washed with EtOAc (1 mL) and dried at 50 $^{\circ}$ C under reduced pressure to afford the desired product (**91**) as a white solid. (564 mg, 43 %); ¹H NMR (400 MHz, DMSO-D₆) δ ppm 0.38 (d, *J* = 7.1 Hz, 3H), 0.59 - 0.75 (m, 4H), 1.22 - 1.36 (m, 1H), 2.24 - 2.36 (m, 1H), 2.43 (s, 3H), 2.70 - 2.90 (m, 4H), 2.95 - 3.19 (m, 3H), 3.39 (m, 4H), 3.49 - 3.64 (m, 2H), 3.80 (d, *J* = 7.8 Hz, 1H), 4.85 (t, *J* = 8.9 Hz, 1H), 5.04 (d, ²*J*_{H-H} = 12.8 Hz, 1H), 5.11 (d, ²*J*_{H-H} = 12.8 Hz, 1H), 6.47 (s, 1H), 7.06 - 7.13 (m, 2H), 7.13 - 7.22 (m, 2H), 7.27 - 7.39 (m, 5H), 7.81 (d,

$J = 8.9$ Hz, 1H), 8.30 (s, 1H), 13.89 (s, 1H); ^{13}C NMR (100 MHz, DMSO) δ ppm 11.0 (CH₃), 13.3 (CH₃), 15.0 (CH₃), 26.3 (CH), 27.9 (CH₂), 32.9 (CH), 34.7 (CH₂), 35.7 (CH₂), 41.6 (CH), 43.1 (CH₂), 45.8 (CH₂), 53.6 (CH), 54.1 (CH), 62.0 (CH), 64.9 (CH₂), 65.4 (CH₂), 65.5 (CH₂), 124.26 (CH), 124.31 (CH), 126.21 (CH), 126.24 (CH), 127.3 (CH), 127.7 (CH), 128.2 (CH), 128.3 (CH), 133.2 (C), 137.0 (C), 140.7 (CH), 142.2 (C), 142.3 (C), 156.2 (C), 162.0 (C), 169.5 (C), 170.3 (C), 171.1 (C); HPLC (Method A) $T_R = 5.79$ min; 99.6% a/a; MS m/z (ESI⁺) 647 ([M+H]⁺).

6.2.5.2 Preparation of (3R,6R)-6-((S)-sec-Butyl)-3-(2,3-dihydro-1H-inden-2-yl)-1-((R)-1-(2-methyloxazol-4-yl)-2-morpholino-2-oxoethyl)piperazine-2,5-dione (5; GSK221149)



A solution of (2R,3S)-2-((R)-2-(((benzyloxy)carbonyl)amino)-2-(2,3-dihydro-1H-inden-2-yl)-N-((R)-1-(2-methyloxazol-4-yl)-2-morpholino-2-oxoethyl)acetamido)-3-methylpentanoic acid (**91**) (511 mg, 0.790 mmol) in *i*-PrOH (20 mL) was hydrogenated over 10% Pd/C (256 mg, 0.24 mmol) at 20 °C and 1 bar for 160 min. The catalyst was removed by filtration through Celite[®] and was washed with *i*-PrOH (10 mL). The filtrate was concentrated to dryness under reduced pressure to afford a clear glass which was dissolved in EtOAc (1.8 mL). Spontaneous crystallisation occurred to give a suspension which was stirred at 20 °C for 18 h. The solids were filtered, washed with EtOAc (2 x 0.5 mL) and dried at 45 °C under reduced pressure to afford the desired product (**5**) as a white solid and 2:1 EtOAc solvate (7.1% w/w) (312 mg, 74%); ^1H NMR (400 MHz, DMSO-D₆) δ ppm 0.58 (d, $J = 7.1$ Hz, 3H), 0.67 (t, $J = 7.2$ Hz, 3H), 0.77 - 0.93 (m, 1H), 1.27 - 1.41 (m, 1H), 1.49 - 1.61 (m, 1H), 2.42 (s, 3H), 2.68 (m, 1H), 2.80 - 3.04 (m, 4H), 3.20 - 3.55 (br m, 8H), 3.76 (dd, $J = 10.6, 4.5$ Hz, 1H), 4.08 (d, $J = 6.1$ Hz, 1H), 6.33 (s, 1H), 7.07 - 7.14 (m, 2H), 7.16 - 7.22 (m, 2H), 8.20 (s, 1H), 8.32 (d, $J = 4.5$ Hz,

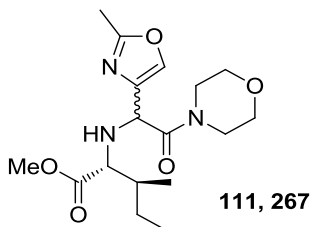
1H), peaks relating to EtOAc are not given; ^{13}C NMR (100 MHz, DMSO-D₆) δ ppm 11.2 (CH₃), 13.3 (CH₃), 15.3 (CH₃), 24.7 (CH₂), 36.2 (CH₂), 36.4 (CH₂), 38.6 (CH), 42.5 (CH₂) 44.8 (CH), 45.5 (CH₂) 52.2 (CH), 59.1 (CH), 62.5 (CH), 65.8 (CH₂), 66.0 (CH₂), 124.2 (CH), 124.3 (CH), 126.2 (CH), 126.3 (CH), 133.2 (C), 140.2 (CH), 141.6 (C), 142.5 (C), 161.6 (C), 166.1 (C), 167.3 (C), 167.7 (C), peaks relating to EtOAc are not given; HPLC (Method A) $T_R = 4.53$ min, 100% a/a; MS m/z (ESI⁺) 495 ([M+H]⁺). HRMS (ESI⁺) m/z calcd. for C₂₇H₃₅N₄O₅ [M+H]⁺ 495.2602, found 495.2589.

6.2.5.3 Re-crystallisation of (3R,6R)-6-((S)-sec-Butyl)-3-(2,3-dihydro-1H-inden-2-yl)-1-((R)-1-(2-methyloxazol-4-yl)-2-morpholino-2-oxoethyl)piperazine-2,5-dione (**5**; GSK221149)

(3R,6R)-6-((S)-sec-Butyl)-3-(2,3-dihydro-1H-inden-2-yl)-1-((R)-1-(2-methyloxazol-4-yl)-2-morpholino-2-oxoethyl)piperazine-2,5-dione (**5**) (185 mg, 0.35 mmol) was suspended in 2-butanol (0.69 mL) and heated to 75 °C to afford a clear solution. The solvent was evaporated in a nitrogen stream. Further 2-butanol (0.69 mL) was charged, and the mixture was heated to 75 °C to afford a solution and then concentrated to dryness under reduced pressure. 2-Butanol (0.34 mL) was then charged again, and the mixture was again heated to 75 °C to afford a clear solution. Heptane (0.52 mL) was added, maintaining the temperature at 75 °C. The clear solution was cooled to 50 °C, seeded and aged for 20 min. The slurry was cooled to 20 °C over approx 30 min and heptane (2.6 mL) was added *via* syringe pump over 1 h. The slurry was stirred at 20 °C for 20 h. The solids were collected by filtration, washed with heptane (2 x 0.76 mL) and dried under reduced pressure at 55 °C for 6 h to afford GSK221149 as a white solid (103 mg, 60%). The spectral data were in agreement with those described in section 6.2.5.2.

6.2.6 Experimental Procedures for Section 3.7.1

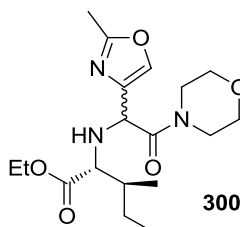
6.2.6.1 Preparation of (2*R*,3*S*)-Methyl 3-methyl-2-((1-(2-methyloxazol-4-yl)-2-morpholino-2-oxoethyl)amino)pentanoate (111/267)



1-(2-Methyloxazol-4-yl)-2-morpholinoethane-1,2-dione (**102**) (10 g, 44.6 mmol) was dissolved in toluene (100 mL) to afford a clear red solution and (2*R*,3*S*)-methyl 2-amino-3-methylpentanoate hydrochloride (**66**) (8.10 g, 44.6 mmol) was added and washed in with toluene (50 mL) to afford a suspension. The suspension was cooled to 0-5 °C and TMEDA (16.8 mL, 112 mmol) was added. Titanium tetrachloride (49.1 mL of a 1 M solution in toluene, 49.1 mmol) was added over approximately 30 min and the resultant dark brown reaction mixture was stirred at 0-5 °C for 1 h until HPLC showed the reaction was complete. The reaction was quenched by the addition of K₂CO₃ (61.6 g, of a 10% w/w aqueous solution, 44.6 mmol) and stirred vigorously to afford a cream slurry. Celite[®] (10 g) was charged and the mixture was stirred for a further 10 min. The triphasic mixture was then filtered through a bed of Celite[®] (10 g) which was washed with toluene (2 x 50 mL). The liquid phases were separated and the organic phase was dried (MgSO₄) and concentrated to dryness under reduced pressure to afford the intermediate (2*R*,3*S*)-ethyl 3-methyl-2-((1-(2-methyloxazol-4-yl)-2-morpholino-2-oxoethylidene) amino)pentanoate (**110**) (11.66 g, 75 %) as an orange/red oil. The intermediate was dissolved in EtOH (116 mL) and 10% wt Pd/C (5.8 g) was charged. The resultant suspension was hydrogenated at 20 °C and 3.5 bar for 210 min until HPLC confirmed the reaction was complete. The catalyst was removed by filtration and the filtrate was concentrated to dryness under reduced pressure to afford an orange oil which was dissolved in dichloromethane (100 mL) and extracted into HCl (40 mL of a 0.5 M aqueous solution). The aqueous phase was neutralised with NaOH (50 mL of a 0.5 M

aqueous solution) and extracted into dichloromethane (50 mL), which was washed with water (10 mL). The organic phase was dried (MgSO_4) and concentrated to dryness under reduced pressure to afford (2*R*,3*S*)-methyl-3-methyl-2-((1-(2-methyloxazol-4-yl)-2-morpholino-2-oxoethyl) amino)pentanoate as a mixture of diastereoisomers (**111/267**) (3.29 g, 21%). HPLC (Method B) (diastereoisomer 1): $T_R = 1.69$ min 57.2% a/a, (diastereoisomer 2): $T_R = 1.75$ min 38.6% a/a; MS m/z (ESI⁺) 354 ($[\text{M}+\text{H}]^+$); the spectral data were consistent with those described in section 6.2.3.4.

6.2.6.2 Preparation of (2*R*,3*S*)-Ethyl 3-methyl-2-((1-(2-methyloxazol-4-yl)-2-morpholino-2-oxoethyl)amino)pentanoate (**300**)



1-(2-Methyloxazol-4-yl)-2-morpholinoethane-1,2-dione (**102**) (10 g, 44.6 mmol) was dissolved in toluene (100 mL) to afford a clear red solution and (2*R*,3*S*)-ethyl 2-amino-3-methylpentanoate hydrochloride (8.73 g, 44.6 mmol) was added and washed in with toluene (50 mL) to afford a suspension. The suspension was cooled to 0-5 °C and TMEDA (16.8 mL, 112 mmol) was added. Titanium tetrachloride (49.1 mL, of a 1 M solution in toluene, 49.1 mmol) was added over approx 30 min and the resultant dark brown reaction mixture was stirred at 0-5 °C for 1 h and HPLC analysis indicated a complete reaction. The reaction was quenched by the addition of K_2CO_3 (61.6 g of a 10% w/w aqueous solution, 44.6 mmol) and stirred vigorously to afford a cream slurry. Celite[®] (10 g) was charged and the mixture was stirred for a further 10 min. The triphasic mixture was then filtered through a bed of Celite[®] (10 g) and washed with toluene (2 x 50 mL). The liquid phases were separated and the organic phase was dried (MgSO_4) and concentrated to dryness under reduced pressure to afford the intermediate (2*R*,3*S*)-ethyl 3-methyl-2-((1-(2-methyloxazol-4-yl)-2-morpholino-2-oxoethylidene) amino)pentanoate (12.93 g, 79 %) as a red oil. The intermediate was dissolved in EtOH

(116 mL) and 10% wt Pd/C (5.8 g, 54.5) was charged. The resultant suspension was hydrogenated at 20 °C and 3.5 bar for 3 h until HPLC confirmed the reaction was complete. The catalyst was removed by filtration and the filtrate was concentrated to dryness under reduced pressure to afford an orange oil which was dissolved in dichloromethane (100 mL) and extracted into HCl (2 x 30 mL of a 1 M aqueous solution). The combined aqueous layers were neutralised with NaOH (70 mL of a 1 M aqueous solution) and extracted with dichloromethane (50 mL). The organic phase was dried (MgSO₄) and concentrated to dryness under reduced pressure to afford (2*R*,3*S*)-ethyl 3-methyl-2-((1-(2-methyloxazol-4-yl)-2-morpholino-2-oxoethyl) amino) pentanoate as an equal mixture of diastereoisomers (**300**) (5.15 g, 31%). ¹H NMR (400 MHz, CDCl₃) Signals arising from diastereoisomer 1: δ ppm 0.91 (d, *J* = 7.1 Hz, 3H), 1.24 (t, *J* = 7.1 Hz, 3H), 3.22 (d, *J* = 5.4 Hz, 1H), 4.13 (q, *J* = 7.1 Hz, 2H), 4.62 (s, 1H), 7.50 (s, 1H); Signals arising from diastereoisomer 2: δ ppm 0.93 (d, *J* = 6.9 Hz, 3H), 1.26 (t, *J* = 7.1 Hz, 3H), 3.44 (d, *J* = 4.2 Hz, 1H), 4.15 (q, *J* = 7.1 Hz, 2H), 4.57 (s, 1H), 7.54 (s, 1H); Signals arising from a combination of the diastereoisomers which could not be distinguished: δ ppm 0.85 (t, *J* = 7.8 Hz, 3H), 1.16 – 1.31 (m, 1H), 1.41 – 1.52 (m, 1H), 1.74 – 1.82 (m, 1H), 2.41 (s, 3H), 2.71 (br. s, 1H), 3.52 – 3.72 (m, 8H); HPLC (Method B) diastereoisomer 1: *T_R* = 1.79 min 48.0% a/a, diastereoisomer 2: *T_R* = 1.86 min 49.0% a/a; MS *m/z* (ESI⁺) 368 ([M+H]⁺);

6.2.6.3 Experimental Procedures for Table 12

The results documented in Table 12 were part of a wider enzyme screen carried out according to the procedure described below.

(2*R*,3*S*)-Ethyl 3-methyl-2-((1-(2-methyloxazol-4-yl)-2-morpholino-2-oxoethyl)amino) pentanoate (**111/267**) (250 mg, 0.680 mmol) and (2*R*,3*S*)-methyl 3-methyl-2-((1-(2-methyloxazol-4-yl)-2-morpholino-2-oxoethyl)amino)pentanoate (**300**) (250 mg, 0.707 mmol) were dissolved separately in pH 7 phosphate buffer (50 mL of a 0.05 mM aqueous solution). Aliquots (1 mL) of each of the above solutions were added to vials containing the dried enzymes (5 mg) as shown (Table 37). The resultant reaction mixtures were stirred at 30 °C for 4 days. Aliquots (0.5 mL) of the reaction mixtures

were taken, filtered and analysed directly by HPLC (Method B). The results are shown (Table 37). Reactions which gave over 1% conversion to the desired amino acid from either the methyl or ethyl ester are highlighted in bold and shown in Table 12.

Type	Strain	From Methyl		From Ethyl	
		89 (% a/a)	268 (% a/a)	89 (% a/a)	268 (% a/a)
Control	<i>none</i>	0.00	0.00	0.00	0.00
Lipase A	<i>Alcaligenes</i>	0.17	0.10	0.24	0.13
Lipase B	<i>Alcaligenes</i>	0.14	0.34	0	0.26
Lipase C	<i>Alcaligenes</i>	0.26	0.09	0.08	0.06
Lipase	<i>Pseudomonas stutzeri</i>	0.25	0.60	0.10	0.18
Lipase	<i>Pseudomonas cepacia</i>	0.49	0.07	1.34	0.26
Lipase A	<i>Candida ruaosa</i>	0.35	0.16	0.36	0.06
Lipase D	<i>Alcaligenes sp.</i>	0.16	0.08	0.19	0.36
Lipase E	<i>Alcaligenes sp.</i>	0.11	0	0.19	0.26
Lipase B	<i>Candida ruaosa</i>	0.15	0.20	0.24	0.13
Lipase F	<i>Alcaligenes sp.</i>	0.19	0.08	0.09	0.32
Lipase	<i>from Fungal Scource</i>	0.13	0	0	0.25
Protease A	<i>Bacillus subtilis</i>	0.12	0.05	0	0.18
Phytase	N/A	0.10	0	0.10	0.16
Alkaline Protease A	N/A	0.07	0.08	0	0.13
Alkaline Lipase A	N/A	0.13	0.06	0.13	0.15
Lipase	<i>Bromeliaceae sp.</i>	0	0.25	0.22	0.09
Lipase	<i>Carcia papaya</i>	0	0.25	0.07	0.03
Neutral Protease A	N/A	0.43	0.46	0.43	0.48
Alkaline Protease B	N/A	6.17	4.17	8.01	7.84
Acidic Protease A	N/A	0.26	0.07	0.18	0.12
Protease A	<i>Aspergillus oryzae</i>	0.25	0.10	0.18	0.08
Protease B	<i>Bacillus subtilis</i>	1.70	0.58	0.87	0.41
Acylase	<i>Aspergillus sp.</i>	0.42	0.22	0.58	0.37
Lipase B	<i>Candida ruaosa</i>	0.13	0.10	0.15	0.05
Lipase	<i>Rhizopus niveus</i>	0.12	0.08	0.21	0.13
Protease	<i>Bacillus stearothermophilus</i>	0.12	0	0.10	0.13
Lipase	<i>Aspergillus niger</i>	0.09	0.06	0.09	0.26
Lipase	<i>Penicillium roquefort</i>	0.11	0	0.11	0.30
Protease	<i>Aspergillus niger</i>	0.14	0.09	0.19	0.21
Lipase	<i>Aspergillus oryzae</i>	0.71	0.22	0.52	0.26
Protease	<i>Aspegillus mellus</i>	0.67	0.36	1.02	0.52
Lipase	<i>Penicillium camembertii</i>	0.11	0.09	0.12	0.15
Protease C	<i>Bacillus subtilis</i>	7.06	5.69	6.05	7.00

Protease B	<i>Aspergillus oryzae</i>	0.64	0.25	0.44	0.18
Lipase	<i>Pseudomonas fluorescens</i>	0.16	0.34	0.13	0.48
Lipase A	<i>Burkholderia cepacia</i>	0.13	0.11	0.14	0.42
Lipase B	<i>Burkholderia cepacia</i>	0.13	0.10	0.09	0.32
Lipase A	<i>Rizomucor miehei</i>	0.12	0	0.09	0.24
Lipase B	<i>Candida antarctica</i>	0.23	0.07	0.31	0.13
Lipase	<i>Rizomucor miehei</i>	0.11	0.05	0.15	0.23
Protease	<i>Bacillus sp.</i>	1.23	1.05	2.28	2.44
Lipase B	<i>Candida antarctica</i>	0.17	0.06	0.31	0.18
Lipase A	<i>Candida antarctica</i>	0.14	0.12	0.06	0.12
Protease B	<i>Bacillus sp.</i>	1.12	0.89	2.03	2.11
Lipase	<i>Thermomyces lanuainosus</i>	0.12	0.06	0	0.40
Lipase C	<i>Rhizomucor miehei</i>	0.20	0.06	0	0.41

Table 37 – Complete enzyme screen results

6.2.6.4 Enzymatic Hydrolysis of Amine 111/267 in Organic Solvent

Water wet solvents (toluene, 2-MeTHF, TBME, methyl *iso*-butylketone, di*iso*-propyl ether & MeCN) were prepared by mixing the solvents with an excess of water so that a biphasic mixture was formed. The organic phases were decanted. In the case of MeCN, 10% v/v water was charged. Six solutions of (2*R*,3*S*)-methyl 3-methyl-2-((1-(2-methyloxazol-4-yl)-2-morpholino-2-oxoethyl)amino)pentanoate (**111/267**) (5 mg, 0.014 mmol) were prepared in each of the wet solvents (1 mL) and each of the six enzymes (lipase - *Pseudomonas cepacia*, alkaline protease B, protease B - *Bacillus subtilis*, protease C - *Bacillus subtilis*, protease B - *Bacillus sp.*, protease C - *Bacillus sp.*, 5 mg) was added to the solutions in an orthogonal manner such that each solvent was used in conjunction with each enzyme. The resultant reaction mixtures were heated to 35 °C and stirred for 48 h. An aliquot (0.25 mL) of each reaction was taken and diluted with MeCN (0.25 mL) and analysed by HPLC (Method B). Product was not observed in any reaction.

6.2.7 Experimental Procedures for Section 3.7

6.2.7.1 General Procedure 9: Imine Formation with Benzyl D-*allo*-isoleucinate

Titanium tetrachloride (A) was added to a solution of 1-(2-methyl-1,3-oxazol-4-yl)-2-(4-morpholinyl)-2-oxoethanone (**102**) (B), (2*R*,3*S*)-benzyl 2-amino-3-methylpentanoate (**108**) (C) and base (D) in solvent (E) at temperature (F) and the resultant reaction mixture was stirred for time (G). Conversion to imine **7** was monitored by quenching an aliquot (20 μ L) into ammonium bicarbonate (1 mL of a 10 mM aqueous solution) and analysing by LCMS or HPLC (Method C) (H).

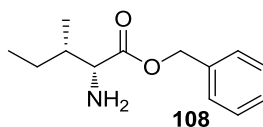
6.2.7.2 Work-up Procedure 2

Potassium carbonate (I) was added to the complete reaction mixture and stirred vigorously to afford a cream coloured slurry. Celite[®] (J) was added and the suspension was filtered through further Celite[®] (J), washing through with toluene (K). The resultant biphasic mixture was separated and the organic phase was washed with water (L), dried (MgSO₄) and concentrated to dryness under reduced pressure to afford (2*R*,3*S*)-benzyl 3-methyl-2-(1-(2-methyloxazol-4-yl)-2-morpholino-2-oxoethylidene)amino)pentanoate (**229**) as a red/orange oil (M).

6.2.7.3 Isolation of Impurity 301

Crude (2*R*,3*S*)-phenyl 3-methyl-2-((1-(2-methyloxazol-4-yl)-2-morpholino-2-oxoethylidene)amino)pentanoate (**301**) (100 mg, 0.242 mmol), prepared according to general procedure 9; Table 13, entry 5, was dissolved in MeOH (1 mL) and purified by MDAP (MeCN/10 mM ammonium bicarbonate). Fractions containing *m/z* (ESI⁺) 647 were combined and concentrated to dryness under reduced pressure to afford a yellow oil (10 mg). ¹H NMR (400 MHz, CDCl₃) Shows absence of oxazole *CH* at $\delta = 7.5 - 8.5$ ppm; HPLC (Method C) *T_R* = 3.57 min, 87.7% a/a; MS *m/z* (ESI⁺) 647 ([M+H]⁺).

6.2.7.4 Preparation of (2*R*,3*S*)-Benzyl 2-amino-3-methylpentanoate (5)



A solution of potassium carbonate (5.27 g, 38.1 mmol) in water (25 mL) was added to a suspension of (2*R*,3*S*)-benzyl 2-amino-3-methylpentanoate, 4-methylphenylsulfonate (**108**) (10 g, 25.4 mmol) in toluene (100 mL) and water (75 mL) and the solids dissolved to afford a clear, colourless biphasic mixture. The phases were separated and the organic phase was washed with water (2 x 50 mL). The organic phase was concentrated under reduced pressure, more toluene (100 mL) was added and the solution was again concentrated. This procedure was repeated to ensure the absence of water in the concentrate and to afford (2*R*,3*S*)-benzyl 2-amino-3-methylpentanoate (**108**) as a colourless oil containing 9.3% w/w toluene (5.97 g, 96 %); ¹H NMR (400 MHz, CDCl₃) δ ppm 0.81 (d, *J* = 6.9 Hz, 3H) 0.91 (t, *J* = 7.3 Hz, 3H) 1.22 - 1.29 (m, 1H) 1.35 (br. s, 2H) 1.39 - 1.50 (m, 1H) 1.79 - 1.89 (m, 1H), 3.49 (d, *J* = 4.2 Hz, 1H) 5.15 (d, ²*J*_{H-H} = 12.5 Hz, 1H), 5.16 (d, ²*J*_{H-H} = 12.5 Hz, 1H), 7.29 - 7.38 (m, 5H); HPLC (Method B) *T*_R = 1.78 min, 85.6% a/a; MS *m/z* (ESI⁺) 221 ([M+H]⁺).

6.2.7.5 Experimental Procedures for Table 13

The experiments documented in Table 13 were carried out according to general procedure 9; details for each entry are provided below. When product was isolated, work-up procedure 2 was followed. Differences in processing are recorded for each entry where applicable.

Entry 1. A: 25 µl, 0.22 mmol; B: 50 mg, 0.22 mmol; C: 4-methylphenylsulfonic acid salt (97 mg, 0.25 mmol); D: triethylamine (93 µl, 0.67 mmol); E: THF (1 mL); F: 0 °C; G: 5 min; H: 41.1% a/a

Entry 2. A: 0.89 mL of a 1 M solution in dichloromethane, 0.89 mmol; B: 200 mg, 0.89 mmol; C: 4-methylphenylsulfonic acid salt (351 mg, 0.89 mmol); D: triethylamine (497 µl, 3.57 mmol); E: dichloromethane (2 mL); F: 0 °C; G: 5 min; H: 62.2% a/a

Entry 3. A: 0.89 mL of a 1 M solution in dichloromethane, 0.89 mmol; B: 200 mg, 0.89 mmol; C: freebase (219 mg of a 90% w/w oil, 0.89 mmol); D: triethylamine (373 μ l, 2.68 mmol); E: dichloromethane (2 mL); F: 0 °C; G: 5 min; H: 66.2% a/a

Entry 4. A: 0.98 mL of a 1 M solution in dichloromethane, 0.98 mmol; B: 200 mg, 0.89 mmol; C: hydrochloride salt (241 mg, 0.94 mmol); D: TMEDA (337 μ l, 2.23 mmol); E: dichloromethane (2 mL); F: 0 °C; G: 2 h; H: 77.2 % a/a

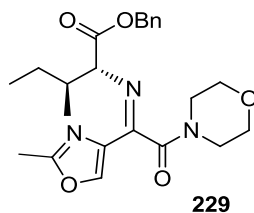
Entry 5. A: 2.65 mL of a 1 M solution in dichloromethane, 2.63 mmol; B: 535 mg, 2.34 mmol; C: 4-methylphenylsulfonate salt (983 mg, 2.51 mmol); D: TMEDA (900 μ l, 5.97 mmol); E: dichloromethane (5.4 mL); F: 0 °C; G: 2 h; H: 77.4 % a/a.

Entry 6. A: 0.98 mL of a 1 M solution in toluene, 0.98 mmol; B: 200 mg, 0.89 mmol; C: hydrochloride salt (241 mg, 0.94 mmol); D: TMEDA (337 μ l, 2.23 mmol); E: toluene (2 mL); F: 0 °C; G: 2 h; H: 88.7 % a/a

Entry 7. A: 0.98 mL of a 1 M solution in toluene, 0.98 mmol; B: 200 mg, 0.89 mmol; C: 4-methylphenylsulfonate salt (368 mg, 0.94 mmol); D: TMEDA (337 μ l, 2.23 mmol); E: toluene (2 mL); F: 0 °C; G: 2 h 30; H: 87.3 % a/a

Entry 8. A: 0.98 mL of a 1 M solution in toluene, 0.98 mmol; B: 200 mg, 0.89 mmol; C: 4-methylphenylsulfonate salt (368 mg, 0.94 mmol); D: TMEDA (269 μ l, 1.78 mmol); E: toluene (2 mL); F: 0 °C; G: 2 h 30; H: 76.0 % a/a

6.2.7.6 Experimental Procedures for the Preparation of (2R,3S)-Benzyl 3-methyl-2-(1-(2-methyloxazol-4-yl)-2-morpholino-2-oxoethylidene)amino)pentanoate (229)



Mixture of *E* and *Z* imines

The experiments for the preparation of (2R,3S)-benzyl 3-methyl-2-(1-(2-methyloxazol-4-yl)-2-morpholino-2-oxoethylidene)amino)pentanoate (**229**) were carried out according to general procedure 9; details for each entry are provided below. When product was isolated, work-up procedure 2 was followed. Differences in processing are recorded for each entry where applicable. For isolated products, full characterisation was carried out for a single batch; the remainder were analysed by HPLC and ¹H NMR. ¹H NMR spectroscopic data matched that given below with the exception of signals arising from residual solvents and minor impurities.

Experiment 1. A: 9.81 mL of a 1 M solution in toluene, 9.8 mmol; B: 2.0 g, 8.9 mmol; C: 4-methylphenylsulfonate salt (3.68 g, 9.4 mmol); D: TMEDA (3.37 mL, 22.3 mmol); E: toluene (30 mL); F: 0 °C; G: 3 h; H: HPLC showed the absence of the ketoamide (**102**); I: 12.3 g of a 10% w/w aqueous solution, 8.9 mmol; J: 4 g; K: 20 mL; L: none; M: 3.23 g, 85%.

Experiment 2. A: 24.5 mL of a 1 M solution in toluene, 24.5 mmol; B: 5.0 g, 22.3 mmol; C: 4-methylphenylsulfonate salt (9.19 g, 23.4 mmol); D: TMEDA (8.4 mL, 55.8 mmol); E: toluene (75 mL); F: 0 °C; G: 1 h 30; H: HPLC showed the presence of 5.0% a/a amine **5**. The reaction was stirred for a further 1 h and re-analysed by HPLC. 4.5% a/a amine **5** was observed and so the reaction was worked up; I: 30.8 g of a 10% w/w aqueous solution, 22.3 mmol; J: 10 g; K: 2 x 25 mL; L: 20 mL; M: 8.66 g, 91%.

Experiment 3. A: 245 mL of a 1 M solution in toluene, 245 mmol; B: 50 g, 233 mmol; C: 4-methylphenylsulfonate salt (88 g, 233 mmol); D: TMEDA (84 mL, 558 mmol); E: toluene (750 mL); F: 0 °C; G: 3 h; H: HPLC showed the presence of <2% a/a of the amine (**108**); I: 308 g of a 10% w/w aqueous solution, 223 mmol; J: 100 g; K: 2 x 250 mL; L: 250 mL; M: 83.05 g, 87%.

Experiment 4. A: 98 mL of a 1 M solution in toluene, 98 mmol; B: 20 g, 89 mmol; C: 4-methylphenylsulfonate salt (35 g, 89 mmol); D: TMEDA (33.7mL, 223 mmol); E: toluene (300 mL); F: 0 °C; G: 3 h; H: HPLC showed the presence of <2% a/a of the amine (**108**); I: 123 g of a 10% w/w aqueous solution, 89 mmol; J: 20 g; K: 2 x 100 mL; L: 50 mL; M: 31.12 g, 82%.

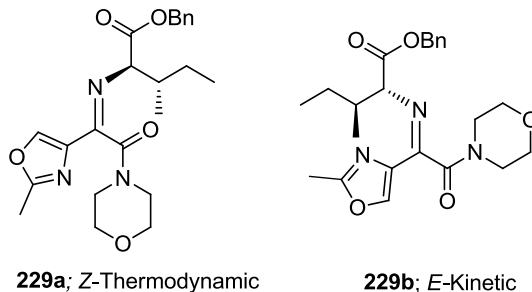
Experiment 5. A: 245 mL of a 1 M solution in toluene, 245 mmol; B: 50 g, 233 mmol; C: 4-methylphenylsulfonate salt (88 g, 233 mmol); D: TMEDA (84 mL, 558 mmol); E: toluene (750 mL); F: 0 °C; G: 2 h 30; H: HPLC showed the presence of <2.6% a/a of the amine (**108**); I: 308 g of a 10% w/w aqueous solution, 223 mmol; J: 100 g; K: 2 x 250 mL; L: 250 mL; M: 79.3 g, 83%. The washed organic solution was stirred with Norit SX[®] activated carbon (25 g) and filtered prior to evaporation.

Experiment 6. A: 123 mL of a 1 M solution in toluene, 123 mmol; B: 25 g, 112 mmol; C: 4-methylphenylsulfonate salt (44 g, 112 mmol); D: TMEDA (42 mL, 279 mmol); E: toluene (375 mL); F: 0 °C; G: 3 h; H: HPLC showed the presence of 2.4% a/a of the amine (**108**); I: 154 g of a 10% w/w aqueous solution, 112 mmol; J: 75 g; K: 2 x 125 mL; L: 125 mL; M: 41.9 g, 88%. The washed organic solution was stirred with Norit SX[®] activated carbon (25 g) and filtered prior to evaporation.

Experiment 7. A: 7.4 mL of a 1 M solution in toluene, 7.4 mmol; B: 1.5 g, 6.7 mmol; C: 4-methylphenylsulfonic acid salt (2.6 g, 6.7 mmol); D: TMEDA (2.5 mL, 16.7 mmol); E: toluene (22.5 mL); F: 0 °C; G: 3 h; H: HPLC showed the presence of <3% a/a of the amine (**108**); I: 9.3 g of a 10% w/w aqueous solution, 6.7 mmol; J: 4.5 g; K: 2 x 7.5 mL; L: 7.5 mL; M: 2.63 g, 83%. The washed organic solution was stirred with Norit SX[®] activated carbon (1.5 g) and filtered prior to evaporation. The 1-(2-methyl-1,3-

oxazol-4-yl)-2-(4-morpholinyl)-2-oxoethanone (**102**) used for this reaction was produced *via* a significantly altered process.¹¹⁸

6.2.7.7 Experimental Procedure for Characterisation of Imines **229a** & **229b**



The crude (2*R*,3*S*)-benzyl 3-methyl-2-((1-(2-methyloxazol-4-yl)-2-morpholino-2-oxoethylidene)amino)pentanoate (**229**) was prepared according to general procedure 9, experiment 7; 87 mg of this isomeric material was separated by MDAP (MeCN/10 mM ammonium bicarbonate). The resulting fractions were concentrated to dryness under reduced pressure to afford the isomerically pure imines.

Z-isomer (**229a**) (36 mg, 41%); ¹H NMR (400 MHz, CDCl₃) δ ppm 0.89 (t, *J* = 7.3 Hz, 3H), 0.97 (d, *J* = 6.9 Hz, 3H), 1.07 - 1.18 (m, 1H), 1.34 - 1.46 (m, 1H), 2.13 - 2.25 (m, 1H), 2.47 (s, 3H), 3.04 - 3.84 (m, 8H), 4.08 (d, *J* = 5.6 Hz, 1H), 5.16 (d, ²*J*_{H-H} = 12.0 Hz, 1H), 5.19 (d, ²*J*_{H-H} = 12.0 Hz, 1H), 7.27 - 7.38 (m, 5H), 8.02 (s, 1H); HPLC (Method C) *T*_R = 2.88 min, 87% a/a. MS *m/z* (ESI⁺) 428 ([M+H]⁺).

E-isomer (**229b**) (37 mg, 42%); ¹H NMR (400 MHz, CDCl₃) δ ppm 0.84 (t, *J* = 7.6 Hz, 3H), 1.01 (d, *J* = 7.3 Hz, 3H), 1.16 - 1.26 (m, 1H), 1.32 - 1.45 (m, 1H), 2.10 - 2.21 (m, 1H), 2.38 (s, 3H), 3.04 - 3.84 (m, 8H), 4.08 (d, *J* = 5.6 Hz, 1H), 5.11 (d, ²*J*_{H-H} = 12.2 Hz, 1H), 5.14 (d, ²*J*_{H-H} = 12.2 Hz, 1H), 7.29 - 7.40 (m, 5H), 7.95 (s, 1H); HPLC (Method C) *T*_R = 3.02 min, 82% a/a. MS *m/z* (ESI⁺) 428 ([M+H]⁺).

6.2.7.8 Experimental Procedures for Figure 26 & Figure 27

The fractions obtained from MDAP purification of (2*R*,3*S*)-benzyl 3-methyl-2-((1-(2-methyloxazol-4-yl)-2-morpholino-2-oxoethylidene)amino)pentanoate (**229**) as described

in section 6.2.7.7 were held at ambient temperature and analysed by HPLC (Method C). % peak areas of the two imines are given in Table 38 and Table 39 below.

Time (h)	% a/a Z-Isomer (229a)	% a/a E-Isomer (229b)
2	96.6	3.2
4	93.4	6.5
20	83.6	16.4
25	82.8	17.2
42	81.9	18.1

Table 38 – Data for Figure 26

Time	% a/a Z-Isomer (229a)	% a/a E-Isomer (229b)
1	9.1	90.9
17	68.2	31.8
22	72.9	27.1
38	80.3	19.7
42	79.6	20.4

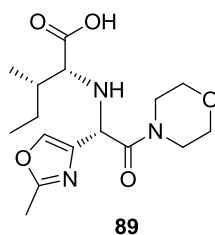
Table 39 – Data for Figure 27

6.2.8 Experimental Procedures for Section 3.8

6.2.8.1 General Procedure 10: Catalytic hydrogenation of Imine **229**

(2*R*,3*S*)-Benzyl-3-methyl-2-((1-(2-methyloxazol-4-yl)-2-morpholino-2-oxoethylidene)amino)pentanoate (**229**) (283 mg, 0.662 mmol) and catalyst (A) were taken up in ethanol (4.5 mL) and hydrogenated for 2 h at temperature (B) and pressure (C). Aliquots (20 μ L) of each reaction were taken and diluted with 1:1 v/v MeOH/ammonium bicarbonate (1 mL of a 10 mM aqueous solution) and analysed by HPLC (Method C). % Peak areas of the desired amino acid (**89**) (D) and diastereomeric excess (E) were recorded. A negative value for the diastereomeric excess indicates preference for the undesired diastereoisomer.

6.2.8.2 Experimental Procedure for the Preparation of Amino Acid **89** by Heterogeneous Benzyl Ester Hydrogenolysis



2*R*,3*S*)-Benzyl 3-methyl-2-((1-(2-methyloxazol-4-yl)-2-morpholino-2-oxoethylidene)amino)pentanoate (**229**) (80 g, 187 mmol) and 10% Pd/C (40 g) were suspended in MeOH (1200 mL) and hydrogenated at 25 °C and 3 bar for 110 min. The catalyst was removed by filtration through Celite[®] under nitrogen, washed through with MeOH (2 x 275 mL) and concentrated to dryness under reduced pressure to afford an orange oil which was dissolved in *i*-PrOH (264 mL) and stirred at ambient temp for 72 h. The resultant slurry was cooled to 0 °C and stirred for a further 2 h. The solids were then collected by filtration under vacuum, washed with *i*-PrOH (2 x 40 mL) and sucked dry. The damp cake was dried under reduced pressure at 40 °C for 2 h to afford the desired product as a single diastereoisomer (**89**) with spectral data consistent with those

described in section 6.2.4.4, (16.53 g, 26 %); HPLC (Method A) $T_R = 2.15$ min, 93.8% a/a.

6.2.8.3 Experimental Procedures for Table 14

The experiments documented in Table 14 were carried out according to general procedure 10, details for each entry are provided below.

Entry 1. A: Pd/C – E101; B: 25 °C; C: 3 bar; D: 33; E: -17.6%.

Entry 2. A: Pd/C – E101; B: 25 °C; C: 1 bar; D: 32; E: -13.6%.

Entry 3. A: Pd/C – E101; B: 50 °C; C: 1 bar; D: 33; E: -14.3%.

Entry 4. A: Pd/C – Type 39; B: 25 °C; C: 3 bar; D: 27; E: -23.5%.

Entry 5. A: Pt/C – B103032; B: 25 °C; C: 3 bar; D: 1.5; E: N/A.

Entry 6. A: Rh/C – 592; B: 25 °C; C: 3 bar; D: 11; E: -16.3%.

Entry 7. A: Rh-Ru/C – 118072; B: 25 °C; C: 3 bar; D: 2.7; E: N/A.

Entry 8. A: Rh/Alumina; B: 25 °C; C: 3 bar; D: 4; E: N/A.

Entry 9. A: Pd(OH)₂; B: 25 °C; C: 3 bar; D: 26; E: -10.5%.

Entry 10. A: Pd/C – Type 457; B: 25 °C; C: 3 bar; D: 26; E: -20.5%.

Entry 11. A: Pd/C – E101; B: 25 °C; C: 3 bar; D: 2.6; E: -17.0%. Reaction performed in toluene.

6.2.9 Experimental Procedures for Section 3.9

6.2.9.1 General Procedure 11: Catalytic Asymmetric Hydrogenation of Imine **229**

(2*R*,3*S*)-Benzyl 3-methyl-2-((1-(2-methyloxazol-4-yl)-2-morpholino-2-oxoethylidene)amino)pentanoate (**229**) (A) was dissolved in solvent (B) and a solution of catalyst (C) was added. The resultant reaction mixture was hydrogenated at temperature (D) and pressure (E) for time (F) then analysed by HPLC or LCMS (G).

6.2.9.2 General Procedure 12: Preparation of Hydrogenation Catalysts

[Ru(*p*-cymene)Cl₂]₂ (A) and ligand (B) were dissolved in 3:1 EtOH/dichloromethane (20 mL) and heated to 50 °C for 2 h then concentrated to dryness under reduced pressure to afford catalyst (C) which was used without further purification.

6.2.9.3 Experimental Procedures for Table 19

The experiments documented in Table 19 were carried out using general procedure 11; details for each entry are provided below. Differences in processing are recorded for each entry where applicable.

Entry 1. A: 200 mg, 0.47 mmol; B: toluene (2 mL); C: [RuCl((*R*)-BINAP)(*p*-cymene)]Cl (21 mg, 0.02 mmol) in toluene (1 mL); D: 50 °C; E: 4 bar; F: 4 h; G: HPLC showed 4.2% a/a of the amine (**89**). The hydrogenation was continued for a further 24 h and the reaction was re-analysed by HPLC which showed 9.0% a/a of the amine (**89**) and 9.2% a/a of an impurity with MH⁺ = 445.

Entry 2. A: 200 mg, 0.47 mmol; B: toluene (2 mL); C: [RuCl((*R*)-BINAP)(*p*-cymene)]Cl (21 mg, 0.02 mmol) in toluene (1 mL); D: 80 °C; E: 4 bar; F: 4 h; G: HPLC showed 16.5% a/a of the amine (**89**). The hydrogenation was continued for a further 24 h and the reaction was re-analysed by HPLC which showed 23.3% a/a of the amine (**89**) and 22.6% a/a of an impurity with MH⁺ = 445. The reaction mixture was concentrated to dryness under reduced pressure and taken up in MeOH (3 mL), Pd/C (100 mg) was charged and the reaction mixture was hydrogenated at 20 °C and 2 bar for 2 h. HPLC

and LCMS analysis showed the presence of a single peak corresponding to the desired diastereoisomer (**89**). The undesired diastereoisomer (**268**) was not observed.

Entry 3. A: 200 mg, 0.47 mmol; B: toluene (2 mL); C: RuCl[*((R)*-H₈-BINAP)(*p*-cymene)]Cl (21 mg, 0.02 mmol) in toluene (1 mL); D: 50 °C; E: 4 bar; F: 4 h; G: HPLC showed 9.6% a/ of the amine (**89**). The hydrogenation was continued for a further 24 h and the reaction was re-analysed by HPLC which showed 11.2% a/a of the amine (**89**) and 17.8% a/a of an impurity with MH⁺ = 445.

Entry 4. A: 200 mg, 0.47 mmol; B: toluene (2 mL); C: RuCl[*((R)*-H₈-BINAP)(*p*-cymene)]Cl (21 mg, 0.02 mmol) in toluene (1 mL); D: 80 °C; E: 4 bar; F: 4 h; G: HPLC showed 19.2% a/a of the amine (**89**). The hydrogenation was continued for a further 24 h and the reaction was re-analysed by HPLC which showed 20.3% a/a of the amine (**89**) and 29.4% a/a of an impurity with MH⁺ = 445.

Entry 5. A: 200 mg, 0.47 mmol; B: DME (2 mL); C: RuCl[*((R)*-BINAP)(*p*-cymene)]Cl (21 mg, 0.02 mmol) in DME (1 mL); D: 50 °C; E: 4 bar; F: 4 h; G: HPLC showed neither the amine (**89**) nor the imine (**229**).

Entry 6. A: 200 mg, 0.47 mmol; B: DME (2 mL); C: RuCl[*((R)*-BINAP)(*p*-cymene)]Cl (21 mg, 0.02 mmol) in DME (1 mL); D: 80 °C; E: 4 bar; F: 4 h; G: HPLC showed 26.5% a/a of the amine (**89**). The hydrogenation was continued for a further 24 h and the reaction was re-analysed by HPLC which showed 30.8% a/a of the amine (**89**) and 19.6% a/a of an impurity with MH⁺ = 445.

Entry 7. A: 200 mg, 0.47 mmol; B: DME (2 mL); C: RuCl[*((R)*-H₈-BINAP)(*p*-cymene)]Cl (21 mg, 0.02 mmol) in DME (1 mL); D: 50 °C; E: 4 bar; F: 4 h; G: HPLC showed 27.8% a/a of the amine (**89**). The hydrogenation was continued for a further 24 h and the reaction was re-analysed by HPLC which showed 27.5% a/a of the amine (**89**) and 11.1% a/a of an impurity with MH⁺ = 445.

Entry 8. A: 200 mg, 0.47 mmol; B: DME (2 mL); C: RuCl[*((R)*-H₈-BINAP)(*p*-cymene)]Cl (21 mg, 0.02 mmol) in DME (1 mL); D: 80 °C; E: 4 bar; F: 4 h; G: HPLC showed 31.4% a/a of the amine (**89**). The hydrogenation was continued for a further 24 h

and the reaction was re-analysed by HPLC which showed 32.5% a/a of the amine (**89**), and 23.4% a/a of an impurity with $MH^+ = 445$. The reaction mixture was concentrated to dryness under reduced pressure and taken up in MeOH (3 mL), Pd/C (100 mg) was charged and the reaction mixture was hydrogenated at 20 °C and 2 bar for 2 h. HPLC and LCMS analysis showed the presence of a single peak corresponding to the desired diastereoisomer (**89**). The undesired diastereoisomer (**268**) was not observed.

6.2.9.4 Experimental procedures for Table 20

The experiments documented in Table 19 were carried out using general procedure 11; details for each entry are provided below. Differences in processing are recorded for each entry where applicable.

Entry 1. A: 200 mg, 0.47 mmol; B: DME (2 mL); C: $RuCl[(R)\text{-SEGPHOS}(p\text{-cymene})]Cl$ (21 mg, 0.02 mmol) in DME (1 mL); D: 80 °C; E: 4 bar; F: 18 h; G: HPLC showed 38.2% a/a of the amine (**89**) and 9.4% a/a of an impurity with $MH^+ = 445$. Hydrogen generated from the electrolysis of water was used.

Entry 2. A: 200 mg, 0.47 mmol; B: DME (2 mL); C: $RuCl[(R)\text{-SEGPHOS}(p\text{-cymene})]Cl$ (21 mg, 0.02 mmol) in DME (1 mL); D: 80 °C; E: 4 bar; F: 18 h; G: HPLC showed 13.8% a/a of the amine (**89**) and 32.4% a/a of an impurity with $MH^+ = 445$. Water (42 μ L, 0.023 mmol) was charged to the reaction mixture prior to hydrogenation.

Entry 3. A: 200 mg, 0.47 mmol; B: DME (2 mL); C: $RuCl[(R)\text{-SEGPHOS}(p\text{-cymene})]Cl$ (21 mg, 0.02 mmol) in DME (1 mL); D: 80 °C; E: 4 bar; F: 18 h; G: HPLC showed 46.3% a/a of the amine (**89**) and 10.7% a/a of an impurity with $MH^+ = 445$. Hydrogen from a lecture bottle was used.

6.2.9.5 Experimental Procedures for the Preparation of Catalysts

The preparation of ruthenium hydrogenation catalysts was carried using general procedure 12; details for each catalyst are provided below. Differences in processing are recorded for each entry where applicable.

Catalyst 1. A: 20 mg; B: (*R*)-BINAP (**151**) (46.8 mg) C: RuCl[*((R)*-BINAP)(*p*-cymene)]Cl Spectral data consistent with those described in the literature¹⁶³ (69 mg, 103%); ³¹P NMR (162 MHz, CDCl₃) δ ppm 24.1 (d, ²J_{P-P} = 73.4 Hz), 40.5 (d, ²J_{P-P} = 73.4 Hz).

Catalyst 2. A: 20 mg; B: (*R*)-(5,5'-dichloro-6,6'-dimethoxy-[1,1'-biphenyl]-2,2'-diyl)bis(diphenylphosphine) (**311**) (48.9 mg) C: RuCl[*((R)*-Cl OMe BIPHEP)(*p*-cymene)]Cl (69 mg, 102%).

Catalyst 3. A: 20 mg; B: (*R*)-5,5'-bis(diphenylphosphino)-4,4'-bibenzo[d][1,3]dioxole (**317**) (45.9 mg) C: RuCl[*((R)*-SEGPPOS)(*p*-cymene)]Cl (67 mg, 102%); ³¹P NMR (162 MHz) δ ppm 26.5 (d, ²J_{P-P} = 61.5 Hz), 41.3 (d, ²J_{P-P} = 61.5 Hz).

Catalyst 4. A: 20 mg; B: (*R*)-(6,6'-dimethoxy-[1,1'-biphenyl]-2,2'-diyl)bis(diphenylphosphine) (**320**) (43.8 mg) C: RuCl[*((R)*-MeO BIPHEP)(*p*-cymene)]Cl (66 mg, 103%).

Catalyst 5. A: 20 mg; B: (*R*)-(6,6'-dimethoxy-[1,1'-biphenyl]-2,2'-diyl)bis(di(furan-2-yl)phosphine) (**321**) (40.7 mg) C: RuCl[*((R)*-Furyl BIPHEP)(*p*-cymene)]Cl (62 mg, 102%).

Catalyst 6. A: 20 mg; B: (*R*)-(6,6'-dimethoxy-[1,1'-biphenyl]-2,2'-diyl)bis(diisopropylphosphine) (**322**) (33.5 mg) C: RuCl[*((R)*-iPr BIPHEP)(*p*-cymene)]Cl (59 mg, 110%).

Catalyst 7. A: 20 mg; B: (*R*)-7,7'-bis(diphenylphosphino)-4,4'-dimethyl-3,3',4,4'-tetrahydro-2H,2'H-8,8'-bibenzo[b][1,4]oxazine (**319**) (49.9 mg) C: RuCl[*((R)*-SOLPHOS)(*p*-cymene)]Cl (70 mg, 100%).

Catalyst 8. A: 20 mg; B: (*R*)-5,5'-bis(diphenylphosphino)-4,4'-bibenzo[d][1,3]dioxole (**317**) (45.9 mg) C: RuCl[*((R)*-SEGPPOS)(*p*-cymene)]Cl (67 mg, 105%); ³¹P NMR (162 MHz, CDCl₃) δ ppm 26.5 (d, ²J_{P-P} = 61.1 Hz), 41.3 (d, ²J_{P-P} = 61.1 Hz). The reaction and isolation was carried out under strictly anaerobic conditions.

6.2.9.6 Experimental Procedures for Table 21

The experiments documented in Table 21 were carried out using general procedure 11; details for each entry are provided below. Differences in processing are recorded for each entry where applicable.

Entry 1. A: 200 mg, 0.47 mmol; B: DME (2 mL); C: RuCl[*((R)*-SEGP_{HOS})(*p*-cymene)]Cl (21 mg, 0.02 mmol) in DME (1 mL); D: 80 °C; E: 4 bar; F: 20 h; G: HPLC showed 36.4% a/a of the amine (**89**), 4.7% a/a of the imine (**229**) and 17.2% a/a of an impurity with MH⁺ = 445. Commercially sourced catalyst was used.

Entry 2. A: 200 mg, 0.47 mmol; B: DME (2 mL); C: RuCl[*((R)*-SEGP_{HOS})(*p*-cymene)]Cl (21 mg, 0.02 mmol) in DME (1 mL); D: 80 °C; E: 4 bar; F: 20 h; G: HPLC showed 16.3% a/a of the amine (**89**), 7.5% a/a of the imine (**229**) and 34.1% a/a of an impurity with MH⁺ = 445. Catalyst prepared in the laboratory was used.

Entry 3. A: 200 mg, 0.47 mmol; B: DME (2 mL); C: RuCl[*((R)*-Cl OMe BIPHEP)(*p*-cymene)]Cl (22 mg, 0.02 mmol) in DME (1 mL); D: 80 °C; E: 4 bar; F: 20 h; G: HPLC showed 0.7% a/a of the amine (**89**), 23.0% a/a of the imine (**229**) and 29.1% a/a of an impurity with MH⁺ = 445. Catalyst prepared in the laboratory was used.

Entry 4. A: 200 mg, 0.47 mmol; B: DME (2 mL); C: RuCl[*((R)*-SOLPHOS)(*p*-cymene)]Cl (23 mg, 0.02 mmol) in DME (1 mL); D: 80 °C; E: 4 bar; F: 20 h; G: HPLC showed 5.4% a/a of the amine (**89**), 7.4% a/a of the imine (**229**). Catalyst prepared in the laboratory was used.

Entry 5. A: 200 mg, 0.47 mmol; B: DME (2 mL); C: RuCl[*((R)*-MeO BIPHEP)(*p*-cymene)]Cl (21 mg, 0.02 mmol) in DME (1 mL); D: 80 °C; E: 4 bar; F: 20 h; G: HPLC showed 16.1% a/a of the amine (**89**), 12.3% a/a of the imine (**229**) and 28.9% a/a of an impurity with MH⁺ = 445. Catalyst prepared in the laboratory was used.

Entry 6. A: 200 mg, 0.47 mmol; B: DME (2 mL); C: RuCl[*((R)*-Furyl BIPHEP)(*p*-cymene)]Cl (20 mg, 0.02 mmol) in DME (1 mL); D: 80 °C; E: 4 bar; F: 20 h; G: HPLC showed 43.2% a/ of the amine (**89**), 6.0% a/a of the imine (**229**) and 9.7% a/a of an impurity with MH⁺ = 445. Catalyst prepared in the laboratory was used.

Entry 7. A: 200 mg, 0.47 mmol; B: DME (2 mL); C: RuCl[*((R)-i-Pr BIPHEP)*(*p*-cymene)]Cl (18 mg, 0.02 mmol) in DME (1 mL); D: 80 °C; E: 4 bar; F: 20 h; G: HPLC showed 1.1% a/a of the amine (**89**), 36% a/a of the imine (**229**) and 28.2% a/a of an impurity with MH⁺ = 445. Catalyst prepared in the laboratory was used.

6.2.9.7 Experimental Procedures for Table 22

The experiments documented in Table 22 were carried out using general procedure 11; details for each entry are provided below. Differences in processing are recorded for each entry where applicable.

Entry 1. A: 200 mg, 0.47 mmol; B: DME (2 mL); C: RuCl[*((R)-SEGPPOS)*(*p*-cymene)]Cl (21 mg, 0.02 mmol) in DME (1 mL); D: 80 °C; E: 4 bar; F: 20 h; G: HPLC showed 38.2% a/a of the amine (**89**), 22.5% a/a of the imine (**229**) and 9.4% a/a of an impurity with MH⁺ = 445. Commercially sourced catalyst was used.

Entry 2. A: 200 mg, 0.47 mmol; B: DME (2 mL); C: RuCl[*((R)-SEGPPOS)*(*p*-cymene)]Cl (21 mg, 0.02 mmol) in DME (1 mL); D: 80 °C; E: 4 bar; F: 20 h; G: HPLC showed 39.8% a/a of the amine (**89**), 26.9% a/a of the imine (**229**) and 8.0% a/a of an impurity with MH⁺ = 445. Catalyst prepared under air was used.

Entry 3. A: 200 mg, 0.47 mmol; B: DME (2 mL); C: RuCl[*((R)-SEGPPOS)*(*p*-cymene)]Cl (21 mg, 0.02 mmol) in DME (1 mL); D: 80 °C; E: 4 bar; F: 20 h; G: HPLC showed 22.5% a/a of the amine (**89**), 38.3% a/a of the imine (**229**) and 7.3% a/a of an impurity with MH⁺ = 445. Catalyst prepared under strictly anaerobic conditions was used.

6.2.9.8 Experimental Procedures for Table 23

The experiments documented in Table 23 were carried out using general procedure 11; details for each entry are provided below. Differences in processing are recorded for each entry where applicable.

Entry 1. A: 200 mg, 0.47 mmol; B: DME (2 mL); C: RuCl[*((R)-SEGPPOS)*(*p*-cymene)]Cl (21 mg, 0.02 mmol) in DME (1 mL); D: 80 °C; E: 4 bar; F: 20 h; G: HPLC

showed 38.2% a/a of the amine (**89**), 22.5% a/a of the imine (**229**) and 9.4% a/a of an impurity with $MH^+ = 445$. Commercially sourced catalyst was used.

Entry 2. A: 200 mg, 0.47 mmol; B: DME (2 mL); C: $[NH_2Me_2][RuCl((R)\text{-SEGPHOS})_2(\mu\text{-Cl})_3]$ (19 mg, 0.01 mmol) in DME (1 mL); D: 80 °C; E: 4 bar; F: 20 h; G: HPLC showed 17.1% a/a of the amine (**89**), 19.4% a/a of the imine (**229**) and 17.7% a/a of an impurity with $MH^+ = 445$. Commercially sourced catalyst was used.

Entry 3. A: 200 mg, 0.47 mmol; B: DME (2 mL); C: $[RuCl(OAc)_2((R)\text{-SEGPHOS})]Cl$ (19 mg, 0.02 mmol) in DME (1 mL); D: 80 °C; E: 4 bar; F: 20 h; G: HPLC showed 75.2% a/a of the imine (**229**), the amine (**89**) was not observed. Commercially sourced catalyst was used.

6.2.9.9 Experimental Procedures for Table 24

The experiments documented in Table 24 were carried out using general procedure 11; details for each entry are provided below. Differences in processing are recorded for each entry where applicable.

Entry 1. A: 200 mg, 0.47 mmol; B: DME (2 mL); C: $RuCl[((R)\text{-SEGPHOS})(p\text{-cymene})]Cl$ (21 mg, 0.02 mmol) in DME (1 mL); D: 80 °C; E: 4 bar; F: 20 h; G: HPLC showed 46.3% a/a of the amine (**89**) and 10.7% a/a of an impurity with $MH^+ = 445$. Commercially sourced catalyst was used.

Entry 2. A: 200 mg, 0.47 mmol; B: DME (2 mL); C: $RuCl[((R)\text{-SEGPHOS})(p\text{-cymene})]Cl$ (21 mg, 0.02 mmol) in DME (1 mL); D: 80 °C; E: 6 bar; F: 20 h; G: HPLC showed 40.0% a/a of the amine (**89**) and 12.7% a/a of an impurity with $MH^+ = 445$. Commercially sourced catalyst was used.

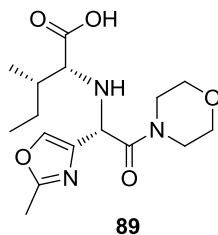
Entry 3. A: 200 mg, 0.47 mmol; B: DME (2 mL); C: $RuCl[((R)\text{-SEGPHOS})(p\text{-cymene})]Cl$ (21 mg, 0.02 mmol) in DME (1 mL); D: 80 °C; E: 8 bar; F: 20 h; G: HPLC showed 51.0% a/a of the amine (**89**) and 6.0% a/a of an impurity with $MH^+ = 445$. Commercially sourced catalyst was used.

Entry 4. A: 200 mg, 0.47 mmol; B: toluene (2 mL); C: RuCl[(*R*)-SEGPHOS](*p*-cymene)]Cl (21 mg, 0.02 mmol) in toluene (1 mL); D: 80 °C; E: 8 bar; F: 20 h; G: HPLC showed 34.5% a/a of the amine (**89**) and 16.1% a/a of an impurity with MH⁺ = 445. Commercially sourced catalyst was used.

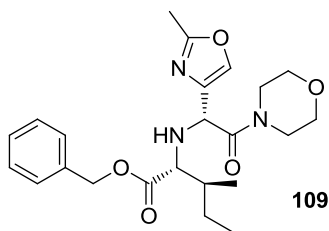
6.2.9.10 Experimental Procedure for the Scale-out of the Asymmetric Reduction of Imine **229**

(*2R,3S*)-Benzyl 3-methyl-2-((1-(2-methyloxazol-4-yl)-2-morpholino-2-oxoethylidene)amino)pentanoate (**229**) (1.4 g, 3.27 mmol) was taken up in DME (14 mL), split into seven equal portions and charged to seven parallel hydrogenator vessels. A slurry of [RuCl(*R*)-SEGPHOS](*p*-cymene)]Cl (150 mg, 0.16 mmol) in DME (7 mL) was also split into seven equal portions and charged to the hydrogenation vessels. The resultant reaction mixtures were hydrogenated at 80 °C and 8 bar (g) for 20 h until HPLC confirmed the reaction was complete. The solutions were cooled to ambient temperature, combined and concentrated to dryness under reduced pressure. The residue was dissolved in MeOH (14 mL) and charged to a larger hydrogenation vessel along with 10% w/w Pd/C (0.7 g). The slurry was hydrogenated at 25 °C and 1 bar (g) for 50 min and HPLC confirmed the reaction was complete. The catalyst was removed by filtration through Celite[®] and washed with MeOH (14 mL). The combined filtrate and wash was concentrated to dryness to afford a brown gum which was triturated with *i*-PrOH (7 mL). The slurry was cooled to 0 °C and stirred for 4 h. The solids were collected by filtration, washed with *i*-PrOH (2 x 3 mL) and dried at 40°C under reduced pressure to afford (*2R,3S*)-3-methyl-2-(((*R*)-1-(2-methyloxazol-4-yl)-2-morpholino-2-oxoethyl)amino)pentanoic acid (**89**) as an off white solid with spectral data consistent with those described in section 6.2.4.4. (522 mg, 1.54 mmol, 47 %); HPLC (Method A) $T_R = 2.15$ min, 99.4% a/a.

6.2.9.11 Experimental Procedure for the Preparation of Amino Acid **89** via Asymmetric Hydrogenation and Benzyl Ester Cleavage



(*2R,3S*)-Benzyl 3-methyl-2-(((*R*)-1-(2-methyloxazol-4-yl)-2-morpholino-2-oxoethylidene) amino)pentanoate (**229**) (38.9 g, 91 mmol) was dissolved in DME (389 mL) and charged to a 1 L Kiloclave[®] hydrogenator. A slurry of [RuCl(*R*)-SEGPHOS](*p*-cymene)]Cl (8.35 g, 9.10 mmol) in DME (195 mL) was charged and the resultant reaction mixture was hydrogenated at 80 °C and 2 bar (g) for 3 h until HPLC confirmed the reaction was complete. The solution was cooled to ambient temperature and concentrated to dryness under reduced pressure. The residue was dissolved in MeOH (500 mL) and re-charged to the hydrogenation vessel along with 10% w/w (50% wet) Pd/C (12.3 g, 116 mmol). The slurry was hydrogenated at 25 °C and 1 bar (g) for 70 min and HPLC confirmed the reaction was complete. The catalyst was removed by filtration through Celite[®] and the filter bed was washed with MeOH (150 mL). The combined filtrate and wash was concentrated to dryness to afford a brown gum which was triturated with *i*-PrOH (200 mL). The slurry was stirred overnight at ambient temperature then cooled to 0 °C and stirred for a further 3 h. The solids were collected by filtration, washed with *i*-PrOH (2 x 80 mL) and dried at 40 °C under reduced pressure to afford (*2R,3S*)-3-methyl-2-(((*R*)-1-(2-methyloxazol-4-yl)-2-morpholino-2-oxoethyl) amino)pentanoic acid (**89**) as an off white solid with spectral data consistent with those described in section 6.2.4.4. (19.9 g, 64 %); HPLC (Method A) $T_R = 2.15$ min, 99.6% a/a.

6.2.9.12 Characterisation of Amine Benzyl Ester **109**

(2*R*,3*S*)-Benzyl 3-methyl-2-(((*R*)-1-(2-methyloxazol-4-yl)-2-morpholino-2-oxoethyl) amino)pentanoate (**229**) (100 mg, 0.233 mmol) (prepared according to section 6.2.9.11) was dissolved in MeOH (1 mL) and purified by MDAP (MeCN/Water & TFA). Fractions containing product were combined and concentrated under reduced pressure to afford (2*R*,3*S*)-benzyl 3-methyl-2-(((*R*)-1-(2-methyloxazol-4-yl)-2-morpholino-2-oxoethyl) amino)pentanoate (**109**) as a colourless oil (62 mg, 62%); ¹H NMR (400 MHz, CDCl₃) δ ppm 0.88 (t, *J* = 7.3 Hz, 3H), 0.97 (d, *J* = 7.1 Hz, 3H), 1.01 - 1.13 (m, 1H), 1.49 - 1.60 (m, 1H), 1.95 - 2.06 (m, 1H), 2.37 (s, 3H), 3.14 - 3.28 (m, 1H), 3.39 - 3.66 (m, 6H), 3.70 - 3.78 (m, 1H), 3.81 (d, *J* = 3.7 Hz, 1H), 5.11 (d, ²*J*_{H-H} = 12.0 Hz 1H), 5.15 (d, ²*J*_{H-H} = 12.0 Hz 1H), 5.65 (s, 1H), 7.15 (s, 1H), 7.31 - 7.41 (m, 5H), 7.70 (s, 1H); ¹³C NMR (100 MHz, CDCl₃) δ ppm 11.5 (CH₃), 13.7 (CH₃), 15.3 (CH₃), 24.8 (CH₂), 36.9 (CH), 43.1 (CH₂), 45.7 (CH₂), 54.0 (CH), 62.8 (CH), 66.0 (CH₂), 66.4 (CH₂), 68.1 (CH₂), 128.75 (C), 128.77 (CH), 128.9 (CH), 131.9 (CH), 134.5 (C), 139.6 (CH), 163.0 (C), 164.9 (C), 169.9 (C); HPLC (Method A) *T*_R = 4.11 min, 100% a/a. MS *m/z* (ESI⁺) 430 ([M+H]⁺).

6.2.10 Experimental Procedures for Section 3.10

6.2.10.1 General Procedure 14: Esterification of *isoleucine*

p-TSA (A) and benzyl alcohol (B) were added to a suspension of *isoleucine* (C) in toluene (D) and the mixture was heated to reflux under Dean-Stark conditions for time (E) until the reaction appeared complete by NMR. The solution was cooled to 80 °C and an aliquot (1 mL) was removed, cooled and sonicated to induce crystallisation. The slurry was diluted with toluene (3 mL) and added to the remainder of the reaction mixture as a seed. The suspension was then aged for 40 min, cooled to 0 °C over 2 h and aged at 0 °C for 1.5 h. The solids were isolated by filtration, washed with toluene (F) and dried at 40 °C under reduced pressure to afford the product (G) as a white solid.

6.2.10.2 General Procedure 15: Imine Formation using *isoleucine* Diastereoisomers

Titanium tetrachloride (A) was added to a solution of 1-(2-methyl-1,3-oxazol-4-yl)-2-(4-morpholinyl)-2-oxoethanone (**102**) (B), benzyl ester (C) and TMEDA (D) in solvent (E) at temperature (F) and the resultant reaction mixture was stirred for time (G) until the reaction was confirmed complete by HPLC (Method C). Potassium carbonate (I) was added to the mixture which was stirred vigorously to afford a cream coloured slurry. Celite[®] (I) was added and the suspension was filtered through further Celite[®] (I), washing through with toluene (J). The biphasic mixture was separated and the organic phase was washed with water (K), dried (MgSO₄) and concentrated to dryness under reduced pressure to afford a mixture of *E* and *Z* imines (L) which were used without further purification.

6.2.10.3 General Procedure 16: Catalytic Hydrogenation of *isoleucine* Imine Diastereoisomers

Imine (A) and Pd/C (B) were taken up in MeOH (C) and hydrogenated at 25 °C and 3 bar for time (D) until the reaction was confirmed complete by HPLC. The catalyst was removed by filtration through Celite[®], washed through with MeOH (E) and concentrated

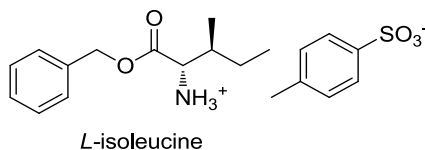
to dryness under reduced pressure to afford the crude amino acid as a mixture of diastereoisomers (F).

6.2.10.4 Purification Procedure 1: Separation of *isoleucine* Amino Acids

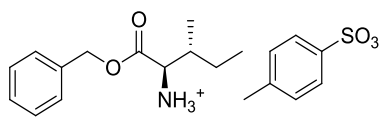
Amino acid mixture (100 mg) (G) was dissolved in MeOH (1 mL) and purified by MDAP (MeCN/Water). Fractions containing product were combined and concentrated to dryness under reduced pressure to afford the diastereomerically pure amino acids as colourless oils (H).

6.2.10.5 Preparation of *iso*Leucine Benzyl Esters **5b-d**

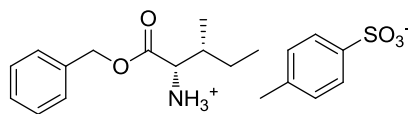
Isoleucine benzyl esters **5b-d** were prepared according to general procedure 14; details for each compound are provided below. Differences in processing are recorded for each entry where applicable.



L-isoleucine. A: 41.7 g, 219 mmol; B: 99 mL, 953 mmol; C: (2*S*,3*S*)-2-amino-3-methylpentanoic acid (25 g, 191 mmol); D: 313 mL; E: 23 h; F: 2 x 100 mL; G: (2*S*,3*S*)-benzyl 2-amino-3-methylpentanoate, 4-methylbenzenesulfonate (49.31 g, 66%); ¹H NMR (400 MHz, DMSO) δ ppm 0.82 (t, *J* = 7.5 Hz, 3H), 0.86 (d, *J* = 6.8 Hz, 3H), 1.17 - 1.28 (m, 1H), 1.32 - 1.46 (m, 1H), 1.82 - 1.93 (m, 1H), 2.28 (s, 3H), 4.01 (d, *J* = 3.7 Hz, 1H), 5.24 (d, ²*J*_{H-H} = 12.2 Hz, 1H), 5.27 (d, ²*J*_{H-H} = 12.2 Hz, 1H), 7.12 (d, *J* = 7.8 Hz, 2H), 7.32 - 7.44 (m, 5H), 7.51 (d, *J* = 7.8 Hz, 2H), 8.36 (br. s, 3H); HPLC (Method A) *p*-TSA: *T*_R = 1.54 min, 80.1% a/a; (2*S*,3*S*)-benzyl 2-amino-3-methylpentanoate: *T*_R = 3.33 min, 15.6% a/a; MS *m/z* (ESI⁺) 222 ([M+H]⁺); Mp 152 – 154 °C.

*D-isoleucine*

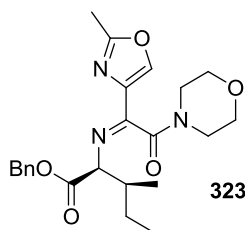
D-isoleucine. A: 4.17 g, 21.9 mmol; B: 9.9 mL, 95.3 mmol; C: (2*R*,3*R*)-2-amino-3-methylpentanoic acid (2.5 g, 19.1 mmol); D: (31 mL); E: 23 h; F: 2 x 10 mL; G: (2*R*,3*R*)-benzyl 2-amino-3-methylpentanoate, 4-methylbenzenesulfonate (4.82 g, 61%); ¹H NMR (400 MHz, DMSO) δ ppm 0.86 (t, *J* = 7.6 Hz, 3H), 0.89 (d, *J* = 7.3 Hz, 3H), 1.1 - 1.29 (m, 1H), 1.33 - 1.49 (m, 1H), 1.81 - 1.92 (m, 1H), 2.28 (s, 3H), 4.03 (d, *J* = 3.9 Hz, 1H), 5.25 (d, ²*J*_{H-H} = 12.2 Hz, 1H), 5.28 (d, ²*J*_{H-H} = 12.2 Hz, 1H), 7.11 (d, *J* = 7.8 Hz, 2H), 7.33 - 7.44 (m, 5H), 7.48 (d, *J* = 7.8 Hz, 2H), 8.32 (br. s, 3H); HPLC (Method A) *p*-TSA: *T*_R = 1.56 min, 82.0% a/a; (2*R*,3*R*)-benzyl 2-amino-3-methylpentanoate: *T*_R = 3.33 min, 15.7% a/a; MS *m/z* (ESI⁺) 222 ([M+H]⁺);

*L-allo-isoleucine*

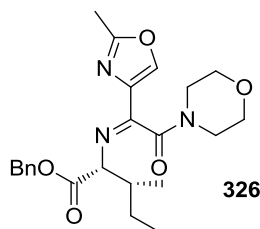
L-allo-isoleucine. A: (810 mg, 4.3 mmol); B: (1.9 mL, 18.5 mmol); C: (2*S*,3*R*)-2-amino-3-methylpentanoic acid (486 g, 3.7 mmol); D: (6.3 mL; E: 48 h; F: 2 x 2.3 mL; G: (2*S*,3*R*)-benzyl 2-amino-3-methylpentanoate, 4-methylbenzenesulfonate (559 mg, 38%); HPLC (Method A) *p*-TSA: *T*_R = 1.53 min, 55.1% a/a; (2*S*,3*R*)-benzyl 2-amino-3-methylpentanoate: *T*_R = 3.31 min, 11.2% a/a; MS *m/z* (ESI⁺) 222 ([M+H]⁺).

6.2.10.6 Preparation of Diastereomeric Imines 323 & 326

Isoleucine benzyl imines were prepared according to general procedure 15; details for each compound are provided below. Differences in processing are recorded for each entry where applicable.



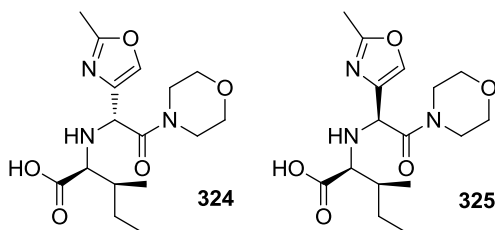
L-isoleucine imines. A: (24.5 mL of a 1 M solution in toluene, 24.5 mmol); B: (5 g, 22.3 mmol); C: (2*S*,3*S*)-benzyl 2-amino-3-methylpentanoate, 4-methylbenzenesulfonate (8.75 g, 22.3 mmol); D: 8.4 mL, 55.8 mmol; E: toluene (25 mL); F: 0 °C; G: 2 h; H: 30.8 g of a 10% w/w aqueous solution, 22.3 mmol; I: 10 g; J: 2 x 25mL; K: 25 mL; L: (2*S*,3*S*)-benzyl-3-methyl-2-((1-(2-methyloxazol-4-yl)-2-morpholino-2-oxoethylidene)amino)pentanoate (**323**) (7.40g, 78 %); LCMS (Method C) (Isomer 1) $T_R = 2.82$ min, 32.1% a/a, (Isomer 2) $T_R = 2.95$ min, 55.5% a/a; MS m/z (ESI+) 428 ($[M+H]^+$).



D-isoleucine imines. A: (12.3 mL, of a 1 M solution in toluene, 12.3 mmol); B: (2.5 g, 11.2 mmol); C: (2*R*,3*R*)-benzyl 2-amino-3-methylpentanoate, 4-methylbenzenesulfonate (4.38 g, 11.2 mmol); D: 4.2 mL, 27.9 mmol; E: toluene (12.5 mL); F: 0 °C; G: 4.5 h; H: 15.4 g of a 10% w/w aqueous solution, 12.2 mmol; I: 5 g; J: 2 x 12.5mL; K: 12.5 mL; L: (2*R*,3*R*)-benzyl-3-methyl-2-((1-(2-methyloxazol-4-yl)-2-morpholino-2-oxoethylidene)amino)pentanoate (**326**) (2.29 g, 52 %); LCMS (Method C) (Isomer 1) $T_R = 2.83$ min, 32.8% a/a, (Isomer 2) $T_R = 2.97$ min, 46.5% a/a; MS m/z (ESI+) 428 ($[M+H]^+$).

6.2.10.7 Preparation of Diastereomeric Amino Acids 324-328

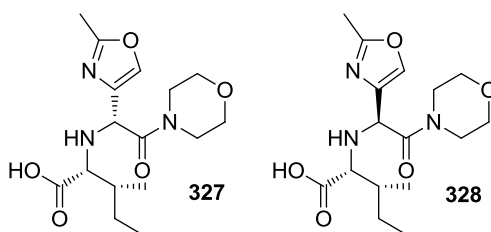
Isoleucine amino acids were prepared according to general procedure 16 and purified according to purification procedure 1, details for each compound are provided below. Differences in processing are recorded for each entry where applicable.



L-isoleucine amino acids. A: (2*S*,3*S*)-Benzyl 3-methyl-2-((1-(2-methyloxazol-4-yl)-2-morpholino-2-oxoethylidene)amino)pentanoate (**323**) (7.0 g, 16.4 mmol); B: 10% wt, 3.5 g; C: 105 mL; D: 90 min; E: 2 x 35 mL; F: (2*S*,3*S*)-3-methyl-2-(((*R*&*S*)-1-(2-methyloxazol-4-yl)-2-morpholino-2-oxoethyl)amino)pentanoic acid (**324** & **325**); (5.59 g, 80%).

Diastereoisomer 1: (18.8 mg); ^1H NMR (400 MHz, MeOD) δ ppm 0.98 (t, $J = 7.5$ Hz, 3H), 1.05 (d, $J = 6.8$ Hz, 3H), 1.38 - 1.53 (m, 1H), 1.55 - 1.67 (m, 1H), 2.08 - 2.23 (m, 1H), 2.48 (s, 3H), 3.18 - 3.34 (m, 2H), 3.36 - 3.50 (m, 1H), 3.55 - 3.72 (m, 5H), 3.96 (d, $J = 2.9$ Hz, 1H), 5.54 (s, 1H), 8.07 (s, 1H), COOH and NH are not observed; ^{13}C NMR (100 MHz, MeOD) δ ppm 12.1 (CH₃), 13.5 (CH₃), 14.8 (CH₃), 27.7 (CH), 37.6 (CH₂) 44.3 (CH₂), 46.9 (CH₂), 56.3 (CH), 65.3 (CH), 67.0 (CH₂), 67.4 (CH₂), 132.3 (C), 141.5 (CH), 164.4 (C), 164.9 (C), 170.3 (C); HPLC (Method A) $T_R = 2.25$ min, 79.7% a/a; MS m/z (ESI⁺) 340 ([M+H]⁺).

Diastereoisomer 2: (23.4 mg); ^1H NMR (400 MHz, MeOD) δ ppm 0.96 (t, $J = 7.3$ Hz, 3H), 1.01 (d, $J = 6.8$ Hz, 3H), 1.38 - 1.50 (m, 1H), 1.54 - 1.65 (m, 1H), 2.10 - 2.21 (m, 1H), 2.46 (s, 3H), 3.19 - 3.27 (m, 2H), 3.34 - 3.48 (m, 1H), 3.58 - 3.74 (m, 5H), 4.07 (d, $J = 3.2$ Hz, 1H), 5.60 (s, 1H), 8.05 (s, 1H), COOH and NH are not observed; ^{13}C NMR (100 MHz, MeOD) δ ppm 12.1 (CH₃), 13.6 (CH₃), 14.7 (CH₃), 27.8 (CH), 37.7 (CH₂) 44.2 (CH₂), 47.1 (CH₂), 55.1 (CH), 63.4 (CH), 67.2 (CH₂), 67.5 (CH₂), 131.6 (C), 142.0 (CH), 164.8 (C), 165.2 (C), 170.5 (C); HPLC (Method A) $T_R = 2.34$ min, 95.9% a/a; MS m/z (ESI⁺) 340 ([M+H]⁺).



D-isoleucine amino acids. A: (2*R*,3*R*)-Benzyl 3-methyl-2-((1-(2-methyloxazol-4-yl)-2-morpholino-2-oxoethylidene)amino)pentanoate (**326**) (2.49 g, 5.8 mmol); B: 10% wt, 1.25 g; C: 37.5 mL; D: 120 min; E: 2 x 12.5 mL; F: (2*R*,3*R*)-3-methyl-2-(((*R*&*S*)-1-(2-methyloxazol-4-yl)-2-morpholino-2-oxoethyl)amino)pentanoic acid (**327** & **328**); (1.63 g, 82%).

Diastereoisomer 1: (19.0 mg); ¹H NMR (400 MHz, MeOD) δ ppm 0.98 (t, *J* = 7.5 Hz, 3H), 1.05 (d, *J* = 6.8 Hz, 3H), 1.38 - 1.53 (m, 1H), 1.55 - 1.67 (m, 1H), 2.08 - 2.23 (m, 1H), 2.48 (s, 3H), 3.18 - 3.34 (m, 2H), 3.36 - 3.50 (m, 1H), 3.55 - 3.72 (m, 5H), 3.96 (d, *J* = 2.9 Hz, 1H), 5.54 (s, 1H), 8.07 (s, 1H), COOH and NH are not observed; ¹³C NMR (100 MHz, MeOD) δ ppm 12.1 (CH₃), 13.5 (CH₃), 14.8 (CH₃), 27.7 (CH), 37.6 (CH₂) 44.3 (CH₂), 46.9 (CH₂), 56.3 (CH), 65.3 (CH), 67.0 (CH₂), 67.4 (CH₂), 132.3 (C), 141.5 (CH), 164.4 (C), 164.9 (C), 170.3 (C); HPLC (Method A) *T_R* = 2.25 min, 91.7% a/a; MS *m/z* (ESI⁺) 340 ([M+H]⁺).

Diastereoisomer 2: (18.7 mg); ¹H NMR (400 MHz, MeOD) δ ppm 0.96 (t, *J* = 7.3 Hz, 3H), 1.01 (d, *J* = 6.8 Hz, 3H), 1.38 - 1.50 (m, 1H), 1.54 - 1.65 (m, 1H), 2.10 - 2.21 (m, 1H), 2.46 (s, 3H), 3.19 - 3.27 (m, 2H), 3.34 - 3.48 (m, 1H), 3.58 - 3.74 (m, 5H), 4.07 (d, *J* = 3.2 Hz, 1H), 5.60 (s, 1H), 8.05 (s, 1H), COOH and NH are not observed; ¹³C NMR (100 MHz, MeOD) δ ppm 12.1 (CH₃), 13.6 (CH₃), 14.7 (CH₃), 27.8 (CH), 37.7 (CH₂) 44.2 (CH₂), 47.1 (CH₂), 55.1 (CH), 63.4 (CH), 67.2 (CH₂), 67.5 (CH₂), 131.6 (C), 142.0 (CH), 164.8 (C), 165.2 (C), 170.5 (C); HPLC (Method A) *T_R* = 2.34 min, 95.8% a/a; MS *m/z* (ESI⁺) 340 ([M+H]⁺).

6.3 Experimental Procedures for Results and Discussion Part 2

6.3.1 General Experimental Procedures for Section 4

6.3.1.1 General Procedure 16 – Catalytic Asymmetric Hydrogenation Reactions

Imine (A) was dissolved in solvent (B) and a solution of catalyst (C) was added. The resultant reaction mixture was hydrogenated at temperature (D) and pressure (E) for time (F) then analysed by HPLC or LCMS (G). The reaction mixture was concentrated to dryness under reduced pressure, dissolved in MeOH and purified by MDAP (H) to afford product (I).

6.3.1.2 General Procedure 17 – Preparation of Ketoamides

NaHMDS (A) was added to a solution of 2-morpholinoacetonitrile (**121**) (B) and an ester (C) in THF (D) at 0-5 °C under nitrogen and stirred for time (E). After HPLC showed the reaction was complete, water (F) was added, the phases were separated and the aqueous phase was washed with methyl *iso*-butyl ketone (G). The washed aqueous phase was cooled to 10 °C and acetic acid (H) and sodium bicarbonate (I) were added. A solution of Oxone[®] (J) in water (50 mL) was added and the reaction mixture was stirred for time (K) until HPLC showed the reaction was complete. Sodium thiosulfate pentahydrate (L) was added stirred until the absence of oxidant was determined using Merckoquant[®] test strips. The aqueous solution was extracted with EtOAc (M) and the combined organic phases were dried (MgSO₄) and concentrated to dryness under reduced pressure. The crude product was purified by chromatography (N) to afford the desired product (O).

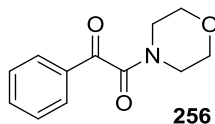
6.3.1.3 General procedure 18 – Imine Formation

Ketone (A) was dissolved in toluene (B) and amine (C) was added. The suspension was cooled to 0 – 5 °C and TMEDA (D) was added. Titanium tetrachloride (E) was added dropwise and the resultant reaction mixtures were stirred for time (F) and analysed by HPLC (G). The mixtures were quenched by addition of 10% aqueous potassium

carbonate (H) and the resultant biphasic suspension was filtered through celite. The phases were separated and the organic phase was concentrated to dryness to afford the crude imines which were purified by MDAP. Fractions containing product were combined and concentrated under reduced pressure to remove the volatiles and then extracted with dichloromethane (I). The organic phase was concentrated to dryness to afford the desired imine (K).

6.3.2 Experimental Procedures for Section 4.3

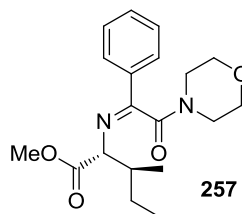
6.3.2.1 Preparation of 2-(4-Morpholinyl)-2-oxo-1-phenylethanone (**256**)



NaHMDS (77.1 mL of a 1 M solution in THF, 77.1 mmol) was added to a solution of 2-morpholinoacetonitrile (**121**) (5.1 g, 40.4 mmol) and methyl benzoate (5.00 g, 36.7 mmol) in THF (25 mL) at 0-5 °C under nitrogen. After stirring for 2 h, the reaction was shown to be incomplete by HPLC. Further NaHMDS (18.3 mL of a 1 M solution in THF, 18.3 mmol) was added and the mixture was stirred at 0-5 °C for 16 h. The reaction was then confirmed to be complete by HPLC. The mixture was warmed to 20 °C and water (70 mL) was added. The phases were separated and the aqueous phase was washed with methyl *iso*-butyl ketone (40 mL). The washed aqueous phase was cooled to 10 °C and acetic acid (4.42 mL, 77.1 mmol) and sodium bicarbonate (7.7 g, 91.8 mmol) were added. A solution of Oxone[®] (11.57 g, 18.7 mmol) in water (50 mL) was added and the reaction mixture was stirred for 22 h. HPLC showed the reaction was incomplete and so a further portion of Oxone[®] (11.57 g, 18.7 mmol) in water (50 mL) was added. After stirring at 10 °C for 1.5 h the reaction was shown to be complete. Sodium thiosulfate pentahydrate (18.2 g, 73.4 mmol) was added and the mixture was stirred for 1 h. The aqueous solution was extracted with EtOAc (2 x 40 mL) and the combined organic phases were washed with saturated sodium bicarbonate solution (50 mL), dried (MgSO₄) and concentrated to dryness under reduced pressure. The crude product was purified by Biotage Chromatography (0 – 100% EtOAc in heptane) to afford the desired product (**256**) as an orange solid with spectral data consistent with the literature¹⁶¹ (5.07 g, 63%); ¹H NMR (400 MHz, CDCl₃) δ ppm 3.35-3.45 (m, 2H) 3.60-3.70 (m, 2H), 3.70-3.90 (m, 4H), 7.53 (dd, *J* = 7.3, 7.2 Hz, 2H), 7.67 (t, *J* = 7.2 Hz, 1H), 7.97 (d, *J* = 7.3 Hz, 2H); ¹³C NMR (100 MHz, CDCl₃) δ ppm 41.6 (CH₂), 46.3 (CH₂), 66.67 (CH₂), 66.74 (CH₂), 129.1 (2 x CH), 129.7 (2 x CH), 133.1 (C) 135.0 (CH), 165.5 (C), 191.2 (C);

HPLC (Method B) $T_R = 1.77$ min 99.3% a/a; MS m/z (ESI⁺) 220 ([M+H]⁺); HRMS (ESI⁺) m/z calcd. for C₁₂H₁₄NO₃ [M+H]⁺ 220.0968, found 220.0963.

6.3.2.2 Preparation of (2*R*,3*S*)-Methyl 3-methyl-2-((2-morpholino-2-oxo-1-phenylethylidene)amino)pentanoate (**257**)



2-(4-Morpholinyl)-2-oxo-1-phenylethanone (**256**) (500 mg, 2.3 mmol) was dissolved in toluene (5 mL) to afford a pale yellow solution and (2*R*,3*S*)-methyl 2-amino-3-methylpentanoate hydrochloride (410 mg, 2.3 mmol) was added. The suspension was cooled to 0-5 °C and TMEDA (0.85 mL, 5.7 mmol) was added to afford a solution. Titanium tetrachloride (2.51 mL, of a 1 M solution in toluene, 2.51 mmol) was added and the resultant dark brown reaction mixture was stirred at 0-5 °C for 16 h until HPLC analysis indicated the reaction was complete. The reaction was quenched by the addition of K₂CO₃ (1.64 g, of a 10% w/w aqueous solution, 1.19 mmol) and stirred vigorously to afford a cream slurry, Celite[®] (1 g) was charged and the mixture was stirred for a further 10 min. The triphasic mixture was then filtered through a bed of Celite[®] (1 g) and the filter bed was washed with toluene (2 x 5 mL). The liquid phases were separated and the organic phase was washed with water (2.5 mL), dried (MgSO₄) and concentrated to dryness under reduced pressure to afford the crude product which was purified by MDAP (Method C). The fractions containing the product were combined and concentrated under reduced pressure to remove the volatiles and extracted with dichloromethane (2 x 10 mL). The organic phases were combined and concentrated to dryness under reduced pressure to afford the desired (2*R*,3*S*)-methyl 3-methyl-2-((2-morpholino-2-oxo-1-phenylethylidene)amino)pentanoate (**257**) as a colourless oil. (155 mg, 20%); ¹H NMR (400 MHz, CDCl₃) δ ppm 0.92 (t, $J = 7.6$ Hz, 3H), 1.03 (d, $J = 6.8$ Hz, 3H), 1.08 - 1.28 (m, 1H), 1.29 - 1.52 (m, 1H), 2.11 - 2.23 (m, 1H), 3.05 - 3.35 (m,

2H), 3.61 - 3.91 (m, 6H), 3.74 (s, 3H), 4.14 (d, $J = 5.1$ Hz, 1H), 7.32 - 7.59 (m, 3H), 7.81 (d, $J = 7.1$ Hz, 2H); HPLC (Method C): $T_R = 2.82$ min 83.7% a/a; MS m/z (ESI⁺) 347 ([M+H]⁺).

6.3.2.3 Experimental Procedures for Table 28

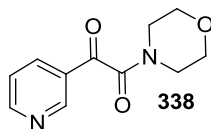
The experiments documented in Table 28 were carried out using general procedure 16; details for each entry are provided below. Differences in processing are recorded for each entry where applicable.

Entry 1. A: (2*R*,3*S*)-methyl 3-methyl-2-((1-(2-methyloxazol-4-yl)-2-morpholino-2-oxoethylidene)amino)pentanoate (**110**) (100 mg, 0.28 mmol); B: DME (5 mL); C: RuCl[*(R)*-SEGPHOS(*p*-cymene)]Cl (26 mg, 0.02 mmol); D: 80 °C; E: 4 bar; F: 17 h; G: HPLC showed complete conversion to the amine (**111**), the undesired diastereoisomer (**267**) was not detected; H: MeCN/Water & TFA, fractions containing product were concentrated to dryness under reduced pressure; I: 98 mg, 98%; HPLC (Method B) $T_R = 1.69$ min, 97.1% a/a; MS m/z (ESI⁺) 354 ([M+H]⁺); Spectral data concordant with that described in section 6.2.3.4.

Entry 2. A: (2*R*,3*S*)-benzyl 3-methyl-2-((1-(2-methyloxazol-4-yl)-2-morpholino-2-oxoethylidene)amino)pentanoate (**229**) (100 mg, 0.23 mmol); B: DME (5 mL); C: RuCl[*(R)*-SEGPHOS(*p*-cymene)]Cl (21 mg, 0.02 mmol); D: 80 °C; E: 4 bar; F: 17 h; G: HPLC showed complete conversion to the amine (**109**); H: MeCN/Water & TFA, fractions containing product were concentrated to dryness under reduced pressure; I: 34 mg, 34%; HPLC (Method B) $T_R = 2.00$ min, 90.7% a/a; MS m/z (ESI⁺) 430 ([M+H]⁺); Spectral data concordant with that described in section 6.2.9.12.

Entry 3. A: (2*R*,3*S*)-methyl 3-methyl-2-((2-morpholino-2-oxo-1-phenylethylidene)amino)pentanoate (**257**) (97 mg, 0.28 mmol); B: DME (5 mL); C RuCl[*(R)*-SEGPHOS(*p*-cymene)]Cl (21 mg, 0.02 mmol); D: 80 °C; E: 4 bar; F: 17 h; G: LCMS shows 55% a/a of the imine (**257**), no evidence of the desired amine. The reaction mixture was discarded.

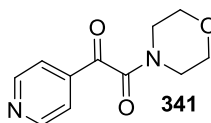
6.3.2.4 Preparation of 1-Morpholino-2-(pyridin-3-yl)ethane-1,2-dione (**338**)



1-Morpholino-2-(pyridin-3-yl)ethane-1,2-dione (**338**) was prepared according to general procedure 17; details are provided below. Differences in processing are recorded where applicable.

A: 30.6 mL of a 1 M solution in THF, 30.6 mmol; B: 2.02 g, 16.0 mmol; C: methyl nicotinate (**337**) (2.0 g, 14.6 mmol); D: 10 mL; E: 2 h; F: 28 mL; G: 16 mL; H: 1.2 mL, 20.4 mmol; I: 3.0 g, 36.5 mmol; J: 4.57 g, 7.4 mmol; K: 1.5 h; L: 3.62 g, 14.6 mmol; M: 2 x 16 mL; N: The crude product was of sufficient purity for onward processing and was not purified; O: (2.48 g, 77%); ^1H NMR (400 MHz, CDCl_3) δ ppm 3.16 - 3.36 (m, 2H), 3.45 - 3.60 (m, 2H), 3.66 (s, 4H), 7.34 (dd, $J = 7.8, 4.9$ Hz, 1H), 8.13 (d, $J = 7.8$ Hz, 1H), 8.71 (dd, $J = 4.9, 1.7$ Hz, 1H), 9.01 (d, $J = 1.7$ Hz, 1H); ^{13}C NMR (100 MHz, CDCl_3) δ ppm 41.9 (CH_2), 46.3 (CH_2), 66.6 (CH_2), 66.8 (CH_2), 128.9 (C), 124.0 (CH), 136.8 (CH), 151.3 (CH) 154.8 (CH), 164.2 (C), 189.4 (C); HPLC (Method B) $T_R = 1.35$ min 95.1% a/a; MS m/z (ESI $^+$) 221 ($[\text{M}+\text{H}]^+$).

6.3.2.5 Preparation of 1-Morpholino-2-(pyridin-4-yl)ethane-1,2-dione (**341**)

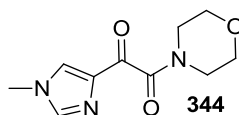


1-Morpholino-2-(pyridin-4-yl)ethane-1,2-dione (**341**) was prepared according to general procedure 17; details are provided below. Differences in processing are recorded where applicable.

A: 30.6 mL of a 1 M solution in THF, 30.6 mmol; B: 2.02 g, 16.0 mmol; C: methyl *isonicotinate* (**340**) (2.0 g, 14.6 mmol); D: 10 mL; E: 2 h; F: 28 mL; G: 16 mL; H: 1.2 mL, 20.4 mmol; I: 3.0 g, 36.5 mmol; J: 4.57 g, 7.4 mmol; K: 1 h 30; L: 3.62 g, 14.6 mmol; M: 2 x 16 mL; N: The crude product was of sufficient purity for onward

processing and was not purified; O: (2.86 g, 89%); ^1H NMR (400 MHz, CDCl_3) δ ppm 3.20 - 3.34 (m, 2H), 3.45 - 3.58 (m, 2H), 3.66 (m, 4H), 7.63 (d, $J = 6.1$ Hz, 2H), 8.73 (d, $J = 6.1$ Hz, 2H); ^{13}C NMR (100 MHz, CDCl_3) δ ppm 41.9 (CH_2), 46.3 (CH_2), 66.6 (CH_2), 66.7 (CH_2), 122.1 (2 x CH), 139.0 (C), 151.2 (2 x CH), 163.9 (C), 189.7 (C); HPLC (Method B) $T_R = 1.26$ min 99.1% a/a; MS m/z (ESI^+) 221 ($[\text{M}+\text{H}]^+$).

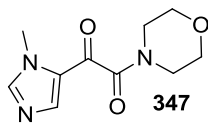
6.3.2.6 Preparation of 1-(1-Methyl-imidazol-4-yl)-2-morpholinoethane-1,2-dione (344)



1-(1-Methyl-imidazol-4-yl)-2-morpholinoethane-1,2-dione (**344**) was prepared according to general procedure 17; details are provided below. Differences in processing are recorded where applicable.

A: 10.0 mL of a 1.5 M solution in THF, 15.0 mmol; B: 0.99 g, 7.9 mmol; C: methyl 1-methyl-imidazole-4-carboxylate (**343**) (1.0 g, 7.1 mmol); D: 10 mL; E: 1 h, followed by the addition of further NaHMDS (2.5 mL of a 1.5 M solution in THF, 3.8 mmol); F: 14 mL; G: 2 x 8 mL; H: 1.14 mL, 20.0 mmol; I: 1.50 g, 17.8 mmol; J: 2.24 g, 3.6 mmol; K: 40 min; L: Not added; M: 2 x 8 mL; N: The crude product was of sufficient purity for onward processing and was not purified; O: (681 mg, 42%); ^1H NMR (400 MHz, CDCl_3) δ ppm 3.35 - 3.56 (m, 2H), 3.64 - 3.79 (m, 6H), 3.78 (s, 3H), 7.55 (s, 1 H), 7.76 (s, 1 H); ^{13}C NMR (100 MHz, CDCl_3) δ ppm 34.0 (CH_3) 41.8 (CH_2), 46.4 (CH_2), 66.6 (CH_2), 66.8 (CH_2), 122.4 (C) 128.3 (CH), 139.8 (CH), 165.5 (C), 180.2 (C); HPLC (Method A) $T_R = 1.64$ min 77.4% a/a; MS m/z (ESI^+) 224 ($[\text{M}+\text{H}]^+$).

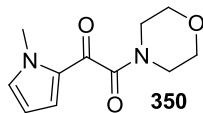
6.3.2.7 Preparation of 1-(1-Methyl-imidazol-5-yl)-2-morpholinoethane-1,2-dione (347)



1-(1-Methyl-imidazol-5-yl)-2-morpholinoethane-1,2-dione (**347**) was prepared according to general procedure 17; details are provided below. Differences in processing are recorded where applicable.

A: 10.0 mL of a 1.5 M solution in THF, 15.0 mmol; B: 0.99 g, 7.9 mmol; C: methyl 1-methyl-imidazole-4-carboxylate (**346**) (1.0 g, 7.1 mmol); D: 10 mL; E: 1 h, followed by the addition of further NaHMDS (2.5 mL of a 1.5 M solution in THF, 3.8 mmol); F: 14 mL; G: 2 x 8 mL; H: 1.14 mL, 20.0 mmol; I: 1.50 g, 17.8 mmol; J: 2.24 g, 3.6 mmol; K: 40 min; L: Not added; M: 2 x 8 mL; N: The crude product was of sufficient purity for onward processing and was not purified; O: (1.02 g, 64%); ¹H NMR (400 MHz, CDCl₃) δ ppm 3.35 - 3.56 (m, 2H), 3.56 - 3.86 (m, 6H), 3.98 (s, 3H), 7.68 (s, 1H), 7.85 (s, 1H); ¹³C NMR (100 MHz, CDCl₃) δ ppm 34.8 (CH₃) 42.0 (CH₂), 46.5 (CH₂), 66.6 (CH₂), 66.8 (CH₂), 128.5 (C), 143.0 (CH), 144.8 (CH), 164.1 (C), 180.5 (C); HPLC (Method A) *T_R* = 1.75 min 92.4% a/a; MS *m/z* (ESI⁺) 224 ([M+H]⁺).

6.3.2.8 Preparation of 1-(1-Methyl-pyrrol-2-yl)-2-morpholinoethane-1,2-dione (350)

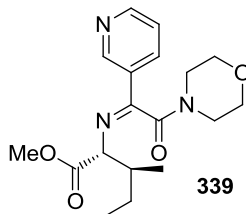


1-(1-Methyl-pyrrol-2-yl)-2-morpholinoethane-1,2-dione (**350**) was prepared according to general procedure 17; details are provided below. Differences in processing are recorded where applicable.

A: 30.2 mL of a 1.0 M solution in THF, 30.2 mmol; B: 1.99 g, 15.8 mmol; C: methyl 1-methyl-pyrrole-2-carboxylate (**349**) (2.0 g, 14.4 mmol); D: 20 mL; E: 30 min; F: 28 mL;

G: 2 x 8 mL; H: 1.14 mL, 20.0 mmol; I: 3.0 g, 35.6 mmol, a white precipitate was observed; J: 2.24 g, 3.6 mmol; K: 40 min, reaction was not observed.

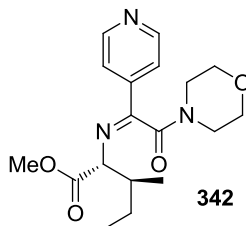
6.3.2.9 Preparation of (2*R*,3*S*)-Methyl 3-methyl-2-((2-morpholino-2-oxo-1-(pyridin-3-yl)ethylidene)amino)pentanoate (**339**)



(2*R*,3*S*)-Methyl 3-methyl-2-((2-morpholino-2-oxo-1-(pyridin-3-yl)ethylidene)amino)pentanoate (**339**) was prepared according to general procedure 18; details are provided below. Differences in processing are recorded where applicable.

A: 1-morpholino-2-(pyridin-3-yl)ethane-1,2-dione (**338**) (246 mg, 1.12 mmol); B: 3.75 mL; C: (2*R*,3*S*)-methyl 2-amino-3-methylpentanoate hydrochloride (203 mg, 1.12 mmol); D: 420 μ L, 2.79 mmol; E: 1.23 mL of a 1 M solution in toluene, 1.23 mmol; F: 3 h; G: Shows complete consumption of the ketone (**338**); H: 2 mL; I: 10 mL; K: 127 mg, 33%; ^1H NMR (400 MHz, CDCl_3) δ ppm 0.92 (t, $J = 7.6$ Hz, 3H), 1.04 (d, $J = 6.6$ Hz, 3H), 1.10 – 1.22 (m, 1H), 1.34 - 1.54 (m, 1H), 2.06 - 2.31 (m, 1H), 3.12 - 3.38 (m, 2H), 3.45 - 3.57 (m, 2H), 3.67 - 3.87 (m, 4H), 3.75 (s, 3H), 4.18 (d, $J = 4.8$ Hz, 1H), 7.38 (dd, $J = 8.0$ Hz, 4.8 Hz, 1H), 8.19 (d, $J = 8.0$ Hz, 1H), 8.70 (dd, $J = 4.7, 1.8$ Hz, 1H), 8.93 (d, $J = 1.8$ Hz, 1 H); ^{13}C NMR (100 MHz, CDCl_3) δ ppm 11.7 (CH_3), 14.9 (CH_3), 26.4 (CH_2), 39.2 (CH_2), 41.3 (CH), 46.3 (CH), 52.1 (CH_3), 66.6 (CH_2), 66.8 (CH_2), 70.7 (CH_2), 123.7 (CH), 130.2 (C), 134.7 (CH), 149.1 (CH) 152.2 (CH), 162.6 (C), 164.0 (C), 171.8 (C); HPLC (Method C): $T_R = 2.29$ min 97.0% a/a; MS m/z (ESI $^+$) 348 ([$\text{M}+\text{H}$] $^+$).

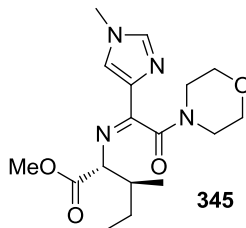
6.3.2.10 Preparation of (2*R*,3*S*)-Methyl 3-methyl-2-((2-morpholino-2-oxo-1-(pyridin-4-yl)ethylidene)amino)pentanoate (**342**)



(2*R*,3*S*)-Methyl 3-methyl-2-((2-morpholino-2-oxo-1-(pyridin-4-yl)ethylidene)amino)pentanoate (**342**) was prepared according to general procedure 18; details are provided below. Differences in processing are recorded where applicable.

A: 1-morpholino-2-(pyridin-4-yl)ethane-1,2-dione (**341**) (246 mg, 1.12 mmol); B: 3.75 mL; C: (2*R*,3*S*)-methyl 2-amino-3-methylpentanoate hydrochloride (**66**) (203 mg, 1.12 mmol); D: 420 μ L, 2.79 mmol; E: 1.23 mL of a 1 M solution in toluene, 1.23 mmol; F: 3 h; G: Shows complete consumption of the ketone (**341**); H: 2 mL; I: 10 mL; K: 97 mg, 25%; ^1H NMR (400 MHz, CDCl_3) δ ppm 0.93 (t, $J = 8.0$ Hz, 3H), 1.02 (d, $J = 6.4$ Hz, 3H), 1.09 – 1.28 (m, 1H), 1.34 - 1.55 (m, 1H), 2.06 - 2.33 (m, 1H), 3.15 - 3.36 (m, 2H), 3.36 - 3.62 (m, 2H), 3.62 - 3.92 (m, 4H), 3.75 (s, 3H), 4. (br. s, 1H), 7.65 (d, $J = 6.0$ Hz, 2H), 8.73 (d, $J = 6.0$ Hz, 2H); ^{13}C NMR (100 MHz, CDCl_3) δ ppm 11.7 (CH_3), 14.9 (CH_3), 26.4 (CH_2), 39.2 (CH), 41.3 (CH_2), 46.3 (CH_2), 52.2 (CH_3), 66.6 (CH_2), 66.8 (CH_2), 70.9 (CH), 121.1 (CH), 141.3 (C), 150.7 (CH), 163.3 (C), 163.7 (C), 171.5 (C); HPLC (Method C): $T_R = 2.33$ min 99.0% a/a; MS m/z (ESI $^+$) 348 ([M+H] $^+$).

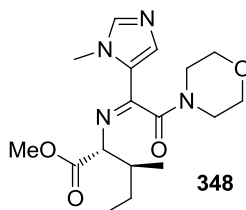
6.3.2.11 Preparation of (2*R*,3*S*)-Methyl 3-methyl-2-((1-(1-methylimidazol-4-yl)-2-morpholino-2-oxoethylidene)amino)pentanoate (**345**)



(2*R*,3*S*)-Methyl 3-methyl-2-((1-(1-methylimidazol-4-yl)-2-morpholino-2-oxoethylidene)amino)pentanoate (**345**) was prepared according to general procedure 18; details are provided below. Differences in processing are recorded where applicable.

A: 1-morpholino-2-(1-methylimidazol-4-yl)ethane-1,2-dione (**344**) (600 mg, 2.69 mmol); B: 11.0 mL; C: (2*R*,3*S*)-methyl 2-amino-3-methylpentanoate hydrochloride (490 mg, 2.69 mmol); D: 780 mg, 6.72 mmol; E: 2.96 mL of a 1 M solution in toluene, 2.96 mmol; F: 18 h; G: Shows complete consumption of the ketone (**344**); H: 4 mL; I: The fractions containing product were evaporated by freeze drying; K: 50 mg, 5%.

6.3.2.12 Preparation of (2*R*,3*S*)-Methyl 3-methyl-2-((1-(1-methylimidazol-5-yl)-2-morpholino-2-oxoethylidene)amino)pentanoate (**348**)



(2*R*,3*S*)-Methyl 3-methyl-2-((1-(1-methylimidazol-5-yl)-2-morpholino-2-oxoethylidene)amino)pentanoate (**348**) was prepared according to general procedure 18; details are provided below. Differences in processing are recorded where applicable.

A: 1-morpholino-2-(1-methylimidazol-5-yl)ethane-1,2-dione (**347**) (600 mg, 2.69 mmol); B: 11.0 mL; C: (2*R*,3*S*)-methyl 2-amino-3-methylpentanoate hydrochloride (490 mg, 2.69 mmol); D: 780 mg, 6.72 mmol; E: 2.96 mL of a 1 M solution in toluene, 2.96 mmol; F: 18 h; G: Shows complete consumption of the ketone (**347**); H: 4 mL; I:

The fractions containing product were evaporated by freeze drying; K: 70 mg, 8%; ^1H NMR (400 MHz, CDCl_3) δ ppm 0.86 (t, $J = 7.3$ Hz, 3H), 0.95 (d, $J = 6.8$ Hz, 3H), 1.00 - 1.14 (m, 1H), 1.27 - 1.40 (m, 1H), 1.86 - 2.12 (m, 1H), 3.02 - 3.32 (m, 2H), 3.32 - 3.46 (m, 1H), 3.46 - 3.58 (m, 1H), 3.58 - 3.85 (m, 4H), 3.66 (s, 3H), 3.90 (s, 3H), 4.04 (d, $J = 4.4$ Hz, 1H), 7.19 (s, 1H), 7.46 (s, 1H); ^{13}C NMR (100 MHz, CDCl_3) δ ppm 11.8 (CH_3), 15.0 (CH_3), 26.6 (CH_2), 35.7 (CH_3), 39.2 (CH), 41.3 (CH_2), 46.7 (CH_2), 52.0 (CH_3), 66.6 (CH_2), 66.8 (CH_2), 69.8 (CH), 127.4 (C), 136.0 (CH), 143.0 (CH), 156.7.1 (C) 163.1 (C), 172.3 (C); %; HPLC (Method C): $T_R = 2.26$ min 94.9% a/a; MS m/z (ESI $^+$) 351 ($[\text{M}+\text{H}]^+$).

6.3.2.13 Experimental procedure for Table 29

The experiments documented in Table 29 were carried out using general procedure 16; details for each entry are provided below. Differences in processing are recorded for each entry where applicable.

Entry 1.

Cat = Ru; A: (2*R*,3*S*)-methyl 3-methyl-2-((1-(2-methyloxazol-4-yl)-2-morpholino-2-oxoethylidene)amino)pentanoate (**110**) (50 mg, 0.14 mmol); B: DME (3 mL); C: $\text{RuCl}[(\textit{R})\text{-SEGPHOS}(\textit{p}\text{-cymene})]\text{Cl}$ (13 mg, 0.01 mmol); D: 80 °C; E: 4 bar; F: 27 h; G: HPLC showed 98% conversion to the amine (**111**) and the undesired diastereoisomer was not detected. The product was not isolated.

Cat = Pd; A: (2*R*,3*S*)-methyl 3-methyl-2-((1-(2-methyloxazol-4-yl)-2-morpholino-2-oxoethylidene)amino)pentanoate (**110**) (5.05 g, 14.4 mmol); B: EtOH (76 mL); C: 10% w. Pd/C (2.5g); D: 25 °C; E: 3 bar; F: 3 h; G: HPLC showed 84% conversion and an equimolar mixture of the two diastereoisomers (**110** & **267**). The catalyst was removed by filtration and the solution was concentrated under reduced pressure to afford the product which was taken on without further purification.

Entry 2.

Cat = Ru; A: (2*R*,3*S*)-Methyl 3-methyl-2-((2-morpholino-2-oxo-1-(pyridin-4-yl)ethylidene)amino)pentanoate (**342**) (50 mg, 0.14 mmol); B: DME (3 mL); C: RuCl[*(R)*-SEGPPOS(*p*-cymene)]Cl (13 mg, 0.01 mmol); D: 80 °C; E: 4 bar; F: 27 h; G: LCMS (Method A) showed 63% a/a of the imine (**342**) and no evidence of the desired amine.

Cat = Pd; A: (2*R*,3*S*)-Methyl 3-methyl-2-((2-morpholino-2-oxo-1-(pyridin-4-yl)ethylidene)amino)pentanoate (**342**) (50 mg, 0.14 mmol); B: DME (3 mL); C: 10% w/w Pd/C (10 mg); D: 25 °C; E: 3 bar; F: 90 min; G: LCMS (Method A) showed 37% conversion to a 1:1 a/a mixture with m/z (ESI⁺) = 350; T_R = 3.46 min and 3.59 min.

Entry 3.

Cat = Ru; A: (2*R*,3*S*)-Methyl 3-methyl-2-((2-morpholino-2-oxo-1-(pyridin-3-yl)ethylidene)amino)pentanoate (**339**) (50 mg, 0.14 mmol); B: DME (3 mL); C: RuCl[*(R)*-SEGPPOS(*p*-cymene)]Cl (13 mg, 0.01 mmol); D: 80 °C; E: 4 bar; F: 27 h; G: LCMS (Method A) showed 38% a/a of the imine (**339**) and no evidence of the desired amine.

Cat = Pd; A: (2*R*,3*S*)-Methyl 3-methyl-2-((2-morpholino-2-oxo-1-(pyridin-3-yl)ethylidene)amino)pentanoate (**339**) (50 mg, 0.14 mmol); B: DME (3 mL); C: 10% w. Pd/C (10 mg); D: 25 °C; E: 3 bar; F: 90 min; G: LCMS (Method A) showed >95% conversion to a 1:1 a/a mixture with m/z (ESI⁺) = 350; T_R = 3.51 min and 3.56 min.

Entry 4.

Cat = Ru; A: (2*R*,3*S*)-Methyl 3-methyl-2-((2-morpholino-2-oxo-1-(1-methylimidazol-4-yl)ethylidene)amino)pentanoate (**345**) (50 mg, 0.14 mmol); B: DME (3 mL); C: RuCl[*(R)*-SEGPPOS(*p*-cymene)]Cl (13 mg, 0.01 mmol); D: 80 °C; E: 4 bar; F: 27 h; G: LCMS (Method A) showed 33% conversion to a compound with m/z (ESI⁺) = 353; T_R = 3.18 min.

Cat = Pd; A: (2*R*,3*S*)-Methyl 3-methyl-2-((2-morpholino-2-oxo-1-(1-methylimidazol-4-yl)ethylidene)amino)pentanoate (**345**) (50 mg, 0.14 mmol); B: DME (3 mL); C: 10%

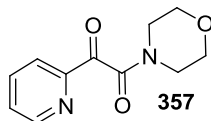
w/w Pd/C (10 mg); D: 25 °C; E: 3 bar; F: 90 min; G: LCMS (Method A) showed 47% conversion to a 1:1 a/a mixture with m/z (ESI⁺) = 353; T_R = 3.18 min and 3.30 min.

Entry 5.

Cat = Ru; A: (2*R*,3*S*)-Methyl 3-methyl-2-((2-morpholino-2-oxo-1-(1-methylimidazol-5-yl)ethylidene)amino)pentanoate (**348**) (50 mg, 0.14 mmol); B: DME (3 mL); C: RuCl[*(R)*-SEGPHOS(*p*-cymene)]Cl (13 mg, 0.01 mmol); D: 80 °C; E: 4 bar; F: 27 h; G: LCMS (Method A) showed 28% a/a of the imine (**348**) and no evidence of the desired amine.

Cat = Pd; A: (2*R*,3*S*)-Methyl 3-methyl-2-((2-morpholino-2-oxo-1-(1-methylimidazol-5-yl)ethylidene)amino)pentanoate (**348**) (50 mg, 0.14 mmol); B: DME (3 mL); C: 10% w/w Pd/C (10 mg); D: 25 °C; E: 3 bar; F: 1 h 30; G: LCMS (Method A) showed 13% conversion to compound with m/z (ESI⁺) = 353; T_R = 3.59 min.

6.3.2.14 Preparation of 1-Morpholino-2-(pyridin-2-yl)ethane-1,2-dione (**357**)

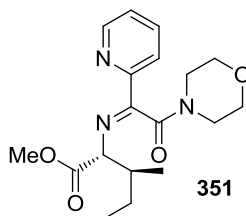


1-Morpholino-2-(pyridin-2-yl)ethane-1,2-dione (**357**) was prepared according to general procedure 17; details are provided below. Differences in processing are recorded where applicable.

A: 30.6 mL of a 1.5 M solution in THF, 45.9 mmol; B: 3.04 g, 24.1 mmol; C: methyl picolinate (**356**) (3.0 g, 21.9 mmol); D: 30 mL; E: 1 h; F: 42 mL; G: 24 mL; H: 3.5 mL, 61.3 mmol; I: 4.6 g, 54.7 mmol; J: 6.86 g, 11.2 mmol; K: 18 h. HPLC showed the reaction was incomplete and so further Oxone[®] (6.86 g, 11.2 mmol) was added and the mixture was stirred for 2 h; L: 10.9 g, 43.8 mmol; M: 2 x 24 mL; N: 100% EtOAc; O: (1.38 g, 29%); ¹H NMR (400 MHz, CDCl₃) δ ppm 3.37 (t, *J* = 4.6 Hz, 2H), 3.71 (t, *J* = 4.6 Hz, 2H), 3.82 (m, 4H), 7.41 - 7.64 (m, 1H), 7.92 (m, 1H), 8.12 (d, *J* = 7.8 Hz, 1H), 8.76 (d, *J* = 4.4 Hz, 1H); ¹³C NMR (100 MHz, CDCl₃) δ ppm 41.6 (CH₂), 46.2 (CH₂),

66.5 (2 x CH₂), 123.2 (CH), 128.2 (CH), 137.3 (CH) 150.0 (CH), 151.2 (C), 166.4 (C), 191.6 (C); HPLC (Method A) T_R = 2.98min 97.1% a/a; MS m/z (ESI⁺) 221 ([M+H]⁺).

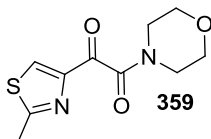
6.3.2.15 Preparation of (2R,3S)-Methyl 3-methyl-2-((2-morpholino-2-oxo-1-(pyridin-2-yl)ethylidene)amino)pentanoate (351)



(2R,3S)-Methyl 3-methyl-2-((2-morpholino-2-oxo-1-(pyridin-2-yl)ethylidene)amino)pentanoate (**351**) was prepared according to general procedure 18; details are provided below. Differences in processing are recorded where applicable.

A: 1-morpholino-2-(pyridin-2-yl)ethane-1,2-dione (**357**) (246 mg, 1.12 mmol); B: 3.75 mL; C: (2R,3S)-methyl 2-amino-3-methylpentanoate hydrochloride (203 mg, 1.15 mmol); D: 420 μ L, 2.79 mmol; E: 1.23 mL of a 1 M solution in toluene, 1.23 mmol; F: 4 h; G: Shows complete consumption of the ketone (**357**); H: 2 mL; I: The fractions containing product were concentrated to remove the volatiles and extracted with dichloromethane. The organic phase was concentrated under an N₂ stream; K: 207 mg, 53%; ¹H NMR (400 MHz, CDCl₃) δ ppm 0.95 (t, J = 8.0 Hz, 3H), 1.06 (d, J = 6.8 Hz, 3H), 1.10 - 1.30 (m, 1H), 1.32 - 1.56 (m, 1H), 2.10 - 2.33 (m, 1H), 3.24 (m, 2H), 3.34 - 3.58 (m, 1H), 3.63 - 3.93 (m, 5H), 3.74 (s, 3H), 4.26 (d, J = 4.9 Hz, 1H), 7.34 (dd, J = 7.4, 4.9 Hz, 1H), 7.77 (dd, J = 7.9, 7.4 Hz, 1H), 8.22 (d, J = 7.9 Hz, 1H), 8.61 (d, J = 4.9 Hz, 1H); HPLC (Method C): T_R = 2.46 min 97.0% a/a; MS m/z (ESI⁺) 348 ([M+H]⁺).

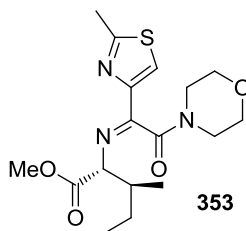
6.3.2.16 Preparation 1-(2-Methylthiazol-4-yl)-2-morpholinoethane-1,2-dione (359)



1-(2-Methylthiazol-4-yl)-2-morpholinoethane-1,2-dione (**359**) was prepared according to general procedure 17; details are provided below. Differences in processing are recorded where applicable.

A: 24.5 mL of a 1.5 M solution in THF, 36.8 mmol; B: 2.43 g, 19.3 mmol; C: ethyl 2-methylthiazole-4-carboxylate (**360**) (3.0 g, 17.5 mmol); D: 30 mL; E: 3.5 h; F: 42 mL; G: 24 mL; H: 2.81 mL, 49.1 mmol; I: 3.68 g, 43.8 mmol; J: 5.49 g, 8.9 mmol; K: 4 h; L: 8.7 g, 35.0 mmol; M: 2 x 24 mL; N: EtOAc; O: (2.16 g, 38.3%); ¹H NMR (400 MHz, CDCl₃) δ ppm 2.77 (s, 3H), 3.43 (t, *J* = 4.6 Hz, 2H), 3.69 (t, *J* = 4.6 Hz, 2H), 3.74 - 3.93 (m, 4H), 8.25 (s, 1H); ¹³C NMR (100 MHz, CDCl₃) δ ppm 19.9 (CH₃) 41.7 (CH₂), 46.3 (CH₂), 66.5 (CH₂), 66.6 (CH₂), 130.1 (CH) 151.4 (C), 165.2 (C), 167.7 (C), 183.8 (C); HPLC (Method A) *T_R* = 2.36 min 92.0% a/a; MS *m/z* (ESI⁺) 241 ([M+H]⁺).

6.3.2.17 Preparation of (2*R*,3*S*)-Methyl 3-methyl-2-((1-(2-methylthiazol-4-yl)-2-morpholino-2-oxoethylidene)amino)pentanoate (**353**)

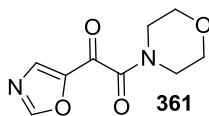


(2*R*,3*S*)-Methyl 3-methyl-2-((1-(2-methylthiazol-4-yl)-2-morpholino-2-oxoethylidene)amino)pentanoate (**353**) was prepared according to general procedure 18; details are provided below. Differences in processing are recorded where applicable.

A: 1-(2-Methylthiazol-4-yl)-2-morpholinoethane-1,2-dione (**359**) (268 mg, 1.12 mmol); B: 3.75 mL; C: (2*R*,3*S*)-methyl 2-amino-3-methylpentanoate hydrochloride (203 mg, 1.15 mmol); D: 420 μL, 2.79 mmol; E: 1.23 mL of a 1 M solution in toluene, 1.23 mmol; F: 4 h; G: Shows complete consumption of the ketone (**359**); H: 2 mL; I: The fractions containing product were concentrated to remove the volatiles and extracted with dichloromethane. The organic phase was concentrated under an N₂ stream; K: 194 mg, 47%; ¹H NMR (Major isomer) (400 MHz, CDCl₃) δ ppm 0.92 (t, *J* = 7.4 Hz, 3H),

1.01 (d, $J = 6.8$ Hz, 3H), 1.07 - 1.30 (m, 1H), 1.30 - 1.56 (m, 1H), 2.04 - 2.28 (m, 1H), 2.71 (s, 3H), 3.29 (m, 2H), 3.40 - 3.58 (m, 1H), 3.58 - 3.88 (m, 5H), 3.73 (s, 3H), 4.13 (d, $J = 5.4$ Hz, 1H), 7.90 (s, 1H); HPLC (Method C): (Major isomer) $T_R = 2.39$ min 92.0% a/a, (Minor isomer) $T_R = 2.52$ min 7.0% a/a; MS m/z (ESI⁺) 368 ([M+H]⁺).

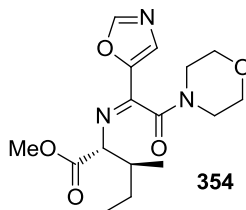
6.3.2.18 Preparation of 1-Morpholino-2-(oxazol-5-yl)ethane-1,2-dione (**361**)



1-Morpholino-2-(oxazol-5-yl)ethane-1,2-dione (**361**) was prepared according to general procedure 17; details are provided below. Differences in processing are recorded where applicable.

A: 29.8 mL of a 1.5 M solution in THF, 44.6 mmol; B: 2.95 g, 23.4 mmol; C: ethyl oxazole-5-carboxylate (**360**) (3.0 g, 21.3 mmol); D: 30 mL; E: 16 h; F: 42 mL; G: 24 mL; H: 3.41 mL, 59.5 mmol; I: 4.46 g, 53.1 mmol; J: 6.66 g, 10.84 mmol; K: 16 h; L: 10.55 g, 42.5 mmol; M: 2 x 24 mL; N: EtOAc; O: the product was isolated as a brown oil (605 mg, 14%); ¹H NMR (400 MHz, CDCl₃) δ ppm 3.42 - 3.65 (m, 2H), 3.65 - 3.87 (m, 6H), 8.04 (s, 1H), 8.13 (s, 1H), ¹³C NMR (100 MHz, CDCl₃) δ ppm 42.4 (CH₂), 46.4 (CH₂), 66.6 (CH₂), 66.8 (CH₂), 137.8 (C) 147.9 (C), 154.7 (CH), 162.3 (C), 176.5 (C); HPLC (Method A) $T_R = 2.02$ min 95.8% a/a; MS m/z (ESI⁺) 211 ([M+H]⁺).

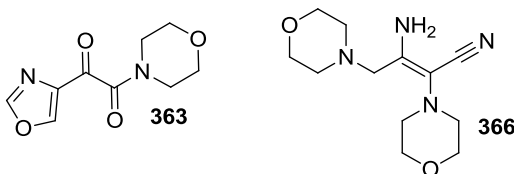
6.3.2.19 Preparation of (2*R*,3*S*)-Methyl 3-methyl-2-((2-morpholino-1-(oxazol-5-yl)-2-oxoethylidene)amino)pentanoate (**354**)



(2*R*,3*S*)-Methyl 3-methyl-2-((2-morpholino-1-(oxazol-5-yl)-2-oxoethylidene)amino)pentanoate (**354**) was prepared according to general procedure 18; details are provided below. Differences in processing are recorded where applicable.

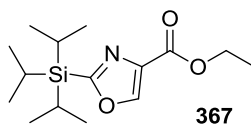
A: 1-morpholino-2-(oxazol-5-yl)ethane-1,2-dione (**361**) (234 mg, 1.12 mmol); B: 3.75 mL; C: (2*R*,3*S*)-methyl 2-amino-3-methylpentanoate hydrochloride (**66**) (203 mg, 1.15 mmol); D: 420 μ L, 2.79 mmol; E: 1.23 mL of a 1 M solution in toluene, 1.23 mmol; F: 4 h; G: Shows complete consumption of the ketone (**361**); H: 2 mL; I: The fractions containing product were concentrated to remove the volatiles and extracted with dichloromethane. The organic phase was concentrated under an N₂ stream; K: 102 mg, 27%; ¹H NMR (Major isomer) (400 MHz, CDCl₃) δ ppm 0.90 (t, *J* = 7.1 Hz, 3H), 1.00 (d, *J* = 6.8 Hz, 3H), 1.06 - 1.28 (m, 1H), 1.42 (m, 1H), 2.19 (m, 1H), 3.14 - 3.42 (m, 2H), 3.42 - 3.66 (m, 2H), 3.66 - 3.90 (m, 4H), 3.75 (s, 3H), 4.10 (d, *J* = 5.2 Hz, 1H), 7.54 (s, 1H), 8.00 (s, 1H); ¹H NMR (Minor isomer) (400 MHz, CDCl₃) δ ppm 0.88 (t, *J* = 7.0 Hz, 3H), 1.00 (d, *J* = 6.8 Hz, 3H), 1.17 - 1.32 (m, 1H), 1.42 (m, 1H), 2.19 (m, 1H), 3.14 - 3.42 (m, 2H), 3.42 - 3.66 (m, 2H), 3.66 - 3.90 (m, 4H), 3.75 (s, 3H), 4.72 (d, *J* = 4.8 Hz, 1H), 7.55 (s, 1H), 7.97 (s, 1H); HPLC (Method C): (Major isomer) *T_R* = 2.13 min 86.0% a/a, (Minor isomer) *T_R* = 2.15 min 13.0% a/a; MS *m/z* (ESI⁺) 338 ([M+H]⁺).

6.3.2.20 Attempted Preparation of 1-Morpholino-2-(oxazol-4-yl)ethane-1,2-dione (363)



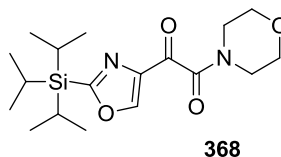
NaHMDS (44.6 mL, of a 1 M solution in THF, 44.6 mmol) was added to a solution of 2-morpholinoacetonitrile (**102**) (2.95 g, 23.3 mmol) and ethyl oxazole-4-carboxylate (**362**) (3 g, 21.3 mmol) in THF (25 mL) at 0-5 °C under nitrogen. After stirring for 1 h, LCMS showed the presence of the unreacted ethyl oxazole-4-carboxylate (**362**) and a peak with m/z (ESI⁺) 253 and m/z (ESI⁺) 166 consistent with the enamine shown (**366**).

6.3.2.21 Preparation of Ethyl 2-(triisopropylsilyl)oxazole-4-carboxylate (367)



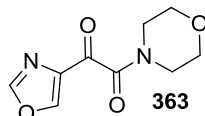
Ethyl oxazole-4-carboxylate (**362**) (5 g, 35.4 mmol) was dissolved in THF (50 mL) and cooled to -65 °C. *n*-Butyllithium (23.2 mL of a 1.6 M solution in hexanes, 37.2 mmol) was added over 15 min maintaining the temperature below -50 °C and the resultant reaction mixture was stirred for 1 h. TIPSOTf (10.1 mL, 37.2 mmol) was added over 10 min maintaining the temperature below -50 °C and the reaction was allowed to warm slowly to ambient temperature and stirred for 18 h. The reaction mixture was quenched by the addition of water (50 mL) and extracted with *i*PrOAc (50 mL). The organic phase was washed with water (50 mL) and concentrated under reduced pressure to afford the crude product which was purified by biotage chromatography (dichloromethane) fractions containing product were combined and concentrated under reduced pressure to afford ethyl 2-(triisopropylsilyl)oxazole-4-carboxylate (**367**) as an orange oil (5.65 g, 53.6 %). ¹H NMR (400 MHz, CDCl₃) δ ppm 1.13 (d, *J* = 7.3 Hz, 18H), 1.37 (t, *J* = 7.1 Hz, 3H), 1.45 (spt, *J* = 7.3 Hz, 3H), 4.38 (q, *J* = 7.1 Hz, 2H), 8.36 (s, 1 H); HPLC (Method A) *T_R* = 7.25 min 94.4% a/a; MS m/z (ESI⁺) 298 ([M+H]⁺).

6.3.2.22 Attempted Preparation of 1-Morpholino-2-(2-(triisopropylsilyl)oxazol-4-yl)ethane-1,2-dione (368)



NaHMDS (0.71 mL of a 1 M solution in THF, 0.71 mmol) was added to a solution of 2-morpholinoacetonitrile (**102**) (47 mg, 0.37 mmol) and ethyl 2-(triisopropylsilyl)oxazole-4-carboxylate (**367**) (100 mg, 0.34 mmol) in THF (1 mL) at 0-5 °C under nitrogen. After stirring for 10 min LCMS showed complete conversion to a peak with $T_R = 7.05$ min and m/z (ESI⁺) 378 consistent with the desired ketonitrile intermediate. Peracetic acid (35 μ L of a 32% w/w solution in AcOH, 0.17 mmol) was added at 0 °C and the mixture was stirred for 10 mins. LCMS showed conversion to a peak with $T_R = 6.15$ min and m/z (ESI⁺) 270 consistent with the silylated oxazole acid (**372**).

6.3.2.23 Attempted Preparation of 1-morpholino-2-(oxazol-4-yl)ethane-1,2-dione (363)



NaHMDS (0.71 mL of a 1 M solution in THF, 0.71 mmol) was added to a solution of 2-morpholinoacetonitrile (**102**) (47 mg, 0.37 mmol) and ethyl 2-(triisopropylsilyl)oxazole-4-carboxylate (**367**) (100 mg, 0.34 mmol) in THF (1 mL) at 0-5 °C under nitrogen. After stirring for 10 min LCMS showed complete conversion to a peak with $T_R = 7.05$ min and m/z (ESI⁺) 378 consistent with the desired ketonitrile intermediate. TBAF (0.37 mL of a 1 M solution in THF, 0.37 mmol) was added at 0 °C and the reaction mixture was stirred for 10 min. LCMS showed conversion to a peak with $T_R = 2.50$ min and m/z (ESI⁺) 222 consistent with the desilylated ketonitrile (**373**). Peracetic acid (35 μ L of a 32% w/w solution in AcOH, 0.17 mmol) was added at 0 °C and the mixture was stirred for 10

mins. LCMS showed complete consumption of the ketoamide (**373**), but no evidence of the desired ketoamide (**363**).

6.3.2.24 Experimental Procedure for Table 30

The experiments documented in Table 30 were carried out using general procedure 16; details for each entry are provided below. Differences in processing are recorded for each entry where applicable.

Entry 1; (2*R*,3*S*)-methyl 3-methyl-2-((1-(2-methyloxazol-4-yl)-2-morpholino-2-oxoethyl)amino)pentanoate (**110**)

See experimental details for Table 28, Entry 1 (Section 6.3.2.3).

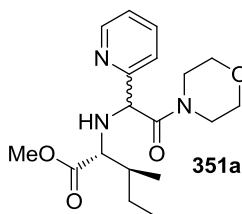
Entry 2; (2*R*,3*S*)-benzyl 3-methyl-2-((1-(2-methyloxazol-4-yl)-2-morpholino-2-oxoethyl)amino)pentanoate (**229**)

See experimental details for Table 28, Entry 2 (Section 6.3.2.3).

Entry 3; (2*R*,3*S*)-methyl 3-methyl-2-((2-morpholino-2-oxo-1-phenylethyl)amino)pentanoate (**257**)

See experimental details for Table 28, Entry 3 (Section 6.3.2.3).

Entry 4. (2*R*,3*S*)-methyl 3-methyl-2-((2-morpholino-2-oxo-1-(pyridin-2-yl)ethyl)amino)pentanoate (**351a**)



Cat = Ru; A: (2*R*,3*S*)-Methyl 3-methyl-2-((2-morpholino-2-oxo-1-(pyridin-2-yl)ethylidene)amino)pentanoate (**351**) (50 mg, 0.14 mmol); B: DME (3.5 mL); C: RuCl[*(R)*-SEGPHOS](*p*-cymene)]Cl (13 mg, 0.01 mmol); D: 80 °C; E: 4 bar; F: 5 h; G: HPLC and LCMS (Method A) showed 32% conversion to the amine (**351a**), present as a

mixture of diastereoisomers. (Isomer 1) $T_R = 2.81$ min, 87.0% a/a, (Isomer 2) $T_R = 3.03$ min 13.0% a/a; MS m/z (ESI⁺) 350 ([M+H]⁺);

Cat = Pd; A: (2*R*,3*S*)-Methyl 3-methyl-2-((2-morpholino-2-oxo-1-(pyridin-2-yl)ethylidene)amino)pentanoate (**351**) (50 mg, 0.14 mmol); B: DME (3 mL); C: 10% w/w Pd/C (10 mg); D: 25 °C; E: 4 bar; F: 6 h; G: HPLC (Method A) and LCMS showed complete conversion to the amine (**351a**), present as a mixture of diastereoisomers. (Isomer 1) $T_R = 2.81$ min, 45.8% a/a, (Isomer 2) $T_R = 3.03$ min 54.2% a/a; MS m/z (ESI⁺) 350 ([M+H]⁺); H: MeCN/Water & TFA. Fractions containing product were neutralised by the addition of NaHCO₃ (10 mL of a 8% w/w aqueous solution) and extracted with dichloromethane (2 x 20 mL) and the combined organic phases were combined and concentrated; I: (2*R*,3*S*)-methyl 3-methyl-2-((2-morpholino-2-oxo-1-(pyridin-2-yl)ethyl)amino) pentanoate (**351a**) (Isomer 1; 19 mg, 38%) (Isomer 2; 25 mg, 100%); ¹H NMR (Isomer 1) (400 MHz, CDCl₃) δ ppm 0.92 (t, $J = 7.4$ Hz, 3H), 0.94 (d, $J = 6.6$ Hz, 3H), 1.08 - 1.38 (m, 1H), 1.40 - 1.62 (m, 1H), 1.74 (br. s, 1H), 1.62 - 1.89 (m, 1H), 3.21 - 3.26 (m, 2H), 3.30 (d, $J = 5.3$ Hz, 1H), 3.40 - 3.70 (m, 6H), 3.56 (s, 3H), 4.77 (s, 1H), 7.19 (ddd, $J = 7.4, 5.0, 0.9$ Hz, 1H), 7.42 (dd, $J = 7.4$ Hz, 0.9 Hz, 1H), 7.67 (ddd, $J = 7.4, 7.4, 1.8$ Hz, 1H), 8.51 (dd, $J = 5.0, 1.8$ Hz, 1H); HPLC (Method C): (Isomer 1) $T_R = 2.81$ min, 98.8% a/a, (Isomer 2) $T_R = 3.03$ min 82.8% a/a; MS m/z (ESI⁺) 350 ([M+H]⁺);

Entry 5. (2*R*,3*S*)-Methyl 3-methyl-2-((2-morpholino-2-oxo-1-(pyridin-4-yl)ethyl)amino) pentanoate (**343**)

See experimental details for Table 29, Entry 2 (Section 6.3.2.13).

Entry 6. (2*R*,3*S*)-Methyl 3-methyl-2-((2-morpholino-2-oxo-1-(pyridin-3-yl)ethyl)amino) pentanoate (**339**)

See experimental details for Table 29, Entry 3 (Section 6.3.2.13).

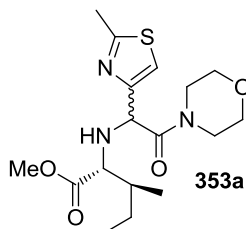
Entry 7. (2*R*,3*S*)-Methyl 3-methyl-2-((1-(1-methyl-1H-imidazol-4-yl)-2-morpholino-2-oxoethyl)amino)pentanoate (**345**).

See experimental details for Table 29, Entry 4 (Section 6.3.2.13).

Entry 8. (2*R*,3*S*)-Methyl 3-methyl-2-((1-(1-methyl-1*H*-imidazol-5-yl)-2-morpholino-2-oxoethyl)amino)pentanoate (**348**).

See experimental details for Table 29, Entry 5 (Section 6.3.2.13).

Entry 9. (2*R*,3*S*)-Methyl 3-methyl-2-((1-(2-methylthiazol-4-yl)-2-morpholino-2-oxoethyl)amino)pentanoate (**353a**)

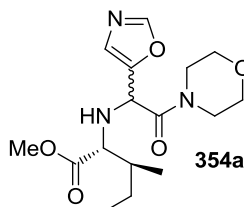


Cat = Ru; A: (2*R*,3*S*)-Methyl 3-methyl-2-((1-(2-methylthiazol-4-yl)-2-morpholino-2-oxoethylidene)amino)pentanoate (**353**) (50 mg, 0.14 mmol); B: DME (3.5 mL); C: RuCl[*(R)*-SEGPHOS](*p*-cymene)]Cl (13 mg, 0.01 mmol); D: 80 °C; E: 4 bar; F: 5 h; G: HPLC (Method A) and LCMS showed 98% conversion to the amine (**353a**), present as a mixture of diastereoisomers. (Isomer 1) $T_R = 2.82$ min, 96.6% a/a, (Isomer 2) $T_R = 2.99$ min 3.4% a/a; MS m/z (ESI⁺) 370 ([M+H]⁺); H: The product was not isolated.

Cat = Pd; A: (2*R*,3*S*)-Methyl 3-methyl-2-((1-(2-methylthiazol-4-yl)-2-morpholino-2-oxoethylidene)amino)pentanoate (**353**) (50 mg, 0.14 mmol); B: DME (3 mL); C: 10% w/w Pd/C (10 mg); D: 25 °C; E: 4 bar; F: 6 h; G: HPLC (Method A) and LCMS showed 91% conversion to the amine (**353a**), present as a mixture of diastereoisomers. (Isomer 1) $T_R = 2.82$ min, 51.3% a/a, (Isomer 2) $T_R = 2.99$ min 48.7% a/a; MS m/z (ESI⁺) 370 ([M+H]⁺); H: MeCN/Water & TFA. Fractions containing product were neutralised by the addition of NaHCO₃ (10 mL of a 8% w/w aqueous solution) and extracted with dichloromethane (2 x 20 mL) and the combined organic phases were combined and concentrated; I: (2*R*,3*S*)-methyl 3-methyl-2-((1-(2-methylthiazol-4-yl)-2-morpholino-2-oxoethyl)amino) pentanoate (**353a**) (Isomer 1; 19 mg, 38%) (Isomer 2; 22 mg, 44%); ¹H NMR (Isomer 1) (400 MHz, CDCl₃) δ ppm 0.90 (t, $J = 7.4$ Hz, 3H), 0.94 (d, $J = 6.8$ Hz, 3H), 1.16 - 1.26 (m, 1H), 1.47 - 1.53 (m, 1H), 2.67 (s, 3H), 2.89 (br. s, 1H), 3.25 (d, $J = 5.4$ Hz, 1H), 3.37 - 3.48 (m, 2H), 3.53 - 3.75 (m, 6H), 3.62 (s, 3H), 4.84 (s, 1H), 7.19 (s,

1H). ¹H NMR (Isomer 2) (400 MHz, CDCl₃) δ ppm 0.81 (t, *J* = 7.4 Hz, 3H), 0.91 (d, *J* = 6.9 Hz, 3H), 1.21 - 1.30 (m, 1H), 1.37 - 1.49 (m, 1H), 2.66 (s, 3H), 2.84 (br. s, 1H), 3.16 (d, *J* = 4.3 Hz, 1H), 3.39 - 3.45 (m, 2H), 3.51 - 3.75 (m, 6H), 3.70 (s, 3H), 4.81 (s, 1H), 7.16 (s, 1H); HPLC (Method C): (Isomer 1) *T_R* = 2.82 min, 97.4 % a/a, (Isomer 2) *T_R* = 2.99 min 89.7% a/a; MS *m/z* (ESI⁺) 370 ([M+H]⁺).

Entry 10. (2*R*,3*S*)-Methyl 3-methyl-2-((2-morpholino-1-(oxazol-5-yl)-2-oxoethyl)amino)pentanoate (**354a**)

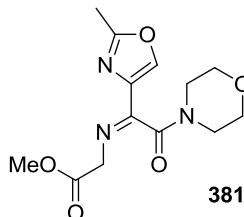


Cat = Ru; A: (2*R*,3*S*)-Methyl 3-methyl-2-((2-morpholino-1-(oxazol-5-yl)-2-oxoethylidene)amino)pentanoate (**354**) (50 mg, 0.15 mmol); B: DME (3.5 mL); C: RuCl[*(R)*-SEGPHOS](*p*-cymene)]Cl (13 mg, 0.01 mmol); D: 80 °C; E: 4 bar; F: 5 h; G: LCMS (Method A) showed 55% a/a of the imine (**354**) and no evidence of the desired amine.

Cat = Pd; A: (2*R*,3*S*)-Methyl 3-methyl-2-((2-morpholino-1-(oxazol-5-yl)-2-oxoethylidene)amino)pentanoate (**354**) (50 mg, 0.15 mmol); B: DME (3 mL); C: 10% w/w Pd/C (10 mg); D: 25 °C; E: 4 bar; F: 6 h; G: HPLC (Method A) and LCMS showed 83% conversion to the amine (**354a**), present as a mixture of diastereoisomers. (Isomer 1) *T_R* = 2.89 min, 43.4 % a/a, (Isomer 2) *T_R* = 3.24 min 56.6% a/a; MS *m/z* (ESI⁺) 340 ([M+H]⁺); H: The product was not isolated.

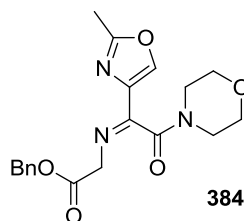
6.3.3 Experimental Procedures for Section 4.4

6.3.3.1 Attempted Preparation of Methyl 2-((1-(2-methyloxazol-4-yl)-2-morpholino-2-oxoethylidene)amino)acetate (**381**)



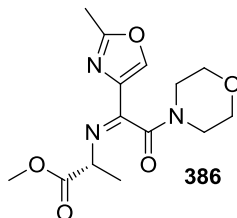
1-(2-Methyloxazol-4-yl)-2-morpholinoethane-1,2-dione (**102**) (500 mg, 2.23 mmol) was dissolved in toluene (5 mL) to afford a clear red solution. Glycine methyl ester hydrochloride (**380**) (280 mg, 2.23 mmol) was added to afford a suspension, washing through with toluene (2.5 mL). The suspension was cooled to 0-5 °C and TMEDA (830 μ L, 5.58 mmol) was added. Titanium tetrachloride (2.45 mL of a 1 M solution in toluene, 24.5 mmol) was added dropwise and the resultant dark brown reaction mixture was stirred at 0-5 °C for 18 h. The reaction was quenched by the addition of K_2CO_3 (3 mL, of a 10% w/w aqueous solution) and stirred vigorously to afford a cream slurry. Celite[®] (1.5 g) was charged and the mixture was stirred for a further 10 min. The triphasic mixture was then filtered through a bed of Celite[®] (1.0 g) and washed with toluene (2 x 10 mL). The liquid phases were separated and the organic phase was dried ($MgSO_4$) and concentrated to dryness under reduced pressure to afford the crude product as a red/brown oil. The crude product was purified by MDAP and the fractions containing product were combined and concentrated under reduced pressure. The concentrated fractions were extracted with dichloromethane (4 x 30 mL). The organic phases were combined, dried ($MgSO_4$) and evaporated to provide methyl 2-((1-(2-methyloxazol-4-yl)-2-morpholino-2-oxoethylidene)amino) acetate (**381**) as an oil (53 mg, 8%). HPLC (Method C) $T_R = 1.37$ min, 36.3% a/a; MS m/z (ESI⁺) 296 ([M+H]⁺).

6.3.3.2 Preparation of Benzyl 2-((1-(2-methyloxazol-4-yl)-2-morpholino-2-oxoethylidene)amino)acetate (**384**)



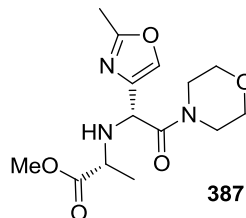
1-(2-Methyloxazol-4-yl)-2-morpholinoethane-1,2-dione (**102**) (500 mg, 2.23 mmol) was dissolved in dichloromethane (5 mL) to afford a clear red solution. Glycine benzyl ester hydrochloride (**382**) (500 mg, 2.23 mmol) was added to afford a suspension, washing through with dichloromethane (2.5 mL). The suspension was cooled to 0-5 °C and TMEDA (830 μ L, 5.58 mmol) was added. Titanium tetrachloride (2.45 mL of a 1 M solution in toluene, 24.5 mmol) was added dropwise and the resultant dark brown reaction mixture was stirred at 0-5 °C for 19 h. The reaction was quenched by the addition of K_2CO_3 (2 mL, of a 10% w/w aqueous solution) and stirred vigorously to afford a cream slurry. Celite[®] (1.5 g) was charged and the mixture was stirred for a further 10 min. The triphasic mixture was then filtered through a bed of Celite[®] (1.0 g) and washed with dichloromethane (2 x 20 mL). The liquid phases were separated and the organic phase was dried ($MgSO_4$) and concentrated to dryness under reduced pressure to afford the crude product as an oil. The crude product was purified by MDAP and the fractions containing product were combined and concentrated under reduced pressure. The concentrated fractions were extracted with dichloromethane (4 x 30 mL). The organic phases were combined, dried ($MgSO_4$) and evaporated to provide benzyl 2-((1-(2-methyloxazol-4-yl)-2-morpholino-2-oxoethylidene)amino) acetate (**384**) as an oil (100 mg, 12%). HPLC (Method C) T_R = 2.26 min, 61.6% a/a; MS m/z (ESI⁺) 372 ([M+H]⁺).

6.3.3.3 Preparation of (*R*)-methyl 2-((1-(2-methyloxazol-4-yl)-2-morpholino-2-oxoethylidene)amino)propanoate (**386**)



1-(2-Methyloxazol-4-yl)-2-morpholinoethane-1,2-dione (**102**) (250 mg, 1.12 mmol) was dissolved in dichloromethane (2.5 mL) to afford a clear red solution. D-Alanine methyl ester hydrochloride (**385**) (156 mg, 1.12 mmol) was added to afford a suspension, washing through with dichloromethane (1.25 mL). The suspension was cooled to 0-5 °C and TMEDA (415 µL, 2.79 mmol) was added. Titanium tetrachloride (1.23 mL of a 1 M solution in toluene, 1.23 mmol) was added dropwise and the resultant dark brown reaction mixture was stirred at 0-5 °C for 16 h. The reaction was quenched by the addition of K₂CO₃ (2 mL, of a 10% w/w aqueous solution) and stirred vigorously to afford a cream slurry. Celite[®] (0.75 g) was charged and the mixture was stirred for a further 10 min. The triphasic mixture was then filtered through a bed of Celite[®] (0.5 g). The liquid phases were separated and the organic phase was dried (MgSO₄) and concentrated to dryness under reduced pressure to afford the crude product as an oil. The crude product was purified by MDAP and the fractions containing product were combined and concentrated under reduced pressure. The concentrated fractions were extracted with dichloromethane (3 x 50 mL). The organic phases were combined, dried (MgSO₄) and evaporated to provide (*R*)-methyl 2-((1-(2-methyloxazol-4-yl)-2-morpholino-2-oxoethylidene)amino)propanoate (**386**) as an oil (85 mg, 25%; ¹H NMR (Major isomer) (400 MHz, CDCl₃) δ ppm 1.52 (d, *J* = 6.6 Hz, 3H), 2.49 (s, 3H), 3.20 - 3.49 (m, 2H), 3.56 - 3.85 (m, 6H), 3.73 (s, 3H), 4.25 (q, *J* = 6.6 Hz, 1H), 7.97 (s, 1H). ¹H NMR (Minor isomer) (400 MHz, CDCl₃) δ ppm 1.56 (d, *J* = 6.8 Hz, 3H), 2.46 (s, 3H), 3.20 - 3.49 (m, 2H), 3.56 - 3.85 (m, 6H), 3.73 (s, 3H), 5.37 (q, *J* = 6.8 Hz, 1H), 7.96 (s, 1H). %). HPLC (Method C): (Major isomer) *T_R* = 1.53 min 68.8% a/a, (Minor isomer) *T_R* = 1.53 min 22.6% a/a; MS *m/z* (ESI⁺) 310 ([M+H]⁺);

6.3.3.4 Preparation of (*R*)-Methyl 2-((1-(2-methyloxazol-4-yl)-2-morpholino-2-oxoethyl)amino)propanoate (**387**)



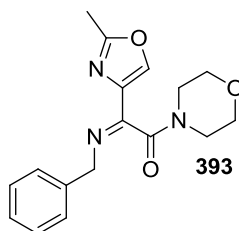
(*R*)-Methyl 2-((1-(2-methyloxazol-4-yl)-2-morpholino-2-oxoethyl)amino)propanoate (**388**) was prepared according to general procedure 16; details are provided below. Differences in processing are recorded where applicable.

Cat = Pd; A: (*R*)-Methyl 2-((1-(2-methyloxazol-4-yl)-2-morpholino-2-oxoethylidene)amino)propanoate (**386**) (50 mg, 0.162 mmol); B: DME (2 mL); C: 10% Pd/C (17 mg) the catalyst was washed in with DME (1 mL); D: 80 °C; E: 4 bar; F: 17 h; G: HPLC (Method A) and LCMS showed complete conversion to the amine (**387**), present as a mixture of diastereoisomers. (Isomer 1) $T_R = 1.45$ min, 41.2% a/a, (Isomer 2) $T_R = 1.74$ min 58.8% a/a; MS m/z (ESI⁺) 312 ([M+H]⁺); H: MeCN/Water & TFA. Fractions containing product were neutralised by the addition of NaHCO₃ (10 mL of a 8% w/w aqueous solution) and extracted with dichloromethane (2 x 20 mL) and the combined organic phases were combined and concentrated; I: (*R*)-methyl 2-((1-(2-methyloxazol-4-yl)-2-morpholino-2-oxoethyl)amino)propanoate (**387**) as a mixture of diastereoisomers. (21 mg, 42%); ¹H NMR (Isomer 1) (400 MHz, CDCl₃) δ ppm 1.34 (d, $J = 7.1$ Hz, 3H), 2.41 (s, 3H), 3.40 (q, $J = 7.1$ Hz, 1H), 3.46 - 3.73 (m, 8 H), 3.70 (s, 3H), 4.68 (s, 1H), 7.50 (s, 1H); ¹H NMR (Isomer 2) (400 MHz, CDCl₃) δ ppm 1.37 (d, $J = 7.1$ Hz, 3H), 2.40 (s, 3H), 3.40 (q, $J = 7.1$ Hz, 1H), 3.46 - 3.73 (m, 8 H), 3.70 (s, 3H), 4.71 (s, 1H), 7.50 (s, 1H); HPLC (Method C): (Isomer 1) $T_R = 1.64$ min, 41.2% a/a, (Isomer 2) $T_R = 1.74$ min 58.8% a/a; MS m/z (ESI⁺) 312 ([M+H]⁺).

Cat = Ru; A: (*R*)-methyl 2-((1-(2-methyloxazol-4-yl)-2-morpholino-2-oxoethylidene)amino)propanoate (**386**) (50 mg, 0.162 mmol); B: DME (2 mL); C: RuCl[*(R)*-SEGPHOS](*p*-cymene)]Cl (14.8 mg, 0.02 mmol). The catalyst was washed in

with DME (1 mL); D: 80 °C; E: 4 bar; F: 17 h. G: HPLC showed the reaction was incomplete. RuCl[*(R)*-SEGPHOS](*p*-cymene)]Cl (14.8 mg, 0.02 mmol) was added and the the mixture was hydrogenated at 4 bar and 80 °C for a further 6 h. HPLC (Method A) and LCMS showed complete conversion to the amine (**387**), present as a mixture of diastereoisomers. (Major isomer) $T_R = 1.65$ min, 87.1% a/a, (Minor isomer) $T_R = 1.76$ min 12.9% a/a; MS m/z (ESI⁺) 312; H: The product was not isolated.

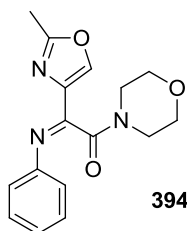
6.3.3.5 Preparation of 2-(Benzylimino)-2-(2-methyloxazol-4-yl)-1-morpholinoethanone (**393**)



2-(Benzylimino)-2-(2-methyloxazol-4-yl)-1-morpholinoethanone (**393**) was prepared according to general procedure 18; details are provided below. Differences in processing are recorded where applicable.

A: 1-(2-methyloxazol-4-yl)-2-morpholinoethane-1,2-dione (**102**) (246 mg, 1.12 mmol); B: 1.25 mL; C: benzylamine (121 μ L, 1.12 mmol); D: 420 μ L, 2.79 mmol; E: 1.23 mL of a 1 M solution in dichloromethane, 1.23 mmol; F: 2.5 h; G: Shows complete consumption of the ketone (**102**); H: 2 mL; I: 2 x 10 mL; K: 120 mg, 34%; ¹H NMR (400 MHz, CDCl₃) δ ppm 2.48 (s, 3H), 3.08 - 3.37 (m, 2H), 3.41 - 3.87 (m, 6H), 4.61 (d, ² $J_{H-H} = 14.2$ Hz, 1H), 4.85 (d, ² $J_{H-H} = 14.2$ Hz, 1H), 7.22 - 7.40 (m, 5H), 7.95 (s, 1H); HPLC (Method C): $T_R = 2.02$ min 84.6% a/a; MS m/z (ESI⁺) 314 ([M+H]⁺).

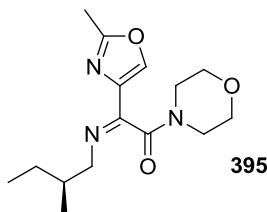
6.3.3.6 Preparation of 2-(2-Methyloxazol-4-yl)-1-morpholino-2-(phenylimino)ethanone (394)



(2*R*,3*S*)-Methyl 2-((2-(dimethylamino)-1-(2-methyloxazol-4-yl)-2-oxoethylidene)amino)-3-methylpentanoate (**394**) was prepared according to general procedure 18; details are provided below. Differences in processing are recorded where applicable.

A: 1-(2-methyloxazol-4-yl)-2-morpholinoethane-1,2-dione (**102**) (500 mg, 2.23 mmol); B: dichloromethane (5 mL); C: aniline (208 mg, 2.23 mmol); D: 834 μ L, 5.58 mmol; E: 2.45 mL of a 1 M solution in dichloromethane, 2.45 mmol; F: 4 h; G: Shows complete consumption of the ketone (**102**); H: 2 mL; I: 2 x 10 mL; K: 539 mg, 66%; ^1H NMR (400 MHz, CDCl_3) δ ppm 2.52 – 2.58 (m, 1H), 2.54 (s, 3H), 2.89 - 3.10 (m, 1H), 3.12 - 3.29 (m, 2H), 3.30 - 3.46 (m, 2H), 3.54 - 3.73 (m, 2H), 7.14 (d, $J = 7.3$ Hz, 2H), 7.19 (t, $J = 7.3$ Hz 1H), 7.35 (dd, $J = 7.3$ Hz 2H), 8.01 (s, 1H); HPLC (Method C): $T_R = 1.86$ min 98.6% a/a; MS m/z (ESI $^+$) 300 ($[\text{M}+\text{H}]^+$).

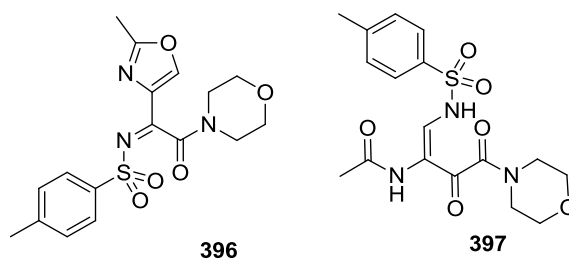
6.3.3.7 Preparation of (S)-2-((2-Methylbutyl)imino)-2-(2-methyloxazol-4-yl)-1-morpholinoethanone (395)



(*S*)-2-((2-Methylbutyl)imino)-2-(2-methyloxazol-4-yl)-1-morpholinoethanone (**395**) was prepared according to general procedure 18; details are provided below. Differences in processing are recorded where applicable.

A: 1-(2-methyloxazol-4-yl)-2-morpholinoethane-1,2-dione (**102**) (250 mg, 1.12 mmol); B: 3.75 mL; C: (*S*)-2-methyl butan-1-amine (97 mg, 1.12 mmol); D: 417 μ L, 2.79 mmol; E: 1.23 mL of a 1 M solution in dichloromethane, 1.23 mmol; F: 22 h; G: Shows complete consumption of the ketone (**102**); H: 2 mL; I: 2 x 10 mL; K: 95 mg, 30%; ^1H NMR (400 MHz, CDCl_3) δ ppm 0.68 - 0.98 (m, 6H), 1.02 - 1.24 (m, 1H), 1.24 - 1.49 (m, 1H), 1.62 - 1.87 (m, 1H), 2.36 (s, 3H), 3.31 - 3.51 (m, 2H), 3.51 - 3.65 (m, 4H), 3.65 - 3.89 (m, 4H), 7.63 (s, 1H). HPLC (Method C): (Major isomer) T_R = 1.92 min, 68.8% a/a (Minor isomer) T_R = 2.11 min, 14.9% a/a; MS m/z (ESI^+) 294 ($[\text{M}+\text{H}]^+$).

6.3.3.8 Attempted Preparation of 4-Methyl-*N*-(1-(2-methyloxazol-4-yl)-2-morpholino-2-oxoethylidene)benzenesulfonamide (**396**)



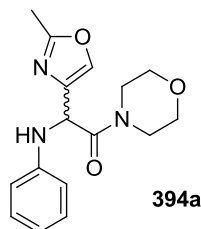
The attempted preparation of 4-methyl-*N*-(1-(2-methyloxazol-4-yl)-2-morpholino-2-oxoethylidene)benzenesulfonamide (**396**) was carried out according to general procedure 18; details are provided below. Differences in processing are recorded where applicable.

A: 1-(2-Methyloxazol-4-yl)-2-morpholinoethane-1,2-dione (**102**) (250 mg, 1.12 mmol); B: dichloromethane 1.25 mL; C: 4-methylbenzenesulfonamide (191 mg, 1.12 mmol); D: 417 μ L, 2.79 mmol; E: 1.51 mL of a 1 M solution in dichloromethane, 1.51 mmol; F: 1 h; G: LCMS (Method C) showed conversion to a peak with T_R = 1.40 min and m/z (ESI^+) 396 consistent with the 1,4-addition product shown (**397**).

6.3.3.9 Experimental procedure for Table 31

The experiments documented in Table 31 were carried out using general procedure 16; details for each entry are provided below. Differences in processing are recorded for each entry where applicable.

Entry 1. 2-(2-Methyloxazol-4-yl)-1-morpholino-2-(phenylamino)ethanone (**394a**)

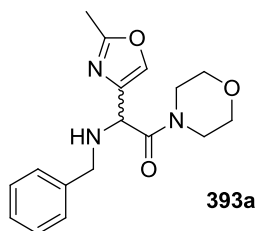


Cat = Ru; A: (2*R*,3*S*)-Methyl 2-((2-(dimethylamino)-1-(2-methyloxazol-4-yl)-2-oxoethylidene) amino)-3-methylpentanoate (**394**) (50 mg, 0.14 mmol); B: DME (3 mL); RuCl₂[(*R*)-SEGPPOS](*p*-cymene)]Cl (19 mg, 0.02 mmol); D: 80 °C; E: 4 bar; F: 12 h; G: HPLC (Method A) and LCMS showed complete conversion to the amine (**394a**); H: MeCN/Water & TFA. Fractions containing product were neutralised by the addition of NaHCO₃ (10 mL of a 8% w/w aqueous solution) and extracted with dichloromethane (2 x 20 mL) and the combined organic phases were combined and concentrated; I: 2-(2-methyloxazol-4-yl)-1-morpholino-2-(phenylamino)ethanone (**394a**) (21 mg, 42%) HPLC (Method A): $T_R = 3.58$ min, 98.7 % a/a; Chiral HPLC: 99.2 : 0.78; MS m/z (ESI⁺) 302 ([M+H]⁺); ¹H NMR (400 MHz, CDCl₃) δ ppm 1.59 (br. s, 1H), 2.35 (s, 3H), 3.42 - 3.48 (m, 1H), 3.50 - 3.77 (m, 6H), 3.79 - 3.95 (m, 1H), 5.22 (d, $J = 3.9$ Hz, 1H), 6.56 (d, $J = 7.8$ Hz, 2H), 6.65 (t, $J = 7.3$ Hz, 1H), 7.08 (dd, $J = 7.3$ Hz, 7.8 Hz, 2H), 7.40 (s, 1H); HPLC (Method A): $T_R = 3.58$ min, 98.7 % a/a; Chiral HPLC: 99.2 : 0.8; MS m/z (ESI⁺) 302 ([M+H]⁺).

Cat = Pd; A: (2*R*,3*S*)-Methyl 2-((2-(dimethylamino)-1-(2-methyloxazol-4-yl)-2-oxoethylidene) amino)-3-methylpentanoate (**394a**) (50 mg, 0.14 mmol); B: DME (3 mL); C: 10% w/w Pd/C (17 mg); D: 80 °C; E: 4 bar; F: 6 h; G: HPLC (Method A) and LCMS showed complete conversion to the amine (**394a**); H: MeCN/Water & TFA. Fractions containing product were neutralised by the addition of NaHCO₃ (10 mL of a

8% w/w aqueous solution) and extracted with dichloromethane (2 x 20 mL) and the combined organic phases were combined and concentrated; I: 2-(2-methyloxazol-4-yl)-1-morpholino-2-(phenylamino)ethanone (**394a**) (34 mg, 67%); $^1\text{H NMR}$ (400 MHz, CDCl_3) δ ppm 1.59 (br. s, 1H), 2.35 (s, 3H), 3.42 - 3.48 (m, 1H), 3.50 - 3.77 (m, 6H), 3.79 - 3.95 (m, 1H), 5.22 (d, $J = 3.9$ Hz, 1H), 6.56 (d, $J = 7.8$ Hz, 2H), 6.65 (t, $J = 7.3$ Hz, 1H), 7.08 (dd, $J = 7.3$ Hz, 7.8 Hz, 2H), 7.40 (s, 1H); HPLC (Method A): $T_R = 3.58$ min, 98.6 % a/a; Chiral HPLC: 49.5 : 50.5; MS m/z (ESI^+) 302 ($[\text{M}+\text{H}]^+$).

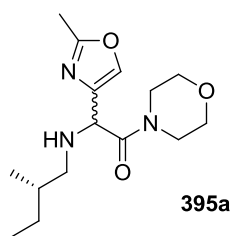
Entry 2. 2-(Benzylamino)-2-(2-methyloxazol-4-yl)-1-morpholinoethanone (**393a**)



Cat = Ru; A: 2-(Benzylimino)-2-(2-methyloxazol-4-yl)-1-morpholinoethanone (**393a**) (50 mg, 0.16 mmol); B: DME (3 mL); $\text{RuCl}[(\text{R})\text{-SEGPHOS}](p\text{-cymene})\text{Cl}$ (18 mg, 0.02 mmol); D: 80 °C; E: 4 bar; F: 12 h; G: LCMS (Method A) showed hydrolysis to the ketone (**102**) and no evidence of the desired amine.

Cat = Pt; A: 2-(Benzylimino)-2-(2-methyloxazol-4-yl)-1-morpholinoethanone (**393a**) (50 mg, 0.16 mmol); B: DME (3 mL); C: 5% w/w Pt/C (62 mg); D: 25 °C; E: 4 bar; F: 6 h; G: HPLC (Method A) and LCMS showed complete conversion to the amine (**393a**); $T_R = 2.52$ min, 61.3 % a/a; MS m/z (ESI^+) 316 ($[\text{M}+\text{H}]^+$); H: The product was not isolated.

Entry 2. (*S*)-2-((2-Methylbutyl)amino)-2-(2-methyloxazol-4-yl)-1-morpholinoethanone (**395a**)

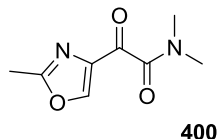


Cat = Ru; A: (*S*)-2-((2-Methylbutyl)imino)-2-(2-methyloxazol-4-yl)-1-morpholinoethanone (**395**) (50 mg, 0.17 mmol); B: DME (3 mL); C: RuCl[*(R)*-SEGPHOS(*p*-cymene)]Cl (16 mg, 0.02 mmol); D: 80 °C; E: 4 bar; F: 12 h; G: LCMS and HPLC (Method A) showed 84% conversion to the amine (**395a**) as a mixture of diastereoisomers; (Isomer 1) $T_R = 8.61$ min, 52.6 % a/a; (Isomer 1) $T_R = 8.67$ min, 29.9 % a/a; MS m/z (ESI⁺) 296 ([M+H]⁺). H: The product was not isolated.

Cat = Pd; A: (*S*)-2-((2-Methylbutyl)imino)-2-(2-methyloxazol-4-yl)-1-morpholinoethanone (**395**) (50 mg, 0.17 mmol); B: DME (3 mL); C: 10% w/w Pd/C (18 mg); D: 25 °C; E: 4 bar; F: 6 h; G: LCMS and HPLC (Method A) showed 92% conversion to the amine (**395**) as a mixture of diastereoisomers; (Isomer 1) $T_R = 8.61$ min, 42.5 % a/a; (Isomer 1) $T_R = 8.67$ min, 33.9 % a/a; MS m/z (ESI⁺) 296 ([M+H]⁺). H: The product was not isolated.

6.3.4 Experimental Procedures for Section 4.5

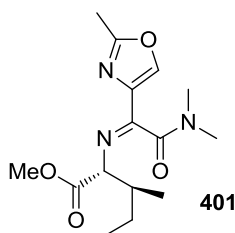
6.3.4.1 Preparation of *N,N*-Dimethyl-2-(2-methyloxazol-4-yl)-2-oxoacetamide (400)



N,N-Dimethyl-2-(2-methyloxazol-4-yl)-2-oxoacetamide (**400**) was prepared according to general procedure 17; details are provided below. Differences in processing are recorded where applicable.

A: 108 mL of a 1 M solution in THF, 180 mmol; B: 2-(dimethylamino)acetonitrile (**39**) (4.77 g, 57 mmol); C: Methyl 2-methyloxazole-4-carboxylate (**84**) (8.0 g, 52 mmol); D: 40 mL; E: 10 min; F: 112 mL; G: 64 mL; H: 4.17 mL, 73 mmol; I: 10.92 g, 130 mmol; J: 15.8 g, in water (80 mL); K: 18 h; L: 12.9 g, 52 mmol; M: 64 mL; N: 12 – 100% EtOAc in heptane; O: *N,N*-dimethyl-2-(2-methyloxazol-4-yl)-2-oxoacetamide (**400**) (1.16 g, 12%); ¹H NMR (400 MHz, CDCl₃) δ ppm 2.53 (s, 3H), 3.08 (s, 6H), 8.35 (s, 1H); HPLC (Method B) *T_R* = 1.31 min 94.5% a/a; MS *m/z* (ESI⁺) 183 ([M+H]⁺).

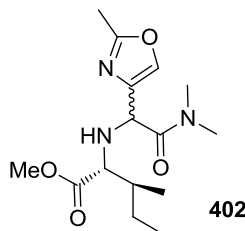
6.3.4.2 Preparation of (2*R*,3*S*)-Methyl 2-((2-(dimethylamino)-1-(2-methyloxazol-4-yl)-2-oxoethylidene)amino)-3-methylpentanoate (401)



(2*R*,3*S*)-Methyl 2-((2-(dimethylamino)-1-(2-methyloxazol-4-yl)-2-oxoethylidene)amino)-3-methylpentanoate (**401**) was prepared according to general procedure 18; details are provided below. Differences in processing are recorded where applicable.

A: *N,N*-Dimethyl-2-(2-methyloxazol-4-yl)-2-oxoacetamide (**400**) (250 mg, 1.37 mmol); B: 1.25 mL; C: (2*R*,3*S*)-methyl 2-amino-3-methylpentanoate hydrochloride (250, 1.37 mmol); D: 510 μ L, 3.43 mmol; E: 1.51 mL of a 1 M solution in dichloromethane, 1.51 mmol; F: 2.5 h; G: Shows complete consumption of the ketone (**400**); H: 2 mL; I: 2 x 10 mL; K: 250 mg, 59%, as a mixture of isomers; $^1\text{H NMR}$ (Isomer 1) (400 MHz, CDCl_3) δ ppm 0.91 (t, $J = 7.3$ Hz, 3H), 0.96 (d, $J = 6.8$ Hz, 3H), 1.07 - 1.26 (m, 1H), 1.40 - 1.48 (m, 1H), 2.04 - 2.20 (m, 1H), 2.47 (s, 3H), 2.88 (s, 3H), 3.07 (s, 3H), 3.72 (s, 3H), 3.97 (d, $J = 5.6$ Hz, 1H), 7.99 (s, 1H); (Isomer 2) (400 MHz, CDCl_3) δ ppm 0.86 (t, $J = 7.4$ Hz, 3H), 1.00 (d, $J = 6.9$ Hz, 3H), 1.07 - 1.26 (m, 1H), 1.40 - 1.48 (m, 1H), 2.04 - 2.20 (m, 1H), 2.44 (s, 3H), 3.07 (s, 3H), 3.16 (s, 3H), 3.73 (s, 3H), 5.09 (d, $J = 3.9$ Hz, 1H), 7.95 (s, 1H); HPLC (Method C): (Isomer 1) $T_R = 2.13$ min 74.2% a/a, (Isomer 2) $T_R = 2.32$ min 23.5% a/a; MS m/z (ESI $^+$) 310 ([M+H] $^+$).

6.3.4.3 Preparation of (2*R*,3*S*)-Methyl 2-((2-(dimethylamino)-1-(2-methyloxazol-4-yl)-2-oxoethyl)amino)-3-methylpentanoate (**402**)



(2*R*,3*S*)-Methyl 2-((2-(dimethylamino)-1-(2-methyloxazol-4-yl)-2-oxoethyl)amino)-3-methylpentanoate (**402**) was prepared according to general procedure 16; details are provided below. Differences in processing are recorded where applicable.

Cat = Pd; A: (2*R*,3*S*)-Methyl 2-((2-(dimethylamino)-1-(2-methyloxazol-4-yl)-2-oxoethylidene)amino)-3-methylpentanoate (**401**) (50 mg, 0.162 mmol); B: DME (2 mL); C: 10% Pd/C (17 mg) the catalyst was washed in with DME (1 mL); D: 80 $^{\circ}\text{C}$; E: 4 bar; F: 6 h. G: HPLC (Method A) and LCMS showed complete conversion to the amine (**402**), present as a mixture of diastereoisomers. (Isomer 1) $T_R = 2.53$ min, 61.1% a/a, (Isomer 2) $T_R = 2.76$ min 38.9% a/a; MS m/z (ESI $^+$) 312 ([M+H] $^+$); H: MeCN/Water & TFA. Fractions containing product were neutralised by the addition of NaHCO_3 (10 mL

of a 8% w/w aqueous solution) and extracted with dichloromethane (2 x 20 mL) and the combined organic phases were combined and concentrated; I: (2*R*,3*S*)-methyl 2-((-2-(dimethylamino)-1-(2-methyloxazol-4-yl)-2-oxoethyl)amino)-3-methylpentanoate (**402**) (Isomer 1; 18 mg, 36%)) (Isomer 2; 25 mg, 50%). ¹H NMR (Isomer 1) (400 MHz, CDCl₃) δ ppm 0.82 (t, *J* = 7.5 Hz, 3H), 0.86 (d, *J* = 6.8 Hz, 3H), 1.03 - 1.25 (m, 1H), 1.41 (m, 1H), 1.62 - 1.77 (m, 1H), 2.01 (br. s, 1H), 2.34 (s, 3H), 2.91 (s, 3H), 2.97 (s, 3H), 3.15 (d, *J* = 5.6 Hz, 1H), 3.59 (s, 3H), 4.56 (s, 1H), 7.53 (s, 1 H); (Isomer 2) (400 MHz, CDCl₃) δ ppm 0.84 (t, *J* = 7.6 Hz, 3H), 0.91 (d, *J* = 6.9 Hz, 3H), 1.10 - 1.28 (m, 1H), 1.39 - 1.50 (m, 1H), 1.69 - 1.87 (m, 1H), 2.34 (br. s, 1H), 2.41 (s, 3H), 2.97 (s, 3H), 3.07 (s, 3H), 3.19 (d, *J* = 4.9 Hz, 1H), 3.68 (s, 3H), 4.62 (s, 1H), 7.41 (s, 1 H); HPLC (Method A): (Isomer 1) *T_R* = 2.53 min, 96.1% a/a, (Isomer 2) *T_R* = 2.75 min 28.8% a/a; MS *m/z* (ESI⁺) 312 ([M+H]⁺).

Cat = Ru; A: (2*R*,3*S*)-Methyl 2-((-2-(dimethylamino)-1-(2-methyloxazol-4-yl)-2-oxoethylidene)amino)-3-methylpentanoate (**401**) (50 mg, 0.162 mmol); B: DME (2 mL); C: RuCl[*(R)*-SEGPHOS(*p*-cymene)]Cl (14.8 mg, 0.02 mmol). The catalyst was washed in with DME (1 mL); D: 80 °C; E: 4 bar; F: 6 h. G: HPLC showed the reaction was incomplete. RuCl[*(R)*-SEGPHOS(*p*-cymene)]Cl (14.8 mg, 0.02 mmol) was added and the the mixture was hydrogenated at 4 bar and 80 °C for a further 6 h. HPLC and LCMS (Method A) showed complete conversion to the amine (**402**), present as a mixture of diastereoisomers. (Major isomer) *T_R* = 2.52 min, 96.4% a/a, (Minor isomer) *T_R* = 2.72 min 3.6% a/a; MS *m/z* (ESI⁺) 312; H: MeCN/Water & TFA. Fractions containing product were neutralised by the addition of NaHCO₃ (10 mL of a 8% w/w aqueous solution) and extracted with dichloromethane (2 x 20 mL) and the combined organic phases were combined and concentrated; I: (2*R*,3*S*)-methyl 2-((-2-(dimethylamino)-1-(2-methyloxazol-4-yl)-2-oxoethyl)amino)-3-methyl pentanoate (**402**) (20 mg, 40%); ¹H NMR (400 MHz, CDCl₃) δ ppm 0.82 (t, *J* = 7.5 Hz, 3H), 0.86 (d, *J* = 6.8 Hz, 3H), 1.03 - 1.25 (m, 1H), 1.41 (m, 1H), 1.62 - 1.77 (m, 1H), 1.99 (br. s, 1H), 2.34 (s, 3H), 2.91 (s, 3H), 2.97 (s, 3H), 3.15 (d, *J* = 5.6 Hz, 1H), 3.59 (s, 3H), 4.56 (s,

1H), 7.53 (s, 1 H); HPLC (Method A) $T_R = 2.53$ min, 96.7% a/a.; MS m/z (ESI⁺) 312 ([M+H]⁺).

7 References

7 References

1. Gimpl, G.; Fahrenholz, F. *Physiol. Rev.* **2001**, *81*, 629-683.
2. Acher, R.; Chauvet, J.; Chauvet, M. T. *Adv. Exp. Med. Biol.* **1995**, *395*, 615-627.
3. du Vigneaud, V.; Ressler, C.; Trippett, S. *J. Biol. Chem.* **1953**, *205*, 949-957.
4. du Vigneaud, V.; Ressler, C.; Swan, J. M.; Roberts, C. W.; Katsoyannis, P. G.; Gordon, S. *J. Am. Chem. Soc.* **1953**, *75*, 4879-4880.
5. Gautvik, K. M.; de Lecea, L.; Gautvik, V. T.; Danielson, P. E.; Tranque, P.; Dopazo, A.; Bloom, F. E.; Sutcliffe, J. G. *Proc. Natl. Acad. Sci. U. S. A.* **1996**, *93*, 8733-8738.
6. Dale, H. H. *J. Physiol. (Oxford, U. K.)* **1906**, *34*, 163-206.
7. Ott, I.; Scott, J. C. *Proc. Soc. Exp. Biol. Med.* **1911**, *8*, 48-49.
8. Witt, D. M. *Neurosci. Biobehav. Rev.* **1995**, *19*, 315-324.
9. Lee, H. J.; Macbeth, A. H.; Pagani, J. H.; Young, W. S. I. *Prog. Neurobiol.* **2009**, *88*, 127-151.
10. Zingg, H. H.; Laporte, S. A. *Trends Endocrinol. Metab.* **2003**, *14*, 222-227.
11. Steer, P. *BJOG* **2005**, *112 Suppl 1*, 1-3.
12. Slattery, M. M.; Morrison, J. J. *Lancet* **2002**, *360*, 1489-1497.
13. Goldenberg, R. L.; Culhane, J. F.; Iams, J. D.; Romero, R. *Lancet* **2008**, *371*, 75-84.
14. Tucker, J. M.; Goldenberg, R. L.; Davis, R. O.; Copper, R. L.; Winkler, C. L.; Hauth, J. C. *Obstet. Gynecol.* **1991**, *77*, 343-347.
15. Iams, J. D.; Romero, R.; Culhane, J. F.; Goldenberg, R. L. *Lancet* **2008**, *371*, 164-175.
16. Papatsonis, D.; Flenady, V.; Cole, S.; Liley, H. *Cochrane Database Syst. Rev.* **2005**, CD004452

17. Corey, R. B. *J. Am. Chem. Soc.* **1938**, *60*, 1598-1604.
18. Martins, M. B.; Carvalho, I. *Tetrahedron* **2007**, *63*, 9923-9932.
19. Raju, R.; Piggott, A. M.; Huang, X. C.; Capon, R. J. *Org. Lett.* **2011**, *13*, 2770-2773.
20. Park, H. B.; Kwon, H. C.; Lee, C. H.; Yang, H. O. *J. Nat. Prod.* **2009**, *72*, 248-252.
21. Szardenings, A. K.; Burkoth, T. S.; Lu, H. H.; Tien, D. W.; Campbell, D. A. *Tetrahedron* **1997**, *53*, 6573-6593.
22. Dinsmore, C. J.; Beshore, D. C. *Tetrahedron* **2002**, *58*, 3297-3312.
23. Akiyama, M.; Katoh, A.; Tsuchiya, Y. *J. Chem. Soc., Perkin Trans. 1* **1989**, 235-239.
24. Wang, D. X.; Liang, M. T.; Tian, G. J.; Lin, H.; Liu, H. Q. *Tetrahedron Lett.* **2002**, *43*, 865-867.
25. Bourne, G. T.; Golding, S. W.; McGeary, R. P.; Meutermans, W. D. F.; Jones, A.; Marshall, G. R.; Alewood, P. F.; Smythe, M. L. *J. Org. Chem.* **2001**, *66*, 7706-7713.
26. Jones, J. H.; Young, G. T. *J. Chem. Soc. C* **1968**, 436-441.
27. Jones, J. H. *J. Chem. Soc. D* **1969**, 1436-1437.
28. Boehm, J. C.; Kingsbury, W. D. *J. Org. Chem.* **1986**, *51*, 2307-2314.
29. Hulme, C.; Morrissette, M. M.; Volz, F. A.; Burns, C. J. *Tetrahedron Lett.* **1998**, *39*, 1113-1116.
30. Keating, T. A.; Armstrong, R. W. *J. Am. Chem. Soc.* **1995**, *117*, 7842-7843.
31. Sollis, S. L. *J. Org. Chem.* **2005**, *70*, 4735-4740.
32. Marcaccini, S.; Pepino, R.; Pozo, M. C. *Tetrahedron Lett.* **2001**, *42*, 2727-2728.
33. Williams, R. M.; Glinka, T.; Kwast, E. *J. Am. Chem. Soc.* **1988**, *110*, 5927-5929.

34. Falorni, M.; Giacomelli, G.; Porcheddu, A.; Taddei, M. *Eur. J. Org. Chem.* **2000**, 1669-1675.
35. O'Reilly, E.; Lestini, E.; Balducci, D.; Paradisi, F. *Tetrahedron Lett.* **2009**, *50*, 1748-1750.
36. Diafi, L.; Couquelet, J.; Tronche, P.; Gardette, D.; Gramain, J. C. *J. Heterocycl. Chem.* **1990**, *27*, 2181-2187.
37. Ugi, I. *Angew. Chem.* **1962**, *74*, 9-22.
38. Mumm, O.; Hesse, H.; Volquartz, H. *Ber. Dtsch. Chem. Ges.* **1915**, *48*, 379-391.
39. Andraos, J. *Org. Process Res. Dev.* **2005**, *9*, 404-431.
40. Chanda, A.; Fokin, V. V. *Chem. Rev.* **2009**, *109*, 725-748.
41. Keating, T. A.; Armstrong, R. W. *J. Am. Chem. Soc.* **1996**, *118*, 2574-2583.
42. Domling, A.; Huang, Y. *Synthesis* **2010**, 2859-2883.
43. Passerini, M.; Ragni, G.; Simone, L. *Gazz. Chim. Ital.* **1931**, *61*, 964-969.
44. Li, X.; Danishefsky, S. J. *J. Am. Chem. Soc.* **2008**, *130*, 5446-5448.
45. Montalbetti, C. A. G. N.; Falque, V. *Tetrahedron* **2005**, *61*, 10827-10852.
46. Carey, J. S.; Webb, M.; Hayes, J. *GlaxoSmithKline* **2005**, Unpublished work.
47. Mattson, A. E.; Bharadwaj, A. R.; Zuhl, A. M.; Scheidt, K. A. *J. Org. Chem.* **2006**, *71*, 5715-5724.
48. Mattson, A. E.; Scheidt, K. A. *Org. Lett.* **2004**, *6*, 4363-4366.
49. Kobayashi, T.; Tanaka, M. *J. Organomet. Chem.* **1982**, *233*, C64-C66.
50. Mueller, P.; Godoy, J. *Tetrahedron Lett.* **1982**, *23*, 3661-3664.
51. Yang, Z.; Zhang, Z.; Meanwell, N. A.; Kadow, J. F.; Wang, T. *Org. Lett.* **2002**, *4*, 1103-1105.
52. Basic Terminology of Stereochemistry. *Pure and Applied Chemistry* **1996**, *68*, 2193-2222.

53. Martinez-Frias, M. L. *Med Clin (Barc)* **2012**, *139*, 25-32.
54. Zipper, J.; Wheeler, R. G.; Potts, D. M.; Rivera, M. *Br Med J (Clin Res Ed)* **1983**, *287*, 1245-1246.
55. Aitken, R. A.; Kilenyi, S. N. *Asymmetric Synthesis* Blackie Academic & Professional: Glasgow, 1992.
56. Harrington, P. J.; Lodewijk, E. *Org. Process Res. Dev.* **1997**, *1*, 72-76.
57. Pope, W. J.; Peachey, S. J. *J. Chem. Soc.* **1899**, *75*, 1066
58. Yang, C. P.; Su, C. S. *J. Org. Chem.* **1986**, *51*, 5186-5191.
59. Ellman, J. A.; Owens, T. D.; Tang, T. P. *Acc. Chem. Res.* **2002**, *35*, 984-995.
60. Klunder, J. M.; Ko, S. Y.; Sharpless, K. B. *J. Org. Chem.* **1986**, *51*, 3710-3712.
61. Klunder, J. M.; Ko, S. Y.; Sharpless, K. B. *J. Org. Chem.* **1986**, *51*, 3710-3712.
62. Molander, G. A. *Science of Synthesis, Stereoselective Synthesis*; Thieme, Stuttgart: 2011; Vol. 2.
63. Osborn, J. A.; Jardine, F. H.; Young, J. F.; Wilkinson, G. *J. Chem. Soc.* **1966**, 1711-1732.
64. Blaser, H. U. *Tetrahedron: Asymm.* **1991**, *2*, 843-866.
65. Knowles, W. S. *Angew. Chem., Int. Ed.* **2002**, *41*, 1998-2007.
66. Kagan, H. B.; Dang, T. P. *J. Chem. Soc. D.* **1971**, 481
67. Miyashita, A.; Yasuda, A.; Takaya, H.; Toriumi, K.; Ito, T.; Souchi, T.; Noyori, R. *J. Am. Chem. Soc.* **1980**, *102*, 7932-7934.
68. Miyashita, A.; Yasuda, A.; Takaya, H.; Toriumi, K.; Ito, T.; Souchi, T.; Noyori, R. *J. Am. Chem. Soc.* **1980**, *102*, 7932-7934.
69. Mashima, K.; Kusano, K.; Ohta, T.; Noyori, R.; Takaya, H. *J. Chem. Soc., Chem. Commun.* **1989**, 1208-1210.
70. Ager, D. J.; Laneman, S. A. *Tetrahedron: Asymm.* **1997**, *8*, 3327-3355.

71. Noyori, R.; Ohkuma, T.; Kitamura, M.; Takaya, H.; Sayo, N.; Kumobayashi, H.; Akutagawa, S. *J. Am. Chem. Soc.* **1987**, *109*, 5856-5858.
72. Noyori, R. *Angew. Chem. Int. Ed.* **2002**, *41*, 2008-2022.
73. Breuer, M.; Ditrich, K.; Habicher, T.; Hauer, B.; Kessler, M.; Stuermer, R.; Zelinski, T. *Angew. Chem., Int. Ed.* **2004**, *43*, 788-824.
74. Ye, Z. Q.; Lan, R. Z.; Yang, W. M.; Yao, L. F.; Yu, X. *J. Int. Med. Res.* **2008**, *36*, 244-252.
75. Blaser, H. U.; Spindler, F. *Chim. Oggi* **2001**, *19*, 17-20.
76. Blaser, H. U. *Adv. Synth. Catal.* **2002**, *344*, 17-31.
77. Xie, J. H.; Zhu, S. F.; Zhou, Q. L. *Chem. Rev.* **2011**, *111*, 1713-1760.
78. Fleury-Bregeot, N.; de la Fuente, V.; Castillon, S.; Claver, C. *ChemCatChem* **2010**, *2*, 1346-1371.
79. Wang, C.; Villa-Marcos, B.; Xiao, J. *Chem. Commun.* **2011**, *47*, 9773-9785.
80. Nugent, T. C.; El-Shazly, M. *Adv. Synth. Catal.* **2010**, *352*, 753-819.
81. Baeza, A.; Pfaltz, A. *Chem. Eur. J.* **2010**, *16*, 4003-4009.
82. Ng Cheong Chan, Y.; Osborn, J. A. *J. Am. Chem. Soc.* **1990**, *112*, 9400-9401.
83. Chan, Y. N. C.; Meyer, D.; Osborn, J. A. *J. Chem. Soc., Chem. Commun.* **1990**, 869-871.
84. Schnider, P.; Koch, G.; Pretot, R.; Wang, G.; Bohnen, F. M.; Kruger, C.; Pfaltz, A. *Chem. - Eur. J.* **1997**, *3*, 887-892.
85. Crabtree, R. *Acc. Chem. Res.* **1979**, *12*, 331-337.
86. Xiao, D.; Zhang, X. *Angew. Chem., Int. Ed.* **2001**, *40*, 3425-3428.
87. Blaser, H. U.; Brieden, W.; Pugin, B.; Spindler, F.; Studer, M.; Togni, A. *Top. Catal.* **2002**, *19*, 3-16.
88. Li, W.; Hou, G.; Chang, M.; Zhang, X. *Adv. Synth. Catal.* **2009**, *351*, 3123-3127.

89. Yang, Q.; Shang, G.; Gao, W.; Deng, J.; Zhang, X. *Angew. Chem., Int. Ed.* **2006**, *45*, 3832-3835.
90. Blaser, H. U. *Adv. Synth. Catal.* **2002**, *344*, 17-31.
91. Shang, G.; Yang, Q.; Zhang, X. *Angew. Chem., Int. Ed.* **2006**, *45*, 6360-6362.
92. Zhong, Y. L.; Krska, S. W.; Zhou, H.; Reamer, R. A.; Lee, J.; Sun, Y.; Askin, D. *Org. Lett.* **2009**, *11*, 369-372.
93. Willoughby, C. A.; Buchwald, S. L. *J. Org. Chem.* **1993**, *58*, 7627-7629.
94. Willoughby, C. A.; Buchwald, S. L. *J. Am. Chem. Soc.* **1994**, *116*, 11703-11714.
95. Collins, S.; Kuntz, B. A.; Taylor, N. J.; Ward, D. G. *J. Organomet. Chem.* **1988**, *342*, 21-29.
96. Willoughby, C. A.; Buchwald, S. L. *J. Am. Chem. Soc.* **1994**, *116*, 8952-8965.
97. Charette, A. B.; Giroux, A. *Tetrahedron Lett.* **1996**, *37*, 6669-6672.
98. Chen, F.; Wang, T.; He, Y.; Ding, Z.; Li, Z.; Xu, L.; Fan, Q. H. *Chem. - Eur. J.* **2011**, *17*, 1109-1113, S1109/1.
99. Noyori, R.; Okhuma, T. *Angew. Chem. Int. Ed.* **2001**, *40*, 40-73.
100. Oppolzer, W.; Wills, M.; Starkemann, C.; Bernardinelli, G. *Tetrahedron Lett.* **1990**, *31*, 4117-4120.
101. Ohkuma, T.; Ooka, H.; Hashiguchi, S.; Ikariya, T.; Noyori, R. *J. Am. Chem. Soc.* **1995**, *117*, 2675-2676.
102. Abdur-Rashid, K.; Lough, A. J.; Morris, R. H. *Organometallics* **2001**, *20*, 1047-1049.
103. Copley, C. J.; Henschke, J. P. *Adv. Synth. Catal.* **2003**, *345*, 195-201.
104. Jackson, M.; Lennon, I. C. *Tetrahedron Lett.* **2007**, *48*, 1831-1834.
105. Bordwell, F. G.; Van der Puy, M.; Vanier, N. R. *J. Org. Chem.* **1976**, *41*, 1883-1885.

106. Taft, R. W.; Bordwell, F. G. *Acc. Chem. Res.* **1988**, *21*, 463-469.
107. Ogata, Y.; Nagura, K. *J. Chem. Soc., Perkin Trans. 2* **1976**, 628-633.
108. Fuson, R. C.; Bull, B. A. *Chem. Rev.* **1934**, *15*, 275-309.
109. Wang, H.; Andemichael, Y. W.; Vogt, F. G. *J. Org. Chem.* **2009**, *74*, 478-481.
110. Wolfe, J. P. *Name React. Funct. Group Transform.* **2007**, 282-290.
111. Camici, L.; Dembech, P.; Ricci, A.; Seconi, G.; Taddei, M. *Tetrahedron* **1988**, *44*, 4197-4206.
112. Leffler, J. E. *J. Org. Chem.* **1951**, *16*, 1785-1787.
113. Cremer, D.; Crehuet, R.; Anglada, J. *J. Am. Chem. Soc.* **2001**, *123*, 6127-6141.
114. Sawaki, Y.; Foote, C. S. *J. Am. Chem. Soc.* **1983**, *105*, 5035-5040.
115. Sawaki, Y.; Foote, C. S. *J. Am. Chem. Soc.* **1979**, *101*, 6292-6296.
116. Zhang, Z.; Yin, Z.; Kadow, J. F.; Meanwell, N. A.; Wang, T. *J. Org. Chem.* **2004**, *69*, 1360-1363.
117. Zhu, J.; Wong, H.; Zhang, Z.; Yin, Z.; Kadow, J. F.; Meanwell, N. A.; Wang, T. *Tetrahedron Lett.* **2005**, *46*, 3587-3589.
118. Garcia, S. *GlaxoSmithKline* **2011**, Unpublished work
119. Payne, G. B.; Deming, P. H.; Williams, P. H. *J. Org. Chem.* **1961**, *26*, 659-663.
120. Cornforth, J. W.; Cornforth, R. H. *J. Chem. Soc.* **1957**, 158-162.
121. Barney, C. L.; Huber, E. W.; McCarthy, J. R. *Tetrahedron Lett.* **1990**, *31*, 5547-5550.
122. Gamble, D. L.; Hems, W. P.; Ridge, B. *J. Chem. Soc., Perkin Trans. 1* **2001**, 248-260.
123. Imai, N.; Achiwa, K. *Chem. Pharm. Bull.* **1987**, *35*, 2646-2655.
124. Faust, R.; Goebelt, B.; Weber, C. *Synlett* **1998**, 64-66.

125. Salmi, C.; Loncle, C.; Letourneux, Y.; Brunel, J. M. *Tetrahedron* **2008**, *64*, 4453-4459.
126. Salmi, C.; Letourneux, Y.; Brunel, J. M. *Lett. Org. Chem.* **2006**, *3*, 396-401.
127. Bouquillon, S.; Henin, F.; Muzart, J. *Synth. Commun.* **2001**, *31*, 39-45.
128. Banik, B. K.; Samajdar, S.; Hackfeld, L. C.; Zegrocka, O.; Becker, F. F. *Abstracts of Papers, 222nd ACS National Meeting, Chicago, IL, United States, August 26-30, 2001* **2001**, ORGN-097.
129. Kwan, E. E.; Huang, S. G. *Eur. J. Org. Chem.* **2008**, 2671-2688.
130. Narasimhan, S.; Balakumar, R. *Aldrichimica Acta* **1998**, *31*, 19-26.
131. Webb, M. *GlaxoSmithKline* **2011**, Unpublished work
132. Remko, M. *Chem. Pap.* **2007**, *61*, 133-141.
133. Carr, W.; Shutt, W. J. *Trans. Faraday Soc.* **1939**, *35*, 579-587.
134. Devos, A.; Remion, J.; Frisque-Hesbain, A. M.; Colens, A.; Ghosez, L. *J. Chem. Soc., Chem. Commun.* **1979**, 1180-1181.
135. Kinnear, K. *GlaxoSmithKline* **2011**, Unpublished work
136. Ironmonger A. *GlaxoSmithKline* **2011**, Unpublished work
137. Ho, T. L.; Olah, G. A. *Proc. Natl. Acad. Sci. U. S. A.* **1978**, *75*, 4-6.
138. Morita, T.; Lim, H. J.; Karube, I. *J. Biotechnol.* **1995**, *38*, 253-261.
139. Mitchell, H. K.; Petersen, N. S.; Buzin, C. H. *Proc. Natl. Acad. Sci. U. S. A.* **1985**, *82*, 4969-4973.
140. Koeller, K. M.; Wong, C. H. *Nature (London)* **2001**, *409*, 232-240.
141. Arnold, F. H. *Nature (London)* **2001**, *409*, 253-257.
142. Srinivas, G.; Periasamy, M. *Tetrahedron Lett.* **2002**, *43*, 2785-2788.
143. Hayes, J. *GlaxoSmithKline* **2011**, Unpublished work

144. Mitchell, M. *GlaxoSmithKline* **2011**, Unpublished work
145. Doucet, H.; Ohkuma, T.; Murata, K.; Yokozawa, T.; Kozawa, M.; Katayama, E.; England, A. F.; Ikariya, T.; Noyori, R. *Angew. Chem. Int. Ed.* **1998**, *37*, 1703-1707.
146. Sandoval, C. A.; Ohkuma, T.; Muniz, K.; Noyori, R. *J. Am. Chem. Soc.* **2003**, *125*, 13490-13503.
147. Noyori, R.; Kitamura, M.; Ohkuma, T. *Proc. Natl. Acad. Sci. U. S. A.* **2004**, *101*, 5356-5362.
148. Hinkelmann, K.; Kempthorne, O. *Design and Analysis of Experiments: Introduction to experimental design*; 2 ed.; Wiley-Interscience: 2007; Vol. 1.
149. Rowan, R., III; Sykes, B. D. *J. Am. Chem. Soc.* **1974**, *96*, 7000-7008.
150. Wan, X.; Sun, Y.; Luo, Y.; Li, D.; Zhang, Z. *J. Org. Chem.* **2005**, *70*, 1070-1072.
151. Touati, R.; Gmiza, T.; Jeulin, S.; Deport, C.; Ratovelomanana-Vidal, V.; Ben Hassine, B.; Genet, J. P. *Synlett* **2005**, 2478-2482.
152. Mitchell, M. *GlaxoSmithKline* **2010**, Unpublished work
153. Shang, G.; Yang, Q.; Zhang, X. *Angew. Chem., Int. Ed.* **2006**, *45*, 6360-6362.
154. Kang, Q.; Zhao, Z. A.; You, S. L. *Adv. Synth. Catal.* **2007**, *349*, 1657-1660.
155. Bayh, O.; Awad, H.; Mongin, F.; Hoarau, C.; Bischoff, L.; Trecourt, F.; Queguiner, G.; Marsais, F.; Blanco, F.; Abarca, B.; Ballesteros, R. *J. Org. Chem.* **2005**, *70*, 5190-5196.
156. Baron, H.; Remfry, F. G. P.; Thorpe, J. F. *J. Chem. Soc.* **1904**, *85*, 1726-1761.
157. Miller, R. A.; Smith, R. M.; Karady, S.; Reamer, R. A. *Tetrahedron Lett.* **2002**, *43*, 935-938.
158. Abdur-Rashid, K.; Lough, A. J. *Acta Crystallogr., Sect. E: Struct. Rep. Online* **2007**, *63*, m246-m248.

159. Sasabe, H.; Nakanishi, S.; Takata, T. *Inorg. Chem. Commun.* **2003**, *6*, 1140-1143.
160. Cambie, M.; D'Arrigo, P.; Fasoli, E.; Servi, S.; Tessaro, D.; Canevotti, F.; Del Corona, L. *Tetrahedron: Asymmetry* **2003**, *14*, 3189-3196.
161. Shanmugapriya, D.; Shankar, R.; Satyanarayana, G.; Dahanukar, V. H.; Kumar, U. K. S.; Vembu, N. *Synlett* **2008**, 2945-2950.
162. Hughes, G.; Devine, P. N.; Naber, J. R.; O'Shea, P. D.; Foster, B. S.; McKay, D. J.; Volante, R. P. *Angew. Chem. Int. Ed.* **2007**, *46*, 1839-1842.
163. Mashima, K.; Kusano, K.; Ohta, T.; Noyori, R.; Takaya, H. *J. Chem. Soc., Chem. Commun.* **1989**, 1208-1210.